



KAPITAŁ LUDZKI
NARODOWA STRATEGIA SPÓJNOŚCI



Politechnika Wrocławska

UNIA EUROPEJSKA
EUROPEJSKI
FUNDUSZ SPOŁECZNY



ROZWÓJ POTENCJAŁU I OFERTY DYDAKTYCZNEJ POLITECHNIKI WROCŁAWSKIEJ

Wrocław University of Technology

Renewable Energy Systems

Robert Łukomski, Tomasz Okon
Kazimierz Wilkosz

POWER SYSTEM MODELLING

Wrocław 2011

Projekt współfinansowany ze środków Unii Europejskiej w ramach
Europejskiego Funduszu Społecznego

Wrocław University of Technology

Renewable Energy Systems

Robert Łukomski, Tomasz Okoń
Kazimierz Wilkosz

POWER SYSTEM MODELLING

Wrocław 2011

Copyright © by Wrocław University of Technology
Wrocław 2011

Reviewer: Eugeniusz Rosołowski

ISBN 978-83-62098-81-1

Published by PRINTPAP Łódź, www.printpap.pl

Contents

1. Introduction. General principles of modelling	7
1.1. Types of models	7
1.1.1. Concrete model	7
1.1.2. Abstract model	7
1.1.3. Physical model	8
1.1.4. Mathematical model	8
1.1.5. Descriptive model	9
1.1.6. Prescriptive model.....	9
1.1.7. Analogue model	9
1.1.8. Symbolic model.....	9
1.2. Classification of models of power systems - domain point of view	9
1.2.1. Phase models	10
1.2.2. Symmetrical component models	10
1.2.3. Single phase models	10
1.2.4. Three-phase models.....	10
1.3. Modelling	10
1.3.1. Mathematical modelling.....	10
1.3.2. Physical modelling	11
Problems	11
References.....	12
2. Models for steady state analyses. Scope of utilization	13
2.1. Introduction.....	13
2.2. Basic components for steady state analysis.....	13
2.2.1. Transmission lines	13
2.2.2. Transformers	14
2.2.3. Shunt capacitors and reactors	18
2.2.4. Loads and generators	19
2.3. Building the network model.....	19
2.3.1. Admittance matrix.....	19
2.3.2. Voltage phasor.....	21
2.3.3. Power equations	22
Problems	22
References.....	23
3. Models for transient analyses. Scope of utilization	24
3.1. Introduction.....	24
3.2. Transient phenomena in power systems.....	25
3.3. Discrete models of electrical networks	26
3.3.1. Discrete models of basic electrical components.....	26
3.4. Non linear and time varying elements modeling.....	30
3.5. Models of power system components	35
3.5.1. Introduction	35
3.5.2. Overhead transmission lines and cables	35
3.5.3. Transformers	43
3.5.4. Rotating machines	46

3.5.5. Loads	52
3.5.6. Circuit breakers	52
3.5.7. Network equivalents for transient analyses	54
3.6. Solution of transients	57
Problems	59
References	60
4. Power system model reduction. Network transformation	62
4.1. General considerations	62
4.2. Network transformation	63
4.2.1. Node elimination	63
4.2.2. Node aggregation using the Dimo's method	70
4.2.3. Node aggregation using the Zhukov's method	72
Problems	75
References	75
5. Power system model reduction. Aggregation of generating units. Equivalent models of the external subsystem	76
5.1. Introduction	76
5.2. Equivalent models of external subsystems	77
5.2.1. Elimination and aggregation nodes	79
5.2.2. Generator coherency recognition	84
5.2.3. Aggregation of generating units	88
5.3. Dynamic external-subsystem-equivalent methods	100
5.4. Aggregation of distribution networks with distributed generation	102
Problems	105
References	108
6. Real-time modelling of power system	110
6.1. Determination of topology model	110
6.1.1. Bus section/circuit breaker topology model	110
6.1.2. Bus/branch topology model	111
6.1.3. Description of topology using incidence matrix	112
6.2. State estimation	113
6.2.1. Measurement data for state estimation	114
6.2.2. Bad data and topology errors in state estimation	114
6.3. Network observability	114
6.4. Bus load forecast factors	115
6.5. External network modelling	115
6.6. Penalty factors	116
6.7. Procedures utilizing results of real-time modelling	116
Problems	116
References	117
7. Weighted least squares power system state estimation	118
7.1. Linear least squareS estimation	118
7.2. Linear weighted least square estimation	119
7.3. Nonlinear weighted least square estimation	123
7.4. Power system state estimation	126
7.4.1. General description	126

7.4.2. Power system model for state estimation	128
Problems	135
References.....	137
8. Alternative formulation of the power system state estimation	139
8.1. Introduction.....	139
8.2. Decoupled formulation of WLS state estimation	139
8.3. Disadvantages of normal equation WLS estimation	141
8.3.2. Hybrid method.....	143
8.3.4. Equality-constrained WLS state estimation	144
8.3.5. Augment matrix approach	145
8.5. Examples of matrices	148
8.5.1. Matrices for normal equation formulation.....	149
8.5.2. Matrices for alternative formulation of WLS estimation method.....	150
Problems	151
References.....	152
9. Network observability analysis.....	153
9.1. Introduction.....	153
9.2. The method based on the nodal model.....	154
9.2.1. Determining the unobservable branches.....	155
9.2.2. Determining the observable island	158
9.3. Topological observability analysis method.....	161
Problems	163
References.....	164
10. Bad data detection and identification	165
10.1. Introduction.....	165
10.2. Features of measurement errors	165
10.3. Types of measurements, bad data detectability and identifiability	166
10.4. Methods for bad data detection and identification	167
10.4.1. Use of χ^2 distribution for bad data detection in WLS state estimation.	167
10.4.2. Utilization of normalized residuals for bad data detection and identification in WLS state estimation	170
10.4.3. Hypothesis testing identification	171
References.....	175
11. Network parameter estimation. Topology error identification	176
11.1. Network parameter estimation	176
11.1.1. Introduction	176
11.1.2. Detection and identification of parameter errors.....	179
11.1.3. Estimation of network parameter	180
11.2. Topology error processing	185
11.2.1. Introduction	185
11.2.2. Characteristics of topology errors.....	186
11.2.4. Influence of topology error on state estimation.....	188
11.2.5. Methods for topology error detection and identification.....	190
11.2.6. Pre-estimation topology error detection and identification	191
11.2.7. Post-estimation topology error detection and identification.....	192
11.2.8. Substation configuration errors	196
Problems	200

References.....	200
12. State estimation using ampere measurements	202
12.1. Introduction.....	202
12.2. Modeling of ampere measurements	202
12.3. Observability analysis for power system with ampere measurements	208
12.3.1. Procedure based on the residual covariance matrix.....	209
12.3.2. Procedure based on the Jacobi matrix	211
12.3.3. Problem of bad data.....	213
Problems	213
References.....	214
13. Distribution power system state estimation – specific problems.....	215
13.1. Introduction.....	215
13.2. Distribution power network characteristic	215
13.3. Models of distribution power system components.....	216
13.3.1. Distribution system structure.....	216
13.3.2. Distribution line models	217
13.3.3. Static load models	218
13.3.4. Load pseudomeasurement estimation.....	221
13.4. Distribution power system state estimation methods	222
13.4.1. Node voltages-based state estimation.....	222
13.4.2. Branch currents-based state estimation	229
13.4.3. Estimation by backward-forward sweep load flow calculations	234
Problems	240
References.....	242
14. Estimation of loads in distribution system.....	244
14.1. Simple load estimation methods	244
14.2. Distribution state estimation based methods	245
14.2.1. Example of load estimation with the use of WLS estimation methods	245
14.3. Statistical load modelling technique	246
14.3.2. Example of statistical load estimation	247
14.4. Fuzzy set based methods.....	248
14.4.1. Application of a fuzzy regression model.....	248
14.4.2. Utilization of operator experience and expert knowledge	248
14.4.3. Application of neural network and fuzzy set techniques.....	249
14.5. Other methods for load estimation	249
14.6. Remarks on methods for load estimation	249
Problems	250
References.....	250

1. INTRODUCTION. GENERAL PRINCIPLES OF MODELLING.

In the most general sense a model is anything used in any way to represent anything else [1.1]-[1.5]. There are also other definitions of the term “model”, e.g.:

1. A model is a simplified representation used to explain the workings of a real world system or event.
2. A model is an object which we study, not for its intrinsic interest, but because it is a formalized or simplified representation of a class of phenomena which can be studied easily.

The reasons of building models are as follows:

1. A model helps us to understand problem.
2. A model makes easier finding possible ways of solving problem.
3. A model helps us to assess possible directions of activities.

The “goodness” of a model depends not on how well it might serve our purposes but on the degree to which it tells the truth.

It should be underlined that if a model is based upon observed data, especially physical data about the real world, then the model must be equally real.

To measure the validity (i.e. the reality) of a model, several criteria are established.

1.1. TYPES OF MODELS

One can distinguish the following types of models:

- concrete and abstract,
- physical and mathematical,
- descriptive and prescriptive,
- analogue and symbolic,

1.1.1. CONCRETE MODEL

A concrete model is a replica of reality.

1.1.2. ABSTRACT MODEL

An abstract model (in another words a conceptual model) is a model that uses ideas to represent other ideas.

The abstract model is:

- a synthetic presentation of the most essential elements of reality,

- a theoretical construct that represents something, with a set of variables and a set of logical and quantitative relationships between them,
- constructed to enable reasoning within an idealized logical framework about certain processes.

1.1.3. PHYSICAL MODEL

A physical model is a physical object that mimics the system.

1.1.4. MATHEMATICAL MODEL

A description of a system where the relationships are expressed in mathematical form is called as a mathematical model.

Classifying mathematical models, one can distinguish the following models:

- static and dynamic,
- deterministic and probabilistic,
- linear and nonlinear.

Static models

A static model presents reality at a specific time instant.

Dynamic models

A dynamic model describes the behaviour of reality in terms of how one qualitative state can turn into another.

Deterministic models

The deterministic model is a mathematical model in which outcomes are precisely determined through known relationships among states and events, without any room for random variation. In such models, a given input will always produce the same output.

Probabilistic models

A statistical (probabilistic) model is a set of mathematical equations which describe the behaviour of an object of study in terms of random variables and their associated probability distributions.

Linear models

If all the operators in a mathematical model exhibit linearity, such a model is called the linear model.

Notes:

The question of linearity and nonlinearity is dependent on context. Linear models may have nonlinear expressions in them.

Nonlinear models

In nonlinear models, some of the operators exhibit nonlinearity.

1.1.5. DESCRIPTIVE MODEL

A descriptive model is a physical, conceptual or mathematical model that describes situations as they are or as they actually appear.

1.1.6. PRESCRIPTIVE MODEL

A prescriptive model is a model that suggests what ought to be done (how things should work) according to some assumptions or standards.

1.1.7. ANALOGUE MODEL

An analogue model explains a phenomenon by reference to some other occurrence.

1.1.8. SYMBOLIC MODEL

Symbolic model contains mathematical symbols used to describe the status of variables at a given time and to define the manner in which they change and interact.

Symbolic models are constructed using either a natural or formal language.

1.2. CLASSIFICATION OF MODELS OF POWER SYSTEMS - DOMAIN POINT OF VIEW

The following models of power systems can be distinguished:

- phase and symmetrical component models,
- one- and three-phase models.

1.2.1. PHASE MODELS

A phase model is a representation of a power system in the natural phase coordinates.

1.2.2. SYMMETRICAL COMPONENT MODELS

A symmetrical component model describes a three-phase power system with use of 3 symmetrical sets of balanced phasors. These sets are the sets of:

- positive sequence components – ABC components,
- negative sequence components – CBA components,
- zero sequence components.

1.2.3. SINGLE PHASE MODELS

A single phase model is the one-phase representation of a three-phase power system.

1.2.4. THREE-PHASE MODELS

A three-phase model is the three-phase representation developed with strong reference to the physical structure of the equipment in actual three-phase power system. It should be underlined, that three-phase model is built for a power system exhibiting a considerable degree of geometric unbalance or load unbalance.

1.3. MODELLING

Modelling is the process of generating a model. Two models of the same phenomenon may be essentially different. It should be also stressed that users of a model need to understand the model's original purpose and the assumptions of its validity.

Modelling processes can be classified as follows:

- mathematical modelling,
- physical modelling

1.3.1. MATHEMATICAL MODELLING

The mathematical modelling is a process of developing a mathematical model. Mathematical modelling is the use of mathematics to:

- describe real-world phenomena,
- investigate important questions about the observed world,

- explain real-world phenomena,
- test ideas,
- make predictions about the real world.

The aim of mathematical modelling is not to produce the most comprehensive, descriptive model but to produce the simplest possible model that incorporates the major features of the phenomenon of interest.

A process of mathematical modelling is presented in the Fig. 1.1.

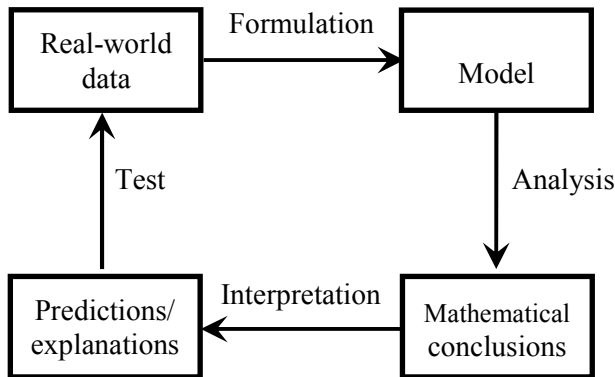


Fig. 1.1. Process of mathematical modelling.

1.3.2. PHYSICAL MODELLING

A typical procedure of physical modelling is cutting a system into subsystems and accounting for the behaviour at the interfaces.

It can be noted that physical modelling is also used for mathematical models built/structured in the same way as physical models. The considered modelling is very convenient for building reusable model libraries.

PROBLEMS

- 1.1. What do you mean by model?
- 1.2. What are the reasons for building models?
- 1.3. Bring out the differences between:
 - a) concrete vs. abstract models,
 - b) physical vs. mathematical models,
 - c) static vs. dynamic models,
 - d) deterministic vs. probabilistic models,
 - e) linear vs. nonlinear models,

- f) descriptive vs. prescriptive models,
 - g) analogue vs. symbolic models,
 - h) phase vs. symmetrical component models,
 - i) one- vs. three-phase models.
- 1.4. What do you mean by modelling? Describe one application of modelling in electrical power engineering.
- 1.5. Differentiate between mathematical and physical modelling.

REFERENCES

- [1.1] E.A. Bender, *An Introduction to Mathematical Modelling*. John Wiley & Sons, New York 1978.
- [1.2] B. S. Bennett, *Simulation Fundamentals*. Prentice-Hall, 1995.
- [1.3] A.M. Law, W.D. Kelton, *Simulation Modelling & Analysis*. McGraw-Hill, New York 1982.
- [1.4] J. Ledin, *Simulation Engineering*. CMP Books, 2001.
- [1.5] M. Pidd, *Systems Modelling: Theory and Practice*. John Wiley & Sons, 2004.

2. MODELS FOR STEADY STATE ANALYSES. SCOPE OF UTILIZATION

2.1. INTRODUCTION

Power system modelling bases on several assumptions: bus loads and branch power flows are three phase and balanced, all series and shunt devices are symmetrical in the three phase. These assumptions allow for a simplification of the three phase power system into single phase model. Nevertheless, these simplifications are fully substantiated because such modelling is accurate enough for steady state analyses of power system [2.1]-[2.5]. Furthermore all network data are expressed in the per-unit system. In order to convert into the per-unit system it is necessary to assume one base apparent power S_b for a whole power system and the base voltage V_b for an individual level of transformation. The remaining base values as the base current I_b , the base impedance Z_b or the base admittance can be obtained in the following way [2.5]:

$$Z_b = \frac{V_b^2}{S_b}, \quad Y_b = \frac{1}{Z_b}, \quad I_b = \frac{S_b}{\sqrt{3}V_b}. \quad (2.1)$$

2.2. BASIC COMPONENTS FOR STEADY STATE ANALYSIS

2.2.1. TRANSMISSION LINES

Transmission lines are described by the equivalent Π -circuit which is defined by two complex parameters: the series impedance \underline{Z}_{km} , and the shunt admittance \underline{Y}_{sh} , where:

$$\begin{aligned} \underline{Z}_{km} &= \underline{Z}_{mk} = R_{km} + jX_{km}, \\ \underline{Y}_{km} &= \underline{Z}_{km}^{-1} = \frac{1}{R_{km} + jX_{km}}, \\ \underline{Y}_{sh} &= G_{sh} + jB_{sh}. \end{aligned} \quad (2.2)$$

Series elements represent resistance and reactance of line. Shunt elements are related with discharge and capacity between lines and ground. All parameters for a transmission line are positive. Sometimes, transmission line is modelled with the use of only the series branch. Expression of line parameters in terms of per-unit can be made in the following way.

$$\begin{aligned}
 \underline{Z}_{km(pu)} &= \underline{Z}_{km} / Z_b \\
 \underline{Y}_{km(pu)} &= \underline{Z}_{km}^{-1} \cdot Z_b \cdot \\
 \underline{Y}_{sh(pu)} &= \underline{Y}_{sh} \cdot Z_b
 \end{aligned}
 \tag{2.3}$$

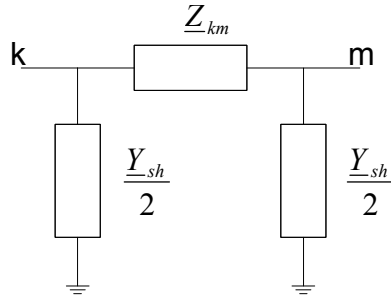


Fig. 2.1. Two port Π -model of transmission line

2.2.2. TRANSFORMERS

Two winding transformers

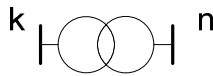


Fig. 2.2. Two winding transformer

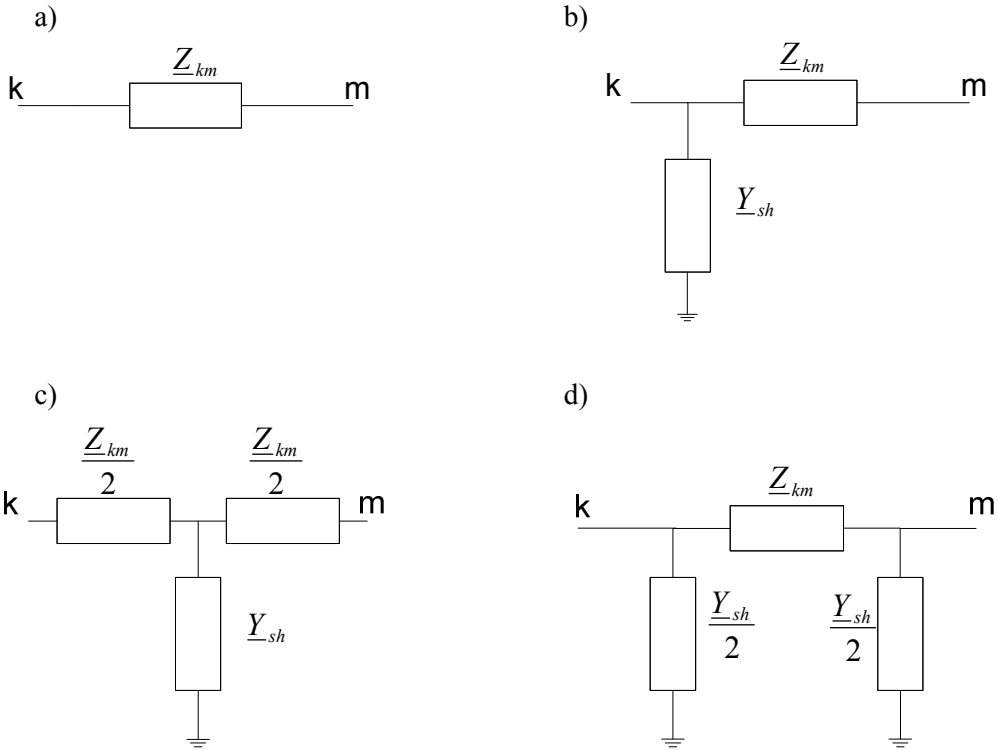


Fig. 2.3. Equivalent circuit for a transformer
 a) the model without shunt elements b) the Γ -model c) the T-model d) the Π -model.

$$Z_{km} = \frac{v_k}{100} \frac{V_N^2}{S_N}, \quad R_{km} = \frac{\Delta P_{Cu}}{S_N} \frac{V_N^2}{S_N}, \quad X_{km} = \sqrt{Z^2 - R^2}, \quad (2.4)$$

$$G_{sh} = \frac{\Delta P_{Fe}}{V_N^2}, \quad B_{sh} = \frac{I_0}{100} \frac{S_N}{V_N^2}, \quad (2.5)$$

where: v_k – a rated value of the short circuit voltage in percentage terms,
 ΔP_{Cu} – total winding active losses,
 ΔP_{Fe} – total magnetic active losses,
 I_0 – an idle current in percent of the rated current of the transformer.

Equivalent parameters of transformers are related to a single phase. They can be related to the primary or secondary voltage and the nominal power of a transformer. In practical computations, these parameters are converted into the per-unit system. For the per-unit system above parameters can be calculated in the following way:

$$Z_{km(pu)} = \frac{v_k V_N^2}{100 S_N} \frac{1}{Z_b} = \frac{v_k V_N^2 S_b}{100 S_N V_N^2} = \frac{v_k S_b}{100 S_N}, \quad (2.6)$$

$$R_{km(pu)} = \frac{\Delta P_{Cu} V_N^2}{S_N S_N} \frac{1}{Z_b} = \frac{\Delta P_{Cu} V_N^2 \cdot S_b}{S_N S_N V_N^2} = \frac{\Delta P_{Cu} S_b}{S_N S_N}, \quad (2.7)$$

$$X_{km(pu)} = \sqrt{Z_{km(pu)}^2 - R_{km(pu)}^2}, \quad (2.8)$$

$$G_{sh(pu)} = \frac{\Delta P_{Fe}}{V_N^2 Y_b} = \frac{\Delta P_{Fe} V_N^2}{V_N^2 S_b} = \frac{\Delta P_{Fe}}{S_b}, \quad (2.9)$$

$$B_{sh(pu)} = \frac{I_0 S_N}{100 V_N^2 Y_b} = \frac{I_0 S_N V_N^2}{100 V_N^2 S_b} = \frac{I_0 S_N}{100 S_b}. \quad (2.10)$$

Three winding transformers

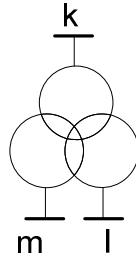


Fig. 2.4. The three winding transformer.

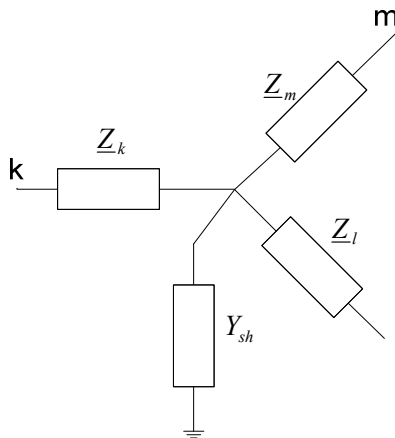


Fig. 2.5. The equivalent circuit for a three winding transformer.

Off-nominal tap transformers and phase shifters

Transformers with off-nominal taps and phase shifters can be modelled as an ideal transformer with complex tap $\underline{t}_{km} = t_{km} e^{j\theta_{km}}$ connected with two port circuit (Π -model, T-model or Γ -model) or series impedance when iron loss and magnetizing reactance is neglected. For practical usage Π -model seems to be the best choice. The following advantages can be enumerated:

- can be used to model also transmission line ($t_{km}=1$). It must be remembered that shunt susceptance, when it is considered, for transmission lines is positive and negative for transformers,
- proper arrangement of shunt reactors allows to build another model of transformers,
- proper arrangement of three of them and shunt reactors allows to model three winding transformer.

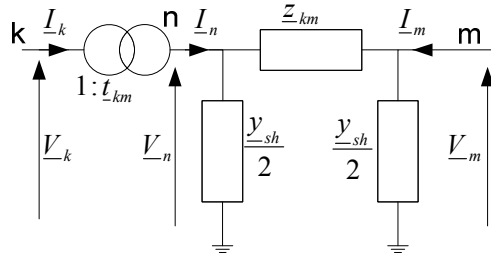


Fig. 2.6. The equivalent Π -circuit for an off-nominal tap transformer or a phase shifter

Series element represents power losses in the winding (real part) and flux leakage (imaginary part). Shunt branches represent iron loss (real part) and magnetizing reactance (imaginary part).

The nodal equations for the equivalent Π -circuit can be derived, using the following relationship with the current flows I_n and I_m :

$$\begin{bmatrix} \underline{I}_n \\ \underline{I}_m \end{bmatrix} = \begin{bmatrix} \underline{y}_{km} + \frac{\underline{y}_{sh}}{2} & -\underline{y}_{km} \\ -\underline{y}_{km} & \underline{y}_{km} + \frac{\underline{y}_{sh}}{2} \end{bmatrix} \begin{bmatrix} \underline{V}_n \\ \underline{V}_m \end{bmatrix}. \quad (2.11)$$

Substituting for \underline{I}_n and \underline{V}_n according to the formulae:

$$\begin{aligned} \underline{I}_n &= \underline{t}_{km}^* \cdot \underline{I}_k, \\ \underline{V}_n &= \underline{V}_k / \underline{t}_{km} \end{aligned} \quad (2.12)$$

we obtain the following relationship among I_k , I_m , V_k and V_m :

$$\begin{bmatrix} \underline{I}_k \\ \underline{I}_m \end{bmatrix} = \begin{bmatrix} \left(\underline{y}_{km} + \frac{\underline{y}_{sh}}{2} \right) / \underline{t}_{km}^2 & -\underline{y}_{km} / \underline{t}_{km}^* \\ -\underline{y}_{km} / \underline{t}_{km} & \underline{y}_{km} + \frac{\underline{y}_{sh}}{2} \end{bmatrix} \begin{bmatrix} \underline{V}_k \\ \underline{V}_m \end{bmatrix}. \quad (2.13)$$

The new relationships for parameters can be derived:

$$\underline{I}_{km} = -\underline{I}_k, \quad (2.14)$$

$$\underline{I}_{mk} = -\underline{I}_m, \quad (2.15)$$

$$\underline{y}_{km}^{tap} = \frac{\underline{y}_{km}}{\underline{t}_{km}^*}, \quad (2.16)$$

$$\underline{y}_{mk}^{tap} = \frac{\underline{y}_{km}}{\underline{t}_{km}}, \quad (2.17)$$

$$\underline{y}_{sh,k}^{tap} = \frac{\underline{y}_{sh}}{2 \cdot \underline{t}_{km}^2} + (1/\underline{t}_{km} - 1) \cdot \underline{y}_{km} / \underline{t}_{km}^*, \quad (2.18)$$

$$\underline{y}_{sh,m}^{tap} = \frac{\underline{y}_{sh}}{2} + (1 - 1/\underline{t}_{km}) \cdot \underline{y}_{km}. \quad (2.19)$$

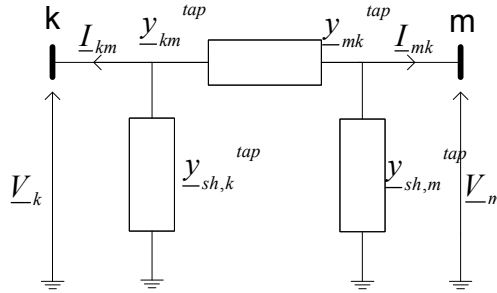


Fig. 2.7. The equivalent circuit of an off-nominal tap transformer or a phase shifter

2.2.3. SHUNT CAPACITORS AND REACTORS

Shunt capacitors or reactors control voltage and reactive power. They are modelled as shunt susceptance at the corresponding bus. Determination of type of shunt element

depends on sign of the susceptance. It will be positive for shunt capacitor and negative for reactor.

2.2.4. LOADS AND GENERATORS

Loads and generators are modeled as equivalent complex power injections. Therefore they are not represented in the network model.

2.3. BUILDING THE NETWORK MODEL

The above-described components can be used to build the model of power system. There are many alternative ways of describing power system to comply with Kirchhoff's laws. The most popular are mesh and nodal method. However the latter one has appeared to be more suitable for digital computer work.

The nodal method has the following advantages:

- very simple the numbering of nodes,
- easy data preparation,
- usually less variables and equations than with the mesh method,
- no difficulties for network crossover branches,
- parallel branches do not increase the number of variables or equations,
- node voltages are available directly from solution, and branch currents are easily calculated,
- off-nominal transformer taps can be easily presented.

Set of equations for power system according to the nodal method has the following form:

$$\mathbf{I} = \begin{bmatrix} I_1 \\ I_2 \\ \vdots \\ I_N \end{bmatrix} = \begin{bmatrix} Y_{11} & Y_{12} & \cdots & Y_{1N} \\ Y_{21} & Y_{22} & \cdots & Y_{2N} \\ \vdots & \vdots & \ddots & \vdots \\ Y_{N1} & Y_{N2} & \cdots & Y_{NN} \end{bmatrix} \cdot \begin{bmatrix} V_1 \\ V_2 \\ \vdots \\ V_N \end{bmatrix} = \mathbf{Y} \cdot \mathbf{V}, \quad (2.20)$$

where: I_k – the current injection phasor at the bus k ,
 V_k – the voltage phasor at the bus k ,
 Y_{km} – the (k,m) element of the admittance matrix \mathbf{Y} ,
 N – number of buses.

2.3.1. ADMITTANCE MATRIX

The admittance matrix \mathbf{Y} has the following properties:

- in general, it is complex, and can be written as $\mathbf{G} + j\mathbf{B}$,
- it is structurally symmetrical and numerical if there is no phase shifters in a power system,
- it is sparse,
- it is non-singular if each island of a power system has at least one shunt connection to the ground.

The admittance matrix is formulated in the following way:

$$\underline{Y}_{kk} = \sum_{m=1}^N \underline{y}_{km}^{tap} + \sum_{j=1}^M \underline{y}_{sh,kj}^{tap}, \quad (2.21)$$

$$\underline{Y}_{km} = -y_{km}^{tap} \quad k, m = 1, 2, \dots, N \quad k \neq m, \quad (2.22)$$

$$\underline{Y}_{mk} = -y_{mk}^{tap} \quad k, m = 1, 2, \dots, N \quad k \neq m, \quad (2.23)$$

where: M -number of shunt elements at the bus k .

Example 2.1

In Fig.2.8, the considered 4-bus power system is presented. Network data and the steady state bus voltages are listed below. The susceptance of the shunt capacitor at bus 3 is given as 0.5 p.u.

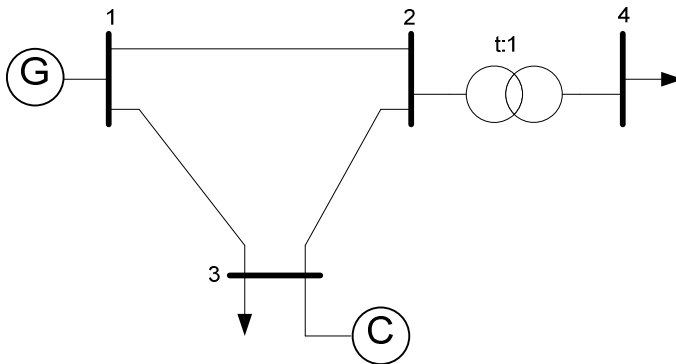


Fig. 2.8. One-line diagram of a 4-bus power system

The parameters of branches are given in Tab.2.1

Tab. 2.1. Data of considered power system

Bus k	Bus m	R p.u.	X p.u.	B p.u.	Tap
1	2	0.02	0.06	0.20	-
1	3	0.02	0.06	0.25	-
2	3	0.05	0.10	0.00	-
2	4	0.00	0.08	0.00	0.98

The admittance matrix for the considered system is:

$$\mathbf{Y} = \begin{bmatrix} 10.00 - j29.77 & -5.00 + j15.00 & -5.00 + j15.00 & 0 \\ -5.00 + j15.00 & 9.00 - j35.91 & -4.00 + j8.00 & j12.75 \\ -5.00 + j15.00 & -4.00 + j8.00 & 9.00 - j22.37 & 0 \\ 0 & j12.75 & 0 & -j12.50 \end{bmatrix}$$

2.3.2. VOLTAGE PHASOR

Voltage phasor can be considered in the polar and rectangular coordinate system. In the polar coordinate system, the bus voltage at the k -th bus is considered in the form $\underline{V}_k = V_k e^{j\delta_k}$ where V_k, δ_k – magnitude and phase angle of the voltage respectively.

In the rectangular coordinate system, $\underline{V}_k = e_k + jf_k$ where e_k, f_k – a real part and an imaginary part of the voltage, respectively.

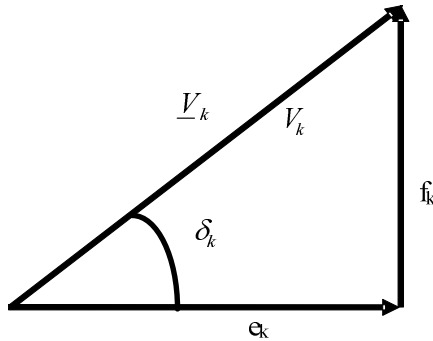


Fig. 2.9. The voltage phasor

2.3.3. POWER EQUATIONS

For the purposes of the steady states modelling, the following relationships for active and reactive power injections, active and reactive power flows and bus voltages can be derived (Fig. 2.7):

$$P_k - jQ_k = \underline{V}_k^* \mathbf{Y}_{row k} \mathbf{V}, \quad (2.24)$$

$$P_{km} - jQ_{km} = \left[-(\underline{y}_{sh,k}^{tap} + \underline{y}_{km}^{tap}) \quad \underline{y}_{km}^{tap} \right] \cdot \left[\underline{V}_k^2 \quad \underline{V}_m \cdot \underline{V}_k^* \right]^T, \quad (2.25)$$

$$P_{mk} - jQ_{mk} = \left[-(\underline{y}_{sh,m}^{tap} + \underline{y}_{mk}^{tap}) \quad \underline{y}_{mk}^{tap} \right] \cdot \left[\underline{V}_m^2 \quad \underline{V}_k \cdot \underline{V}_m^* \right]^T, \quad (2.26)$$

where: P_k, Q_k – an active injection and a reactive one at the k -th bus respectively;
 P_{km}, Q_{km} – an active power flow and a reactive power one between the k -th bus and the m -th one, respectively;
 y_{km}^{tap} – an admittance of the series branch connecting the k -th bus and the m -th one,
 $y_{sh,k}^{tap}$ – an admittance of the shunt branch at the k -th bus,
 $y_{sh,m}^{tap}$ – an admittance of the shunt branch at the m -th bus,
 $\mathbf{Y}_{row k}$ – the k -th row of an admittance matrix,

$$\mathbf{Y}_{row k} = \left[\underline{y}_{k1}, \underline{y}_{k2}, \dots, \underline{y}_{kN} \right], \quad (2.27)$$

$$\mathbf{V} = \left[\underline{V}_1, \underline{V}_2, \dots, \underline{V}_N \right]^T. \quad (2.28)$$

It must be noted that it is assumed convention that currents or power entering a bus is positive.

PROBLEMS

- 2.1. Build the admittance matrix for the power system from example 2.1 if a phase shifting transformer is used instead of the transformer between the buses 2 and 4. Assume that the phase shift is equal to 30 degrees.
- 2.2. Calculate all bus and branch powers in the power system from example 2.1 for the state vector shown in the Tab. P.2.1, if shunt parameters of branches (i) are considered, (ii) are not considered.

Tab. P.2.1. Elements of the state vector of an exemplary power system

bus no.	V , p.u.	δ , degrees
1	1.00	0
2	0.99	-1.72
3	0.97	-3.14
4	1.00	-2.86

REFERENCES

- [2.1] J. A. Momoh, *Electric Power System Application of Optimization Second Edition*. CRC Press, 2008.
- [2.2] A. Meier, *Electric Power Systems: A Conceptual Introduction*. John Wiley & Sons, INC., Hoboken, New Jersey 2006.
- [2.3] A. Abur, A. G. Exposito, *Power System State Estimation: Theory and Implementation*. Marcel Dekker, Inc, New York – Basel, 2004.
- [2.4] A. Monticelly, *State Estimation in Electric Power Systems: A Generalized Approach*, Massachusetts, Kluwer Academic Publisher, 1999.
- [2.5] Z. Kremens, M. Sobierajski, *Analiza systemów elektroenergetycznych*. WNT, Warszawa, 1996.

3. MODELS FOR TRANSIENT ANALYSES. SCOPE OF UTILIZATION

3.1. INTRODUCTION

Electromagnetic transient analysis (transients) plays very important role in power system operation studies. It provides valuable information on dynamic behavior of system resulting from various forms of transient phenomena. Transient phenomena in power systems are caused by change of power network configuration and parameters such as switching operations, faults, lightning strokes. When transients occur, the currents and voltages in some parts of the network may many times exceed their nominal values and may cause malfunction of power network equipment.

The changes of currents, voltages, power and energy during the transients are not instantaneous because the transient processes are attained by the interchange of energy stored in the magnetic field of inductances and the electrical field of capacitances. All transients vanish and, after that new steady-state operation point is established, i.e. transient describes the circuit behavior between two steady-states. It should be noted that in case of power system steady state operation system generation and loads change continuously and the power system never reaches steady-state mode – it operates in fact in quasi steady-state mode.

Mathematical description of electromagnetic transient has in general a form of set of first order differential equations based on Kirchhoff's laws describing circuit response containing resistances, inductions and capacities in presence of specified stimulus. Handling general formulation and analysis of the power networks is very complex due to interactions of electrical, mechanical and thermal phenomena.

Calculation by hand of electromagnetic transients for large scale power systems is practically very challenging or quite impossible. Since late third decade of the last century, power systems were modeled with use of their physical models called transient network analyzers. From the mid of 1960's the transient simulation with digital computers has become possible and pure analog transient network analyzers have been successively replaced by hybrid (analog-digital) or purely digital systems. First version of EMTP software was proposed by Dommel in early 1960's [3.4]. Today's transient simulation software packages are intensively developed, equipped with user friendly, visual "drag and drop" environment, are capable of graphically represent the results, export-import data in different formats etc. Key technical features concern on component library facilities with detailed element modeling, supporting of load flow and short-circuit studies, electric motors, protection devices, power electronics and FACTS simulations, flexible and adaptive simulation modes, time- and frequency (harmonic components) domain analyses etc. Moreover, various special modules and add-ons are offered as an extension of basic version. To the most popular simulation software one can be numbered: ATP-EMTP, PSCAD-EMTDC,

DigSILENT PowerFactory, Matlab Power System Blockset, PowerWorld Simulator, PSS/E.

Further part of the chapter concerns on characteristic of transient phenomena, discrete models of basic circuit elements, formulation and solution of network equations. A concise description power system equipment is also given in order to explain the way the network devices are modeled.

3.2. TRANSIENT PHENOMENA IN POWER SYSTEMS

Electric power system consists of large number of various elements operating for energy generation, transmission, distribution and consumption. In such complex and wide-area distributed system the great variety of transients can occur and they may affect not only single elements or small areas, but also entire system. From physical character point of view the following transient groups can be recognized:

- wave – involving electromagnetic wave propagation,
- electromagnetic – involving interaction between electric and magnetic field stored in power system,
- electromechanic – involving interaction between electrical energy stored in power system and energy generator rotor motion and oscillations,
- thermodynamic – involving control phenomena in thermal power plants.

To the most important electromagnetic transient phenomena one can recognize:

- switching phenomena caused by energization of lines, cables and transformers, capacitor and reactor switching, circuit breaker operation, sudden load changes, electrical motor startup, power electronic equipment operation etc.,
- faults, e.g. symmetrical and unsymmetrical faults, fault removing,
- transient stability, sub-synchronous resonance,
- lightning overvoltages, e.g. direct and indirect lightning strokes.

Electromagnetic transients in power network involve wide time duration from microseconds to minute (Fig. 3.1) and wide frequency range from DC to 50 MHz or even more. Modeling of power network components valid for such wide frequency range is impossible in practice. Therefore, the applied component models should correspond to the specific frequency range of certain transient phenomena.

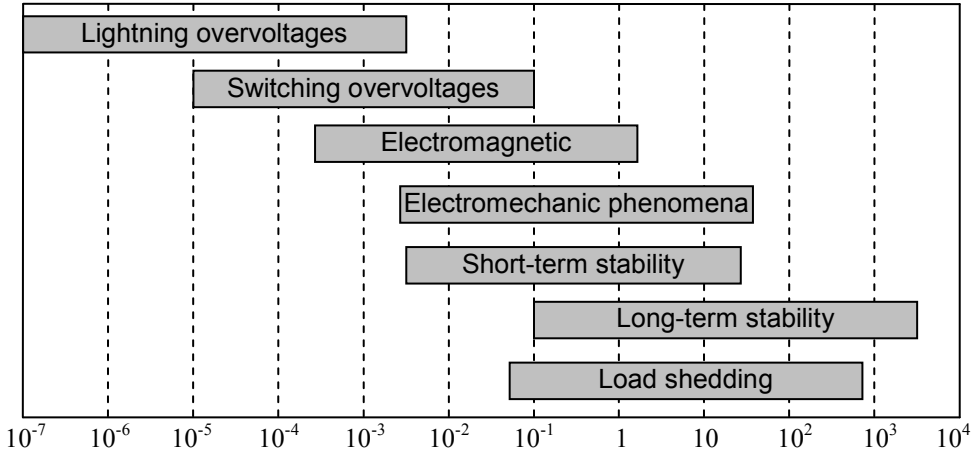


Fig. 3.1. Duration time (in. sec.) of some transient phenomena.

Tab. 3.1 contains brief overview of electromagnetic origins and their frequency ranges. Tab. 3.2 presents the frequency ranges of electrical transients which are classified into four groups with frequency ranges for which specific models of components can be stated.

Although time/frequency characteristic consideration for accurate power network representation is very important it is essential to recognize component non-linearities, to identify reliable model structure and parameters, to consider their mutual/distributed nature and frequency dependence.

3.3. DISCRETE MODELS OF ELECTRICAL NETWORKS

Transient calculations cannot be performed without applying digital computers except to the very simple circuits and with use of classical methods, e.g. Laplace transformations. Electrical variables in power networks are continuous, however, digital simulation is discrete in nature. One of the main problems in digital transient simulation is developing of appropriate models and methods applied for solution of differential and algebraic equations at discrete time instances.

3.3.1. DISCRETE MODELS OF BASIC ELECTRICAL COMPONENTS

Basic electrical component: resistors, capacitors and inductors need to be represented in discrete form for computer calculation of transient studies. These models are applied to formulate discrete model of electrical network suitable for solving by digital computer with the assumed integration rule and time step.

Tab. 3.1. Origin of electromagnetic transients and their frequency ranges [3.3].

Origin	Frequency
Transformer energization Ferroresonance	0,1 Hz – 1 kHz
Load rejection	0,1 Hz – 3 kHz
Fault clearing Fault initiation	50 Hz – 3 kHz 50 Hz – 20 kHz
Line energization Line reclosing	50 Hz – 20 kHz (DC) 50 Hz – 20 kHz
<i>Recovery voltage:</i> Terminal faults Short line faults	50 Hz – 20 kHz 50 Hz – 100 kHz
Multiple re-strikes of circuit breakers	10 kHz – 1 MHz
Lightning surges, Faults in substations	10 kHz – 1 MHz
Disconnecter switching and faults in gas insulated switchgear	100 kHz – 50 MHz

Tab. 3.2. Origin of electromagnetic transients and their frequency ranges [3.3].

Group	Frequency range	Time-domain characteristic	Representation for
I	0,1 Hz – 3 kHz	Low frequency oscillations	Temporary overvoltages
II	50 Hz – 20 kHz	Slow front surges	Switching overvoltages
III	10 kHz – 3 MHz	Fast front surges	Lightning overvoltages
IV	100 kHz – 50 MHz	Very fast front surges	Restrike overvoltages

Resistor is considered as static element and its representation is shown in Fig. 3.2.

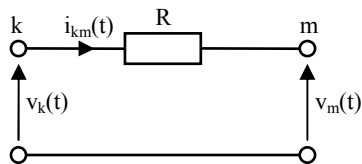


Fig. 3.2. Resistor representation.

Relation between current and voltages in time instance t can be described by equation

$$i_{km}(t) = \frac{1}{R}(v_k(t) - v_m(t)) \quad (3.1)$$

Capacitor and their Norton based representation is presented in Fig. 3.3.:

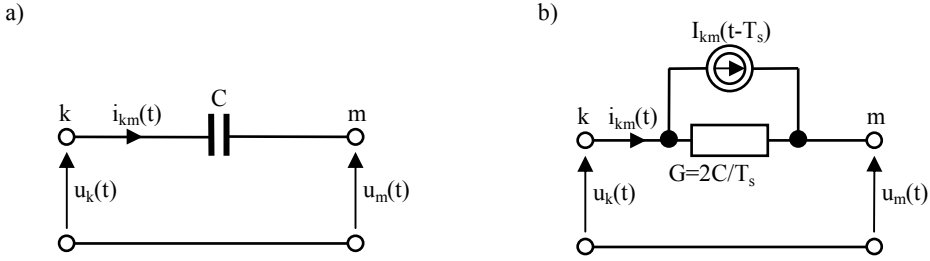


Fig. 3.3. Capacitor (a) and their equivalent circuit (b).

Differential equation describing relation between current and voltage is given by:

$$i_{km}(t) = C \frac{d(v_k(t) - v_m(t))}{dt}. \quad (3.2)$$

Assuming that $i_{km}(t-T_s)$, $v_k(t-T_s)$, $v_m(t-T_s)$ are known (from previous time step), the equation can be integrated for one step T_s :

$$v_k(t) - v_m(t) = v_k(t-T_s) - v_m(t-T_s) + \frac{1}{C} \int_{t-T_s}^t i_{km}(t) dt. \quad (3.3)$$

Applying trapezoidal integration rule one can obtain:

$$\int_{t-T_s}^t i_{km}(t) dt \approx \frac{1}{2} T_s (i_{km}(t) + i_{km}(t-T_s)). \quad (3.4)$$

If the values from preceding time steps are in $I_{km}(t-T_s)$, then:

$$i_{km}(t) = \frac{2C}{T_s} (v_k(t) - v_m(t)) + I_{km}(t-T_s) = G(v_k(t) - v_m(t)) + I_{km}(t-T_s), \quad (3.5)$$

where:

$$I_{km}(t-T_s) = -i_{km}(t-T_s) - \frac{2C}{T_s} (v_k(t-T_s) - v_m(t-T_s)), \quad (3.6)$$

is called current history term.

For inductance described by differential equation:

$$v_L = v_k(t) - v_m(t) = L \frac{di_{km}}{dt}. \quad (3.7)$$

Using similar rules as for capacitance, the current in branch with inductance is given by:

$$i_{km}(t) = \frac{T_s}{2L}(v_k(t) - v_m(t)) + I_{km}(t - T_s) = G(v_k(t) - v_m(t)) + I_{km}(t - T_s), \quad (3.8)$$

and history term:

$$I_{km}(t - T_s) = -i_{km}(t - T_s) - \frac{T_s}{2L}(v_k(t - T_s) - v_m(t - T_s)). \quad (3.9)$$

Norton equivalent circuit for inductance is presented in Fig. 3.4.

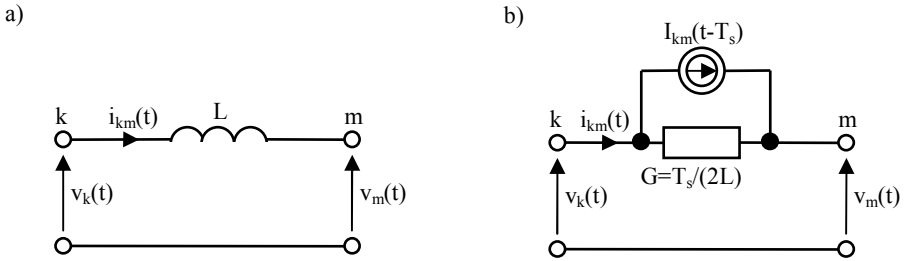


Fig. 3.4. Inductance (a) and their equivalent circuit (b).

Note that applying different integration rules is possible as shown in Tab. 3.3.

Tab. 3.3. Integration formulae for selected discrete integration methods.

Integration method	Capacity model		Induction model	
	G	History term	G	History term
Backward Euler	$\frac{C}{T_s}$	$-\frac{C}{T_s}v(t - T_s)$	$\frac{T_s}{L}$	$i(t - T_s)$
Trapezoidal	$\frac{2C}{T_s}$	$-\frac{2C}{T_s}v(t - T_s) - i(t - T_s)$	$\frac{T_s}{2L}$	$i(t - T_s) + \frac{T_s}{2L}v(t - T_s)$
Gear 2 nd order	$\frac{3C}{2T_s}$	$-\frac{2C}{T_s}v(t - T_s) - \frac{C}{2T_s}v(t - 2T_s)$	$\frac{2T_s}{3L}$	$\frac{4}{3}i(t - T_s) - \frac{1}{3}i(t - 2T_s)$

3.4. NON LINEAR AND TIME VARYING ELEMENTS MODELING

Electrical power networks contain various types of nonlinear elements. The most common are nonlinear inductances representing saturation and hysteresis effects in transformer and reactor cores, nonlinear resistances of surge arresters, time varying resistances of electrical arc. The network contains usually relatively small number of nonlinear elements. Hence methods used for linear networks are adopted to find the solution.

Several modifications have been presented to handle with nonlinear and time varying elements. There are based on a current source representation, piecewise-linear approximation or the compensation method.

With use of compensation method nonlinear elements are represented by current injections. Compensation theory states that the branch with non-linear element can be excluded from the network and simulated as a current source connecting nodes k and m if the non-linear element is considered as load (Fig. 3.5a).

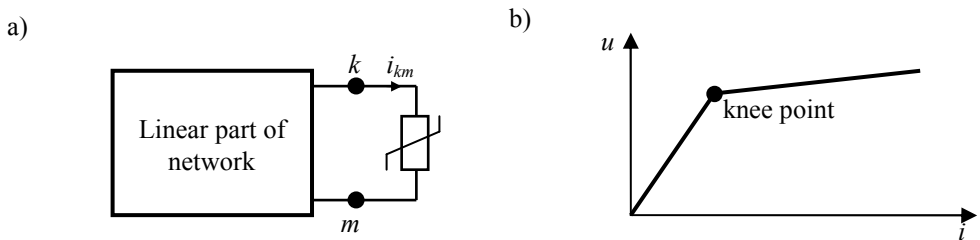


Fig. 3.5. Representing of nonlinear elements: compensation method (a), piecewise linear approximation (b).

First, the solution of the network without nonlinear element is found according to equation:

$$v_{km} = v_{km(0)} - R_{Thev} i_{km}, \quad (3.10)$$

and next, the characteristic of nonlinear element:

$$v_{km} = f\left(i_{km}, \frac{di_{km}}{dt}, t, \dots\right), \quad (3.11)$$

where: $v_{km(0)}$ – voltage across nodes k and m without nonlinear element,
 R_{Thev} – Thevenin equivalent resistance.

Iterative algorithm, e.g. Newton's method is used to find the solution in this step. The compensation method can be used to solve networks with several nonlinear elements, if one nonlinear element is connected to the node.

Piecewise approximation is often used for representation of saturation effect of magnetic cores (Fig. 3.5b). The solution method is linear, but the conductance of element should be changed once the voltage exceeds the knee point.

Formulation and solution of node equations

After replacing network components by Norton equivalents, for network with n nodes the system of n equations can be formed:

$$\mathbf{G}\mathbf{v}(t) = \mathbf{i}(t) - \mathbf{I}_H, \quad (3.12)$$

where: \mathbf{G} – a nodal conductance matrix (size $n \times n$),

$\mathbf{v}(t)$ – a vector of node voltages (size $1 \times n$),

$\mathbf{i}(t)$ – a vector of nodal current source injections (size $1 \times n$),

\mathbf{I}_H – a vector of current history terms (size $1 \times n$).

Some of nodes have known voltages because voltage sources connected to node are grounded (zero potential). The equation (3.12) is rearranged and partitioned into sets with unknown node voltages (A) and known node voltages (B):

$$\begin{bmatrix} \mathbf{G}_{AA} & \mathbf{G}_{AB} \\ \mathbf{G}_{BA} & \mathbf{G}_{BB} \end{bmatrix} \begin{bmatrix} \mathbf{v}_A(t) \\ \mathbf{v}_B(t) \end{bmatrix} = \begin{bmatrix} \mathbf{i}_A(t) \\ \mathbf{i}_B(t) \end{bmatrix} - \begin{bmatrix} \mathbf{I}_{HA} \\ \mathbf{I}_{HB} \end{bmatrix} = \begin{bmatrix} \mathbf{I}_A \\ \mathbf{I}_B \end{bmatrix}. \quad (3.13)$$

The unknown voltages are calculated from:

$$\mathbf{G}_{AA} \mathbf{v}_A(t) = \mathbf{i}_A(t) - \mathbf{I}_{HA} - \mathbf{G}_{AB} \mathbf{v}_B(t) = \mathbf{I}_A - \mathbf{G}_{AB} \mathbf{v}_B(t), \quad (3.14)$$

and currents flowing through voltage sources can be calculated using:

$$\mathbf{G}_{BA} \mathbf{v}_A(t) + \mathbf{G}_{BB} \mathbf{v}_B(t) + \mathbf{I}_{HB} = \mathbf{i}_B(t). \quad (3.15)$$

The set of the linear equations can be solved in efficient way by triangular factorization of the augmented matrix \mathbf{G}_{AA} . The computation algorithm is as follows:

1. Building matrices \mathbf{G}_{AA} and \mathbf{G}_{BB} . Triangularization of \mathbf{G}_{AA} using e.g. Gauss elimination technique.
2. In each time step the vector on right-hand side of (3.15) is updated from known history terms and known current and voltage sources.
3. The system of linear equations is solved for $\mathbf{v}_A(t)$, using transformation during the triangularized matrix \mathbf{G}_{AA} . In this iteration process the symmetry of the matrix is exploited, i.e. the same triangularized matrix used for downward operations is also used in the back substitution.
4. Updating the history terms \mathbf{I}_{HA} and proceeding next time step.

The described algorithm steps are presented in Fig. 3.6 for better clarity.

In case of three phase representation the single element of \mathbf{G} matrix is replaced by 3×3 submatrix. Current and voltage vector elements are replaced by vector of three elements corresponding to the certain phases.

Example 3.1

To illustrate the network solution algorithm transient response for step voltage for simple RLC circuit shown in Fig. 3.7a will be calculated for 2 time points using

trapezoidal integration rule. Transient calculations run with time step $T_s = 0,1$ ms and zero initial conditions, i.e. capacitor voltage and induction current at $t=0$ are equal to zero. The circuit parameters: $E=100$ V, $R=4$ Ω , $L=1$ mH, $C=100$ μ F.

The Norton equivalent of the circuit is shown in Fig. 3.7b. Voltage source is converted to the Norton equivalent (current source with resistance in parallel).

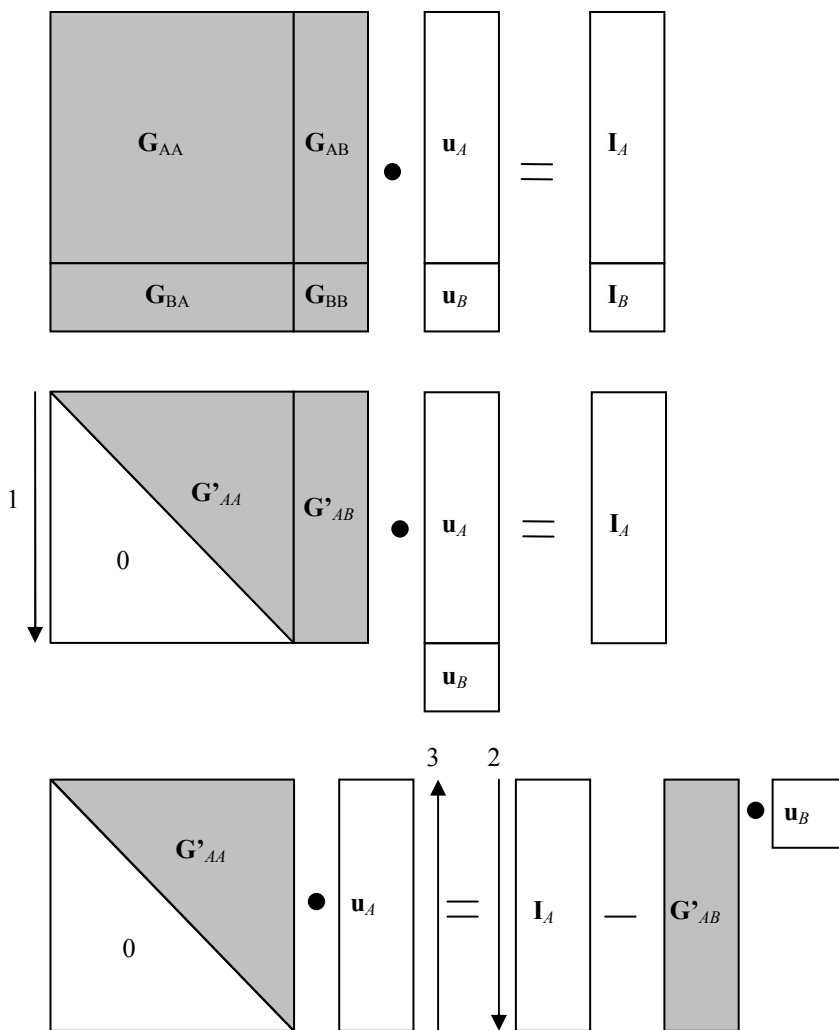


Fig. 3.6. Steps of transient solution algorithm:
1 – triangular factorization, 2 – forward reduction, 3 – backward substitution

According to Norton equivalent scheme (Fig. 3.7b) the nodal equations can be formulated as:

$$\begin{bmatrix} G_R + G_L & -G_L \\ -G_L & G_L + G_C \end{bmatrix} \begin{bmatrix} v_1 \\ v_2 \end{bmatrix} = \begin{bmatrix} G_{11} & G_{12} \\ G_{21} & G_{22} \end{bmatrix} \begin{bmatrix} v_1 \\ v_2 \end{bmatrix} = \begin{bmatrix} i_{10} \\ 0 \end{bmatrix} - \begin{bmatrix} I_{h12} \\ I_{h20} \end{bmatrix}, \quad (3.16)$$

where: $G_R = \frac{1}{R}$, $G_L = \frac{T_s}{2L}$, $G_C = \frac{2C}{T_s}$.

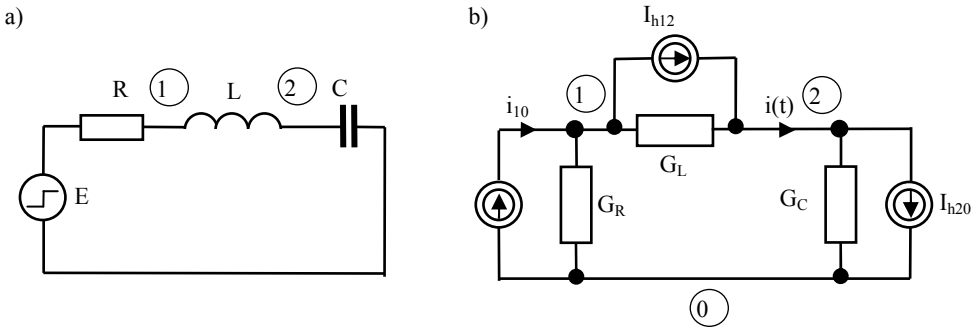


Fig. 3.7. Simple RLC circuit (a) and their equivalent (b).

The result of nodal conductance matrix building:

$$G = \begin{bmatrix} 0.3 & -0.05 \\ -0.05 & 2.05 \end{bmatrix}.$$

Calculations for $t = T_s$

The extended conductance matrix (matrix is extended by vector $\begin{bmatrix} i_{10} \\ 0 \end{bmatrix} - \begin{bmatrix} I_{h12} \\ I_{h20} \end{bmatrix}$):

$$\left[\begin{array}{cc|c} 0.3 & -0.05 & 25 \\ -0.05 & 2.05 & 0 \end{array} \right]$$

Applying Gauss elimination technique to triangularize the matrix:

- division of first row by G_{11} ,
- multiplying of first row by $-G_{21}$ and adding it to the second row, gives the following result:

$$\left[\begin{array}{cc|c} 1 & -0.016 & 83.333 \\ 0 & 2.041 & 4.166 \end{array} \right]$$

c) node voltages $v_1(T_s)$ and $v_2(T_s)$ calculated by backward substitution:

$$v_2(T_s) = \frac{4.166}{2.041} = 2.041 \text{ V},$$

$$v_1(T_s) = 0.016v_2(T_s) + 83.333 = 0.016 \cdot 2.041 + 83.333 = 83.673 \text{ V},$$

d) current flowing in the circuit:

$$i(T_s) = G_L(v_1(T_s) - v_2(T_s)) = 0.05(83.673 - 2.041) = 4.082 \text{ A}$$

The same result is obtained with use of:

$$i(T_s) = G_C(v_2(T_s)) = 2.0(2.041) = 4.082 \text{ A}.$$

Calculations for $t = 2T_s$

The updated values of current history terms:

$$I_{h12}(T_s) = i_{12}(T_s) + G_L(v_1(T_s) - v_2(T_s)) = 8.163 \text{ A},$$

$$I_{h20}(T_s) = -i_{20}(T_s) + G_C(v_2(T_s)) = -8.163 \text{ A}.$$

and updated current vector $\begin{bmatrix} i_{10}(T_s) \\ 0 \end{bmatrix} - \begin{bmatrix} I_{h12}(T_s) \\ I_{h20}(T_s) \end{bmatrix} = \begin{bmatrix} 25 \\ 0 \end{bmatrix} - \begin{bmatrix} 8.163 \\ -8.163 \end{bmatrix} = \begin{bmatrix} 16.836 \\ 8.163 \end{bmatrix}$.

Applying Gauss elimination to the extended matrix:

$$\left[\begin{array}{cc|c} 0.3 & -0.05 & 16.836 \\ -0.05 & 2.05 & 8.163 \end{array} \right],$$

i.e. division of first row by G_{11} , multiplying of first row by $-G_{21}$ and adding it to the second row gives the node voltages:

$$v_2(2T_s) = 9.371 \text{ V and } v_1(2T_s) = 57.684 \text{ V}$$

The circuit current value:

$$i(T_s) = G_L(v_1(T_s) - v_2(T_s)) + I_{h12}(T_s) = 0.05(57.684 - 9.371) + 8.163 = 10.579 \text{ A}$$

The analytical solution for current obtained from inverse Laplace transform gives:

$$i(t) = \frac{50\sqrt{6}}{3} \sin(1000\sqrt{6}t) \exp(-2000t) \quad (3.17)$$

The comparison between discrete and exact values of circuit current is given in the table below.

t, ms	$i(t)$, A	
	discrete value	exact value
0.1	4.082	8.105
0.2	10.579	12.876

3.5. MODELS OF POWER SYSTEM COMPONENTS

3.5.1. INTRODUCTION

An accurate simulation of transient phenomenon requires a representation of network components valid for a very wide frequency range (from DC to several MHz). An acceptable representation of each component throughout this frequency range is usually impossible in practice. This chapter discusses modeling of the most important network components - overhead lines, insulated cables, transformers, arresters, network equivalents, rotating machines, circuit breakers. Their frequency-dependent behavior is considered.

3.5.2. OVERHEAD TRANSMISSION LINES AND CABLES

In general two main model types of overhead lines for time-domain simulations are used: lumped parameters and distributed parameters models. The selection of the model depends on line length and range of frequency to be simulated.

Lumped parameter models are stated for one, usually fundamental frequency and they are suitable for steady-state simulations or for frequencies similar to fundamental frequency. However, much more adequate models for transient analysis are with distributed nature and frequency dependence of parameters.

The common rule for selecting the transmission line model is relation between wave travel time τ_l over line and simulation time step T_s . If $\tau_l < T_s$ then lumped parameter, usually π -section model assumed. Otherwise the frequency depended model should be selected. If the data describing line geometry are not available the Bergeron model can be used.

The general guideline for modeling of power lines in different frequency ranges is presented in Tab. 3.4.

Lumped parameter models

The most common lumped parameter model of transmission lines is nominal (coupled) model, as shown in Fig. 3.8. It should be underlined that it is valid only for fundamental frequency.

An approximation for the distributed nature of a transmission line parameters is also possible by representing of line as an interconnection of many lumped parameter identical sections. Each section can be in form of π , T or Γ equivalent and contains series resistance, series inductance and shunt capacitance (shunt conductance is usually neglected). The parameters of each section are obtained by dividing total R , L , C line parameters by number of sections. The impedance parameters are usually available for typical conductor types and their geometrical configuration.

Tab. 3.4. Guideline for overhead line modeling [3.3].

Topic	0.1 Hz-3kHz	50 Hz-20 kHz	10 kHz-3 MHz	100 kHz-50 MHz
Representation of transposed lines	Lumped parameters multi-phase π circuit	Distributed parameter multi-phase model	Distributed parameter multi-phase model	Distributed parameters single phase model
Line asymmetry	Important	Capacitive asymmetry is important, inductive is important, except for statistical studies, for which it is negligible	Negligible for single-phase simulations, others	Negligible
Frequency dependent parameters	Important	Important	Important	Important
Corona effect	Important if phase conductor voltages can exceeded the corona inception voltage	Negligible	Very important	Negligible

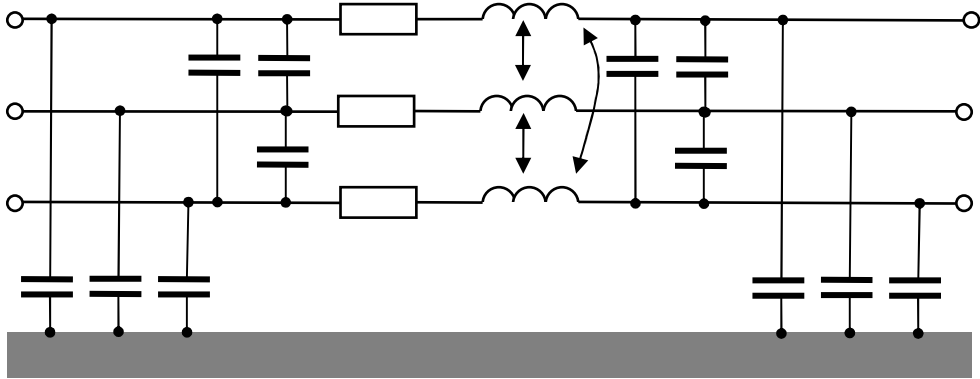


Fig. 3.8. Nominal π coupled model of transmission line.

Linear, lumped parameter networks containing resistors, capacitors, inductors, and voltage and current sources can be represented by the following system of first-order ordinary differential equations and a set of output equations written in the form of state space formulation:

$$\begin{aligned} \dot{\mathbf{x}} &= \mathbf{Ax} + \mathbf{Bu}, & \mathbf{x}(0) &= \mathbf{x}_0, \\ \mathbf{y} &= \mathbf{Cx} + \mathbf{Du}, \end{aligned} \quad (3.18)$$

where: \mathbf{x} – a state vector;

$$\mathbf{A} = \begin{bmatrix} a_{11} & a_{12} & \dots & a_{1n} \\ \vdots & & & \\ a_{n1} & a_{n2} & \dots & a_{nm} \end{bmatrix};$$

$$\mathbf{B} = \begin{bmatrix} b_{11} & b_{12} & \dots & b_{1m} \\ \vdots & & & \\ b_{n1} & b_{n2} & \dots & b_{nm} \end{bmatrix};$$

$$\mathbf{C} = \begin{bmatrix} c_{11} & c_{12} & \dots & c_{1n} \\ \vdots & & & \vdots \\ c_{n1} & c_{n2} & \dots & c_{nm} \end{bmatrix};$$

$$\mathbf{D} = \begin{bmatrix} d_{11} & d_{12} & \dots & d_{1m} \\ \vdots & & & \vdots \\ d_{n1} & d_{n2} & \dots & d_{nm} \end{bmatrix};$$

\mathbf{x}_0 – a vector of initial values;

\mathbf{u} – an excitation vector;

\mathbf{y} – an output vector.

In these equations the state vector \mathbf{x} contains some of the capacitor voltages and inductor currents. Matrices \mathbf{A} , \mathbf{B} , \mathbf{C} , and \mathbf{D} are the constant real matrices with proper dimensions, and their entries depend on the values of the lumped parameters of the network.

The solution in state space equation is given by:

$$\mathbf{x} = e^{\mathbf{A}t} \int_0^t e^{-\mathbf{A}\tau} \mathbf{B} \mathbf{u} d\tau + e^{\mathbf{A}t} \mathbf{x}(0). \quad (3.19)$$

Square matrix \mathbf{A} is called system matrix and $e^{\mathbf{A}t}$ is transient matrix defined as:

$$e^{\mathbf{A}t} = \mathbf{I} + \mathbf{A}t + \frac{1}{2!}(\mathbf{A}t)^2 + \dots + \frac{1}{n!}(\mathbf{A}t)^n + \dots \quad (3.20)$$

For digital analysis the discrete form of state variable equations is suitable. As a result state variable values in discrete time instances are obtained.

Assuming that $t = kT_s$, $k = 0, 1, 2$, the discrete approximation of equation 3.19 by trapezoidal rule gives:

$$\mathbf{x}((k+1)T_s) = \left(\mathbf{I} - \frac{T_s}{2} \mathbf{A} \right)^{-1} \left(\mathbf{I} + \frac{T_s}{2} \mathbf{A} \right) \mathbf{x}(kT_s) + T_s \mathbf{B} \mathbf{u}(kT_s), \quad (3.21)$$

Fig. 3.9 shows the line model represented by connection of identical sections with n state variables. Assuming the capacitor voltages and inductor currents state matrix \mathbf{A} has form:

-R/L	-1/L										
1/C		-1/C									
	1/L	-R/L	-1/L								
		1/C		-1/C							
...
								1/C	-1/C		
								1/L	-R/L	-1/L	
									1/C		

Note that only non zero terms are presented.

Column vector \mathbf{B} with n terms relating input (voltage at the beginning node) with state variables has the form:

$$\mathbf{B} = [1/L \ 0 \ 0 \ \dots \ 0]^T.$$

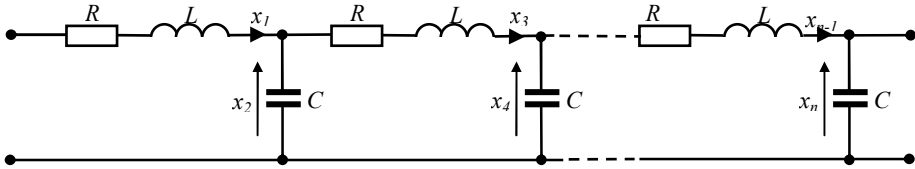


Fig. 3.9. Lumped parameter section transmission line model.

Line models with distributed parameters

Fig. 3.10 shows small length section of transmission line with single conductor parallel to ground.

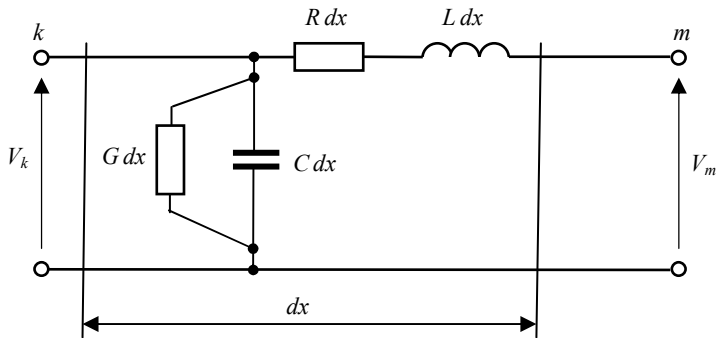


Fig. 3.10. Section of power transmission line with distributed parameters.

Equations describing line currents and voltages in the time domain are as follows:

$$-\frac{\partial v(x,t)}{\partial x} = R' i(x,t) + L' \frac{\partial i(x,t)}{\partial t},$$

$$-\frac{\partial i(x,t)}{\partial x} = G' v(x,t) + C' \frac{\partial v(x,t)}{\partial t},$$

where: $v(x,t)$ – the line voltage;

$i(x,t)$ – the line current;

R', L', G', C' – line parameters per unit length.

The single phase lossless transmission line (resistances R and shunt G conductances are neglected) can be described with use of partial differential equation:

$$-\frac{\partial v(x,t)}{\partial x} = L' \frac{\partial i(x,t)}{\partial t}, \quad (3.22)$$

$$-\frac{\partial i(x,t)}{\partial x} = C' \frac{\partial v(x,t)}{\partial t}, \quad (3.23)$$

The general solution of the equations gives:

$$i(x,t) = f_1(x - \varpi t) + f_2(x + \varpi t), \quad (3.24)$$

$$v(x,t) = Z_c f_1(x - \varpi t) - Z_c f_2(x + \varpi t), \quad (3.25)$$

where: $f_1(x - \varpi t)$, $f_2(x + \varpi t)$ - arbitrary functions representing wave traveling at velocity ϖ in a forward and backward direction respectively;

$Z_c = \sqrt{\frac{L'}{C'}}$ - a surge (characteristic) impedance;

$\varpi = \frac{1}{\sqrt{L'C'}}$ a phase velocity.

Multiplying equation (3.24) by Z_c and inserting into equation (3.25) yields:

$$v(x,t) + Z_c i(x,t) = 2Z_c f_1(x - \varpi t), \quad (3.26)$$

$$v(x,t) - Z_c i(x,t) = -2Z_c f_2(x + \varpi t). \quad (3.27)$$

Line propagation velocity is equal to:

$$\tau = \frac{d}{\varpi} = d\sqrt{L'C'}, \quad (3.28)$$

where: d - a length of the transmission line.

Hence

$$v_k(t - \tau) + Z_c i_{km}(t - \tau) = v_m(t) + Z_c (-i_{km}(t)). \quad (3.29)$$

Rearranging equation 3.29 one can obtain:

$$i_{mk}(t) = \frac{1}{Z_c} v_m(t) + I_m(t - \tau). \quad (3.30)$$

History term is given by:

$$I_m(t - \tau) = -\frac{1}{Z_c} v_k(t - \tau) - i_{km}(t - \tau). \quad (3.31)$$

Current at the node k is:

$$i_{km}(t) = \frac{1}{Z_c} v_k(t) + I_k(t - \tau), \quad (3.32)$$

and the current history term is as follows:

$$I_k(t - \tau) = -\frac{1}{Z_c} v_m(t - \tau) - i_{mk}(t - \tau). \quad (3.33)$$

Fig. 3.11 presents the two-port model. There is no direct impedance connection among nodes k and m . The characteristic impedances and equivalent current sources are connected to the terminals. Current supplied by current source at node k at time instance t depends on the current and voltage at $(t - \tau)$ at the node m and similarly current supplied by source at node m at time t depends on the current and voltage at $(t - \tau)$ at the node k . It should be underlined that wave propagation time τ differs from the multiple of integration time step. History terms of currents of the actual traveling time are interpolated to give the correct traveling time. The presented basic transmission line model is called Bergeron model.

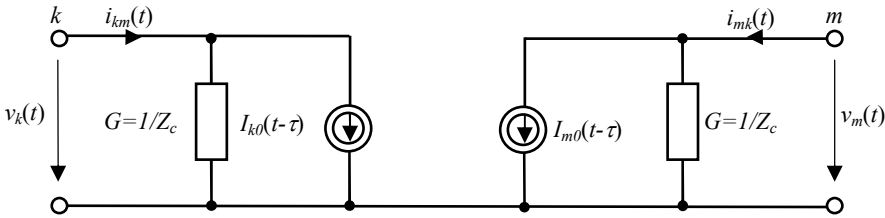


Fig. 3.11. The Bergeron model of a power transmission line.

To decouple multiphase line matrix equations the modal theory is applied. The diagonal matrices are then obtained and each mode can be analyzed independently as a single phase line.

Frequency depended models

Multiconductor transmission line is characterized in frequency domain by the following equations:

$$-\frac{d\mathbf{V}_x(\omega)}{dx} = \mathbf{Z}(\omega)\mathbf{I}_x(\omega), \quad (3.34)$$

$$-\frac{d\mathbf{I}_x(\omega)}{dx} = \mathbf{Y}(\omega)\mathbf{V}_x(\omega), \quad (3.35)$$

where: $\mathbf{Z}(\omega)$, $\mathbf{Y}(\omega)$ – the series impedance and the shunt admittance matrices.

The impedance matrix is complex and symmetric:

$$\mathbf{Z}(\omega) = \mathbf{R}(\omega) + j\omega\mathbf{L}(\omega), \quad (3.36)$$

and their component are frequency dependent.

The shunt admittance is equal to:

$$\mathbf{Y}(\omega) = \mathbf{G} + j\omega\mathbf{C}(\omega). \quad (3.37)$$

Note, that $\mathbf{Z}(\omega)$ and $\mathbf{Y}(\omega)$ are $n \times n$ matrices where n is the number of quantities describing conductors. Line shunt conductance \mathbf{G} is usually neglected for overhead line models.

The relationships among voltages and current at line terminals are as follows:

$$\begin{bmatrix} V_k(\omega) \\ I_{km}(\omega) \end{bmatrix} = \begin{bmatrix} \cosh(\gamma(\omega)l) & Z_c \sinh(\gamma(\omega)l) \\ \frac{1}{Z_c} \sinh(\gamma(\omega)l) & \cosh(\gamma(\omega)l) \end{bmatrix} \begin{bmatrix} V_m(\omega) \\ -I_{mk}(\omega) \end{bmatrix} \quad (3.38)$$

where: $Z_c = \sqrt{\underline{Z}'(\omega)/\underline{Y}'(\omega)}$ – a characteristic impedance;

$\gamma = \underline{Z}'(\omega)\underline{Y}'(\omega)$ – a propagation constant;

l – a total line length;

$\underline{Z}'(\omega)$ – a line impedance specified per unit length;

$\underline{Y}'(\omega)$ – a line admittance specified per unit length.

If the detailed power line configuration is available EMTP program are usually capable of computing the line parameters with use of line input data:

- (x,y) coordinates of each conductor and shield wire,
- bundle size and spacing,
- sag of phase conductors and protecting wires,
- phase rotation at transposition structures,
- physical dimensions of each conductor,
- resistance or resistivity of conductors and shield wires,
- ground resistivity of the ground return path.

Other data used for line modeling in frequency domain:

- lumped-parameter equivalent or nominal π -circuits at the specified frequency,
- constant distributed-parameter model at the specified frequency,
- frequency-dependent distributed parameter model, fitted for a given frequency range,
- capacitance or the susceptance matrix,
- series impedance matrix,

- resistance, inductance, and capacitance per-unit length for zero and positive sequences, at a given frequency or for the specified frequency range,
- surge impedance, attenuation, propagation velocity, and wavelength for zero and positive sequences, at a given frequency or for a specified frequency range.

Overhead line parameters are derived from the forms of Carson or Schellcunoff equations.

It is generally impossible to obtain a closed-form time-domain solution for a general input signal waveform. Therefore, a numerical frequency to time domain transformation is used. It should be underlined that line model in frequency domain is used only for model parameter and transformation determination. Modeling algorithm is the same as in case of losses line with included resistance.

Most of the EMTP programs are also capable of calculating the cable line parameters. Similarly to overhead lines, the basic equations describing cable line are described by equations (3.37) and (3.38). \mathbf{Z} and \mathbf{Y} parameters are calculated with used of cable geometry and material properties such as:

- (x, y) coordinates of each conductor;
- radius of each conductor,
- burial depth of cable system,
- resistivity and permeability of all conductors and surrounding medium,
- permittivity of cable insulation.

The way of transient computation is then similar as in case of overhead lines.

3.5.3. TRANSFORMERS

The modeling of transformer should take into consideration various physical phenomena appearing during transients. Transformer behavior is nonlinear, frequency dependent and many variations on core and coil construction are possible. There are many physical attributes and phenomena whose behavior may need to be correctly represented: core and coil configuration, self- and mutual inductances between coils, leakage fluxes, skin effect and proximity effect in coils, magnetic core saturation, hysteresis, and eddy current losses in core, capacitive effects. EMTP-type programs provide dedicated support to derive detailed transformer model.

Transformers have relatively simple structure. However, their adequate representation in wide frequency range is very difficult. Hence, the guideline for transformer modeling for different frequency ranges was proposed as in Tab. 3.5. It should be noted that for higher frequencies winding capacities are considered and frequency parameter dependence.

Tab. 3.5. Guideline for power transformer modeling [3.3].

Parameter/effect	0.1 Hz-3kHz	50 Hz-20 kHz	10 kHz-3 MHz	100 kHz-50 MHz
Short circuit impedance	Very important	Very important	Important	Negligible
Saturation	Very important	Very important,	Negligible	Negligible
Iron losses	Important ²⁾	Important ¹⁾	Negligible	Negligible
Eddy currents	Very important	Important	Negligible	Negligible
Capacitive coupling	Negligible	Important	Very important	Very important

¹⁾ Only for transformer energization phenomena, otherwise important.

²⁾ Only for resonance phenomena.

Many transformer models have been proposed for low frequency studies and the selection of most proper representation depends on many factors. The following approaches are commonly used in EMTP software to transformer representation for low-frequency and slow-front transients:

- matrix representation based models,
- topology based models.

Matrix representation based models

Matrix representation based models use the single- and three-phase n -winding transformers in the form of an impedance or admittance matrix. The derivation of parameters is possible from manufacturer data. For transformer representation by complex impedance matrix one can write:

$$\underline{\mathbf{V}} = \underline{\mathbf{Z}}\underline{\mathbf{I}} = (\underline{\mathbf{R}} + j\omega\underline{\mathbf{L}})\underline{\mathbf{I}}, \quad (3.39)$$

and for simulation in the time domain:

$$\mathbf{v} = \mathbf{R}\mathbf{i} + \mathbf{L}\frac{d\mathbf{i}}{dt}. \quad (3.40)$$

Using of admittance matrix description, especially in case of very small magnetizing currents is also possible:

$$\underline{\mathbf{I}} = \underline{\mathbf{Y}}\underline{\mathbf{U}}, \quad (3.41)$$

Hence, the currents in time domain are:

$$\frac{d\mathbf{i}}{dt} = \mathbf{L}^{-1}(\mathbf{R}\mathbf{i} + \mathbf{v}). \quad (3.42)$$

The basic equivalent circuit of the single phase transformer model shown is shown in Fig. 3.12. For simplicity the resistances are neglected. It is assumed that it consists of two coupled coils. The voltages at the terminal are given by:

$$\begin{bmatrix} v_k \\ v_m \end{bmatrix} = \begin{bmatrix} L_{kk} & L_{km} \\ L_{mk} & L_{mm} \end{bmatrix} \frac{d}{dt} \begin{bmatrix} i_k \\ i_m \end{bmatrix}, \quad (3.43)$$

where L_{kk}, L_{mm} – self-inductances of winding k and m respectively;
 L_{km}, L_{mk} – mutual inductances between windings.

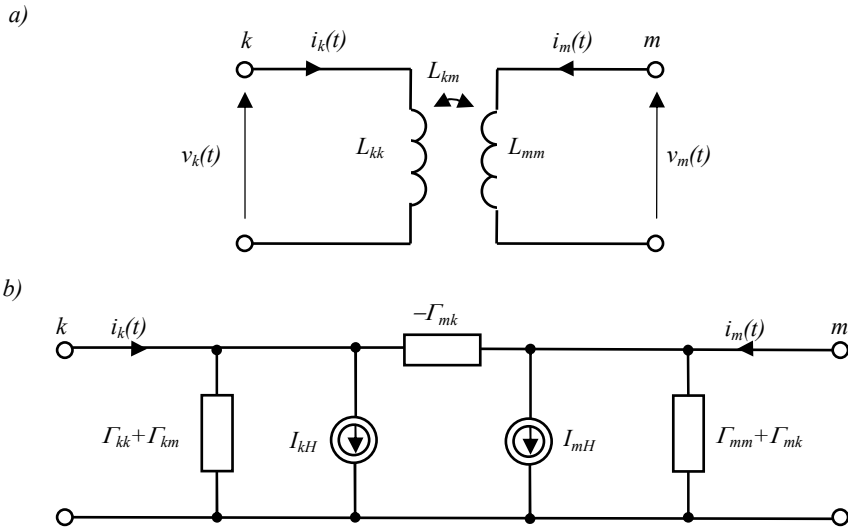


Fig. 3.12. Transformer (a) and its discrete equivalent (b).

The winding currents are expressed as:

$$\frac{d}{dt} \begin{bmatrix} i_k \\ i_m \end{bmatrix} = \begin{bmatrix} \Gamma_{kk} & \Gamma_{km} \\ \Gamma_{mk} & \Gamma_{mm} \end{bmatrix} \begin{bmatrix} v_k \\ v_m \end{bmatrix}, \quad (3.44)$$

where: $\Gamma_{kk} = \frac{L_{mm}}{L_{kk}L_{mm} - L_{km}L_{mk}};$

$$\Gamma_{mm} = \frac{L_{kk}}{L_{kk}L_{mm} - L_{km}L_{mk}};$$

$$\Gamma_{km} = \frac{-L_{mk}}{L_{kk}L_{mm} - L_{km}L_{mk}};$$

$$\Gamma_{mk} = \frac{-L_{km}}{L_{kk}L_{mm} - L_{km}L_{mk}}.$$

Digital implementation of transformer model with use of trapezoidal integration formula can be expressed as:

$$i_k(t) = I_{kH}(t - T_s) + \frac{T_s}{2}(\Gamma_{kk} + \Gamma_{km})v_k(t) + \frac{T_s}{2}\Gamma_{km}(v_k(t) - v_m(t)), \quad (3.45)$$

where: $I_{kH}(t - T_s) = i_k(t - T_s) + \frac{T_s}{2}(\Gamma_{kk} + \Gamma_{km})v_k(t - T_s) + \frac{T_s}{2}\Gamma_{km}(v_k(t - T_s) - v_m(t - T_s))$.

Topology (duality) based models

Topology (duality) based models are derived from a magnetic circuit model with use of the duality principle. The obtained models include the effects of saturation in each individual leg of the core, interphase magnetic coupling, and leakage effects. In the equivalent magnetic circuit, windings are represented by magnetomotive sources, leakage paths appear as linear reluctances, and magnetic cores appear as saturable reluctances. The equations based on Kirchhoff laws for the magnetic circuits, similarly as for electrical networks are also formulated.

Geometric based models use the formulation in which core topology is considered by use of magnetic equations and their coupling with electrical part.

Summarizing of the approaches to transformer modeling is presented in Tab. 3.6.

Tab. 3.6. Summarizing of power transformer models.

Model	Characteristic
Matrix representation	Consideration of phase-to-phase coupling and terminal characteristics, Only linear models can be represented, Saturation can be linked externally at the terminals in the form of non-linear elements, Reasonable accuracy for frequencies below 1 kHz.
Topology (duality) based representation	Duality-based models include the effects of saturation in each individual leg of the core, interphase magnetic coupling, and leakage effects. The mathematical formulation of geometric models is based on the magnetic equations and their coupling to the electrical equations, which is made taking into account the core topology. Models differ from each other in the way in which the magnetic equations are derived.

3.5.4. ROTATING MACHINES

Operation of the rotating machines depends on the interaction of electrical and mechanical part. The simple generator model consisting of electromotive force behind the reactance is adequate only for very short transient. For longer disturbances speed variations have the great influence on machine behavior. The mathematical model of

rotating machine for transient analysis depends on the specified frequency range. Tab. 3.7 shows guideline for modeling of rotating machines.

The detailed representation is required for low frequency transients. The modeling of coils, saturation, mechanical torque should be considered. Also voltage regulator and speed governor representation should be added into the model.

Scheme of electrical part of synchronous generator and an equivalent circuit are shown in Fig. 3.12.

Tab. 3.7. Guideline for rotating machine modeling [3.3].

Parameter/effect	0.1 Hz-3kHz	50 Hz-20 kHz	10 kHz-3 MHz	100 kHz-50 MHz
Representation	Detailed representation of electrical and mechanical parts including saturation effect modeling	A simplified representation of electrical part: an ideal AC source behind the frequency dependent transient impedance	A linear per phase circuit which matches the frequency response of the machine	A capacitance to ground per phase
Voltage control	Very important	Negligible	Negligible	Negligible
Speed control	Important	Negligible	Negligible	Negligible
Capacitance	Negligible	Important	Important	Very important
Frequency dependent parameters	Important	Important	Negligible	Negligible

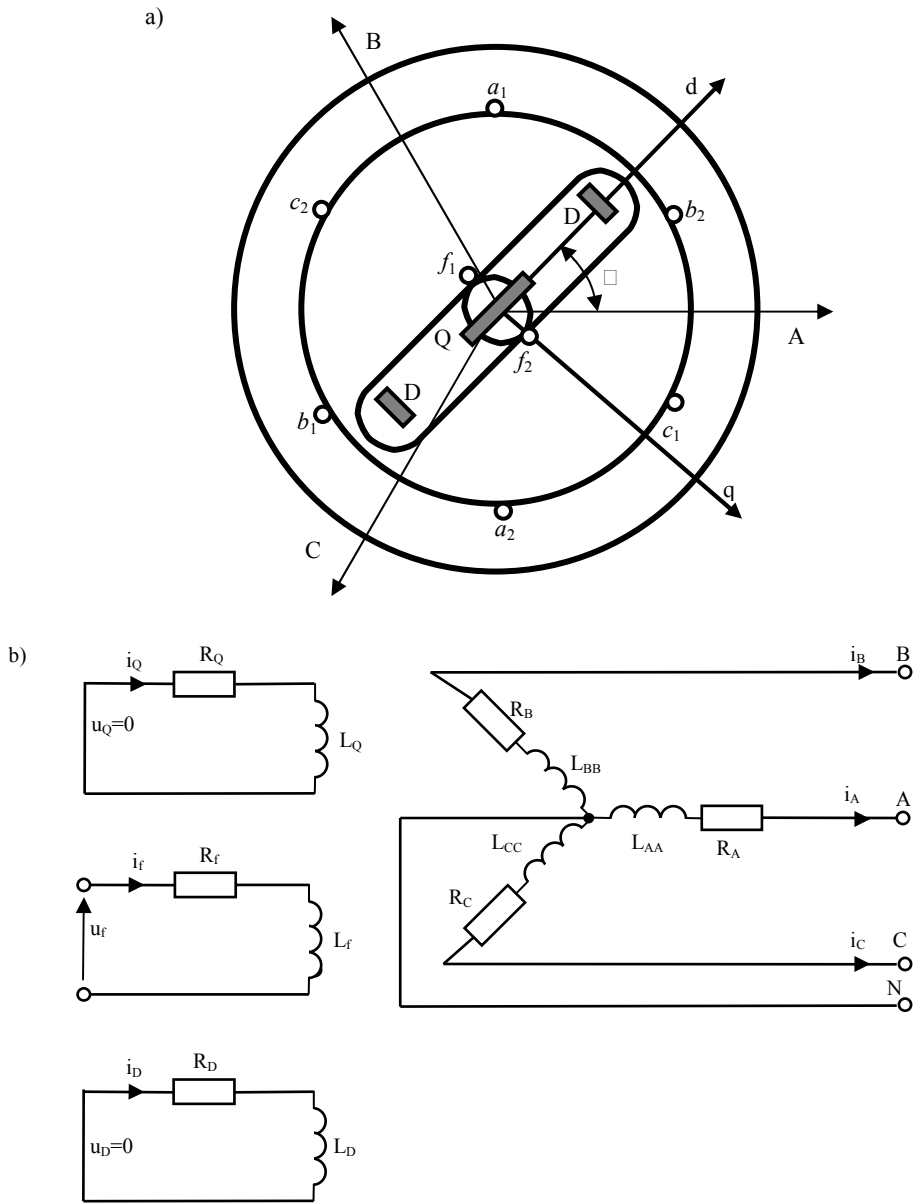


Fig. 3.13. Electrical part of synchronous generator (a) and their electrical equivalent (b).

The electrical part of the synchronous machine is described by the equation:

$$\begin{bmatrix} \Psi_A \\ \Psi_B \\ \Psi_C \\ \Psi_f \\ \Psi_D \\ \Psi_Q \end{bmatrix} = \begin{bmatrix} L_{AA} & L_{AB} & L_{AC} & L_{Af} & L_{AD} & L_{AQ} \\ L_{BA} & L_{BB} & L_{BC} & L_{Bf} & L_{BD} & L_{BQ} \\ L_{CA} & L_{CB} & L_{CC} & L_{Cf} & L_{CD} & L_{CQ} \\ L_{fA} & L_{fB} & L_{fC} & L_{ff} & L_{fD} & L_{fQ} \\ L_{DA} & L_{DB} & L_{DC} & L_{Df} & L_{DD} & L_{DQ} \\ L_{QA} & L_{QB} & L_{QC} & L_{Qf} & L_{QD} & L_{QQ} \end{bmatrix} \begin{bmatrix} i_A \\ i_B \\ i_C \\ i_f \\ i_D \\ i_Q \end{bmatrix} \quad (3.46)$$

or in matrix form:

$$\begin{bmatrix} \Psi_{ABC} \\ \Psi_{fDQ} \end{bmatrix} = \begin{bmatrix} \mathbf{L}_S & \mathbf{L}_{SW} \\ \mathbf{L}_{SW}^T & \mathbf{L}_W \end{bmatrix} \begin{bmatrix} \mathbf{i}_{ABC} \\ \mathbf{i}_{fDQ} \end{bmatrix}, \quad (3.47)$$

where: \mathbf{L}_S – a matrix of armature self and mutual inductances;

\mathbf{L}_W – a matrix of field self and mutual inductances;

\mathbf{L}_{SW} – a matrix of mutual inductances of field and armature.

The self and mutual inductances vary with time and are expressed by the following equations:

$$L_{AA} = L_S + \Delta L_S \cos 2\gamma, \quad L_{BB} = L_S + \Delta L_S \cos\left(2\gamma - \frac{2}{3}\pi\right),$$

$$L_{CC} = L_S + \Delta L_S \cos\left(2\gamma + \frac{2}{3}\pi\right),$$

$$L_{AB} = L_{BA} = -M_S - \Delta L_S \cos 2\left(\gamma + \frac{1}{6}\pi\right),$$

$$L_{BC} = L_{CB} = -M_S - \Delta L_S \cos 2\left(\gamma - \frac{1}{2}\pi\right),$$

$$L_{CA} = L_{AC} = -M_S - \Delta L_S \cos 2\left(\gamma + \frac{5}{6}\pi\right),$$

$$L_{Af} = L_{fA} = M_f \cos \gamma, \quad L_{AD} = L_{DA} = M_D \cos \gamma, \quad L_{AQ} = L_{QA} = M_Q \sin \gamma,$$

$$L_{Bf} = L_{fB} = M_f \cos\left(\gamma - \frac{2}{3}\pi\right), \quad L_{BD} = L_{DB} = M_D \cos\left(\gamma - \frac{2}{3}\pi\right),$$

$$L_{BQ} = L_{QB} = M_Q \sin\left(\gamma - \frac{2}{3}\pi\right),$$

$$L_{Cf} = L_{fc} = M_f \cos\left(\gamma + \frac{2}{3}\pi\right), \quad L_{CD} = L_{DC} = M_D \cos\left(\gamma + \frac{2}{3}\pi\right),$$

$$L_{CQ} = L_{QC} = M_Q \sin\left(\gamma + \frac{2}{3}\pi\right),$$

$$L_{fQ} = L_{Qf} = 0, \quad L_{DQ} = L_{QD} = 0.$$

Solving of these equations is possible in phase quantities. However, they are usually solved after transforming stator quantities into rotor-axis quantities, using the Park's transformation. The transformation matrix is :

$$\mathbf{W} = \sqrt{\frac{2}{3}} \begin{bmatrix} \frac{1}{\sqrt{2}} & \frac{1}{\sqrt{2}} & \frac{1}{\sqrt{2}} \\ \cos \gamma & \cos\left(\gamma - \frac{2}{3}\pi\right) & \cos\left(\gamma + \frac{2}{3}\pi\right) \\ \sin \gamma & \sin\left(\gamma - \frac{2}{3}\pi\right) & \sin\left(\gamma + \frac{2}{3}\pi\right) \end{bmatrix}. \quad (3.48)$$

Application of the transformation yields:

$$\begin{bmatrix} \psi_0 \\ \psi_d \\ \psi_q \\ \psi_f \\ \psi_D \\ \psi_Q \end{bmatrix} = \begin{bmatrix} L_0 & & & & & \\ & L_d & & kM_f & kM_D & \\ & & L_q & & & kM_Q \\ & kM_f & & L_f & L_{fD} & \\ & kM_D & & L_{fD} & L_D & \\ & & kM_Q & & & L_Q \end{bmatrix} \begin{bmatrix} i_0 \\ i_d \\ i_q \\ i_f \\ i_D \\ i_Q \end{bmatrix} \quad (3.49)$$

or in matrix form:

$$\begin{bmatrix} \Psi_{0dq} \\ \Psi_{fDQ} \end{bmatrix} = \begin{bmatrix} \mathbf{L}_{0dq} & k\mathbf{M}_{fDQ} \\ k\mathbf{M}_{fDQ}^T & \mathbf{L}_{fDQ} \end{bmatrix} \begin{bmatrix} \mathbf{i}_{0dq} \\ \mathbf{i}_{fDQ} \end{bmatrix}, \quad (3.50)$$

where: $k = \sqrt{\frac{3}{2}}$,

$$L_0 = L_S - 2M_S,$$

$$L_d = L_S + M_S + \frac{3}{2}\Delta L_S,$$

$$L_q = L_S + M_S - \frac{3}{2}\Delta L_S$$

The flux-current-voltage equations in d - q frame can be written in the following form:

$$\begin{bmatrix} \dot{\Psi}_{0dq} \\ \dot{\Psi}_{fDQ} \end{bmatrix} = - \begin{bmatrix} \mathbf{v}_{0dq} \\ \mathbf{v}_{fDQ} \end{bmatrix} - \begin{bmatrix} \mathbf{r}_{ABC} & \\ & \mathbf{r}_{fDQ} \end{bmatrix} \begin{bmatrix} \mathbf{i}_{0dq} \\ \mathbf{i}_{fDQ} \end{bmatrix} + \begin{bmatrix} \mathbf{\Omega} \\ \mathbf{0} \end{bmatrix} \begin{bmatrix} \Psi_{0dq} \\ \Psi_{fDQ} \end{bmatrix}, \quad (3.51)$$

where: $\mathbf{\Omega} = \mathbf{W}\mathbf{W}^{-1} = \omega \begin{bmatrix} 0 & 0 & 0 \\ 0 & 0 & -1 \\ 0 & 1 & 0 \end{bmatrix}$.

The electromechanical part of generator is described by the following differential equation:

$$\frac{T_m S_r}{\omega_s} \frac{d^2 \delta}{dt^2} = P_m - P_e - D \frac{d\delta}{dt}, \quad (3.52)$$

where: ω_s – a synchronous angular speed;
 δ – a rotor angle;
 T_m – a mechanical time constant;
 S_r – a generator nominal power;
 P_m – a turbine mechanical power;
 P_e – a generator electrical power;
 D – a rotor damping coefficient.

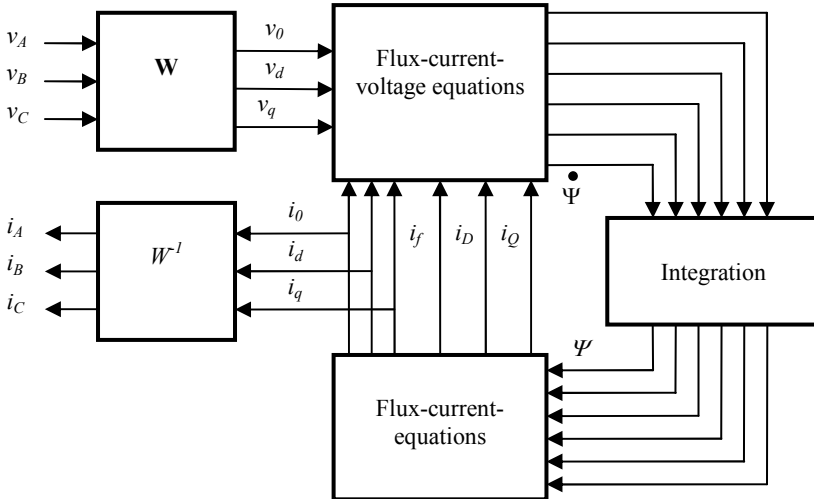


Fig. 3.14. Incorporation of synchronous generator model in EMTP.

3.5.5. LOADS

Loads connected to the power system are non-linear and their characteristics depend on system voltage and frequency. Different load dynamic profiles occur: non-dynamic (e.g. resistive loads), slow dynamic (e.g. manually controlled loads), fast dynamic (induction motors, adjustable speed drives) and non-continuous (protection switching).

Power system loads can be modeled by static and dynamic models. Static models are represented by constant active and reactive power, constant current or constant impedance models or combination of these types. Modeling of load dynamic characteristic load enables sensitivity to voltage and frequency changes. In some cases it is not possible or not feasible to model the dynamic behavior of individual loads and they are grouped into components with similar characteristics. Although there exist many types of loads, the most influential on dynamic behavior are induction motors.

3.5.6. CIRCUIT BREAKERS

Circuit breakers carry and break currents under normal and abnormal (short circuits) conditions. Normally breaker operates at closed position and when the tripping signal is obtained it opens contact and current flow is broken. The separation of the contacts causes the generation of an electric arc. The arc is usually quickly cooled by surrounding gas. The arc phenomenon is very complex and difficult to modeling and there is no generally accepted model. Guideline for circuit breaker modeling in different transient frequency ranges is presented in Tab. 3.8.

In simulation programs circuit breakers are modeled by the following representations:

- Ideal switch that is opened at first zero current crossing, after the obtaining tripping signal. Arc influence on the network is not considered,
- The arc is modeled as a time-varying resistance. Resistance variation is determined with use of the breaker characteristic.
- Dynamically varying resistance.

Models of arc were proposed by Cassie and Mayr. The Cassie model is described by the following equation:

$$\frac{1}{g} \frac{dg}{dt} = \frac{1}{\tau} \left(\frac{v^2}{v_0^2} - 1 \right) = \frac{1}{\tau} \left(\frac{i^2}{v_0^2 g^2} - 1 \right), \quad (3.53)$$

and the Mayr model is expressed by:

$$\frac{1}{g} \frac{dg}{dt} = \frac{1}{\tau} \left(\frac{vi}{P_0} - 1 \right) = \frac{1}{\tau} \left(\frac{i^2}{P_0 g} - 1 \right), \quad (3.54)$$

where: g – an arc conductance,
 v – an arc voltage;
 i – an arc current;
 τ – an arc time constant;
 P_0 – a steady state power loss;
 v_0 – a constant part of the arc voltage.

Usually the following models for closing operation are used:

- Ideal switch representation of circuit breaker. Its impedance changes rapidly from very large to very small value,
- Assuming the existence of closing time when the arc can strike before the circuit breaker contacts are finally closed.

Tab. 3.8. Guideline for modeling circuit breaker [3.3].

Operation	Mode	0.1 Hz-3kHz	50 Hz-20kHz	10 kHz-3 MHz	100 kHz-50 MHz
Closing	Mechanical pole spread	important	very important	negligible	negligible
	Prestrikes (decrease of sparkover voltage vs. time)	negligible	important	important	very important
Opening	High current interruption (arc equations)	important only for interruption capability studies	important only for interruption capability studies	negligible	negligible
	Current chopping (arc instability)	negligible	important only for interruption of small inductive currents	important only for interruption of small inductive currents	negligible
	Restrike characteristic (increase of sparkover voltage vs. time)	negligible	important only for interruption of small inductive currents	very important	very important
	High frequency current interruption	negligible	important only for interruption of small inductive currents	very important	very important

Circuit breakers switching actions may have a significant influence on power network. In some cases modeling of breakers as ideal switch is exact enough. Exact modeling of arc-network interactions requires arc models whose parameters can be obtained only in experimental way.

Application of switching device model can cause numerical oscillation (chatters). In such case voltage and current values oscillating around true values. The common reasons of chatters are a step change in current through an inductor or a step change in voltage across a capacitor. An inductor voltage is equal to:

$$v = L \frac{di}{dt} \quad (3.55)$$

Applying the trapezoidal integration rule one can obtain:

$$i(t) = i(t - T_s) + \frac{T_s}{2L} (v(t) + v(t - T_s)), \quad (3.56)$$

and solving for voltage across inductor:

$$v(t) = -v(t - T_s) + \frac{2L}{T_s} (i(t) - i(t - T_s)) \quad (3.57)$$

Assuming the unity step current change for $i(t \geq 0) = 1.0$, the voltages across inductor are:

$$\begin{aligned} v(t) &= 2L/T_s \\ v(t+T_s) &= -2L/T_s \\ v(t+2T_s) &= 2L/T_s \\ v(t+3T_s) &= -2L/T_s \\ &\dots \quad \dots \end{aligned}$$

The expected values of voltage $v(t > 0)$ is zero and it can be stated that numerical oscillations damage the simulation results. To prevent the numerical oscillations some artificial damping resistors are included in the model. However, the accuracy of simulation can suffer from such modification. Another way is to change the trapezoidal integration rule in case of discontinuity by Euler backward rule or interpolation steps [3.16].

3.5.7. NETWORK EQUIVALENTS FOR TRANSIENT ANALYSES

At present the main efforts concern on to find equivalent in time domain by use of discrete time network equivalent or to replace the external network using of lumped *RLC* circuit or transfer functions with frequency response approximating the characteristic of the original system.

Tab. 3.9. Frequency domain equivalent methods characteristics for EMTP analyses.

Frequency domain	
Direct methods	
Foster equivalent	<p>Equivalent created by Foster method of circuit synthesis. The impedance-frequency characteristic of the external system is described by:</p> $\underline{Z}(f) = \frac{j2}{2\pi} \sum_{i=1}^n i \frac{A_i f}{f_i^2 - f^2},$ <p>where: f_i – i-th resonant frequency, A_i – residual correspondent to the i-th pole Good accuracy for limited frequency range.</p>
Lumped parameter circuit	<p>External system replaced by lumped RLC circuit whose frequency response approximates the response of external system. Model circuit consists of parallel branches corresponding to certain frequencies. The general admittance (resistances are omitted):</p> $Y(s) = \frac{K_s(s + K_0)}{s} + \sum_{i=1}^n i \frac{K_i s}{s^2 + \omega_i^2}.$ <p>where: K_s – constant, K_0, K_i – residues of system admittance, ω_i – series resonance frequencies. The method suitable for systems with available resonant frequencies.</p>
Correction filter	<p>Use of equivalent circuit with parallel RLC branches. Correction filter are used for the frequency ranges with large discrepancy between original and approximated impedance-frequency. The method is simpler and more accurate than optimization methods.</p>
Frequency response approximation	<p>Equivalent circuit based on parallel RLC branches for particular impedance-frequency characteristic. Each branch corresponds to the minimum at certain resonance frequency.</p>
Pole removal	<p>Least square fitting to synthesize RLC equivalent circuit according to the driving-point function with respect to the frequency domain around resonance.</p>
Optimization methods	
Low-order rational function	<p>Network equivalent use the frequency response of the admittance functions over frequency range. The optimization method is used to minimize objective function involving amplitude and phase functions.</p>
Gradient optimization	<p>Minimization of the difference between the actual and equivalent system response according to the formula:</p> $J = h(g(x, A_1), g(x, A_2), \dots, g(x, A_m)),$ <p>where: g – objective function, $A_1, A_2 \dots A_m$ – independent variables at the m sample points, h – error criterion function.</p>

First group, discrete time Norton equivalents are obtained with use of response of external system to a sinusoidal signal used for identification of discrete time model

with use of least square method. The great variety of methods is applied for frequency domain modeling. The general review of these methods (according to [3.7]) is presented in Tab. 3.9.

The direct methods use circuit theory concepts, mainly the circuit synthesis techniques to obtain the adequate frequency response. Optimization methods take the advantage of the network admittance parameter identification.

It should be noted that the equivalents have always the limited accuracy and the verification step is required before application.

Example 3.2

Discrete time Norton equivalent of the external network can be obtained with the use of an excitation signal (the multisinus signal) [3.1]:

$$x(t) = \sum_{k=1}^M A_k \sin(2\pi f_k t + \phi_k), \quad f_k = \frac{l_k}{T} \quad (3.58)$$

where: A_k, f_k, ϕ_k – an amplitude, a frequency and a phase of the k -th component respectively.

The phase of k -th component can be derived from:

$$\phi_m = \phi_1 - \frac{m(m-1)}{M} \pi, \quad m = 2, \dots, M, \quad (3.59)$$

Frequency spectrum of such signal is flat for the specified frequency range which can be adjusted in simple way.

The equivalent can be described by parameter vector θ . The relation between discrete voltages and current of equivalent circuit can be expressed by linear regression equation:

$$\mathbf{Z} = \mathbf{X} \cdot \theta \quad (3.60)$$

where: $\mathbf{Z} = [i(N), i(N-1), \dots, i(p+1)]^T$;

$\theta = [a_1, a_2, \dots, a_p, g_0, g_1, g_2, \dots, g_p]^T$ – a parameter vector;

p – an assumed model order;

$$\mathbf{X} = \begin{bmatrix} i(N-1) & i(N-2) & \cdots & i(N-p) \\ i(N-2) & i(N-3) & \cdots & i(N-p+1) \\ \cdot & \cdot & \cdots & \cdot \\ \cdot & \cdot & \cdots & \cdot \\ \cdot & \cdot & \cdots & \cdot \\ i(p) & i(p-1) & \cdots & i(1) \\ v(N) & v(N-1) & \cdots & v(N-p) \\ v(N-1) & v(N-2) & \cdots & v(N-p+1) \\ \cdot & \cdot & \cdots & \cdot \\ \cdot & \cdot & \cdots & \cdot \\ \cdot & \cdot & \cdots & \cdot \\ v(p+1) & v(p) & \cdots & v(1) \end{bmatrix}.$$

To obtain the circuit discrete equivalent the transient simulation with use of multisinus voltage excitation and discrete current are then registered. Assuming the model the order the \mathbf{X} and \mathbf{Z} matrices are formulated. The parameter estimates can be found with use of the least squares method:

$$\hat{\boldsymbol{\theta}} = (\mathbf{X}^T \mathbf{X})^{-1} \mathbf{X}^T \mathbf{Z}, \quad (3.61)$$

Once the response of equivalent is found the mean square error between equivalent and simulation results is calculated. If the equivalent of the considered order satisfies the adequacy conditions, then it can be incorporated into EMTP solution routine. Otherwise, the model order is updated and the equivalent searching procedure is repeated.

3.6. SOLUTION OF TRANSIENTS

Mathematical description of electromagnetic transient has a form of set of first order differential equations with known initial conditions:

$$\frac{d\mathbf{x}}{dt} = f(\mathbf{x}, t), \quad (3.62)$$

where: \mathbf{x} – a state variable vector,
 $f(\mathbf{x})$ – a vector function of state variables,

and algebraic equations:

$$g(\mathbf{x}, t) = 0. \quad (3.63)$$

The objective is to find \mathbf{x} as a function of t , with the initial values of \mathbf{x} and t equal to \mathbf{x}_0 and t_0 . Numerical integration is used to find the solution $x(t+T_s)$ with use of previous time solutions. T_s is a time interval between two adjacent time points and is called time step. Time step may be maintained constant over the integration interval or may be changed.

Once the discrete equivalent circuits are formulated they are solved at discrete time points with the use of nodal circuit analysis methods. Conductance matrix is usually sparse and some decomposition techniques employed to improve computation speed and accuracy.

Numerical integration methods produce unavoidable errors caused by:

- round-off resulting from finite machine word length, used computer type and programming language,
- truncation resulting from the mathematical approximation of the integral. This type of error depends only on the applied integration algorithm i.e. the way the approximation is made.

During passing the integration algorithm it is expected to suppress numerical truncation error with simulation time, i.e. to preserve a numerical stability. Stability depends on the integrated equation, time step and the applied integration method.

Another important topic is stiffness relating to time constants appearing in power system. Solution of linear differential equation set is linear combination of exponential functions. Each function describes individual system mode defined by system eigenvalues. Stiffness of the system depends on distribution of the eigenvalues: small values are related to slow dynamic changes and large values to fast dynamics. The large differences in system modes may result in some numerical and accuracy problems. Hence, the employed formula should be tailored to equation set stiffness.

Due to great variety of possible power system operation conditions the selected integration scheme should ensure the sufficient accuracy and numerical stability. There are many methods to perform numerical integration, which use Taylor expansion or polynomial approximation. Generally, they can be divided into explicit and implicit. The value of integration of function in an explicit method is obtained without the value $f(\mathbf{x}_{n+1}, t_{n+1})$ (e.g. forward Euler method). Otherwise the integration methods are called implicit (e.g. backward Euler). Some of the basic integration rules are shown in Tab. 3.10.

Tab. 3.10. Basic integration formulae for selected discrete integration methods.
 $T_s = t_{n+1} - t_n$ - integration time step.

Integration method	Integration formula	Order
Forward Euler	$\mathbf{x}_{n+1} = \mathbf{x}_n + T_s f(\mathbf{x}_n, t_n)$	1
Backward Euler	$\mathbf{x}_{n+1} = \mathbf{x}_n + T_s f(\mathbf{x}_{n+1}, t_{n+1})$	1
Trapezoidal	$\mathbf{x}_{n+1} = \mathbf{x}_n + \frac{T_s}{2} [f(\mathbf{x}_n, t_n) + f(\mathbf{x}_{n+1}, t_{n+1})]$	1
Gears 2 nd order	$\mathbf{x}_{n+1} = \frac{4}{3} \mathbf{x}_n - \frac{1}{3} \mathbf{x}_{n-1} + \frac{2T_s}{3} f(\mathbf{x}_{n+1}, t_{n+1})$	2

The first order methods are able to self-start. Higher order methods use the past values of the integrated function, it is not possible to solve $n+1$ term for $n = 0$. In such case first terms in simulation are calculated with selected first order method. Higher order methods provide “smooth” approximation of integrated function and linear approximation is applied in first order methods. Therefore the accuracy for the same time step is usually better when higher order methods are used.

The trapezoidal integration rule is mostly used in transient analyses. It is easy to programming, numerically stable and has reasonable accuracy. However, if the great accuracy is required, the small integration time step should be applied and computational efforts grow considerably.

PROBLEMS

3.1. Find the discrete Norton equivalents for circuits shown in Fig. 3.15 applying trapezoidal integration rule.

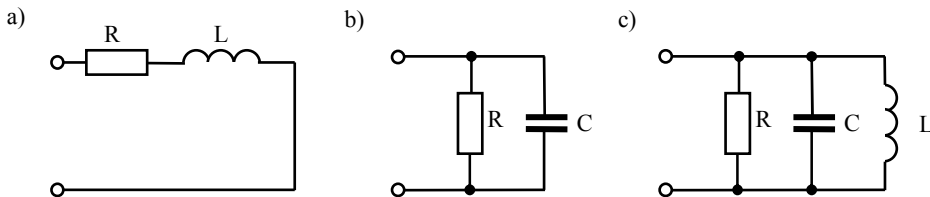


Fig. 3.15. Circuits for Problem 3.1.

3.2. Form the discrete Norton equivalent for circuit presented in Fig. 3.16 applying trapezoidal rule and write the node equations. Solve them for three time points $(0, T_s, 2T_s)$. Circuit parameters: E – step voltage 40 V (applied at $t=0$),

$R_1 = 2 \Omega$, $R_2 = 5 \Omega$, $R_3 = 5 \Omega$, $L_1 = 1 \text{ mH}$, $L_2 = 1 \text{ mH}$, $C_1 = 1 \mu\text{F}$, $T_s = 1 \text{ ms}$.
Zero initial conditions.

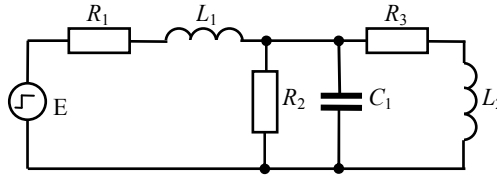


Fig. 3.16. Circuit for Problem 3.2.

REFERENCES

- [3.1] A. Abur, H. Singh, *Time domain modeling of external systems for electromagnetic transient programs*, *IEEE Trans. on Power Systems*, Vol. 8, No. 2, May 1993, pp. 671-676.
- [3.2] L. O. Chua, P. M. Lin, *Computer-aided analysis of electronic circuits. Algorithms and computational techniques*, Prentice-Hall, Englewood Cliffs, New Jersey, 1975.
- [3.3] CIGRE Working Group 33.02, *Guidelines for representation of network elements when calculating transients*, 1990.
- [3.4] H. W. Dommel, *Digital computer solution of electromagnetic transients in single- and multiphase networks*, *IEEE Trans. on Power Apparatus and Systems*, Vol. 88, April 1969, pp. 388-399.
- [3.5] H. W. Dommel, *Nonlinear and time-varying elements in digital simulation of electromagnetic transients*, *IEEE Trans. on Power Apparatus and Systems*, Vol. 90, Nov. 1971, pp. 2561-2567.
- [3.6] H. W. Dommel, *Electromagnetic transient program reference manual (EMTP theory book)*, Bonneville Power Administrator, Portland, 1986.
- [3.7] A. I. Ibrahim, *Frequency dependent network equivalents for electromagnetic transient studies: a bibliographical survey*, *Electrical Power and Energy Systems*, Vol. 25, 2003, pp. 193-199.
- [3.8] P. Kundur, *Power system stability and control*, McGraw Hill, 1994.
- [3.9] J. Machowski, J. Bialek, J. Bumby, *Power system dynamics, stability and control*, John Wiley&Sons, New York, 2008.
- [3.10] J. A. Martinez, B. Gustavsen, D. Durbak, *Parameter determination for modeling system transients – Part I: Overhead lines*, *IEEE Trans. on Power Delivery*, Vol. 20, No. 3, July 2005, pp. 2038-2044.

- [3.11] J. A. Martinez, B. Gustavsen, D. Durbak, ***Parameter determination for modeling system transients – Part II: Insulated cables***, *IEEE Trans. on Power Delivery*, Vol. 20, No. 3, July 2005, pp. 2045-2050.
- [3.12] J. A. Martinez, R. Walling, B. A. Mork, J. Martin-Arnedo, D. Durbak, ***Parameter determination for modeling system transients – Part III: Transformers***, *IEEE Trans. on Power Delivery*, Vol. 20, No. 3, July 2005, pp. 2051-2062.
- [3.13] J. A. Martinez, B. Johnson, C. Grande-Moran, ***Parameter determination for modeling system transients – Part IV: Rotating machines***, *IEEE Trans. on Power Delivery*, Vol. 20, No. 3, July 2005, pp. 2063-2072.
- [3.14] J. A. Martinez, J. Mahseredjian, B. Khodabakhchian, ***Parameter determination for modeling system transients – Part VI: Circuit breakers***, *IEEE Trans. on Power Delivery*, Vol. 20, No. 3, July 2005, pp. 2079-2085.
- [3.15] A. L. Shenkman, ***Transient analysis of electric power circuits handbook***, Springer, 2005.
- [3.16] N. Watson, J. Arrillaga, ***Power system electromagnetic transient simulation***, IEE, London, UK, 2003.

4. POWER SYSTEM MODEL REDUCTION. NETWORK TRANSFORMATION

4.1. GENERAL CONSIDERATIONS

Power-system model reductions are made because of [4.1]-[4.3]:

- practical computational limitations (the required size of computer memory, and computing time),
- there is no necessity to model parts of the system far away from a disturbance with great accuracy,
- parts of the system, which do not belong to the considered utility, are considered as external subsystems,
- maintaining the relevant databases, in which data from the whole system are collected, would be very difficult and expensive.

The methods for producing the equivalents of an external subsystem can be divided as follows [4.2]:

- methods which do not require any knowledge of the external subsystem,
- methods requiring certain knowledge of the configuration and the parameters of the external subsystem itself.

The latter of the mentioned methods are model-reduction ones.

One can distinguish the following groups of model-reduction methods:

- methods of physical reduction,
- methods of topological reduction,
- methods of modal reduction.

Methods of physical reduction ensure choosing appropriate models for the system elements (generators, loads etc.). They select models depending on how influential an individual element is in determining the system response to a particular disturbance. Elements, which are electrically close to the disturbance, are modelled with higher accuracy.

Methods of topological reduction rely on eliminating and/or aggregating selected nodes in order to reduce the size of the equivalent network and the number of generating units modelled. If they are used together with physical reduction, they give an equivalent model that comprises equivalents of standard system elements such as generating units, lines, nodes etc.

The methods of topological reduction are also called methods of network transformation.

The third group of the model-reduction methods includes methods of modal reduction. These methods use linearised models of the external subsystem to eliminate, or neglect, the unexcited system modes

4.2. NETWORK TRANSFORMATION

4.2.1. NODE ELIMINATION

While the process of elimination of network nodes is performed the following rule is in force: when nodes are eliminated from the network model, the currents and nodal voltages at the retained nodes are unchanged.

In this subsection, node elimination by matrix partitioning is considered.

Before any nodes are eliminated from the network (Fig. 4.1) we have:

$$\begin{bmatrix} \bar{\mathbf{I}}_R \\ \bar{\mathbf{I}}_E \end{bmatrix} = \begin{bmatrix} \bar{\mathbf{Y}}_{RR} & \bar{\mathbf{Y}}_{RE} \\ \bar{\mathbf{Y}}_{ER} & \bar{\mathbf{Y}}_{EE} \end{bmatrix} \begin{bmatrix} \bar{\mathbf{V}}_R \\ \bar{\mathbf{V}}_E \end{bmatrix}, \quad (4.1)$$

where: E – denotes the set of eliminated nodes,

R – denotes the set of retained nodes,

$\bar{\mathbf{I}}$ – a vector of current injection,

$\bar{\mathbf{V}}$ – a vector of nodal voltages,

$\bar{\mathbf{Y}}$ – a submatrix of the nodal admittance matrix.

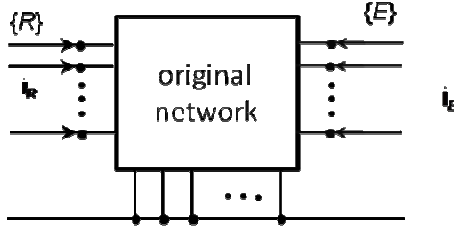


Fig. 4.1. The representation of the considered network before elimination of nodes.

Transforming the equations (4.1), we have

$$\begin{bmatrix} \bar{\mathbf{I}}_R \\ \bar{\mathbf{V}}_E \end{bmatrix} = \begin{bmatrix} \bar{\mathbf{Y}}_R & \bar{\mathbf{K}}_I \\ \bar{\mathbf{K}}_V & \bar{\mathbf{Y}}_{EE}^{-1} \end{bmatrix} \begin{bmatrix} \bar{\mathbf{V}}_R \\ \bar{\mathbf{I}}_E \end{bmatrix}, \quad (4.2)$$

$$\text{where: } \bar{\mathbf{Y}}_R = \bar{\mathbf{Y}}_{RR} - \bar{\mathbf{Y}}_{RE} \bar{\mathbf{Y}}_{EE}^{-1} \bar{\mathbf{Y}}_{ER}, \quad (4.3)$$

$$\bar{\mathbf{K}}_I = -\bar{\mathbf{Y}}_{RE} \bar{\mathbf{Y}}_{EE}^{-1}, \quad (4.4)$$

$$\bar{\mathbf{K}}_V = -\bar{\mathbf{Y}}_{EE}^{-1} \bar{\mathbf{Y}}_{ER}. \quad (4.5)$$

Taking into account the equations (4.1) and (4.2), one can ascertain, that

$$\bar{\mathbf{I}}_R = \bar{\mathbf{Y}}_R \bar{\mathbf{V}}_R + \Delta \bar{\mathbf{I}}_R. \quad (4.6)$$

where:

$$\Delta \bar{\mathbf{I}}_R = \bar{\mathbf{K}}_I \bar{\mathbf{I}}_E. \quad (4.7)$$

The vector $\bar{\mathbf{I}}_E$ as well as the vector $\bar{\mathbf{V}}_E$ are not directly present in the equation (4.6). It should be noted that the vector $\Delta \bar{\mathbf{I}}_R$ depends upon the vectors $\bar{\mathbf{I}}_E$ and $\bar{\mathbf{V}}_E$.

The equation (4.6) can be considered as the equation describing the reduced network (Fig. 4.2), in which the above-mentioned eliminated nodes (from the set E) are not present. In the new network, the current injections differ from the ones at the same nodes of the original network. The difference is shown by equation (4.7).

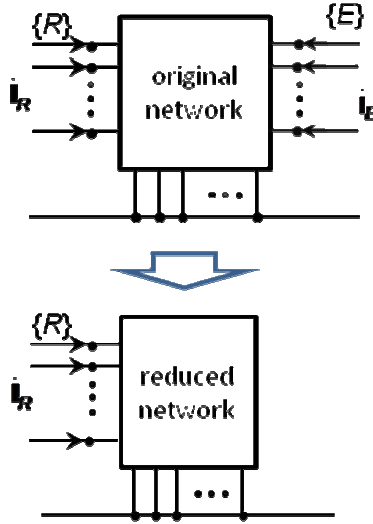


Fig. 4.2. The reduction of the network by elimination of nodes.

The matrix $\bar{\mathbf{Y}}_R$ in the equation (4.6) is called a transfer admittance matrix and the matrix $\bar{\mathbf{K}}_I$ in the equation (4.7) is called a distribution matrix.

Apart from the presented way of modelling the original network one can consider another one, assuming that a current injection at each eliminated node is equal to zero. In this situation, a load at each eliminated node is represented by the admittance

$$\bar{\mathbf{Y}}_{Ei} = \frac{\bar{\mathbf{S}}_{Ei}^*}{V_{Ei}^2}. \quad (4.8)$$

where: i – an index of the node,

$\bar{\mathbf{S}}_{Ei}$ – a complex power at the node i , belonging to the set of nodes E ,

V_{Ei} – a magnitude of the voltage at the node i .

The admittance \bar{Y}_{Ei} is taken into account when the self admittance at the node i is determined. In the considered case, the self admittance at the node i differs from the one in the earlier case by \bar{Y}_{Ei} .

In the considered case, we have the following two sets of equations derived from (4.1)

$$\bar{\mathbf{I}}_R = \bar{\mathbf{Y}}_{RR} \bar{\mathbf{V}}_R + \bar{\mathbf{Y}}_{RE} \bar{\mathbf{V}}_E . \quad (4.9)$$

$$0 = \bar{\mathbf{I}}_E = \bar{\mathbf{Y}}_{ER} \bar{\mathbf{V}}_R + \bar{\mathbf{Y}}_{EE} \bar{\mathbf{V}}_E . \quad (4.10)$$

From the equation (4.10) we have

$$\bar{\mathbf{V}}_E = -\bar{\mathbf{Y}}_{EE}^{-1} \bar{\mathbf{Y}}_{ER} \bar{\mathbf{V}}_R , \quad (4.11)$$

and taking into consideration the equation (4.9), we get

$$\begin{aligned} \bar{\mathbf{I}}_R &= \bar{\mathbf{Y}}_{RR} \bar{\mathbf{V}}_R + \bar{\mathbf{Y}}_{RE} \left(-\bar{\mathbf{Y}}_{EE}^{-1} \bar{\mathbf{Y}}_{ER} \bar{\mathbf{V}}_R \right) = \\ &= \left(\bar{\mathbf{Y}}_{RR} - \bar{\mathbf{Y}}_{RE} \bar{\mathbf{Y}}_{EE}^{-1} \bar{\mathbf{Y}}_{ER} \right) \bar{\mathbf{V}}_R = \bar{\mathbf{Y}}_R \bar{\mathbf{V}}_R . \end{aligned} \quad (4.12)$$

In the considered case, the vector $\Delta \bar{\mathbf{I}}_R$, which occurs in the equation (4.6), is equal to the vector with zero elements.

The second from the considered methods of node elimination by matrix partitioning, has a certain drawback. In the transformed model, the equivalent shunt branches have large conductance values, and in effect the branches of the equivalent network may have a poor X/R ratio causing convergence problems for some load-flow computer programs.

Example 4.1.

Let us consider the power system from Fig. 4.3. Parameters of the branches of that system are in Tab. 4.1. Voltages at the nodes, power and current injections in the power system from Fig. 4.3 are in Tab. 4.2. The nodal admittance matrix for the considered system is in Tab. 4.5. Let us assume that: (i) the set $\{1, 2, 3\}$ is the set of retained nodes, (ii) the set $\{4, 5, 6, 7, 8, 9\}$ is the set of eliminated nodes. In this situation, the vectors of currents $\bar{\mathbf{I}}_R$, $\bar{\mathbf{I}}_E$, the vectors of voltages $\bar{\mathbf{V}}_R$, $\bar{\mathbf{V}}_E$ and the matrices $\bar{\mathbf{Y}}_{RR}$, $\bar{\mathbf{Y}}_{RE}$, $\bar{\mathbf{Y}}_{ER}$, $\bar{\mathbf{Y}}_{EE}$ are as it is shown in Tab. 4.3 – Tab. 4.9. Utilizing the equations (4.3), (4.4), we calculate the matrices: $\bar{\mathbf{Y}}_R$, $\bar{\mathbf{K}}_I$. These matrices are presented in Tab. 4.10 and Tab. 4.11. $\bar{\mathbf{Y}}_R \bar{\mathbf{V}}_R$ and $\Delta \bar{\mathbf{I}}_R$, i.e. components of the sum in the formula (4.6) and also $\bar{\mathbf{I}}_R$ calculated from this formula are shown in Tab. 4.12. The currents $\bar{\mathbf{I}}_R$ are calculated under assumption, that at the nodes 1, 2 and 3 are the same voltages as before elimination of the nodes: 4, 5, 6, 7, 8 and 9. Finally, we can ascertain that after elimination of the nodes: 4, 5, 6, 7, 8 and 9 the currents and nodal voltages at the retained nodes, i.e. at the nodes: 1, 2 and 3 are unchanged.

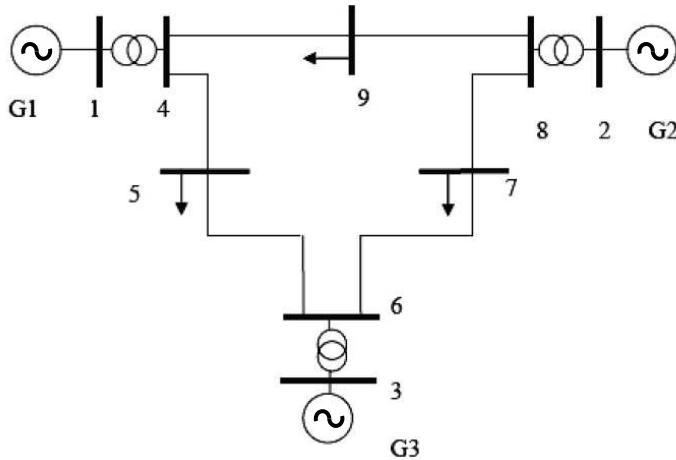


Fig. 4.3. The considered power system.

Tab. 4.1. The parameters of the branches of the power system from Fig. 4.3.

i	j	R_{ij}	X_{ij}	B_{ij}
1	4	0.0000	0.0576	0.0000
4	5	0.0170	0.0920	0.1580
5	6	0.0390	0.1700	0.3580
3	6	0.0000	0.0586	0.0000
6	7	0.0119	0.1008	0.2090
7	8	0.0085	0.0720	0.1490
8	2	0.0000	0.0625	0.0000
8	9	0.0320	0.1610	0.3060
9	4	0.0100	0.0850	0.1760

Tab. 4.2. Voltages at the nodes, power and current injections in the power system from Fig. 4.3.

i	V_i	δ_{Vi}	P_{gi}	Q_{gi}	P_{Li}	Q_{Li}	I_i	δ_{li}
1	1.00	0	71.95	24.07	0.00	0.00	0.76	-18.50
2	1.00	9.67	163.00	14.46	0.00	0.00	1.67	4.60
3	1.00	4.77	85.00	-3.65	0.00	0.00	0.85	7.23
4	0.99	-2.41	0.00	0.00	0.00	0.00	0.00	0.00
5	0.98	-4.02	0.00	0.00	90.00	30.00	0.97	-22.45
6	1.00	1.93	0.00	0.00	0.00	0.00	0.00	0.00
7	0.99	0.62	0.00	0.00	100.00	35.00	1.08	-18.67
8	1.00	3.80	0.00	0.00	0.00	0.00	0.00	0.00
9	0.96	-4.35	0.00	0.00	125.00	50.00	1.41	-26.15

Tab. 4.3. The elements of the vectors $\bar{\mathbf{I}}_R$, $\bar{\mathbf{V}}_R$.

No. of element	No. of node	$\bar{\mathbf{I}}_R$		$\bar{\mathbf{V}}_R$	
		Magnitude p.u.	Phase angle degrees	Magnitude p.u.	Phase angle degrees
1	1	0.76	-18.50	1.00	0.00
2	2	1.64	4.60	1.00	9.67
3	3	0.85	7.23	1.00	4.77

Tab. 4.4. The elements of the vectors \bar{I}_E, \bar{V}_E .

No. of element	No. of node	\bar{I}_E		\bar{V}_E	
		Magnitude p.u.	Phase angle degrees	Magnitude p.u.	Phase angle degrees
1	4	0.00	0.00	0.99	-2.41
2	5	0.97	-22.45	0.98	-4.02
3	6	0.00	0.00	1.00	1.93
4	7	1.07	-18.67	0.99	0.62
5	8	0.00	0.00	1.00	3.80
6	9	1.41	-26.15	0.96	-4.35

Tab. 4.5. The nodal admittance matrix for the power system from Fig. 4.3.

	1	2	3	4	5	6	7	8	9
1	j 17.36	0	0	j 17.36	0	0	0	0	0
2	0	-j 16.00	0	0	0	0	0	j 16.00	0
3	0	0	j 17.06	0	0	j 17.06	0	0	0
4	j 17.36	0	0	3.31-j 39.31	-1.94+j 10.51	0	0	0	-1.37+j 11.60
5	0	0	0	-1.94+j 10.51	3.22-j 15.84	-1.28+j 5.59	0	0	0
6	0	0	j 17.06	0	-1.28+j 5.59	2.44-j 32.15	-1.16+j 9.78	0	0
7	0	0	0	0	0	-1.16+j 9.78	2.77-j 23.30	-1.62+j 13.70	0
8	0	j 16.00	0	0	0	0	-1.62+j 13.70	2.8-j 35.45	-1.19+j 5.98
9	0	0	0	-1.37+j 11.6	0	0	0	-1.19+j 5.98	2.55-j 17.34

Tab. 4.6. The matrix \bar{Y}_{RR} .

	1	2	3
1	j 17.36	0	0
2	0	-j 16.00	0
3	0	0	j 17.06

Tab. 4.7. The matrix \bar{Y}_{RE} .

	1	2	3	4	5	6
1	j 17.36	0	0	0	0	0
2	0	0	0	0	j 16.00	0
3	0	0	j 17.06	0	0	0

Tab. 4.8. The matrix \bar{Y}_{ER} .

	1	2	3
1	j 17.36	0	0
2	0	0	0
3	0	0	j 17.06
4	0	0	0
5	0	j 16.00	0
6	0	0	0

Tab. 4.9. The matrix \bar{Y}_{EE} .

	1	2	3	4	5	6
1	3.31- j 39.31	-1.94+ j 10.51	0	0	0	-1.37+ j 11.60
2	-1.94+ j 10.51	3.22- j 15.84	-1.28+ j 5.59	0	0	0
3	0	-1.28+ j 5.59	2.44- j 32.15	-1.16+ j 9.78	0	0
4	0	0	-1.16+ j 9.78	2.77- j 23.30	-1.62+ j 13.70	0
5	0	0	0	-1.62+ j 13.70	2.8- j 35.45	-1.19+ j 5.98
6	-1.37+ j 11.6	0	0	0	-1.19+ j 5.98	2.55- j 17.34

Tab. 4.10. The matrix \bar{Y}_R .

	1	2	3
1	0.54-j 4.34	-0.24+j 2.43	-0.30+j 2.42
2	-0.24+j 2.43	0.39-j 4.95	-0.15+j 2.95
3	-0.30+j 2.42	-0.15+j 2.95	0.45-j 4.90

Tab. 4.11. The matrix \bar{K}_f .

	1	2	3	4	5	6
1	0.75-j 0.03	0.55-j 0.02	0.14+j 0.02	0.15+j 0.02	0.15+j 0.01	0.55-j 0.03
2	0.14+j 0.01	0.15+j 0.01	0.17+j 0.009	0.48-j 0.01	0.69-j 0.02	0.33+j 0.01
3	0.14+j 0.02	0.35+j 0.006	0.71-j 0.03	0.41-j 0.006	0.18+j 0.01	0.16+j 0.02

Tab. 4.12. The elements of the vector \bar{I}_R calculated from the formula (4.6), and the elements of the vectors $\bar{Y}_R \bar{V}_R$, and $\Delta \bar{I}_R$, which are components of the sum in the formula (4.6).

No. of element	No. of node	\bar{I}_R		$\bar{Y}_R \bar{V}_R$		$\Delta \bar{I}_R$	
		Magnitude p.u.	Phase angle degrees	Magnitude p.u.	Phase angle degrees	Magnitude p.u.	Phase angle degrees
1	1	0.76	-18.50	0.72	146.69	1.46	-25.68
2	2	1.64	4.60	0.80	43.49	1.13	-21.56
3	3	0.85	7.23	0.46	101.15	1.00	-20.37

4.2.2. NODE AGGREGATION USING THE DIMO'S METHOD

The aim of the method is replacing a group of nodes $\{A\}$ by an equivalent node a (Fig. 4.4) [4.1]-[4.3].

In the first step of the transformation, some fictitious branches are added to the aggregated nodes, constituting the set $\{A\}$.

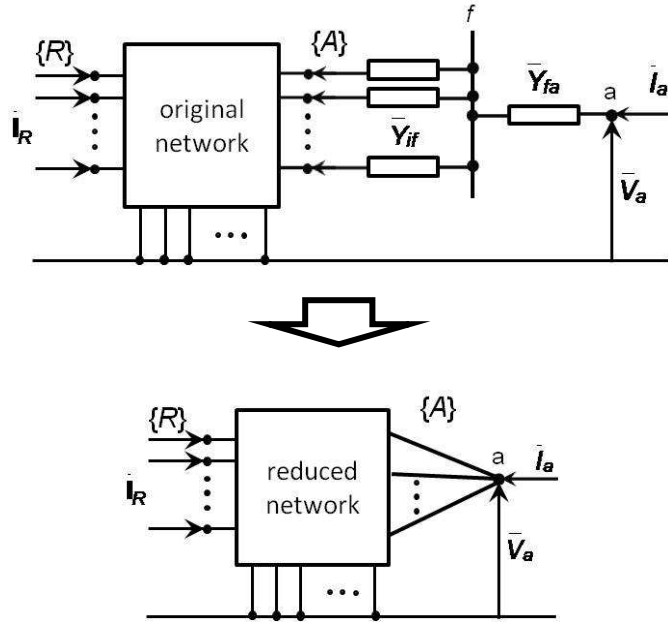


Fig. 4.4. The reduction of the network by aggregation of nodes using the Dimo's method.

The admittance of each of the fictitious branches is expressed by the formula

$$\bar{Y}_{if} = \frac{\bar{S}_i^*}{V_i^2} \quad \text{for } i \in \{A\}. \quad (4.13)$$

To obtain an equivalent node operating at nonzero voltage an extra fictitious branch with negative admittance is usually added to node a (Fig. 4.4)

$$\bar{Y}_{fa} = \frac{\bar{S}_a^*}{V_a^2}, \quad (4.14)$$

where: $\bar{S}_a = \sum_{i \in \{A\}} \bar{S}_i$,

$$\bar{V}_a = \frac{\sum_{i \in \{A\}} \bar{S}_i}{\sum_{i \in \{A\}} \left(\frac{\bar{S}_i}{\bar{V}_i} \right)^*}.$$

Features of aggregation of nodes using Dimo's method

4. If the assumption, that admittances of the fictitious branches are constant, is not valid, the obtained equivalent will only imitate the external network accurately.
5. The Dimo's method produces a large number of fictitious branches due to the elimination of node f and nodes $\{A\}$.
6. A result of the Dimo's method may be branches with negative admittances, of which real parts have essential significance. This fact may cause convergence problems during calculations

4.2.3. NODE AGGREGATION USING THE ZHUKOV'S METHOD

Aim of the Zhukov's method is the same as it is for the Dimo's method, i.e. it is replacing a set of nodes $\{A\}$ by a single equivalent node a (Fig. 4.5) [4.2].

The method ensures satisfaction of the conditions:

1. The currents and voltages, i.e. $\bar{\mathbf{I}}_R$ and $\bar{\mathbf{V}}_R$, at the retained nodes cannot be changed.
2. $\bar{\mathbf{S}}_a = \sum_{i \in \{A\}} \bar{\mathbf{S}}_i$, where $\bar{\mathbf{S}}_i$ - power injection at the aggregated node i .

Before aggregation of nodes, the network is described by the formula

$$\begin{bmatrix} \bar{\mathbf{I}}_R \\ \bar{\mathbf{I}}_A \end{bmatrix} = \begin{bmatrix} \bar{\mathbf{Y}}_{RR} & \bar{\mathbf{Y}}_{RA} \\ \bar{\mathbf{Y}}_{AR} & \bar{\mathbf{Y}}_{AA} \end{bmatrix} \begin{bmatrix} \bar{\mathbf{V}}_R \\ \bar{\mathbf{V}}_A \end{bmatrix}, \quad (4.15)$$

where A – denotes the set of aggregated nodes.

After aggregation of nodes, the following relationship is valid

$$\begin{bmatrix} \bar{\mathbf{I}}_R \\ \bar{\mathbf{I}}_a \end{bmatrix} = \begin{bmatrix} \bar{\mathbf{Y}}_{RR} & \bar{\mathbf{Y}}_{Ra} \\ \bar{\mathbf{Y}}_{aR} & \bar{\mathbf{Y}}_{aa} \end{bmatrix} \begin{bmatrix} \bar{\mathbf{V}}_R \\ \bar{\mathbf{V}}_a \end{bmatrix} \quad (4.16)$$

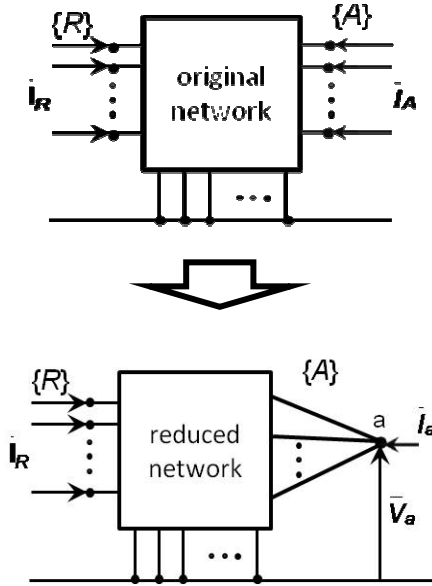


Fig. 4.5. The reduction of the network by aggregation of nodes using the Zhukov's method.

The condition: „The currents and voltages $\bar{\mathbf{I}}_R$ and $\bar{\mathbf{V}}_R$, at the retained nodes cannot be changed.” is satisfied when

$$\bar{\mathbf{Y}}_{RR} \bar{\mathbf{V}}_R + \bar{\mathbf{Y}}_{RA} \bar{\mathbf{V}}_A = \bar{\mathbf{Y}}_{RR} \bar{\mathbf{V}}_R + \bar{\mathbf{Y}}_{Ra} \bar{\mathbf{V}}_a \quad (4.17)$$

or

$$\bar{\mathbf{Y}}_{RA} \bar{\mathbf{V}}_A = \bar{\mathbf{Y}}_{Ra} \bar{\mathbf{V}}_a. \quad (4.18)$$

If the above condition is to be satisfied for any vector $\bar{\mathbf{V}}_A$, it must hold that

$$\bar{\mathbf{Y}}_{Ra} = \bar{\mathbf{Y}}_{RA} \bar{\mathbf{G}}, \quad (4.19)$$

where $\bar{\mathbf{G}} = \bar{\mathbf{V}}_a^{-1} \bar{\mathbf{V}}_A$.

The condition: $\bar{\mathbf{S}}_a = \sum_{i \in \{A\}} \bar{\mathbf{S}}_i$ is satisfied when

$$\bar{\mathbf{V}}_a \bar{\mathbf{I}}_a^* = \bar{\mathbf{V}}_A^* \bar{\mathbf{I}}_A^*, \quad (4.20)$$

what is equivalent with

$$\bar{\mathbf{V}}_a \bar{\mathbf{Y}}_{aR}^* \bar{\mathbf{V}}_R^* + \bar{\mathbf{V}}_a \bar{\mathbf{Y}}_{aa}^* \bar{\mathbf{V}}_a^* = \bar{\mathbf{V}}_A^T \bar{\mathbf{Y}}_{AR}^* \bar{\mathbf{V}}_R^* + \bar{\mathbf{V}}_A^T \bar{\mathbf{Y}}_{AA}^* \bar{\mathbf{V}}_A^*. \quad (4.21)$$

If the equation (4.21) is to be satisfied for any vector $\bar{\mathbf{V}}_A$, it must hold that

$$\bar{\mathbf{Y}}_{aR} = \bar{\mathbf{G}}^{*T} \bar{\mathbf{Y}}_{AR} \quad (4.22)$$

and

$$\bar{\mathbf{Y}}_{aA} = \bar{\mathbf{G}}^{*T} \bar{\mathbf{Y}}_{AA} \bar{\mathbf{G}}. \quad (4.23)$$

One can note, that:

1. The admittances of the equivalent branches linking the equivalent node with the retained nodes depend on $\bar{\mathbf{G}}$, and hence on the voltage angle at the equivalent node δ_a .
2. To have equivalent branches with low resistances the angle δ_a is assumed to be calculated from:

for steady-state analysis

$$\delta_a = \frac{\sum_{i \in \{A\}} S_i \delta_i}{\sum_{i \in \{A\}} S_i}, \quad (4.24)$$

for aggregation of a group of generators in the transient stability model

$$\delta'_a = \frac{\sum_{i \in \{A\}} M_i \delta'_i}{\sum_{i \in \{A\}} M_i}, \quad (4.25)$$

where $M_i = T_{mi} S_{ni} / \omega_s$ the inertia coefficient of the unit installed at the i -th aggregated node.

Features of aggregation of nodes using the Zhukov's method

1. The admittances in the equivalent Zhukov's network depend on the vector $\bar{\mathbf{G}}$. This means that an equivalent network obtained for an initial (pre-fault) state is only valid for other states (transient or steady-state), if $\bar{\mathbf{G}}_i$ $i \in \{A\}$ can be assumed to remain constant.
2. The Zhukov's method does not introduce fictitious branches between the retained nodes $\{R\}$. The Zhukov's aggregation introduces some equivalent shunt admittances at these nodes.
3. If the vector $\bar{\mathbf{G}}$ is complex then Zhukov's equivalent admittance matrix is not generally symmetric ($\bar{\mathbf{Y}}_{aR} \neq \bar{\mathbf{Y}}_{Ra}^T$). This means that if $\bar{Y}_{ia} \neq \bar{Y}_{ai}$ for $i \in \{R\}$, then

the values of the admittances in the equivalent branches obtained after aggregation are direction dependent.

PROBLEMS

- 4.1. What are the reasons for power-system model reductions?
- 4.2. How can we distinguish model-reduction methods?
- 4.3. What is an admittance of the fictitious branch, which is added to the node a (Fig. 4.5), when the node aggregation with the use of the Dimo's method is utilized? What does this admittance depend on?
- 4.4. What is the nodal admittance matrix after node aggregation with the use of the Zhukov's method?
- 4.5. What are differences between the Dimo's method and the Zhukov's method?

REFERENCES

- [4.1] P. Dimo, *Nodal Analysis of Power Systems*. Taylor & Francis, 1975.
- [4.2] J. Machowski, J.W. Bialek, J.R. Bumby, *Power System Dynamics and Stability*. John Wiley and Sons, 1997.
- [4.3] S.C. Savulescu, *Equivalents for Security Analysis of Power Systems*. *IEEE Trans. on Power Apparatus and Systems*, Vol. 100, No. 5, May 1981, pp. 2672 – 2682.

5. POWER SYSTEM MODEL REDUCTION. AGGREGATION OF GENERATING UNITS. EQUIVALENT MODELS OF THE EXTERNAL SUBSYSTEM

5.1. INTRODUCTION

Continued development and interconnection of power systems results in increase in model dimension and complexity. Modeling and analysis of systems with more and more complex structure is challenging task. Despite the rapid growth of computing capabilities there is still need of using system equivalents. Equivalent can be defined as simplified model which can represent the original system without loss of any significant characteristic behavior. It can be stated that in practice usually there is no need to model entire power system in details. Using equivalents seems to be advantageous:

- simplified representation by eliminating the elements that are influential in power system operation but they are out of interest,
- avoiding serious difficulties with construction of detailed full scale system model, e.g. problems with data availability,
- improving computational efficiency and simplification of result analysis.

Some drawback of using equivalents concerns on possibility of obtaining inaccurate results. In addition, using simplified representation is usually valid over a limited range of operating conditions. It is worth noting that applying of simplification rules may lead to creation the models with elements and parameters not existed in original system.

Generally, model reduction methods can be classified into the following groups:

- physical reduction – elements without great influence on operation of analyzed system are replaced by very simple models,
- topological reduction – using circuit-theoretic methods do develop equivalents. elimination and/or aggregation of power network nodes in order to simplify the network structure and reduce the number of generating units,
- modal reduction – reduction of the linearized differential equation set describing system in order to suppress the irrelevant system modes.
- identification technique reduction – using real-time data to develop the equivalent by identification or parameter estimation methods without detailed description of the power network.

Topological reduction combined with physical reduction techniques are mainly used in practice. The presented further topology reduction techniques are particularly suitable for static analyses such as load flow. These methods extended by generator coherency recognition and aggregation are also used for dynamic studies, e.g. transient stability. It is worth noting that topological reduction methods can be easily incorporated into power system analysis software. Some other power system equivalent types and application are reviewed in [5.1].

For developing the power system equivalent the whole system is divided into *internal subsystem* and *external subsystem*, as shown in Fig. 5.1.

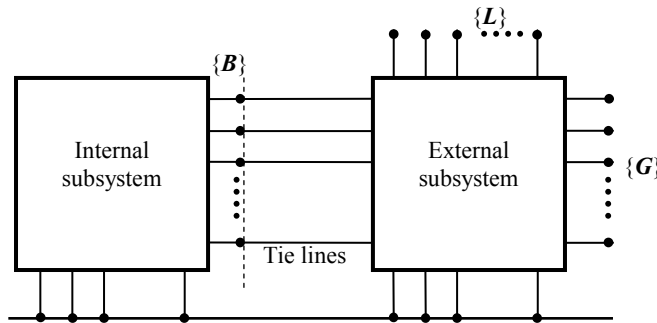


Fig. 5.1. Partitioning of power system into internal and external subsystem. $\{B\}$ – set of boundary nodes, $\{G\}$ – set of external subsystem generator nodes, $\{L\}$ – set of external subsystem load nodes.

The external subsystem is connected with internal one via tie lines adjacent to boundary buses. Internal subsystem is part of the system under study and with detailed representation of network elements, usually equipped with own energy management system. External subsystem is replaced by equivalent network which contains only a few boundary nodes and some nodes remained after original network transformations. Eliminated nodes are completely removed from equivalent and aggregated group of nodes is replaced by one node. In addition, branch parameters of equivalent are also modified.

5.2. EQUIVALENT MODELS OF EXTERNAL SUBSYSTEMS

The node elimination and aggregation presented in Chapter 4 can be used to develop the equivalent for static steady state. After identification of boundary nodes which cannot be eliminated, eliminated and aggregated nodes are selected. The network transformation are applied in order to obtain static equivalent.

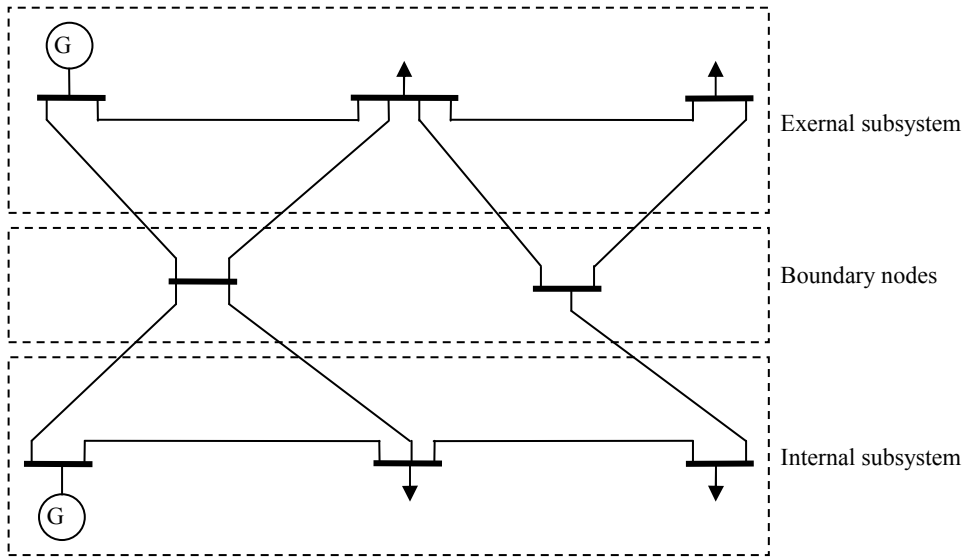


Fig. 5.2. Example power system divided into internal subsystem, external subsystem, and boundary nodes.

Equivalent for the external subsystem for dynamic studies is made in the following steps:

1. Identification of external subsystem and boundary nodes.
2. Elimination/aggregation of the load nodes in the external subsystem.
3. Recognition of coherent groups of generators.
4. Aggregation of the coherent groups of generators.

After dividing power system into internal and external subsystem the sets of retained and eliminated nodes in external network are distinguished. Retained nodes belong to external subsystem being also a node of equivalent network. Nodes which are in original external subsystem but do not appear in of equivalent (their presence is approximated by equivalent) are defined as eliminated nodes. Load nodes are eliminated from external subsystem by topological reduction. After identification of coherent generating units, each coherent group is represented by one equivalent generator. The resulting equivalent network of external subsystem contains only border nodes and nodes with aggregated generating units connected.

5.2.1. ELIMINATION AND AGGREGATION NODES

Considering the external subsystem in separately from internal part as shown in Fig. 5.2 the following network equations can be derived:

$$\begin{bmatrix} \underline{\mathbf{I}}_B \\ \underline{\mathbf{I}}_G \\ \underline{\mathbf{I}}_L \end{bmatrix} = \begin{bmatrix} \underline{\mathbf{Y}}_{BB} & \underline{\mathbf{Y}}_{BG} & \underline{\mathbf{Y}}_{BL} \\ \underline{\mathbf{Y}}_{GB} & \underline{\mathbf{Y}}_{GG} & \underline{\mathbf{Y}}_{GL} \\ \underline{\mathbf{Y}}_{LB} & \underline{\mathbf{Y}}_{LG} & \underline{\mathbf{Y}}_{LL} \end{bmatrix} \begin{bmatrix} \underline{\mathbf{V}}_B \\ \underline{\mathbf{V}}_G \\ \underline{\mathbf{V}}_L \end{bmatrix}, \quad (5.1)$$

where: $\underline{\mathbf{I}}_B$, $\underline{\mathbf{I}}_G$, $\underline{\mathbf{I}}_L$ – injection current vectors for boundary, generation and load nodes respectively;

$\underline{\mathbf{V}}_B$, $\underline{\mathbf{V}}_G$, $\underline{\mathbf{V}}_L$ – nodal voltage vectors for boundary, generation and load nodes respectively;

$\underline{\mathbf{Y}}_{BB}$, $\underline{\mathbf{Y}}_{GG}$, $\underline{\mathbf{Y}}_{LL}$ –self-admittance matrix derived for boundary generation and load nodes respectively;

$\underline{\mathbf{Y}}_{BG}$, $\underline{\mathbf{Y}}_{BL}$ – mutual-admittance matrices for boundary nodes;

$\underline{\mathbf{Y}}_{GB}$, $\underline{\mathbf{Y}}_{GL}$ – mutual-admittance matrices for generation nodes;

$\underline{\mathbf{Y}}_{LB}$, $\underline{\mathbf{Y}}_{LG}$ – mutual-admittance matrices for load nodes.

After elimination of load nodes, the node currents for retained nodes (boundary and generating nodes) can be calculated from:

$$\begin{bmatrix} \underline{\mathbf{I}}_B \\ \underline{\mathbf{I}}_G \end{bmatrix} = \begin{bmatrix} \underline{\mathbf{Y}}_B - \underline{\mathbf{Y}}_{BL} \underline{\mathbf{Y}}_{LL}^{-1} \underline{\mathbf{Y}}_{LB} & \underline{\mathbf{Y}}_{BG} - \underline{\mathbf{Y}}_{BL} \underline{\mathbf{Y}}_{LL}^{-1} \underline{\mathbf{Y}}_{LG} \\ \underline{\mathbf{Y}}_{GB} - \underline{\mathbf{Y}}_{GL} \underline{\mathbf{Y}}_{LL}^{-1} \underline{\mathbf{Y}}_{LB} & \underline{\mathbf{Y}}_G - \underline{\mathbf{Y}}_{GL} \underline{\mathbf{Y}}_{LL}^{-1} \underline{\mathbf{Y}}_{LG} \end{bmatrix} \begin{bmatrix} \underline{\mathbf{V}}_B \\ \underline{\mathbf{V}}_G \end{bmatrix} + \begin{bmatrix} \underline{\mathbf{Y}}_{BL} \underline{\mathbf{Y}}_{LL}^{-1} \\ \underline{\mathbf{Y}}_{GL} \underline{\mathbf{Y}}_{LL}^{-1} \end{bmatrix} \underline{\mathbf{I}}_L. \quad (5.2)$$

The load node elimination can be expressed in simpler form. Let assume that generating and boundary nodes belong to the retained node set $\{\mathbf{R}\}$. The equation (5.2) can be re-written in the form:

$$\begin{bmatrix} \underline{\mathbf{I}}_R \\ \underline{\mathbf{I}}_L \end{bmatrix} = \begin{bmatrix} \underline{\mathbf{Y}}_{RR} & \underline{\mathbf{Y}}_{RL} \\ \underline{\mathbf{Y}}_{LR} & \underline{\mathbf{Y}}_{LL} \end{bmatrix} \begin{bmatrix} \underline{\mathbf{V}}_R \\ \underline{\mathbf{V}}_L \end{bmatrix}. \quad (5.3)$$

Elimination of load nodes by network transformation yields:

$$\underline{\mathbf{I}}_R = \underline{\mathbf{Y}}_R \underline{\mathbf{V}}_R + \underline{\mathbf{K}}_I \underline{\mathbf{I}}_L, \quad (5.4)$$

where: $\underline{\mathbf{Y}}_R = \underline{\mathbf{Y}}_{RR} - \underline{\mathbf{Y}}_{RL} \underline{\mathbf{Y}}_{LL}^{-1} \underline{\mathbf{Y}}_{LR}$,

$$\underline{\mathbf{K}}_I = \underline{\mathbf{Y}}_{RL} \underline{\mathbf{Y}}_{LL}^{-1}.$$

The matrix $\underline{\mathbf{Y}}_{RR}$ is also called transfer matrix and matrix $\underline{\mathbf{K}}_I$ is distribution matrix. It should be underlined that the currents in retained nodes depend on load node current.

If the loads in eliminated nodes are replaced by constant admittances then node currents $\underline{I}_L = \mathbf{0}$ and then term $\underline{K}_L \underline{I}_L$ in (5.3) vanishes. For load power $\underline{S}_{Li} = P_{Li} + jQ_{Li}$ in the node i and the node voltage \underline{V}_i the equivalent load admittance is derived from:

$$\underline{Y}_{Li} = \frac{P_{Li}}{V_i^2} - j \frac{Q_{Li}}{V_i^2}. \quad (5.5)$$

The equivalent admittances are added (with appropriate sign) to corresponding diagonal terms of \underline{Y}_{LL} matrix.

Equation (5.2) and (5.3) describe the equivalent network consisting only of boundary and generator nodes. Hence, it is also called *PV* equivalent (similarly as generating node type in load flow studies) or *PV-Ward* equivalent (this equivalent method was originally proposed by J. B. Ward in the mid of the 20-th century) [5.11].

It should be underlined that Ward equivalent is accurate at the operating point at which is derived. If the operating point moves away from the base point then the equivalent model does not represent the external subsystem accurately.

Some analyses require adjustment of power demand in external subsystem and flows through tie lines. In such case some selected nodes are replaced by the Dimo's REI equivalent.

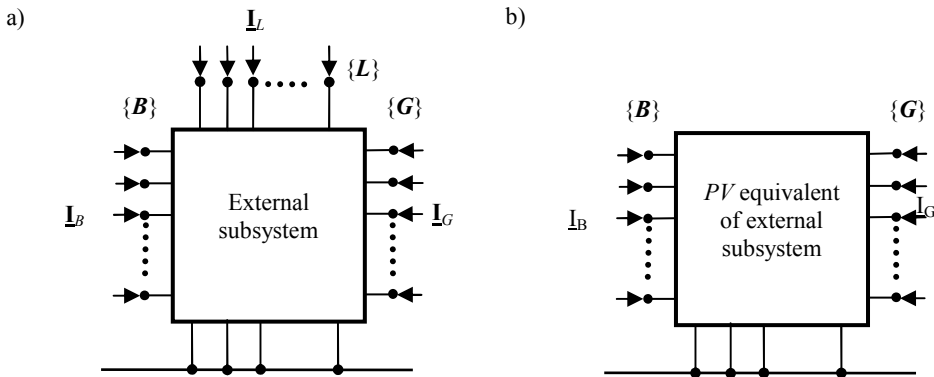


Fig. 5.3. Load node elimination: network before transformation (a), network after transformation (b).
 $\{B\}$ – set of boundary nodes, $\{G\}$ – set generation nodes, $\{L\}$ – set of load nodes.

The objective of radial equivalent independent (REI) method originally proposed by Dimo [5.3] is to replace external network by aggregating injections of a group of the nodes belonging to external subsystem. Radial links connect fictitious node which is added to the internal system and aggregated node. Each radial branch admittance is chosen in a such way as to make the terminal voltage of all the added branches equal. The nodes in external system are grouped according to a certain common criterion

such as geographical or electrical distance, operation control area, generation or load type.

Steps of formulation REI equivalent for external subsystem are shown in Fig. 5.4.

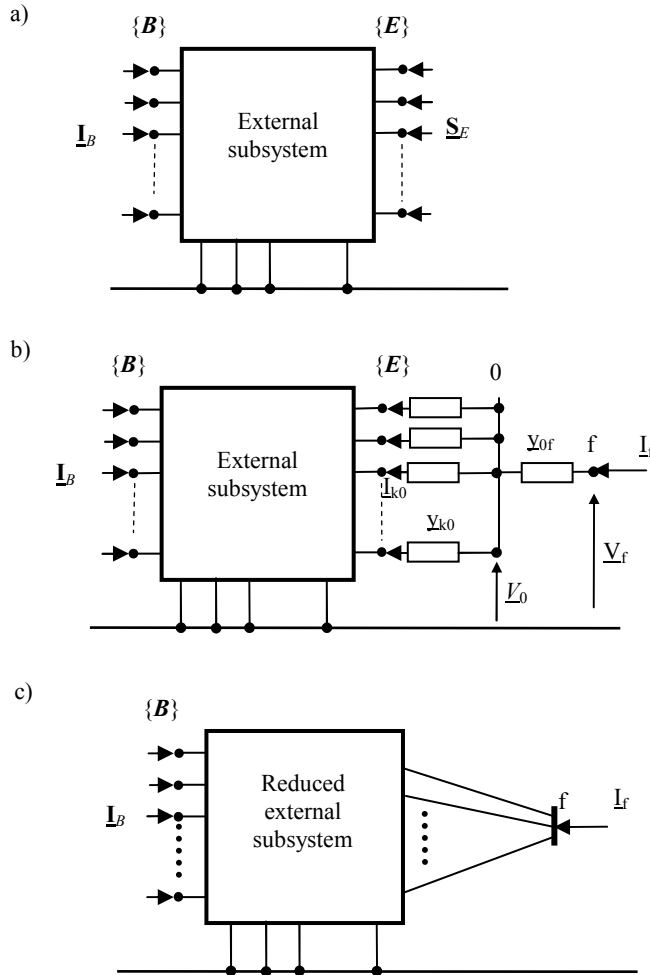


Fig. 5.4. External subsystem reduction using REI method: original subsystem (a), network with additional branches (b), network after elimination of node 0 (c).
 $\{B\}$ – boundary node set, $\{E\}$ – external subsystem node set.

Complex power \underline{S}_f injected into node f is an algebraic sum of node power \underline{S}_k in external subsystem:

$$\underline{S}_f = \sum_{k \in \{E\}} \underline{S}_k \cdot \quad (5.6)$$

Node currents for f and k can be calculated from the relationships:

$$\underline{I}_f = \underline{I}_{f0} = \left(\frac{\underline{S}_f}{\underline{V}_f} \right)^* = y_{\underline{0}f} (\underline{V}_f - \underline{V}_0), \quad (5.7)$$

$$\underline{I}_k = \left(\frac{\underline{S}_k}{\underline{V}_k} \right)^* = y_{\underline{0}k} (\underline{V}_0 - \underline{V}_k). \quad (5.8)$$

It is convenient to set $\underline{V}_0 = 0$. Hence, the REI admittances are:

$$y_{\underline{0}f} = \frac{I_f^2}{\underline{S}_f}, \quad (5.9)$$

$$y_{\underline{0}k} = -\frac{\underline{S}_k^*}{V_f^2}. \quad (5.10)$$

The voltage \underline{V}_f at the equivalent node is equal to the weighted average of the voltages at the aggregated nodes:

$$\underline{V}_f = \frac{\sum_{k \in \{E\}} \underline{S}_k}{\sum_{k \in \{E\}} \left(\frac{\underline{S}_k}{\underline{V}_k} \right)^*}. \quad (5.11)$$

Network matrix equation for REI equivalent shown in Fig. 5.4b is as follows:

$$\begin{bmatrix} \underline{I}_B \\ \underline{I}_f \\ \underline{I}_E \\ \underline{I}_0 \end{bmatrix} = \begin{bmatrix} \underline{Y}_{BB} & \mathbf{0} & \underline{Y}_{BE} & \mathbf{0} \\ \mathbf{0} & \underline{Y}_{ff} & \mathbf{0} & -y_{\underline{0}f} \\ \underline{Y}_{EB} & \mathbf{0} & \underline{Y}_{EE} & \underline{Y}_{E0} \\ \mathbf{0} & -y_{\underline{0}f} & \underline{Y}_{0E} & \underline{Y}_{00} \end{bmatrix} \begin{bmatrix} \underline{V}_B \\ \underline{V}_f \\ \underline{V}_E \\ \underline{V}_0 \end{bmatrix}. \quad (5.12)$$

Because V_0 and node current I_E and I_0 are equal to zero the matrix equation (5.12) can be rewritten in the following form:

$$\begin{bmatrix} \underline{I}_B \\ \underline{I}_f \\ \mathbf{0} \\ 0 \end{bmatrix} = \begin{bmatrix} \underline{Y}_{BB} & \mathbf{0} & \underline{Y}_{BE} & \mathbf{0} \\ \mathbf{0} & \underline{Y}_{ff} & \mathbf{0} & -\underline{y}_{0f} \\ \underline{Y}_{EB} & \mathbf{0} & \underline{Y}_{EE} & \underline{Y}_{E0} \\ \mathbf{0} & -\underline{y}_{0f} & \underline{Y}_{0E} & \underline{Y}_{00} \end{bmatrix} \begin{bmatrix} \underline{V}_B \\ \underline{V}_f \\ \underline{V}_E \\ 0 \end{bmatrix}, \quad (5.13)$$

where: \underline{Y}_{BB} – a self admittance matrix for boundary nodes;

$\underline{Y}_{EB}, \underline{Y}_{BE}$ – mutual admittance matrices for boundary and external subsystem nodes;

$$\underline{Y}_{00} = \underline{y}_{0f} + \sum_{k \in \{E\}} \underline{y}_{k0};$$

$$\underline{Y}_{ff} = \underline{y}_{0f}; \quad \underline{Y}_{E0} = [\dots \quad -\underline{y}_{k0} \quad \dots]^T,$$

$$\underline{Y}_{0E} = [\dots \quad -\underline{y}_{k0} \quad \dots], \quad k \in \{E\}.$$

Node 0 and nodes from set $\{E\}$ can be eliminated with use of the node elimination method (e.g. with Gauss elimination). After removing these nodes the network equation of the equivalent :

$$\begin{bmatrix} \underline{I}_B \\ \underline{I}_f \end{bmatrix} = \begin{bmatrix} \underline{Y}'_{BB} & \underline{Y}'_{Bf} \\ \underline{Y}'_{fB} & \underline{Y}'_{ff} \end{bmatrix} \begin{bmatrix} \underline{V}_B \\ \underline{V}_f \end{bmatrix}. \quad (5.14)$$

where: \underline{Y}'_{BB} – a self admittance matrix for boundary nodes after elimination;

$\underline{Y}'_{Bf}, \underline{Y}'_{fB}$ – mutual admittances for boundary and equivalent node;

\underline{Y}'_{ff} – a self admittance of equivalent node.

REI networks can be also derived multiple equivalent nodes, e.g. for generating and load power separately (Fig. 5.5).

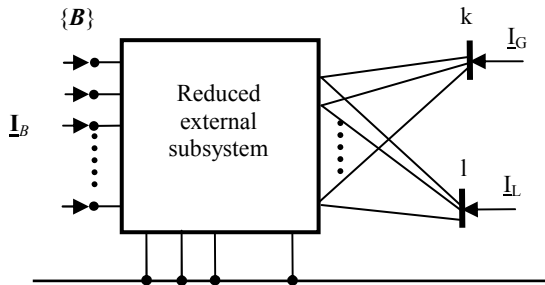


Fig. 5.5. External subsystem reduction using REI for generating and load nodes.

Summarizing, in Ward equivalents it is difficult to analyze generation and load variations in external subsystem. Due to the presence of generation and load node (or nodes) in the REI network, investigation of generation and load changes in the subsystem is much more convenient. However, admittances of fictitious branches in the REI network (significant resistances, negative admittances) do not have simple physical interpretation.

5.2.2. GENERATOR COHERENCY RECOGNITION

The step before aggregation of generating units is identification of coherent groups of generators. The classical method for coherency identification is simulation in time domain. The response of the system to the specified disturbance is computed and rotor angle changes of generators are compared. The generators which swing together (have similar speed deviation) are considered as coherent (Fig. 5.6).

The generating nodes can be aggregated if the coherency condition is satisfied:

$$|\delta_i(t) - \delta_j(t)| = |\delta_{ij0}(t)| \leq \varepsilon, \quad t \in (0, T), \quad (5.15)$$

where: $\delta_i(t), \delta_j(t)$ – generator rotor angles;
 ε – an assumed angle tolerance level;
 T – a simulation time.

Several methods for generator coherence identification can be divided into the following groups:

- simulation of the system perturbation with use of non-linear model,
- simulation of the system perturbation with use of linearized model,
- using relationships describing system parameters and perturbation without simulation – coherence prediction.

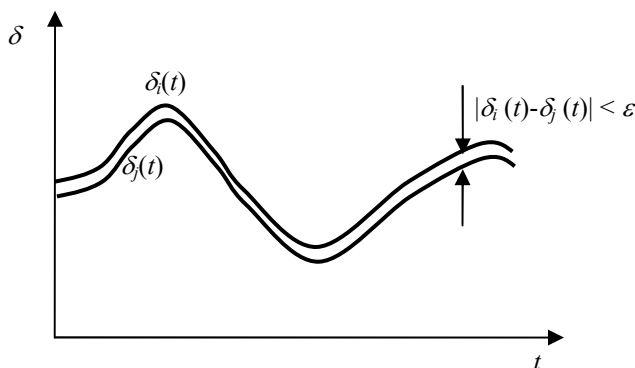


Fig. 5.6. Rotor angle variations of coherent generators

The methods of coherency identification use various techniques to recognize such coherent groups, e.g.:

- concept of distance measure,
- singular point analysis,
- equal angular deviation,
- mean square criterion,
- Taylor series expansion,
- frequency response,
- energy function.

Identification of generator coherent groups in the presence of certain perturbation and system parameters is also possible without making time domain simulation, i.e. the coherence prediction.

The real power produced by the i -th generator in the external subsystem is [5.6]:

$$P_i = V_i^2 G_{ii} + \sum_{k \in \{B\}} V_i V_k [B_{ik} \sin(\theta'_i - \theta_k) + G_{ik} \cos(\theta'_i - \theta_k)] + \sum_{l \in \{G\}} V_i V_l [B_{il} \sin(\theta'_i - \theta_l) + G_{il} \cos(\theta'_i - \theta_l)] \quad (5.16)$$

where: V_i – a transient electromotive force of the i -th generator;

V_k – a voltage at the border node,

$\theta'_i, \theta_k, \theta_l$ – node voltage angles ;

$G_{ii}, G_{ik}, G_{il}, B_{ik}, B_{il}$ – elements of a transfer admittance matrix (conductances and susceptances),

$\{B\}$ – a set of boundary nodes,

$\{G\}$ – a set of generator nodes.

Neglecting G_{ik}, G_{il} and assuming that the perturbation cause the change in voltage angle of the border node k from initial value θ_{k0} by $\Delta\theta_k$, i.e. $\theta_k = \theta_{k0} + \Delta\theta_k$ and voltages of remaining nodes do not change, for $\Delta\theta_k \approx 0$, $\cos \Delta\theta_k \approx 1$ and $\sin \Delta\theta_k \approx \Delta\theta_k$, the change of active power as a function of $\Delta\theta_k$ is given by:

$$\Delta P_i(\Delta\theta_k) \approx h_{ik} \Delta\theta_k, \quad (5.17)$$

where: $h_{ik} = V_i V_k B_{ik} \cos(\theta_i - \theta_{k0})$ – synchronization power between i -th generator and k -th border node.

The change in synchronization power cause the rotor acceleration:

$$a_i = \frac{d^2 \delta_i}{dt^2} = \frac{\Delta P_i(\Delta\theta_k)}{M_i} = \frac{h_{ik}}{M_i} \Delta\theta_k, \quad i \in \{G\}, k \in \{B\}. \quad (5.18)$$

where: M_i – an inertia of i -th generator;

δ_i – a rotor angle of i -th generator.

If the rotor accelerations of generators i and j caused by the perturbation are equal, the generator are considered as electromechanically coherent:

$$\frac{h_{ik}}{M_i} = \frac{h_{jk}}{M_j}, \quad i \in \{\mathbf{G}\}, k \in \{\mathbf{B}\}. \quad (5.19)$$

The equation corresponds to the fact that the parameter h_{ik} of equivalent branch determines the influence of change in electrical state of node k to the power injected by i -th generator. The value $\frac{h_{ik}}{M_i}$ determines the generator rotor acceleration. The change in electrical state of node k cause the same rotor accelerations of coherent generators.

The condition of coherence is not usually exactly satisfied. The practical rule for identification the coherence is the difference between maximal and minimal value of synchronization power does not exceed the assumed tolerance level ε_h :

$$\max_{i \in G} \frac{h_{ik}}{M_i} - \min_{j \in G} \frac{h_{jk}}{M_j} \leq \varepsilon_h, \quad i, j \in \{\mathbf{G}\}, k \in \{\mathbf{B}\}. \quad (5.20)$$

The value ε_h is usually assumed to be dependent on distance of a certain generator from border nodes.

The coherency identification algorithm contains the following steps [5.6]:

1. Elimination of load nodes and obtaining PV -equivalent.
2. Grouping all the generators in the external subsystem in one coherent group.
3. Ordering all the equivalent lines in ascending order according to the values of synchronization power.
4. Taking the next equivalent line with terminal nodes i and j until no lines left. If all the lines are taken stop the algorithm.
5. If the generator i or j is not suitable for grouping, go to p. 4.
6. If the condition (5.10) is not satisfied for pair i and j go to p. 4. Otherwise create group $\{\mathbf{g}\}$ consisting generators i and j .
7. Search all the generators for a given generator e which satisfy the condition (5.10) for the group $\{\mathbf{g}, e\}$ and gives a minimum value for the difference $\max_{i \in G} \frac{h_{ik}}{M_i} - \min_{i \in G} \frac{h_{ik}}{M_i}$. If such generator cannot be found create new group $\{\mathbf{g}\}$ and go to p. 4. Otherwise go to p. 8.

8. Mark generator g as non-eligible and include it to group $\{\mathbf{g}\}$. Go to p. 7.

Simplified flowchart of the algorithm is presented in Fig. 5.7.

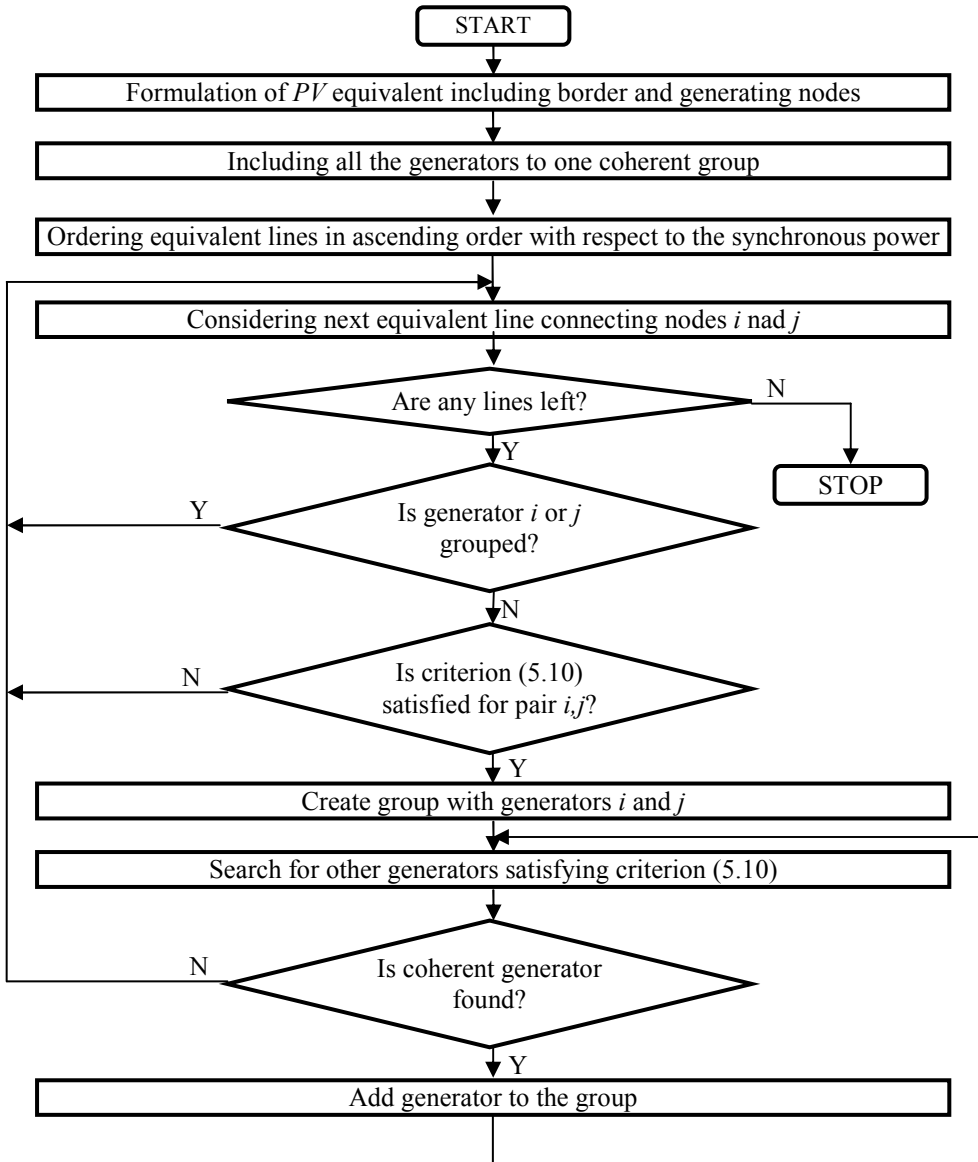


Fig. 5.7. The flow chart of the coherent prediction algorithm.

5.2.3. AGGREGATION OF GENERATING UNITS

After identification of coherent groups, each group is aggregated and replaced to one equivalent generating units as shown in Fig. 5.8. In addition the network is modified to preserve the steady state power flow conditions. Generator nodes belonging to coherent group are linked together and network parameters are updated with use of the selected method.

In dynamic analyses the generator in coherent group can be represented by classical generator model with electromotive force behind transient reactance. Such modeling method assumes neglecting of the control system that exists in the generating units.

Classical model is valid only for few cycles after disturbance. Otherwise, the swing equation should be solved to simulated rotor angle and speed changes in time domain. Considering group coherent generators $\{g\}$, and using the second order motion equation description gives:

$$\begin{aligned} M_i \frac{d\omega_i}{dt} + D_i \omega_i &= P_{m_i} + P_{e_i}, \\ \frac{d\delta_i}{dt} &= \omega_i \end{aligned} \quad (5.21)$$

where: M_i – an inertia;

ω_i – a rotor speed of the i -th generator;

δ_i – a rotor angle of the i -th generator;

D_i – a dumping coefficient;

P_{m_i} – a mechanical power of the i -th generator;

P_{e_i} – an electrical power of the i -th generator; $i \in \{g\}$.

The power generated by equivalent unit is equal to the sum of power generated by the aggregated units. It corresponds to the synchronous rotation of masses one common rigid shaft. The motion equation for equivalent generator is:

$$\left(\sum_{i \in \{g\}} M_i \right) \frac{d\omega}{dt} = \sum_{i \in \{g\}} P_{m_i} - \sum_{i \in \{g\}} P_{e_i} - \left(\sum_{i \in \{g\}} D_i \right) \omega. \quad (5.22)$$

The inertia of the equivalent generator is given by:

$$M_g = \sum_{i \in \{g\}} M_i, \quad (5.23)$$

damping coefficient:

$$D_g = \sum_{i \in \{g\}} D_i, \quad (5.24)$$

electrical and mechanical power:

$$P_{mg} = \sum_{i \in \{g\}} P_{m_i} \quad P_{eg} = \sum_{i \in \{g\}} P_{e_i} . \quad (5.25)$$

For classical generator model the equivalent transient reactance is calculated from parallel connection of reactances of aggregated generators:

$$X'_{d_g} = \frac{1}{\sum_{i \in \{g\}} \frac{1}{X'_{d_i}}} . \quad (5.26)$$

Although aggregation with use classical models is still able to provide a good approximation a detailed aggregation of the control systems: exciter, power system stabilizer, governor is also takes into account. These control system equivalent parameters are obtained from identification procedure. Inclusion of control parameters usually improves the accuracy during time domain simulations.

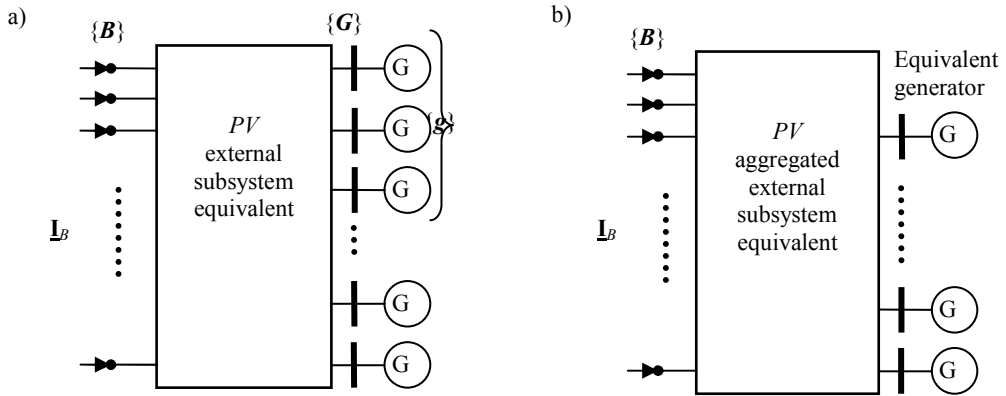


Fig. 5.8. Aggregation of coherent group of generators: network before aggregation (a), network after aggregation (b). $\{g\}$ – coherent group.

Zhukov aggregation method

After insertion of equivalent generator for each coherent group network should be updated to preserve steady state load flow. Due to identification of n coherent generator groups the network equation needs to be re-arranged into the following form:

$$\begin{bmatrix} \underline{\mathbf{I}}_B \\ \underline{\mathbf{I}}_{g1} \\ \vdots \\ \underline{\mathbf{I}}_{gn} \end{bmatrix} = \begin{bmatrix} \underline{\mathbf{Y}}'_{BB} & \underline{\mathbf{Y}}_{Bg1} & \cdots & \underline{\mathbf{Y}}_{Bg2} \\ \underline{\mathbf{Y}}_{g1B} & \underline{\mathbf{Y}}_{g1g2} & \cdots & \underline{\mathbf{Y}}_{g1gn} \\ \vdots & \vdots & \ddots & \vdots \\ \underline{\mathbf{Y}}_{gnB} & \underline{\mathbf{Y}}_{ng2} & \cdots & \underline{\mathbf{Y}}_{ngn} \end{bmatrix} \begin{bmatrix} \underline{\mathbf{V}}_B \\ \underline{\mathbf{V}}_{g1} \\ \vdots \\ \underline{\mathbf{V}}_{gn} \end{bmatrix}, \quad (5.27)$$

where: $\underline{\mathbf{Y}}_{Bgi}$ – an admittance matrix for the network regarding to boundary nodes and generating nodes belonging to the i -th coherent group, $i = 1, 2, \dots, n$;

$\underline{\mathbf{Y}}_{gigj}$ – an admittance matrix for the network regarding to nodes belonging to the i -th and j -th coherent group; $i, j = 1, 2, \dots, n$;

$\underline{\mathbf{V}}_{gi}$ – a voltage vector for nodes belonging to the i -th coherent group;

$\underline{\mathbf{I}}_{gi}$ – a current vector for nodes belonging to the i -th coherent group.

Aggregation of generating nodes for each coherent group yields:

$$\begin{bmatrix} \underline{\mathbf{I}}_B \\ \underline{\mathbf{I}}^a_{g1} \\ \vdots \\ \underline{\mathbf{I}}^a_{gn} \end{bmatrix} = \begin{bmatrix} \underline{\mathbf{Y}}'_{BB} & \underline{\mathbf{Y}}^a_{Bg1} & \cdots & \underline{\mathbf{Y}}^a_{Bgn} \\ \underline{\mathbf{Y}}^a_{g1B} & \underline{\mathbf{Y}}^a_{g1g1} & \cdots & \underline{\mathbf{Y}}^a_{g1gn} \\ \vdots & \vdots & \ddots & \vdots \\ \underline{\mathbf{Y}}^a_{gnB} & \underline{\mathbf{Y}}^a_{ng1} & \cdots & \underline{\mathbf{Y}}^a_{ngn} \end{bmatrix} \begin{bmatrix} \underline{\mathbf{V}}_B \\ \underline{\mathbf{V}}^a_{g1} \\ \vdots \\ \underline{\mathbf{V}}^a_{gn} \end{bmatrix}, \quad (5.28)$$

The admittances can be calculated by applying Zhukov aggregation from the following equations:

$$\underline{\mathbf{Y}}^a_{giB} = \underline{\mathcal{G}}^*_{giB} \underline{\mathbf{Y}}_{giB}, \quad (5.29)$$

where: $\underline{\mathcal{G}}_{giB} = (\underline{\mathbf{V}}^a_{gi})^{-1} \underline{\mathbf{V}}_{gi}$, $i = 1, 2, \dots, n$,

$$\underline{\mathbf{Y}}^a_{gigj} = \underline{\mathcal{G}}^*_{gigj} \underline{\mathbf{Y}}_{gigj} \underline{\mathcal{G}}_{gigj}, \quad (5.30)$$

where: $\underline{\mathcal{G}}_{gigj} = (\underline{\mathbf{V}}^a_{gi})^{-1} \underline{\mathbf{V}}_{gj}$, $i, j = 1, 2, \dots, n$,

$$\underline{\mathbf{Y}}^a_{Bgi} = \underline{\mathbf{Y}}_{Bgi} \underline{\mathcal{G}}_{Bgi}, \quad (5.31)$$

where: $\underline{\mathcal{G}}_{Bgi} = (\underline{\mathbf{V}}^a_{gi})^{-1} \underline{\mathbf{V}}_{gi}$, $i = 1, 2, \dots, n$.

The voltage magnitude and phase for aggregated nodes in steady state static analysis can be calculated as:

$$V_{gi}^a = \frac{\sum_{j \in \{g_i\}} S_j V_j}{\sum_{j \in \{g_i\}} M_j}, \quad \theta_{gi}^a = \frac{\sum_{j \in \{g_i\}} S_j \theta_j}{\sum_{i \in \{g_i\}} S_j}, \quad (5.32)$$

where: S_j – an apparent power injected into the j -th node;

$\{g_i\}$ – a set of nodes belonging to the i -th coherent generator group,

For dynamic analyses equivalent node voltage is weighted sum of aggregated node voltages:

$$V_{gi} = \frac{\sum_{j \in \{g_i\}} M_j V_j}{\sum_{j \in \{g_i\}} M_j}, \quad \theta_{gi} = \frac{\sum_{j \in \{g_i\}} M_j \theta_j}{\sum_{i \in \{g_i\}} M_j}, \quad (5.33)$$

where: M_j – an inertia of generating unit at j -th node;

$\{g_i\}$ – a set of nodes belonging to i -th coherent generator group.

Example 5.1

Replace the external subsystem shown in Fig. 5.9 by PV aggregated equivalent for dynamic study. Generators connected to nodes 2 and 3 are recognized as coherent and modeled as electromotive force behind transient reactance $X'_{d2} = X'_{d3} = 0.015$. Nodes 2' and 3' are internal generator nodes. Inertia of generators $M_2 = M_3 = 6.5$.

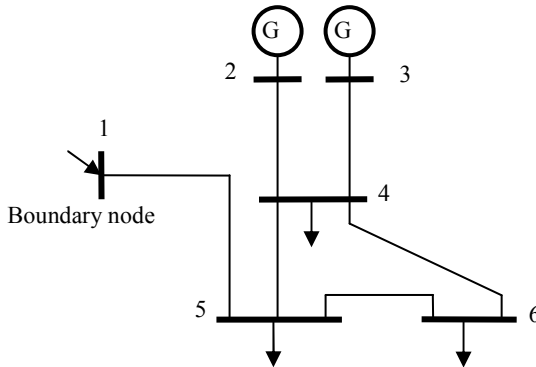


Fig. 5.9. Example external subsystem for dynamic PV aggregated equivalent.

Branch and node parameters are given in Tab. 5.1.

Tab. 5.1. Branch parameters of system shown in Fig. 5.9.

Node i	Node j	R , p.u.	X , p.u.	B , p.u.
1	5	0,02	0,50	0,0
2	4	0,02	0,10	0,0
3	4	0,02	0,10	0,0
4	5	0,03	0,12	0,0
4	6	0,07	0,15	0,0
5	6	0,07	0,20	0,0
2	2'	0,00	0,015	0,0
3	3'	0,00	0,015	0,0

Tab. 5.2. Node data obtained from load flow study.

Node, i	P_{Gi} , p.u.	Q_{Gi} , p.u.	P_{Li} , p.u.	Q_{Li} , p.u.	V_i , p.u.	I_i , p.u.
1	-	-	-	-	1,032-j0,038	0,129-j0,055
2	0.250	0.021	-	-	1,018-j0,061	0,244-j0,038
3	0.250	0.021	-	-	1,018-j0,061	0,244-j0,038
4			0.200	0.020	1,009-j0,085	-0,195+j0,040
5			0.250	0.025	1,003-j0,101	-0,244+j0,050
6			0.180	0.020	0,996-j0,106	-0,177+j0,040

Alternatively, load connected to eliminated nodes can be replaced by constant shunt admittances:

$$y_{L4} = \frac{P_{L4} - jQ_{L4}}{V_4^2} = \frac{0.200 - j0.020}{1.009^2 + 0.085^2} = 0.195 - j0.023,$$

$$y_{L5} = \frac{P_{L5} - jQ_{L5}}{V_5^2} = \frac{0.250 - j0.025}{1.003^2 + 0.101^2} = 0.246 - j0.025,$$

$$y_{L6} = \frac{P_{L6} - jQ_{L6}}{V_6^2} = \frac{0.180 - j0.020}{0.996^2 + 0.106^2} = 0.179 - j0.021,$$

and then load node currents are zero $\mathbf{I}_L = \mathbf{0}$.

The electromotive forces of generators:

$$\underline{E}_2 = \underline{V}_2 + jX'_{d2}I_2 = 1.018 - j0.061 + j0.015(0.244 - j0.038) = 1.018 - j0.057,$$

$$\underline{E}_3 = \underline{V}_3 + jX'_{d3}I_3 = 1.018 - j0.061 + j0.015(0.244 - j0.038) = 1.018 - j0.057.$$

Admittance matrix $\underline{\mathbf{Y}}$ constructed for network with admittance load representation:

	1	2'	3'	2	3	4	5	6
1	0,08- j2,00	0	0	0	0	0	-0,08+ j2,00	0
2'	0	-j66,67	0	j66,67	0	0	0	0
3'	0	0	-j66,67	0	j66,67	0	0	0
2	0	j66,67	0	1,92- j76,28	0	-1,92+ j9,62	0	0
3	0	0	j66,67	0	1,92- j76,28	-1,92+ j9,62	0	0
4	0	0	0	-1,92+ j9,62	-1,92+ j9,62	8,56- j32,57	-1,96+ j7,84	-2,55+ j5,47
5	-0,08+ j2,00	0	0	0	0	-1,96+ j7,84	3,85- j14,32	-1,56+ j4,45
6	0	0	0	0	0	-2,55+ j5,47	-1,56+ j4,45	4,29- j9,95

Set of retaining nodes (generator and boundary nodes): $\{\mathbf{R}\} = \{\mathbf{B}\} \cup \{\mathbf{G}\} = \{1, 2', 3'\}$ and set of eliminated load nodes $\{\mathbf{L}\} = \{2, 3, 4, 5, 6\}$. Matrix $\underline{\mathbf{Y}}$ is split into the self and mutual admittance submatrices:

$$\underline{\mathbf{Y}}_{RR} = \begin{bmatrix} 0.08 - j2.00 & 0 & 0 \\ 0 & -j66.67 & 0 \\ 0 & 0 & -j66.67 \end{bmatrix},$$

$$\underline{\mathbf{Y}}_{RL} = \begin{bmatrix} 0 & 0 & 0 & -0.08 + j2.00 & 0 \\ 0 & 0 & 0 & 0 & 0 \\ j66.67 & 0 & 0 & 0 & 0 \end{bmatrix},$$

$$\underline{\mathbf{Y}}_{LR} = \begin{bmatrix} 0 & j66.67 & 0 \\ 0 & 0 & j66.67 \\ 0 & 0 & 0 \\ -0.08 + j2.00 & 0 & 0 \\ 0 & 0 & 0 \end{bmatrix},$$

$$\underline{\mathbf{Y}}_{LL} = \begin{bmatrix} 1.92 - j76.28 & 0 & -1.92 + j9.62 & 0 & 0 \\ 0 & 1.92 - j76.28 & -1.92 + j9.62 & 0 & 0 \\ -1.92 + j9.62 & -1.92 + j9.62 & 8.56 - j32.57 & -1.96 + j7.84 & -2.55 + j5.47 \\ 0 & 0 & -1.96 + j7.84 & 3.85 - j14.32 & -1.56 + j4.45 \\ 0 & 0 & -2.55 + j5.47 & -1.56 + j4.45 & 4.29 - j9.95 \end{bmatrix}$$

Transfer matrix calculated from (5.4):

$$\underline{\mathbf{Y}}_R = \begin{bmatrix} 0.149 - j1.542 & -0.026 + j0.756 & -0.026 + j0.756 \\ -0.026 + j0.756 & 0.874 - j4.614 & -0.593 + j3.825 \\ -0.026 + j0.756 & -0.593 + j3.825 & 0.874 - j4.614 \end{bmatrix}.$$

The next step is aggregation of nodes 2' and 3'. The voltage in aggregated node:

$$V_{g1}^q = \frac{M_2 E_{2'} + M_3 E_{3'}}{M_2 + M_3} = \frac{6.5 \cdot 1.021 + 6.5 \cdot 1.021}{6.5 + 6.5} = 1.021,$$

$$\theta_{g1}^a = \frac{M_2 \theta_{2'} + M_3 \theta_{3'}}{M_2 + M_3} = \frac{6.5 (-0.056) + 6.5 (-0.056)}{6.5 + 6.5} = -0.056.$$

Voltage of aggregated node is equal to electromotive forces of generator. Hence, transformation ratio is simply:

$$\underline{\mathcal{G}}_{1,g1} = \underline{\mathcal{G}}_{g1,1} = \underline{\mathcal{G}}_{1,1} = 1,$$

Admittance matrices for aggregated PV equivalent are calculated with use of rearranged transfer matrix $\underline{\mathbf{Y}}_R$ are calculated from (5.28) - (5.31) and then:

$$\underline{\mathbf{Y}}'_{BB} = 0.149 - j1.542,$$

$$\underline{\mathbf{Y}}^a_{B,g1} = -0.052 + j1.512,$$

$$\underline{\mathbf{Y}}^a_{g1,B} = -0.052 + j1.512,$$

$$\underline{\mathbf{Y}}^a_{g1,g1} = 0.563 - j1.578.$$

Equivalent network matrix:

$$\underline{\mathbf{Y}}_{eq} = \begin{bmatrix} \underline{\mathbf{Y}}'_{BB} & \underline{\mathbf{Y}}^a_{B,g1} \\ \underline{\mathbf{Y}}^a_{g1,B} & \underline{\mathbf{Y}}^a_{g1,g1} \end{bmatrix} = \begin{bmatrix} 0.149 - j1.542 & -0.052 + j1.512 \\ -0.052 + j1.512 & 0.563 - j1.578 \end{bmatrix}.$$

Slow coherence aggregation algorithm

The coherent generators are aggregated at generator internal nodes. The machine internal node voltages are computed and these nodes are linked to a common bus via phase shifters to preserve power flows. Let consider the part of the system containing two coherent generators as shown in Fig. 5.10.

The algorithm is as follows [5.1]:

1. Computation of voltages of machine internal nodes with use power flow calculation results. Using complex nodal power the node current injection is calculated.
2. Creating the common node p . Calculation of common bus voltage \underline{V}_p with use of inertial weighted average of the internal generator voltages $\underline{E}_i, i \in \{a, b\}$.

$$\underline{V}_p = \frac{M_a \underline{E}_a + M_b \underline{E}_b}{M_a + M_b} \quad (5.34)$$

where: M_i – inertia of i -th generator;

\underline{E}_i – complex internal generator voltage i -th generator.

3. Adding new lines connecting bus p with buses a and b . Calculation of complex voltage transformation ratios:

$$\underline{g}_i = \frac{\underline{V}_p}{\underline{E}_i} = g_i e^{j\phi_i}, \quad i \in \{a, b\}. \quad (5.35)$$

The parameters of new lines are the series connection of reactance jX_{di} and transformer with complex ratio $\underline{g}_i, i \in \{a, b\}$ (Fig. 5.10b). Shunt parameters are neglected.

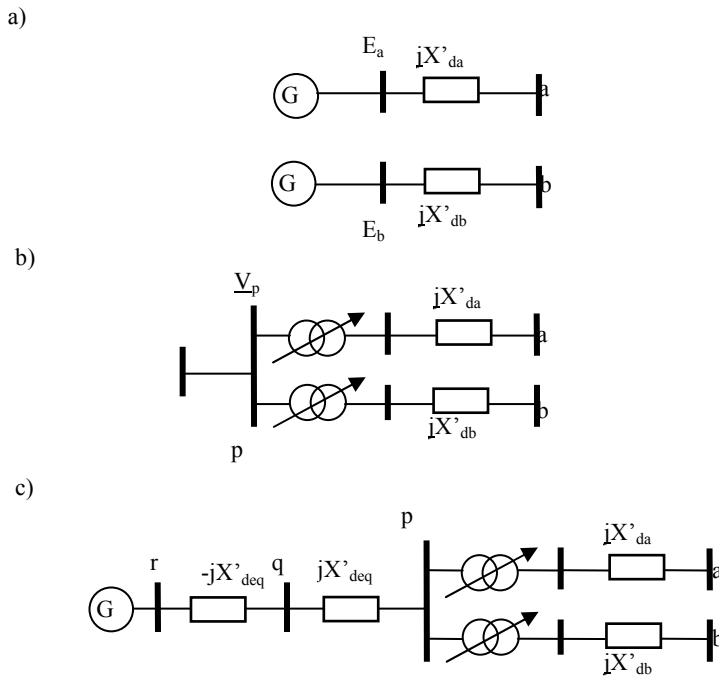


Fig. 5.10. Inertial coherency generator aggregation steps.

4. Computation of inertia and transient reactance of the equivalent generator:

$$M_{eq} = M_a + M_b \quad (5.36)$$

$$X'_{deq} = \frac{1}{\frac{1}{X'_{da}} + \frac{1}{X'_{db}}} \quad (5.37)$$

5. Creating of bus q . This bus cannot be used as generator internal node and the branch connecting nodes p and q with reactance $-jX'_{deq}$ is added, and then to a bus r with line reactance jX'_{deq} . The node p has the same voltage as node r . Bus q is used as terminal and bus r as aggregated generator internal voltage. The voltage at bus q is equal to \underline{V}_q and the power flow to the buses a and b .
6. Adjusting generation at buses a , b , q . Generations at buses a , b are set to zero. The generation on the new terminal bus q is set equal to the power transfer to buses a and b . Bus p does not have any generator or load, and can be eliminated (Fig. 5.10c).

Example 5.2

Aggregate generating units connected to the nodes 4 and 5 as shown in Fig. 5.11 with use of inertial coherence method. Assume classical generator model (electromotive force behind transient reactance). Branch data are as in Example 5.1. Node data obtained from load flow study are presented in Tab. 5.3.

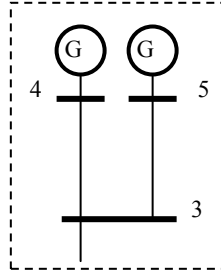


Fig. 5.11. Example system for dynamic inertial aggregation.

Tab. 5.3. Load flow study results for system presented in Fig. 5.11.

Node, <i>i</i>	$P_{Gi,}$ p.u.	$Q_{Gi,}$ p.u.	$P_{Li,}$ p.u.	$Q_{Li,}$ p.u.	$\underline{V}_i,$ p.u.	$\underline{I}_i,$ p.u.
4	0.30	0.085	-	-	1.0035 - j0.114	0.285 - j0.117
5	0.30	0.061	-	-	1.0085 - j0.084	0.291 - j0.084

Generating unit data:

Inertia: $M_4 = 6.5, M_5 = 3.0,$

Transient reactances: $X'_{d4} = 0.12, X'_{d5} = 0.18.$

Inertial aggregation of generating unit is made in the following steps:

1. Generator internal voltages calculated from data:

Electromotive forces behind transient reactances:

$$\underline{E}_4 = \underline{V}_4 + jX'_{d4}\underline{I}_4 = 1.0035 - j0.1140 + j0.12(0.2858 - j0.1167) = 1.0173 - j0.0797,$$

$$\underline{E}_5 = \underline{V}_5 + jX'_{d5}\underline{I}_5 = 1.0085 - j0.0842 + j0.18(0.2905 - j0.0843) = 1.0234 - j0.0319.$$

or in polar form:

$$\underline{E}_4 = 1.0204e^{-j0.0781}, \underline{E}_5 = 1.0239e^{-j0.0311}$$

2. Common bus voltage:

$$\underline{V}_p = \frac{M_4 \underline{E}_4 + M_5 \underline{E}_5}{M_4 + M_5} = \frac{6.5(1.0173 - j0.0797) + 3.0(1.0234 - j0.0319)}{6.5 + 3.0} = 1.0192 - j0.0646$$

3. Voltage transformation ratios:

$$\underline{g}_4 = \frac{V_p}{E_4} = \frac{1.0192 - j0.0646}{1.0173 - j0.0797} = 1.0007 + j0.0149 = 1.0008e^{j0.0149},$$

$$\underline{g}_5 = \frac{V_p}{E_5} = \frac{1.0192 - j0.0646}{1.0234 - j0.0319} = 0.9969 - j0.0320 = 0.9974e^{-j0.0321}.$$

4. Equivalent inertia and transient reactance:

$$M_{eq} = M_4 + M_5 = 6.5 + 3.0 = 9.5,$$

$$X'_{d_{eq}} = \frac{1}{\frac{1}{X'_{d4}} + \frac{1}{X'_{d5}}} = \frac{1}{\frac{1}{0.12} + \frac{1}{0.18}} = 0.072$$

The network scheme with aggregated units is shown in Fig. 5.12.

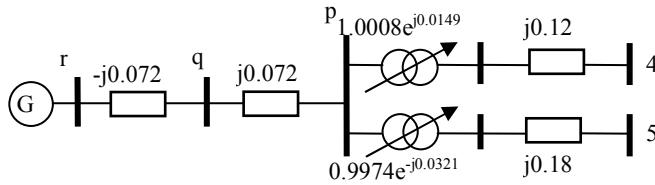


Fig. 5.12. Inertial coherency generator aggregation results.

Slow coherency aggregation algorithm

The slow coherency aggregation uses an impedance modification to the inertial aggregation. Hence, the slow coherency aggregation can be considered as an inertial aggregation with impedance correction.

Slow coherency aggregation procedure uses the linearization at the generator terminal buses. The fast inter-machine variables are then eliminated, and the power network is reconstructed from the reduced linearized model.

The slow coherency aggregation is as follows [5.1]:

1. After performing the steps 1 and 2 for inertial coherency algorithm the swing equations for generators at the operating point are linearized.

$$2H_i \Delta \ddot{\delta}_i = -\frac{E_{i0} V_{i0} \cos(\delta_{i0} - \theta_{i0})}{X'_{di}} \Delta \delta_i - \frac{E_{i0} \sin(\delta_{i0} - \theta_{i0})}{X'_{di}} \Delta V_i + \frac{E_{i0} V_{i0} \cos(\delta_{i0} - \theta_{i0})}{X'_{di}} \Delta \theta_i, \quad (5.38)$$

$$\Delta L_i = -\frac{E_{i0}}{X'_{di}} \Delta \delta_i + \frac{e^{j\theta_{i0}}}{jX'_{di}} \Delta V_i + \frac{V_{i0}}{X'_{di}} \Delta \theta_i, \quad i \in \{a, b\}, \quad (5.39)$$

where: H_i – an inertia,

E_{i0} – an internal generator voltage magnitude,

V_{i0} – a generator terminal voltage,

θ_{i0} – a terminal bus voltage angle,

δ_{i0} – a rotor angle,

ΔI_j – a current injection.

Defining the following vectors:

$$\mathbf{x} = \begin{bmatrix} \Delta \delta_a \\ \Delta \delta_b \end{bmatrix}, \quad \mathbf{z} = \begin{bmatrix} \Delta V_a \\ \Delta V_b \\ \Delta \theta_a \\ \Delta \theta_b \end{bmatrix}, \quad \Delta \mathbf{I} = \begin{bmatrix} \Delta I_a \\ \Delta I_b \end{bmatrix}.$$

The equations can be written in matrix form as:

$$\ddot{\mathbf{x}} = \mathbf{K}_1 \mathbf{x} + \mathbf{K}_2 \mathbf{z}, \quad \Delta \mathbf{I} = \mathbf{K}_3 \mathbf{x} + \mathbf{K}_4 \mathbf{z} \quad (5.40)$$

2. Transforming into slow and fast variables.

When the machines form a slow coherent group, their centre of angle as the slow variables can be obtained, and the inter-machine oscillations as the fast variables. To perform the slow coherency aggregation, the original machine angles are transformed to slow and fast variables. The slow aggregate variable and fast local variable are defined as:

$$\delta_s = \frac{H_a \delta_a + H_b \delta_b}{H_a + H_b} \quad \delta_f = \delta_b - \delta_a. \quad (5.41)$$

The linearized model after applying the transformation results in:

$$\begin{bmatrix} \Delta \ddot{\delta}_s \\ \Delta \ddot{\delta}_f \end{bmatrix} = \begin{bmatrix} \mathbf{K}_{11} & \mathbf{K}_{12} \\ \mathbf{K}_{13} & \mathbf{K}_{14} \end{bmatrix} \begin{bmatrix} \Delta \delta_s \\ \Delta \delta_f \end{bmatrix} + \begin{bmatrix} \mathbf{K}_{21} \\ \mathbf{K}_{22} \end{bmatrix} \mathbf{z}, \quad (5.42)$$

$$\Delta \mathbf{I} = \begin{bmatrix} \mathbf{K}_{31} & \mathbf{K}_{32} \end{bmatrix} \begin{bmatrix} \Delta \delta_s \\ \Delta \delta_f \end{bmatrix} + \mathbf{K}_4 \mathbf{z}. \quad (5.43)$$

3. Creating of slow subsystem.

Neglecting the fast dynamic component $\Delta \delta_f$, the quasi steady-state of slow component:

$$\Delta \bar{\delta}_f = -\mathbf{K}_{14}^{-1} (\mathbf{K}_{13} \Delta \bar{\delta}_s + \mathbf{K}_{22} \mathbf{z}). \quad (5.44)$$

After neglecting $\Delta\hat{\delta}_f$ one can obtain:

$$\Delta\bar{\delta}_s = \mathbf{K}_{1s}\Delta\bar{\delta}_s + \mathbf{K}_{2s}\mathbf{z} \quad \Delta\bar{\mathbf{I}} = \mathbf{K}_{3s}\Delta\bar{\delta}_s + \mathbf{K}_{4s}\mathbf{z}, \quad (5.45)$$

where: $\mathbf{K}_{1s} = \mathbf{K}_{11} - \mathbf{K}_{12}\mathbf{K}_{14}^{-1}\mathbf{K}_{13}$,

$$\mathbf{K}_{2s} = \mathbf{K}_{21} - \mathbf{K}_{12}\mathbf{K}_{14}^{-1}\mathbf{K}_{22},$$

$$\mathbf{K}_{3s} = \mathbf{K}_{31} - \mathbf{K}_{32}\mathbf{K}_{14}^{-1}\mathbf{K}_{13},$$

$$\mathbf{K}_{4s} = \mathbf{K}_4 - \mathbf{K}_{32}\mathbf{K}_{14}^{-1}\mathbf{K}_{22}.$$

Equation (5.42) represents the linearized model for the slow subsystem. The next step is to reconstruct a power network whose linearization would yield equation (5.45). The terms K_{1s} , K_{2s} and K_{3s} are needed to construct lines connecting bus to the original generator terminal buses a and b , and the term K_{4s} is needed for the lines interconnecting buses a and b . The reconstruction will in general require phase shifters. In addition, the reconstruction from K_{4s} will not satisfy the network flow condition. As a result, balancing the power flow is achieved by adding loads to these buses. It is also possible that the impedances from the K_{4s} reconstruction are much larger than those from the K_{2s} , such that the K_{4s} terms can be neglected.

5.3. DYNAMIC EXTERNAL-SUBSYSTEM-EQUIVALENT METHODS

The great variety of methods for obtaining external system equivalent for both steady state and transient operation have been proposed. Topological reduction and coherency approach rely on elimination and aggregation of nodes to reduce equivalent network complexity are presented previously. The other main approaches to dynamic equivalent system are as follows:

- Infinite bus approach: external system is represented by voltage source with constant voltage magnitude and frequency. Dynamical interactions between internal and external subsystem are neglected. The model is very simple but inaccurate.
- Modal approach: set of nonlinear differential equations is linearized and eigenvalues are analyzed. The system matrix is diagonalized and modes having small influence on system are neglected. Assuming the linearized state equation describing the power system:

$$\begin{aligned} \Delta\dot{\mathbf{x}} &= \mathbf{A}\Delta\mathbf{x} + \mathbf{B}\Delta\mathbf{u} \\ \Delta\mathbf{y} &= \mathbf{C}\Delta\mathbf{x} + \mathbf{D}\Delta\mathbf{u} \end{aligned} \quad (5.46)$$

where: \mathbf{A} , \mathbf{B} , \mathbf{C} , \mathbf{D} – state matrices;

$\Delta \mathbf{x}$ – a state vector;

$\Delta \mathbf{u}$ – an input vector;

$\Delta \mathbf{y}$ – an output vector,

the eigensolution is given by:

$$\Delta \mathbf{x}(t) = \sum_{i=1}^n \underline{\Phi}_i e^{\lambda_i t} (\underline{\Psi}_i \Delta \mathbf{x}(0)), \quad (5.47)$$

where: $\underline{\Phi}_i$ – the i -th right eigenvector;

$\underline{\Psi}_i$ – the i -th left eigenvector;

λ_i – the i -th eigenvalue;

n – a system order.

The participation of each state on the mode $e^{\lambda_i t}$ regarding intensity and phase angle is described by the complex right eigenvector $\underline{\Phi}_i$. The excitation of the modes depends on the left eigenvector $\underline{\Psi}_i$ and the initial state.

The reduction of the system order relies on elimination of the modes having small influence on system. Different criteria for mode rejection can be applied. The concept of participation factors assessment is often proposed. Usually the single modes and given state variable dependence is investigated with used of participation factors defined as the sensitivity of the i -th eigenvalue to the k -th diagonal element of state matrix \mathbf{A} :

$$p_{ik} = \frac{\partial \lambda_i}{\partial a_{kk}}. \quad (5.48)$$

where: p_{ik} – a complex participation factor of the state variable \mathbf{x}_k and eigenvalue λ_i .

Using this approach full knowledge on power system parameters is required. New variables obtained during modal analysis do not have simple physical interpretation.

- Identification approach: data obtained from internal system are used. The external system is represented by equivalent with much more simpler structure. An error objective function is used to adjust equivalent parameters subject to minimize discrepancies between original and equivalent system response. It requires few information on external system and external system complexity may be significantly reduced.

Summary of the power reduction methods is presented in Tab. 5.4.

5.4. AGGREGATION OF DISTRIBUTION NETWORKS WITH DISTRIBUTED GENERATION

Distributed Generation (DG) are small generating units embedded in distribution network. With the constantly increase in DG penetration their impact on power network is noticeable, e.g. changes in power flow values and directions, influence on stability etc. and cannot be neglected.

Typically, the power network with DG consists a great amount of generating units, transformers, lines and feeders, capacitor banks etc. Building the detailed model of such network requires many efforts and usually long computation time at simulation step. Instead of using complete model, employing the simplified equivalent following the behavior of the network with satisfied accuracy can be considered.

Most of these units, such as small thermal and hydro power plant, wind turbines, are based on using induction generators. Further, such type of unit is considered.

An example of typical distribution power network with DG is shown in Fig. 5.13.

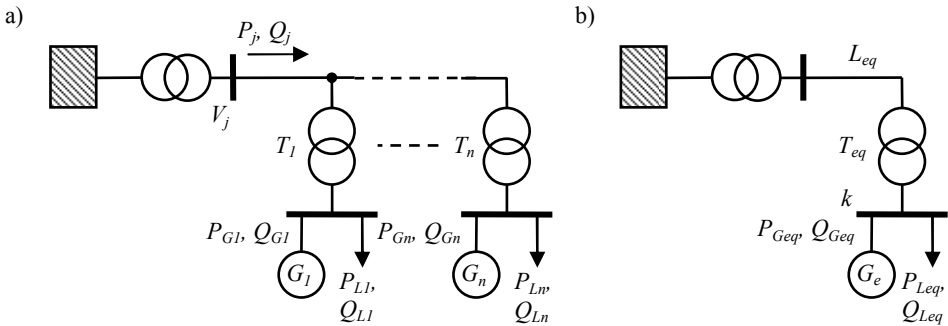


Fig. 5.13. Power network with connected distributed generators (a) and their equivalent (b).

According to 0 the following assumption for creating the equivalent are made:

- active and reactive power flows in the considered network are known,
- generator terminal voltages are assumed to be nominal,
- aggregated induction generator parameters are derived from no-load and rotor-lock test of the parallel operation of individual machines.

No load impedance of i -th machine is as follows:

$$\underline{Z}_{nl,i} = R_{s,i} + j(X_{s,i} + X_{m,i}), \quad (5.49)$$

where: $R_{s,i}$ – a stator resistance;
 $X_{s,i}$ – a stator leakage reactance;
 $X_{m,i}$ – a magnetizing reactance.

Hence, the equivalent no-load impedance:

$$\underline{Z}_{nl,eq} = \frac{1}{\sum_{i=1}^n \frac{1}{\underline{Z}_{nl,i}}} = R_{s,eq} + j(X_{s,eq} + X_{m,eq}), \quad (5.50)$$

where: n – a number of machines in a group.

The impedance of i -th machine for rotor lock:

$$\underline{Z}_{rl,i} = (R_{s,i} + R_{r,i}) + j(X_{s,i} + X_{r,i}), \quad (5.51)$$

where: $R_{r,i}$ – a rotor resistance;

$X_{r,i}$ – a rotor reactance,

and the equivalent impedance of n parallel induction generators:

$$\underline{Z}_{rl,eq} = \frac{1}{\sum_{i=1}^n \frac{1}{\underline{Z}_{rl,i}}} = (R_{s,eq} + R_{r,eq}) + j(X_{s,eq} + X_{r,eq}), \quad (5.52)$$

where: n – a number of machines in a group.

It should be underlined that different types of machines can differ in parameters, so they can be divided into the corresponding sub-groups.

Equivalent generating active and reactive power is obtained from:

$$P_{G,eq} = \sum_{i=1}^g P_{G,i}, \quad (5.53)$$

$$Q_{G,eq} = \sum_{i=1}^g Q_{G,i}, \quad (5.54)$$

where: $P_{G,i}$, $Q_{G,i}$ – an active and a reactive power of the i -th generating unit;

g – a number of generating units.

Similarly, the equivalent load power is derived as:

$$P_{L,eq} = \sum_{i=1}^L P_{L,i}, \quad (5.55)$$

$$Q_{L,eq} = \sum_{i=1}^L Q_{L,i}, \quad (5.56)$$

where: $P_{L,i}$, $Q_{L,i}$ – an active and a reactive power of the i -th load;

L – a number of loads.

The slip of aggregated generator is obtained from 0:

$$s_{eq} = \frac{\sum_{i=1}^g P_i s_i}{P_{G,eq}}, \quad (5.57)$$

where: s_i – a slip of the i -th machine.

Equivalent inertia constant:

$$H_{eq} = \frac{\sum_{i=1}^g H_i P_i}{P_{G,eq}}, \quad (5.58)$$

and equivalent moment of inertia:

$$J_{eq} = \frac{2H_{eq}P_{eq}}{\omega_s^2}, \quad (5.59)$$

where: ω_s – a synchronous angular speed.

Aggregated transformer parameters are derived from the losses of each device. The overall active and reactive power losses:

$$\Delta P_{T,eq} = 3 \sum_{i=1}^t R_{T,i} I_i^2, \quad (5.60)$$

$$\Delta Q_{T,eq} = 3 \sum_{i=1}^t X_{T,i} I_i^2, \quad (5.61)$$

where: $R_{T,i}, X_{T,i}$ – a resistance and a reactance of the i -th transformer;

I_i – a phase current in the branch representing the i -th transformer;

t – a number of transformers.

Hence, the parameters of equivalent transformer:

$$R_{T,eq} = \frac{\Delta P_{T,eq}}{3I_{eq}^2}, \quad (5.62)$$

$$X_{T,eq} = \frac{\Delta Q_{T,eq}}{3I_{eq}^2}, \quad (5.63)$$

where: $I_{eq} = \frac{\sqrt{(P_{G,eq} - P_{L,eq})^2 + (Q_{G,eq} + Q_{L,eq})^2}}{\sqrt{3}V_k}$ – a current magnitude for the aggregated

system;

V_k – a line voltage magnitude the node k (see Fig. 5.13).

Equivalent line parameters are derived from the following equations:

$$R_{B,eq} = \frac{P_M + P_{G,eq} - P_{L,eq} - \Delta P_{T,eq}}{3I_j^2}, \quad (5.64)$$

$$X_{B,eq} = \frac{Q_M - Q_{G,eq} - Q_{L,eq} - \Delta Q_{T,eq}}{3I_j^2}, \quad (5.65)$$

where: $I_j = \frac{\sqrt{P_j^2 + Q_j^2}}{\sqrt{3}V_j}$ – a feeder current magnitude;

V_j – a line voltage magnitude at the node j .

Applying the equivalent procedure is advantageous especially when significant number of generator operates in parallel, e.g. in wind farms. However, it should be underlined that model simplification can lead to the inaccuracies and the equivalent should be assessed if it is capable of giving satisfactory results.

Tab. 5.4. Power network equivalent technique summary.

Equivalence approach	Requirements	Application	Equivalent form
Infinite bus	No	On-line	Voltage source with constant voltage and frequency
Modal analysis	Linearized detailed model	Off-line with small disturbances	Modal quantities
Topological reduction and coherency	Detailed model	Off-line with large disturbances	Aggregated equivalent model
Identification techniques	Impedance characteristics of boundary nodes	On-line	Equivalent circuit

PROBLEMS

- 5.1. In Fig. P.5.1 power system shown where an internal and external subsystems are distinguished. Determine static Ward and REI equivalent of external subsystem. Network parameters and load flow results for base case are in Tab. P.5.1-Tab.P.5.3.

Tab. P.5.1. Branch data for Problem 5.1.

Nodes		Parameters	
i	j	R , p.u.	X , p.u.
6	11	0,09498	0,19890

6	12	0,12291	0,25581
6	13	0,06615	0,13027
9	10	0,03181	0,08450
9	14	0,12711	0,27038
10	11	0,08205	0,19207
12	13	0,22092	0,19988
13	14	0,17093	0,34802

Tab. P.5.2. Load flow data of external system for Problem 5.1.

Node i	V_i , p.u.	θ_i , rad	P_{Li} , p.u.	Q_{Li} , p.u.
10	1,05	-0,26	0,09	0,058
11	1,06	-0,26	0,035	0,018
12	1,06	-0,26	0,061	0,016
13	1,05	-0,26	0,14	0,058
14	1,04	-0,28	0,15	0,05

Tab. P.5.3. Boundary node voltages and injections for Problem 5.1.

Node i	V_i , p.u.	θ_i , rad	$P_{inj,i}$, p.u.	$Q_{inj,i}$, p.u.
6	1,07	-0,25	0,33	0,13
9	1,06	-0,26	0,15	0,078

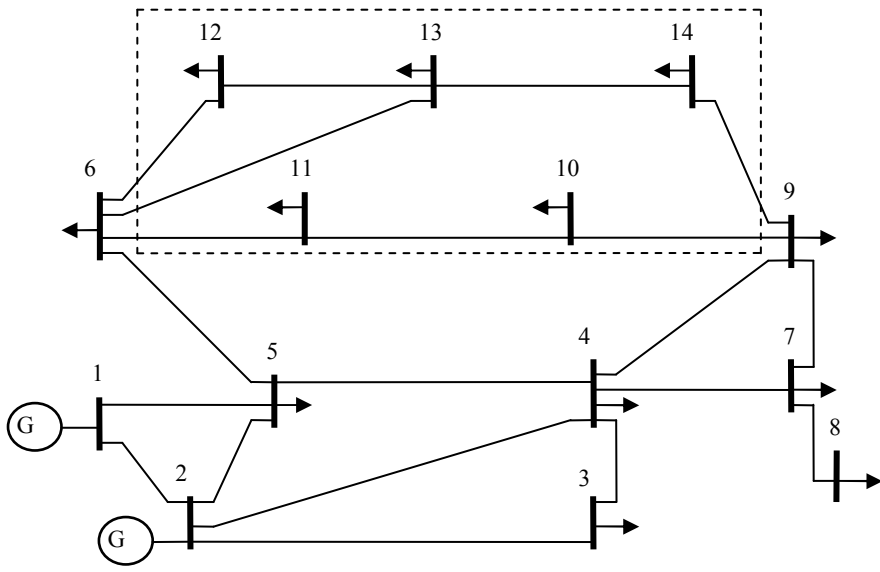


Fig. P.5.1. Power system for Problem 5.1. external subsystem.

5.2. Check the coherency of the generators in power system shown in Fig. P.5.2. If the coherency conditions are satisfied form coherent group and perform the aggregation of generating units with use of Zhukov and inertial coherence algorithm. Assume that generators are represented by classical model (electromotive force behind transient reactance). The system data are given in Tab. P.5.4-Tab.P.5.7.

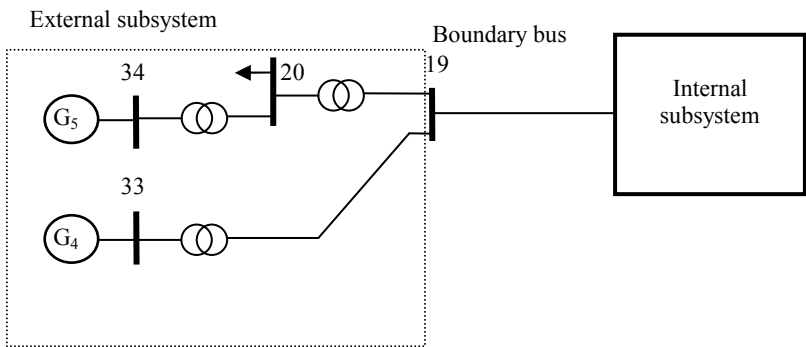


Fig. P.5.2. External subsystem scheme for Problem 5.2.

Tab. P.5.4. Generator data for Problem 5.2.

Generator	M , p.u.	X'_{ds} p.u.
G_4	28,6	0,043
G_5	26,0	0,132

Tab. P.5.5. Branch parameters for Problem 5.2.

Node $i-j$	R , p.u.	X , p.u.	tap, p.u.
19-20	0.00	0.014	1.06
19-33	0.00	0.014	1.07
20-34	0.00	0.018	1.009

Tab. P.5.6. Load flow data for Problem 5.2.

Node, i	V_i , p.u.	θ_i , rad	P_{Gi} , p.u.	Q_{Gi} , p.u.	P_{Li} , p.u.	Q_{Li} , p.u.
20	0.99	-0.0799	-	-	6.80	1.03
33	0.997	0.0358	6.32	1.0897	-	-
34	1.01	0.0107	5.08	1.6700	-	-

Tab. P.5.7. Boundary node voltages and injections for Problem 5.2.

Node i	V_i , p.u.	θ_i , rad	$P_{inj,i}$, p.u.	$Q_{inj,i}$, p.u.
19	1.05	-0.055	-4.54	-0.597

REFERENCES

- [5.1] A. Akhaveina, M. Fotuhi Firuzabadi, R. Billinton, D. Farokhzad, **Review of reduction techniques in the determination of composite system adequacy equivalents**, *Electric Power Systems Research*, Vol. 80, 2010, pp. 1385–1393.
- [5.2] J. H. Chow, R. Galarza, P. Accari, W. W. Price, **Inertial and slow coherency aggregation algorithms for power system dynamic model reduction**, *IEEE Trans. on Power Systems*, Vol. 10, No. 2, May 1995, pp. 680-685.
- [5.3] P. Dimeo, **Nodal analysis of power systems**, Taylor & Francis, 1975.
- [5.4] T. E. Dyliacono, S. C. Savulescu, K. A. Ramarao, **An on-line topological equivalent of a power system**, *IEEE Trans. on Power Apparatus and Systems*, Vol. PAS-97, No.5, Sept/Oct 1978.

- [5.5] A. J. Germond, R. Padmore, ***Dynamic aggregation of generating unit models***, *IEEE Trans. on Power Apparatus and Systems*, Vol. 97, No. 4, 1978, pp. 1060-1069.
- [5.6] Y. Lei, G. Burt, Y. Anaya-Lara, J. McDonald, ***Aggregated modelling of distributed networks with distributed generation***, *The 42nd Universities Power Engineering Conf. (UPEC)*, 2007.
- [5.7] J. Machowski, J. W. Bialek, J. R. Bumby, ***Power system dynamic and stability***, John Wiley & Sons, Chichester 2005.
- [5.8] J. Machowski, A. Cichy, F. Gubina, P. Omahen, ***External subsystem equivalent model for steady-state and dynamic security assessment***, *IEEE Trans. on Power Systems*, Vol.3, No.4, Nov. 1988, pp. 1456-1463.
- [5.9] A. Monticelli, S. Deckmann, A. Garcia, B. Stott, ***Real-time external equivalents for static security analysis***, *IEEE Trans. on Power Apparatus and Systems*, Vol. 98, No.2, March/April 1979.
- [5.10] R. Nath, S. S. Lamba, K. S. Prakasa Rao, ***Coherency based decomposition into study an external areas using weak coupling***, *IEEE Trans. on Power Apparatus and Systems*, Vol. 104, June 1985, pp. 1443-1449.
- [5.11] J. R. Winkelman, J. H. Chow, B. C. Bowler, B. Avramovic, P. V. Kokotovic, ***An analysis of interarea dynamics of multi-machine systems***, *IEEE Trans. on Power Apparatus Systems*, Vol. 100, Feb. 1981, pp. 754-763.
- [5.12] J. B. Ward, ***Equivalent circuits for power flow studies***, *AIEE Trans.*, Vol. 68, 1949.

6. REAL-TIME MODELLING OF POWER SYSTEM

A real-time model is a quasi-static computer based mathematical representation of current conditions in a power network [6.1], [6.2]. The real-time model is extracted at intervals from „snapshots” of real-time measurements as well as from static network data. Real-time measurements are analog measurements and the status of switching devices. Static network data include a basic configuration and parameters of a network.

The process of building real-time power system model is presented in the Fig. 6.1

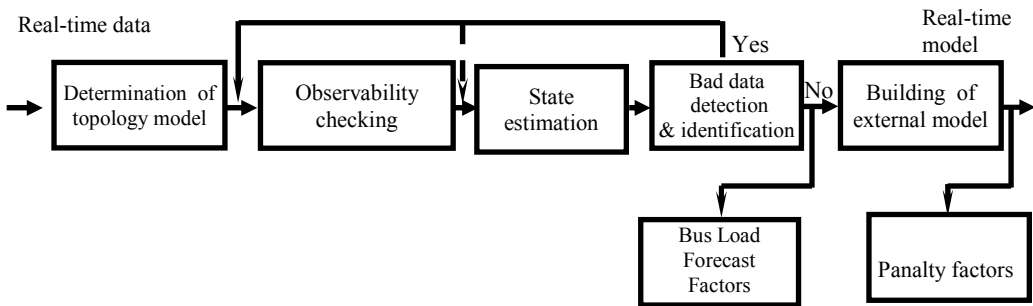


Fig. 6.1. The process of building real-time power system model.

6.1. DETERMINATION OF TOPOLOGY MODEL

The topology model says about present connections in a power system [6.1]-[6.6], [6.10]. Topology model is determined by the network topology processor from the telemetered status of circuit breakers.

Network topology can be described using terms of:

- bus sections and circuit breakers,
- buses and branches.

6.1.1. BUS SECTION/CIRCUIT BREAKER TOPOLOGY MODEL

All equipment (generators, load feeders, shunt reactors, transformers, transmission lines, etc.) are connected to bus-sections. Bus-sections within one voltage level at a substation may be connected together by circuit breakers. An exemplary power system with this level of detail is shown in Fig. 6.2. The data associated with a part of the exemplary power system, which is distinguished by the gray circles, are given in Tab. 6.1.

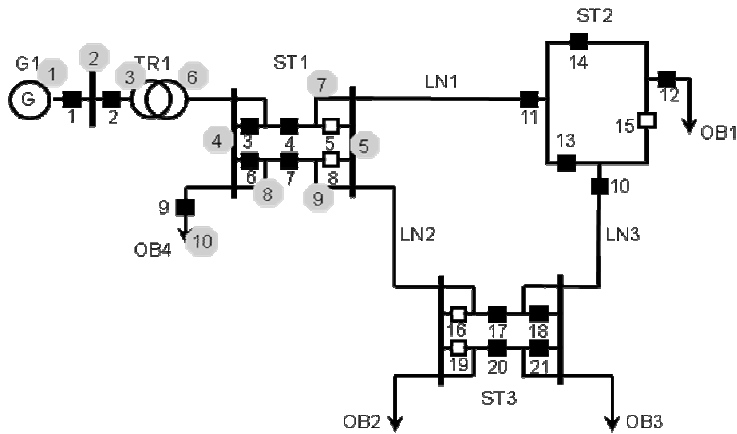


Fig. 6.2. The example of a bus section/circuit breaker topology model.

Tab. 6.1. Description of topology using terms of bus section and circuit breaker.

Sub-station	Bus Sections			Circuit Breakers			
	No	Type	Eq. Ident.	Nc	From B. Sec	To B. Sec	Status
1	1	gen. unit	G1	1	1	2	ON
	2	connection		2	2	3	ON
	3	transf.	TR1	3	6	4	ON
	4	connection		4	6	7	ON
	5	connection		5	7	5	OFF
	6	transf.	TR2	6	4	8	ON
	7	line	LN1	7	8	9	ON
	8	connection		8	9	5	OFF
	9	line	LN2	9	10	8	ON
	10	load	OB4				

6.1.2. BUSBRANCH TOPOLOGY MODEL

In the bus/branch topology model, buses and branches are distinguished. A bus, more exactly an electrical bus is a common electrical connection among different elements of a power system such as power lines, transformers, generators, loads, shunts, etc. A branch represents a power line or a transformer.

The bus/branch topology model is determined using circuit breaker status data. If a circuit breaker is on, a connection is modeled. If a circuit breaker is off, no connection is modeled. Each of the buses must be identified together with the generation, loads, and shunts at these buses.

Status of circuit breakers changes in real time and therefore the bus/branch topology is expected to change. In this situation, whenever there is a change of status of circuit breakers, the network topology processor must determine the new topology. There are several methods to convert bus section/circuit breaker topology into bus/branch topology.

The bus/branch topology model for an exemplary power system is shown in Fig. 6.3. That exemplary system is the same as the system for which the bus section/circuit breaker topology model is presented in Fig. 6.2. The data associated with the model from Fig. 6.3, are collected in Tab. 6.1.

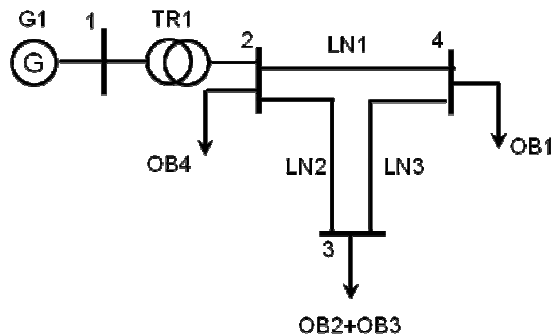


Fig. 6.3. The example of a bus/branch topology model.

6.1.3. DESCRIPTION OF TOPOLOGY USING INCIDENCE MATRIX

An incidence matrix of a power network represents interconnection of the branches with respect to the nodes. As it was previously, the branch represents a power line or a transformer. Saying “node”, we mean “electrical node”.

Let:

\mathbf{C} - an incidence matrix,

n - a number of nodes in a power network,

b – a number of branches in a power network.

Under the mentioned assumptions \mathbf{C} is a $b \times n$ matrix and:

- $C_{ij} = -1$ if the branch i is incident to the node j and it is directed away,
- $C_{ij} = 1$ if the branch i is incident to the node j and it is directed towards,
- $C_{ij} = 0$ if the branch i is not incident to the node j .

where: $i \in \{1, 2, \dots, b\}$,

$j \in \{1, 2, \dots, n\}$.

Tab. 6.2. Description of topology using terms of bus and branch.

No	Name	From bus	To bus	Status at the bus "from"	Status at the bus "to"
1	G1	1	0	ON	
2	TR1	1	2	ON	ON
3	LN1	2	4	ON	ON
4	LN2	2	3	ON	ON
5	LN3	3	4	ON	ON
6	OB1	4	0	ON	
7	OB2+OB3	3	0	ON	
8	OB4	2	0	ON	

In Fig. 6.4, there is presented the incidence matrix for the power system, for which the bus section/circuit breaker topology model is shown in Fig. 6.2 and the bus/branch topology model in Fig. 6.3.

	1	2	3	4
TR1	1	-1	0	0
LN1	0	1	0	-1
LN2	0	-1	1	0
LN3	0	0	-1	1

Fig. 6.4. The example of an incidence matrix for the power system.

The incidence matrix is determined on the base of the bus/branch topology model.

6.2. STATE ESTIMATION

The state estimation is a calculation process which enables obtaining the best estimate of the power system state vector [6.1], [6.2], [6.7]-[6.9]. Power system state vector is a vector whose elements are bus voltage magnitudes and angles throughout the network.

State estimation is a key function for obtaining a real-time network model. Inputs for a state estimation are:

- a topology model,
- measurement data from a power network.

6.2.1. MEASUREMENT DATA FOR STATE ESTIMATION

In the classical approach, the set of measurement data for state estimation includes:

- active and reactive power flows,
- active and reactive power injections,
- voltage magnitudes,
- current magnitudes (sometimes).

In the modern approach, we also utilise:

- voltage phasors,
- current phasors.

6.2.2. BAD DATA AND TOPOLOGY ERRORS IN STATE ESTIMATION

Problems of bad data and topology errors are essential problems in state estimation [6.1], [6.2], [6.7]-[6.9]. Bad data is a data burdened with unusually large measurement error (caused by meter-communication system failures). Usually, we assume that such an error has a module which is much larger than standard deviation of distribution describing measurement noise, e.g. larger than 6 standard deviations. Topology error is improper modelling of any connection in a power network.

Bad data and topology errors have disadvantageous impact on state estimation. They can be cause of divergence of an estimation process. They can decrease accuracy of state estimation results, as well. Therefore, there is necessity of detection and identification of bad data and topology errors in or also before state estimation starts.

Detection means a test to determine whether bad data or topology errors are present. Identification means determination of data which are bad or connection which is improperly modelled.

It should be underlined that topology errors occur rare but their consequences are much more severe than it is in the case of bad data.

Identified bad data are eliminated from a data set utilized by state estimation. In the case of identification of topology error the correction of topology model is made. The next step is repetition of observability checking and estimation calculations. Such iteration process is repeated until tests do not detect bad data or topology errors in inputs for state estimation calculations.

6.3. NETWORK OBSERVABILITY

A network is observable, when sufficient measurement data are available so that the entire state vector can be estimated [6.1], [6.2]. In other words, for the observable network the state estimation can be made.

Network observability is dependent on:

- the locations and types of available measurements,
- the network topology.

Normally, the metering system for the controlled portion of the network is designed so that the network will not only be observable, but also redundant. The network is redundant if the metering system provides measurement data whose number is larger than $2n - 1$ (n – a number of nodes).

There are different methods for checking network observability. They can be divided into the following classes:

- numerically based methods,
- topologically based methods.

An observability test is performed every time when there is a change in the set of available measurement data or the network topology. If the entire network is not observable, unobservable buses should be determined. The unobservable buses have to be either removed from the state estimator calculation or made observable by adding pseudo-measurements.

If there are unobservable buses, a state estimation is performed for observable islands of buses.

6.4. BUS LOAD FORECAST FACTORS

Using results of state estimation, the ratio of each bus MW load to the system MW load (and also the power factor) is calculated every few minutes [6.1], [6.2]. The mentioned factors are utilized for forecasting the bus loads for a given system MW load and a given month, day, and time. Purposes of the considered forecast are:

- utilization of the forecasted complex loads as pseudo-measurements to make the buses observable if they are unobservable due to communication and RTU failure,
- automatic specification of all the bus loads from a given system MW load.

6.5. EXTERNAL NETWORK MODELLING

The internal system is the observable part of a system solved by the state estimator [6.1], [6.2]. It is assumed that the unobservable parts of a system are either lumped into the external system or made observable by using pseudomeasurements

6.6. PENALTY FACTORS

In the economic dispatching of generation, the sensitivity of the transmission losses to the individual generation levels is taken into account by penalizing the incremental cost functions of the generators [6.1], [6.2].

The penalty factors are given by:

$$PF_i = \frac{1}{1 - \frac{\partial L}{\partial P_{gi}}} \quad (6.1)$$

where: L – the system loss,

P_{gi} – the real power output of the i -th generator

With the availability of the real-time network model it is possible to calculate the penalty factors right after the external model calculation is completed.

6.7. PROCEDURES

UTILIZING RESULTS OF REAL-TIME MODELLING

The most important procedures, which utilize results of real-time modelling, are:

- contingency analysis,
- optimal power flow with security constraints,
- optimal power flow with security constraints and post-contingency rescheduling,
- dispatcher training simulator.

PROBLEMS

- 6.1. What is a purpose of real-time modelling of a power system?
- 6.2. What are the main stages of real-time modelling of a power system?
- 6.3. Describe the topology of any power system using terms of bus section and circuit breaker.
- 6.4. Create a bus/branch topology model for the power system considered in the previous problem.
- 6.5. What is a purpose of utilization of the power-system state estimation?
- 6.6. What is necessary condition to perform a power-system state estimation process?
- 6.7. Where are utilized results of power-system state estimation?

REFERENCES

- [6.1] A. Bose, K.A. Clements, *Real-time modeling of power networks. Proceedings of the IEEE*, Vol. 75, No. 12, Dec. 1987, pp. 1607 – 1622.
- [6.2] A. Bose, T.A. Green, *New Modeling, Analysis and Computation Techniques Needed for Power System Control Centers. Inter. Journal of Electrical Power & Energy Systems*, Vol. 15, No. 3, June 1993, pp. 163-168.
- [6.3] R. Łukomski, K. Wilkosz, *Power system topology determination: survey of the methods. The 16th Inter. Conf. on Systems Science*, Wrocław, Poland, 4-6 Sept. 2007. Vol. 3, pp. 149-157.
- [6.4] R. Łukomski, K. Wilkosz, *Power system topology verification method: utilization of different types of artificial neural networks. The 16th Inter.l Conf. on Systems Science*, Wrocław, Poland, 4-6 Sept. 2007. Vol. 3, pp. 149-157.
- [6.5] R. Łukomski, K. Wilkosz, *Method for Power System Topology Verification with Use of Radial Basis Function Networks. Lecture Notes in Computer Science*, Vol. 4507, 2007, pp. 862 - 869.
- [6.6] R. Lukomski, K. Wilkosz, *Power Network Observability for State Estimation Review of the Method. The 9th Inter. Scientific Conf. on Electric Power Engineering (EPE)*, Brno, Czech Republic, May 13-15, 2008, pp. 183-190.
- [6.7] A. Monticelli, *State Estimation in Electric Power Systems. A Generalized Approach*. Boston, Kluwer Academic Publishers, 1999.
- [6.8] A. Monticelli, *Electric power system state estimation. Proceedings of the IEEE*, Vol. 88, No. 2, Feb. 2000, pp. 262 – 282.
- [6.9] T. Okoń, K. Wilkosz, *Weighted-least-squares power system state estimation in different coordinate systems. Przegląd Elektrotechniczny*, nr 11a, R. 86, 2010, s. 54-58.
- [6.10] K. Wilkosz, *A Multi-Agent System Approach to Power System Topology Verification. Lecture Notes in Computer Science*, Vol. 4881, 2007, pp. 970 - 979.

7. WEIGHTED LEAST SQUARES POWER SYSTEM STATE ESTIMATION

7.1. LINEAR LEAST SQUARES ESTIMATION

The name least squares or weighted least squares results from the criterion for finding the solution of the overdetermined set of equations made if more measurements than state variables are available. The linear form of the equations is assumed:

$$\mathbf{y} = \mathbf{A}\mathbf{x}, \quad (7.1)$$

where: $\mathbf{y} = [y_1, y_2, \dots, y_m]^T$ – a measurement (output) vector;

$\mathbf{x} = [x_1, x_2, \dots, x_n]^T$ – a state variable vector;

m - a number of measurements,

n - a number of state variables,

\mathbf{A} – a $m \times n$ matrix with, $m > n$ (matrix has more rows than columns).

In general, the equation (7.1) does not have the solution. In addition, measurement data are burdened by errors and therefore one can write:

$$\mathbf{y} = \mathbf{A}\mathbf{x} + \mathbf{e}, \quad (7.2)$$

where: \mathbf{e} – a vector representing measurement errors.

The solution of least square problem is based on the assumption that measurement errors are independent random variables and they have the same distribution with zero mean and variance equal to 1:

$$E\{\mathbf{e}\} = \mathbf{0} \quad E\{\mathbf{e}\mathbf{e}^T\} = \mathbf{I}. \quad (7.3)$$

Searching for the estimates of state variables can be considered as the optimization problem based on the minimization of the following objective function:

$$J(\hat{\mathbf{x}}) = E\{(\mathbf{y} - \mathbf{A}\hat{\mathbf{x}})^T(\mathbf{y} - \mathbf{A}\hat{\mathbf{x}})\} = \mathbf{y}\mathbf{y}^T - 2\mathbf{y}^T\mathbf{A}\hat{\mathbf{x}} - \hat{\mathbf{x}}^T\mathbf{A}^T\mathbf{A}\hat{\mathbf{x}}. \quad (7.4)$$

The conditions for the minimum of the objective function are following:

$$\frac{\partial J(\hat{\mathbf{x}})}{\partial \hat{\mathbf{x}}} = \mathbf{0} \quad \frac{\partial^2 J(\hat{\mathbf{x}})}{\partial \hat{\mathbf{x}}^2} > 0. \quad (7.5)$$

The solution for the power system state estimation is:

$$\hat{\mathbf{x}} = (\mathbf{A}^T\mathbf{A})^{-1}\mathbf{A}^T\mathbf{y}. \quad (7.6)$$

7.2. LINEAR WEIGHTED LEAST SQUARE ESTIMATION

Let suppose that for measurement errors $E\{\mathbf{e}\} = \mathbf{0}$ and the covariance matrix is as follows:

$$\mathbf{R} = E\{\mathbf{e}\mathbf{e}^T\},$$

where $E\{e_i e_j\} = 0, i, j = 1, 2, \dots, m, i \neq j$.

The objective function for the weighted least square estimation is to minimize:

$$J(\hat{\mathbf{x}}) = E\{(\mathbf{y} - \mathbf{A}\hat{\mathbf{x}})^T \mathbf{R}^{-1}(\mathbf{y} - \mathbf{A}\hat{\mathbf{x}})\} = \mathbf{y}\mathbf{R}^{-1}\mathbf{y}^T - 2\mathbf{y}^T \mathbf{R}^{-1} \mathbf{A}\hat{\mathbf{x}} - \hat{\mathbf{x}}^T \mathbf{A}^T \mathbf{R}^{-1} \mathbf{A}\hat{\mathbf{x}}, \quad (7.7)$$

and the solution of the estimation is:

$$\hat{\mathbf{x}} = (\mathbf{A}^T \mathbf{R}^{-1} \mathbf{A})^{-1} \mathbf{A}^T \mathbf{R}^{-1} \mathbf{y}. \quad (7.8)$$

Assuming that the matrix \mathbf{R} is diagonal (the measurement errors are not correlated):

$$\mathbf{R} = \begin{bmatrix} \sigma_{11}^2 & 0 & 0 & 0 \\ 0 & \sigma_{22}^2 & 0 & 0 \\ \vdots & \vdots & \ddots & \vdots \\ 0 & 0 & 0 & \sigma_{mm}^2 \end{bmatrix}, \quad (7.9)$$

then the objective function is:

$$J(\hat{\mathbf{x}}) = E\{(\mathbf{y} - \mathbf{A}\hat{\mathbf{x}})^T \mathbf{R}^{-1}(\mathbf{y} - \mathbf{A}\hat{\mathbf{x}})\} = \sum_{i=1}^m \frac{(y_i - \hat{y}_i)^2}{\sigma_{ii}}, \quad (7.10)$$

where: $\hat{\mathbf{y}} = \mathbf{A}\hat{\mathbf{x}}$.

The difference between measured and estimated value:

$$\mathbf{r} = \mathbf{y} - \hat{\mathbf{y}} \quad (7.11)$$

is called measurement residuals. The expected value and covariance matrix of residuals are:

$$E\{\mathbf{r}\} = \mathbf{0} \quad \text{cov}(\mathbf{r}) = \mathbf{A}(\mathbf{A}^T \mathbf{W}^{-1} \mathbf{A})^{-1} \mathbf{A}^T. \quad (7.12)$$

and diagonal (random variables are independent).

Example 7.1

Calculate the state estimates obtained with use of least squares for the overdetermined set of equations:

$$\begin{cases} 4x_1 + 7x_2 + x_3 = 10 \\ 3x_1 - x_2 + 2x_3 = 1 \\ 2x_1 + 3x_2 - x_3 = 3 \\ 6x_1 + 4x_2 + x_3 = 8 \\ 9x_1 + 5x_2 - 2x_3 = 7 \end{cases}$$

Compare the estimation results for the following cases:

- without weighting matrix (or with unity weighting matrix),
- with weighting matrix

$$\mathbf{R} = \begin{bmatrix} 1 & 0 & 0 & 0 & 0 \\ 0 & 1 & 0 & 0 & 0 \\ 0 & 0 & 1 & 0 & 0 \\ 0 & 0 & 0 & 0.1 & 0 \\ 0 & 0 & 0 & 0 & 0.1 \end{bmatrix}.$$

Writing equations in matrix form, one can obtain:

$$\mathbf{A} = \begin{bmatrix} 4 & 7 & 1 \\ 3 & -1 & 2 \\ 2 & 3 & -1 \\ 6 & 4 & 1 \\ 9 & 5 & -2 \end{bmatrix}, \quad \mathbf{y} = [10 \ 1 \ 3 \ 8 \ 7]^T$$

a) according to equation (7.8), the estimate of vector \mathbf{x} is calculated as follows:

$$\hat{\mathbf{x}} = \left(\begin{bmatrix} 4 & 7 & 1 \\ 3 & -1 & 2 \\ 2 & 3 & -1 \\ 6 & 4 & 1 \\ 9 & 5 & -2 \end{bmatrix}^T \begin{bmatrix} 4 & 7 & 1 \\ 3 & -1 & 2 \\ 2 & 3 & -1 \\ 6 & 4 & 1 \\ 9 & 5 & -2 \end{bmatrix} \right)^{-1} \begin{bmatrix} 4 & 7 & 1 \\ 3 & -1 & 2 \\ 2 & 3 & -1 \\ 6 & 4 & 1 \\ 9 & 5 & -2 \end{bmatrix}^T \begin{bmatrix} 10 \\ 1 \\ 3 \\ 8 \\ 7 \end{bmatrix} = \begin{bmatrix} 0.3261 \\ 1.1564 \\ 0.8118 \end{bmatrix};$$

the residuals:

$$\mathbf{r} = \mathbf{y} - \mathbf{Ax} = \begin{bmatrix} 10 \\ 1 \\ 3 \\ 8 \\ 7 \end{bmatrix} - \begin{bmatrix} 4 & 7 & 1 \\ 3 & -1 & 2 \\ 2 & 3 & -1 \\ 6 & 4 & 1 \\ 9 & 5 & -2 \end{bmatrix} \begin{bmatrix} 0.3261 \\ 1.1564 \\ 0.8118 \end{bmatrix} = \begin{bmatrix} -0.2109 \\ -0.4455 \\ -0.3095 \\ 0.6061 \\ -0.0931 \end{bmatrix}.$$

b) the weighted least square estimates calculated with used of equation (7.8):

$$\hat{\mathbf{x}} = \left(\begin{bmatrix} 4 & 7 & 1 \\ 3 & -1 & 2 \\ 2 & 3 & -1 \\ 6 & 4 & 1 \\ 9 & 5 & -2 \end{bmatrix}^T \begin{bmatrix} 1 & 0 & 0 & 0 & 0 \\ 0 & 1 & 0 & 0 & 0 \\ 0 & 0 & 1 & 0 & 0 \\ 0 & 0 & 0 & 0.1 & 0 \\ 0 & 0 & 0 & 0 & 0.1 \end{bmatrix}^{-1} \begin{bmatrix} 4 & 7 & 1 \\ 3 & -1 & 2 \\ 2 & 3 & -1 \\ 6 & 4 & 1 \\ 9 & 5 & -2 \end{bmatrix} \right)^{-1} \times$$

$$\times \begin{bmatrix} 4 & 7 & 1 \\ 3 & -1 & 2 \\ 2 & 3 & -1 \\ 6 & 4 & 1 \\ 9 & 5 & -2 \end{bmatrix}^T \begin{bmatrix} 1 & 0 & 0 & 0 & 0 \\ 0 & 1 & 0 & 0 & 0 \\ 0 & 0 & 1 & 0 & 0 \\ 0 & 0 & 0 & 0.1 & 0 \\ 0 & 0 & 0 & 0 & 0.1 \end{bmatrix}^{-1} \begin{bmatrix} 10 \\ 1 \\ 3 \\ 8 \\ 7 \end{bmatrix} = \begin{bmatrix} 0.3566 \\ 1.1724 \\ 1.0168 \end{bmatrix}$$

and the residuals:

$$\mathbf{r} = \mathbf{y} - \mathbf{Ax} = \begin{bmatrix} 10 \\ 1 \\ 3 \\ 8 \\ 7 \end{bmatrix} - \begin{bmatrix} 4 & 7 & 1 \\ 3 & -1 & 2 \\ 2 & 3 & -1 \\ 6 & 4 & 1 \\ 9 & 5 & -2 \end{bmatrix} \begin{bmatrix} 0.3566 \\ 1.1724 \\ 1.0168 \end{bmatrix} = \begin{bmatrix} -0.6500 \\ -0.9310 \\ -0.2136 \\ 0.1539 \\ -0.0380 \end{bmatrix}.$$

It can be noticed that the considerable reduction of residuals is obtained for measurement with better accuracy stated by weighting factors in matrix \mathbf{R} .

Example 7.2

Calculate estimates of voltages at nodes 1 and 2 in the DC circuit shown in Fig. 7.1. Find branch current and voltage estimates of sources. Meter readings are $z_1=5.1\text{V}$, $z_2=4.2\text{V}$, $z_3=13.7\text{A}$, $z_4=11.4\text{A}$. Resistances of all branches are assumed $R=0.5\Omega$.

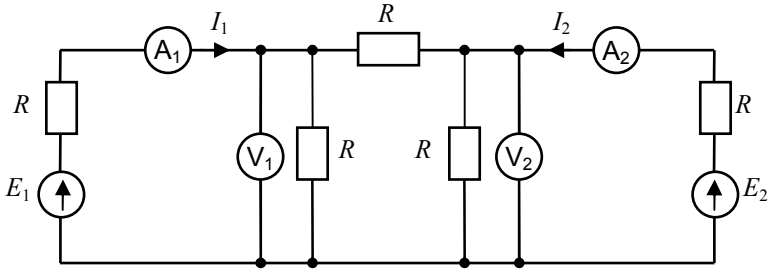


Fig. 7.1. DC circuit for the state estimation calculations.

The state vector contains node voltages

$$\mathbf{x} = [V_1 \quad V_2]^T.$$

Knowing nodal voltages enables all other voltages and currents in circuit to be calculated.

According the Kirchoff and Ohm's laws the functions related measurements and state variables can be evaluated:

$$z_1 = V_1 + e_1,$$

$$z_2 = V_2 + e_2,$$

$$z_3 = \frac{1}{R}V_1 + \frac{1}{R}(V_1 - V_2) + e_3 = \frac{2}{R}V_1 - \frac{1}{R}V_2 + e_3,$$

$$z_4 = -\frac{1}{R}(V_1 - V_2) + \frac{1}{R}V_2 + e_4 = -\frac{1}{R}V_1 + \frac{2}{R}V_2 + e_4.$$

Voltage measurement are assumed to be more accurate than ampmeter readings and the weight matrix is as follows:

$$\mathbf{R} = \begin{bmatrix} 0.1 & 0 & 0 & 0 \\ 0 & 0.1 & 0 & 0 \\ 0 & 0 & 1 & 0 \\ 0 & 0 & 0 & 1 \end{bmatrix}.$$

The measurement function is linear (state variable estimates can be calculated directly). Hence:

$$\mathbf{H} = \begin{bmatrix} 1 & 0 \\ 0 & 1 \\ \frac{2}{R} & -\frac{1}{R} \\ -\frac{1}{R} & \frac{2}{R} \end{bmatrix} = \begin{bmatrix} 1 & 0 \\ 0 & 1 \\ 4 & -2 \\ -2 & 4 \end{bmatrix}.$$

Node voltage estimates are calculated from:

$$\hat{\mathbf{x}} = \begin{bmatrix} \hat{V}_1 \\ \hat{V}_2 \end{bmatrix} = (\mathbf{H}^T \mathbf{R}^{-1} \mathbf{H})^{-1} \mathbf{H}^T \mathbf{R}^{-1} \mathbf{z} = \left(\begin{bmatrix} 1 & 0 \\ 0 & 1 \\ 4 & -2 \\ -2 & 4 \end{bmatrix}^T \begin{bmatrix} 0.1 & 0 & 0 & 0 \\ 0 & 0.1 & 0 & 0 \\ 0 & 0 & 1 & 0 \\ 0 & 0 & 0 & 1 \end{bmatrix}^{-1} \begin{bmatrix} 1 & 0 \\ 0 & 1 \\ 4 & -2 \\ -2 & 4 \end{bmatrix} \right)^{-1} \times$$

$$\times \begin{bmatrix} 1 & 0 \\ 0 & 1 \\ 4 & -2 \\ -2 & 4 \end{bmatrix}^T \begin{bmatrix} 0.1 & 0 & 0 & 0 \\ 0 & 0.1 & 0 & 0 \\ 0 & 0 & 1 & 0 \\ 0 & 0 & 0 & 1 \end{bmatrix}^{-1} \begin{bmatrix} 5.1 \\ 4.2 \\ 13.7 \\ 11.4 \end{bmatrix} = \begin{bmatrix} 5.362 \\ 4.866 \end{bmatrix}$$

The branch current estimates:

$$\hat{I}_1 = 4\hat{V}_1 - 2\hat{V}_2 = 11.715 \text{ A},$$

$$\hat{I}_2 = -2\hat{V}_1 + 4\hat{V}_2 = 8.741 \text{ A}.$$

The estimates of source voltages are:

$$\hat{E}_1 = R\hat{I}_1 + \hat{V}_1 = 0.5 \cdot 11.715 + 5.362 = 11.219 \text{ V},$$

$$\hat{E}_2 = R\hat{I}_2 + \hat{V}_2 = 0.5 \cdot 8.741 + 4.866 = 9.237 \text{ V}.$$

7.3. NONLINEAR WEIGHTED LEAST SQUARE ESTIMATION

From practical point of view very important is the case when the measurements are a nonlinear function of the state variables:

$$\mathbf{z} = h(\mathbf{x}) + \mathbf{e}, \quad (7.13)$$

where: \mathbf{z} – a measurement vector;

$h(\mathbf{x})$ – a non-linear function of state variables,

\mathbf{e} – a measurement-error vector with zero-mean ($E(\mathbf{e})=0$) and with the covariance matrix:

$$E(\mathbf{e}\mathbf{e}^T) = \mathbf{R}. \quad (7.14)$$

The state estimate $\hat{\mathbf{x}}$ should minimize the objective function:

$$J(\hat{\mathbf{x}}) = [\mathbf{z} - h(\hat{\mathbf{x}})]^T \mathbf{R}^{-1} [\mathbf{z} - h(\hat{\mathbf{x}})]. \quad (7.15)$$

Using Taylor series expansion around the point $\mathbf{x}^{(k)}$ and neglecting higher order terms the measurement function can be linearized:

$$h(\mathbf{x}) \approx h(\mathbf{x}^{(k)}) + \left. \frac{\partial h(\mathbf{x})}{\partial \mathbf{x}} \right|_{\mathbf{x}^{(k)}} (\mathbf{x} - \mathbf{x}^{(k)}) = h(\mathbf{x}^{(k)}) + \mathbf{H}(\mathbf{x} - \mathbf{x}^{(k)}), \quad (7.16)$$

where: \mathbf{H} – the Jacobi matrix, i.e. the matrix of partial derivatives of the measurement function elements with respect to state variables:

$$\mathbf{H} = \begin{bmatrix} \frac{\partial h_1(\mathbf{x})}{\partial x_1} & \frac{\partial h_1(\mathbf{x})}{\partial x_2} & \cdots & \frac{\partial h_1(\mathbf{x})}{\partial x_n} \\ \frac{\partial h_2(\mathbf{x})}{\partial x_1} & \frac{\partial h_2(\mathbf{x})}{\partial x_2} & \cdots & \frac{\partial h_2(\mathbf{x})}{\partial x_n} \\ \vdots & \vdots & \ddots & \vdots \\ \frac{\partial h_m(\mathbf{x})}{\partial x_1} & \frac{\partial h_m(\mathbf{x})}{\partial x_2} & \cdots & \frac{\partial h_m(\mathbf{x})}{\partial x_n} \end{bmatrix}. \quad (7.17)$$

The incremental version of equation (7.8) can be written as:

$$\mathbf{H}^T \mathbf{R}^{-1} \mathbf{H} \Delta \hat{\mathbf{x}} = \mathbf{H}^T \mathbf{R}^{-1} \Delta \mathbf{z} \quad (7.18)$$

where: $\Delta \hat{\mathbf{x}} = \hat{\mathbf{x}} - \hat{\mathbf{x}}^{(k)}$,

$\Delta \mathbf{z} = \mathbf{z} - h(\hat{\mathbf{x}}^{(k)})$.

The matrix defined as:

$$\mathbf{G} = \mathbf{H}^T \mathbf{R}^{-1} \mathbf{H} \quad (7.19)$$

is called also the gain matrix.

The estimate of state is given by:

$$\Delta \hat{\mathbf{x}} = (\mathbf{H}^T \mathbf{R}^{-1} \mathbf{H})^{-1} \mathbf{H}^T \mathbf{R}^{-1} \Delta \mathbf{z} = \mathbf{G}^{-1} \mathbf{H}^T \mathbf{R}^{-1} (\mathbf{z} - h(\hat{\mathbf{x}}^{(k)})). \quad (7.20)$$

The estimate can be found with use the iterative scheme:

$$\hat{\mathbf{x}}^{(k+1)} = \hat{\mathbf{x}}^{(k)} + \left(\mathbf{H}^{(k)T} \mathbf{R}^{-1} \mathbf{H}^{(k)} \right)^{-1} \mathbf{H}^{(k)T} \mathbf{R}^{-1} \left(\mathbf{z} - h(\hat{\mathbf{x}}^{(k)}) \right), \quad (7.21)$$

where: k – an iteration number.

Example 7.3

Find the state estimate with use of nonlinear weighted least squares for:

$$h(x) = \begin{bmatrix} x^2 - 6x + 9 \\ 2x - 3 \end{bmatrix}, \quad \mathbf{z} = \begin{bmatrix} 6 \\ 2 \end{bmatrix}, \quad \mathbf{R}^{-1} = \begin{bmatrix} 1 & 0 \\ 0 & 1 \end{bmatrix}. \text{ Assume the iteration}$$

starting point $\hat{x}^{(0)} = 1.0$ and the iteration stop condition $|x^{(k+1)} - x^{(k)}| < 10^{-3}$.

The Jacobi matrix of measurement function:

$$\mathbf{H} = \frac{dh(\hat{x})}{d\hat{x}} = \begin{bmatrix} 2\hat{x} - 6 \\ 2 \end{bmatrix}.$$

The state variable estimate value at the k -th iteration can be calculated from:

$$\hat{x}^{(k+1)} = \hat{x}^{(k)} + \left(\begin{bmatrix} 2\hat{x}^{(k)} - 6 \\ 2 \end{bmatrix}^T \begin{bmatrix} 1 & 0 \\ 0 & 1 \end{bmatrix}^{-1} \begin{bmatrix} 2\hat{x}^{(k)} - 6 \\ 2 \end{bmatrix} \right)^{-1} \begin{bmatrix} 2\hat{x}^{(k)} - 6 \\ 2 \end{bmatrix}^T \begin{bmatrix} 1 & 0 \\ 0 & 1 \end{bmatrix}^{-1} \times$$

$$\times \left(\begin{bmatrix} 6 \\ 2 \end{bmatrix} - \begin{bmatrix} (x^{(k)})^2 - 6x^{(k)} + 9 \\ 2x^{(k)} - 3 \end{bmatrix} \right) = \hat{x}^{(k)} + \frac{1}{(2\hat{x}^{(k)} - 6)^2 + 4} \begin{bmatrix} 2\hat{x}^{(k)} - 6 & 2 \end{bmatrix} \begin{bmatrix} (x^{(k)})^2 - 6x^{(k)} - 3 \\ 2x^{(k)} - 1 \end{bmatrix}$$

The solution for each iteration is shown in Tab. 7.1.

Tab. 7.1. The estimation solutions for each iteration.

k	$\hat{x}^{(k)}$
1	0.9000
2	0.8560
3	0.8378
4	0.8304
5	0.8274
6	0.8262
7	0.8258

7.4. POWER SYSTEM STATE ESTIMATION

7.4.1. GENERAL DESCRIPTION

Theoretical background for power system state estimation was originally proposed in early 1970's [7.3]-[7.5]. State of the power system is described by node voltage magnitudes and angles (voltages can be also express in rectangle form). Only the voltage magnitudes can be measured directly. However, it is possible to calculate phase angle values using redundant real-time data acquired from the system. These data are processed by state estimator. It is special computational routine calculating bus voltage magnitudes and angles. Using state variables other estimated quantities can be calculated (e.g. not measured voltage magnitudes, branch power flows). State estimation produces results which are similar to these obtained from standard power flow. The difference is in applied computational method and used input data.

The general scheme for power system real-time modeling is presented in Fig. 7.2.

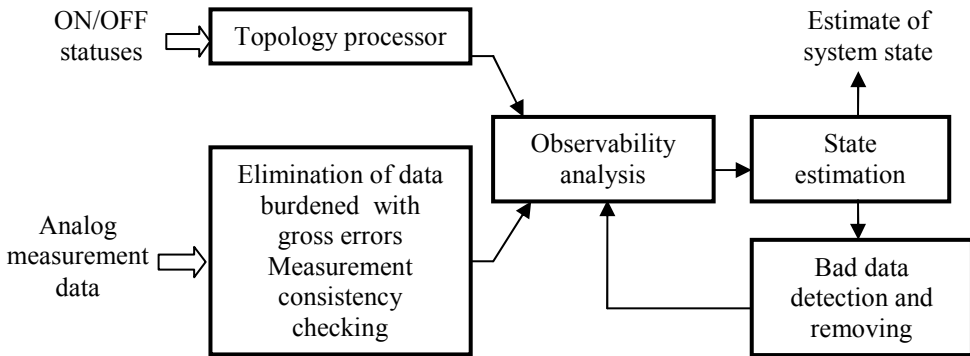


Fig. 7.2. Real-time power system modeling steps.

The state estimator acquires the measurements delivered by Supervisory Control and Data Acquisition (SCADA): voltage magnitudes at most of the buses, active and reactive power flows in lines and transformers, active and reactive power injections at buses with generators and loads, discrete statuses of switching devices. Every short period of time (usually few seconds) the measurement units are scanned and the measurement set is sent to the control center. Topology processing step determines the current power network connectivity with use of reported ON/OFF statuses of switching equipment. The result is bus-branch connectivity model or more detailed topology model at the bus section level. In the initial step some measurement data with outstanding gross errors are rejected and measurement set consistency test is performed.

In real-time environment some of measurements may be unavailable and some network configuration changes may occur. The observability test checks whether sufficient measurement data set is available so that the state vector can be estimated.

Bad data detection module decides whether bad measurements with large errors are present using redundant measurement data set and state estimation results. After rejection of detected bad measurement data, state estimation is re-calculated. Finally, state estimation produces average estimate of the all state variables being the best fit of the input measurement data.

In state estimation the number of processed data is much greater than in the number of data required for standard power flow. As a consequence the number of equations is also greater than the number of state variables. However, the data redundancy is advantage because it enables elimination of bad data and perform estimation in case when the part of measurement set is unavailable.

To compute power system state estimation non-linear weighted least squares procedure is adopted. Flow chart for calculation of state estimates is presented in Fig. 7.3

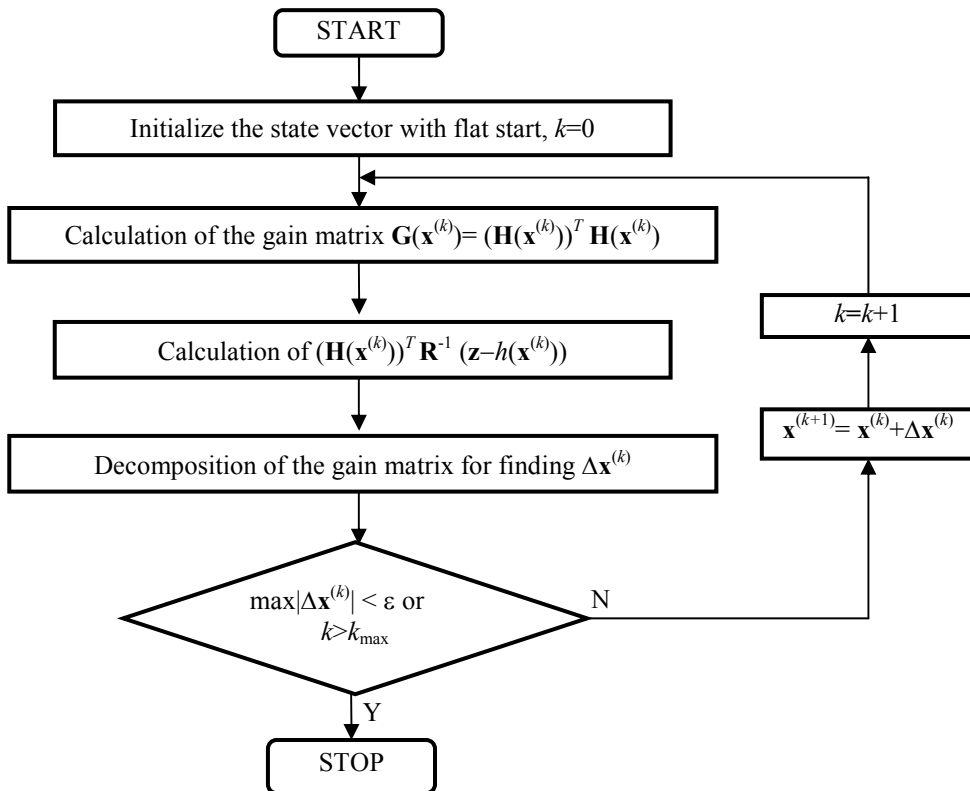


Fig. 7.3. Algorithm for calculations of power system state estimation.

First, flat starting point is assumed as initial values of state vector estimates. The Jacobi and gain matrices are constructed with use of initial state vector. The next step in algorithm is calculation of differences between measurement values and measurement function values $h(\mathbf{x})$. Gain matrix is decomposed for finding the incremental values of state estimates $\Delta \mathbf{x}^{(k)}$. Convergence criterion is checked. If the performance is not met the state vector is updated and iteration counter is incremented. Next iteration of computations is performed. The calculations are continued until reaching the convergence or maximal number of iterations (if the convergence is not reached).

7.4.2. POWER SYSTEM MODEL FOR STATE ESTIMATION

State variable vector contains node voltage angles and magnitudes:

$$\mathbf{x} = [\theta_2 \quad \theta_3 \quad \dots \quad \theta_n \quad V_1 \quad V_2 \quad \dots \quad V_n]^T, \quad (7.22)$$

where: n – a number of nodes in power network.

Note that voltage angle θ_1 is not included in state vector. Similarly as in conventional power flow it is reference and their value is assumed to be zero.

Network equations relating node current injections and node voltages:

$$\begin{bmatrix} \underline{I}_1 \\ \underline{I}_2 \\ \vdots \\ \underline{I}_n \end{bmatrix} = \begin{bmatrix} \underline{Y}_{11} & \underline{Y}_{12} & \dots & \underline{Y}_{1n} \\ \underline{Y}_{21} & \underline{Y}_{22} & \dots & \underline{Y}_{2n} \\ \vdots & \vdots & \ddots & \vdots \\ \underline{Y}_{n1} & \underline{Y}_{n2} & \dots & \underline{Y}_{nn} \end{bmatrix} \begin{bmatrix} \underline{V}_1 \\ \underline{V}_2 \\ \vdots \\ \underline{V}_n \end{bmatrix} \quad (7.23)$$

or in matrix form:

$$\underline{\mathbf{I}} = \underline{\mathbf{Y}}\underline{\mathbf{V}} \quad (7.24)$$

where: $\underline{\mathbf{I}}$ – a node current injection vector;

$\underline{\mathbf{V}}$ – a node voltage vector;

$\underline{\mathbf{Y}}$ – an admittance matrix.

The term \underline{Y}_{ij} is mutual admittance between the nodes i and j and it has the sign which is opposed to the sign of the branch series admittance. The self admittance \underline{Y}_{ii} is equal to the sum of series admittances of branches connected to node i and shunt admittances at node i . The assumed branch model for deriving measurement function is shown in Fig. 7.4.

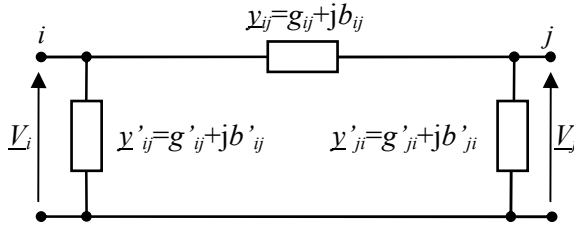


Fig. 7.4. Two port π branch equivalent.

The active and reactive power injected at node i are:

$$\begin{aligned}
 P_i &= V_i \sum_{j=1}^n V_j (G_{ij} \cos(\theta_i - \theta_j) + B_{ij} \sin(\theta_i - \theta_j)) = \\
 &= G_{ii} V_i^2 + V_i \sum_{j=1, j \neq i}^n V_j (G_{ij} \cos(\theta_i - \theta_j) + B_{ij} \sin(\theta_i - \theta_j))',
 \end{aligned} \tag{7.25}$$

$$\begin{aligned}
 Q_i &= V_i \sum_{j=1}^n V_j (G_{ij} \sin(\theta_i - \theta_j) - B_{ij} \cos(\theta_i - \theta_j)) = \\
 &= -B_{ii} V_i^2 + V_i \sum_{j=1, j \neq i}^n V_j (G_{ij} \sin(\theta_i - \theta_j) - B_{ij} \cos(\theta_i - \theta_j))',
 \end{aligned} \tag{7.26}$$

where: P_i, Q_i – a nodal active and reactive power at the node i ;
 n – a number of nodes in a power network;

$\underline{Y}_{ij} = G_{ij} + jB_{ij}$ – the i - j element of an admittance matrix;

The presented form of network equations is called hybrid form because admittances are given in rectangular coordinates and voltages in polar coordinates.

Branch active and reactive power flows

$$P_{ij} = V_i^2 (g'_{ij} + g_{ij}) - V_i V_j (g_{ij} \cos(\theta_i - \theta_j) + b_{ij} \sin(\theta_i - \theta_j)), \tag{7.27}$$

$$Q_{ij} = -V_i^2 (b'_{ij} + b_{ij}) - V_i V_j (g_{ij} \sin(\theta_i - \theta_j) - b_{ij} \cos(\theta_i - \theta_j)), \tag{7.28}$$

where: P_{ij}, Q_{ij} – at the node i ;

$\underline{y}_{ij} = g_{ij} + jb_{ij}$ – an admittance of the series branch connecting the buses i and j .

$\underline{y}'_{ij} = g'_{ij} + jb'_{ij}$ – an admittance of the shunt branch connected at the bus j .

Branch current magnitudes are calculated from:

$$I_{ij} = \frac{\sqrt{P_{ij}^2 + Q_{ij}^2}}{V_i}, \tag{7.29}$$

$$I_{ij} = \sqrt{(g_{ij}^2 + b_{ij}^2)(V_i^2 + V_j^2 - 2V_iV_j \cos(\theta_i - \theta_j))}, \quad (7.30)$$

The measurement Jacobi matrix is constructed with use of the following structure:

$$\mathbf{H} = \begin{bmatrix} \frac{\partial \mathbf{P}_{inj}}{\partial \theta_2} & \cdots & \frac{\partial \mathbf{P}_{inj}}{\partial \theta_n} & \frac{\partial \mathbf{P}_{inj}}{\partial V_1} & \cdots & \frac{\partial \mathbf{P}_{inj}}{\partial V_n} \\ \frac{\partial \mathbf{Q}_{inj}}{\partial \theta_2} & \cdots & \frac{\partial \mathbf{Q}_{inj}}{\partial \theta_n} & \frac{\partial \mathbf{Q}_{inj}}{\partial V_1} & \cdots & \frac{\partial \mathbf{Q}_{inj}}{\partial V_n} \\ \frac{\partial \mathbf{P}_{brn}}{\partial \theta_2} & \cdots & \frac{\partial \mathbf{P}_{brn}}{\partial \theta_n} & \frac{\partial \mathbf{P}_{brn}}{\partial V_1} & \cdots & \frac{\partial \mathbf{P}_{brn}}{\partial V_n} \\ \frac{\partial \mathbf{Q}_{brn}}{\partial \theta_2} & \cdots & \frac{\partial \mathbf{Q}_{brn}}{\partial \theta_n} & \frac{\partial \mathbf{Q}_{brn}}{\partial V_1} & \cdots & \frac{\partial \mathbf{Q}_{brn}}{\partial V_n} \\ \frac{\partial \mathbf{I}_{brn}}{\partial \theta_2} & \cdots & \frac{\partial \mathbf{I}_{brn}}{\partial \theta_n} & \frac{\partial \mathbf{I}_{brn}}{\partial V_1} & \cdots & \frac{\partial \mathbf{I}_{brn}}{\partial V_n} \\ \mathbf{0} & \mathbf{0} & \mathbf{0} & \frac{\partial \mathbf{V}}{\partial V_1} & \cdots & \frac{\partial \mathbf{V}}{\partial V_n} \end{bmatrix}, \quad (7.31)$$

where: \mathbf{P}_{inj} – a vector of active power node injection measurements;
 \mathbf{Q}_{inj} – a vector of reactive power node injection measurements;
 \mathbf{P}_{brn} – a vector of active power flow measurements at branch terminal;
 \mathbf{Q}_{brn} – a vector of reactive power flow measurements at branch terminal;
 \mathbf{I}_{brn} – a vector of branch current magnitude measurements;
 \mathbf{V} – a vector of node voltage magnitude measurements.

Elements of the Jacobi matrix are partial derivatives of P_i , Q_i , P_{ij} , Q_{ij} (the equations (7.25) - (7.28)) with respect to state variables. The equations (7.25) - (7.28) used for calculation of P_i , Q_i , P_{ij} , Q_{ij} are derived for the branch model shown in Fig. 7.4. The terms of the Jacobi matrix are as follows:

a) active and reactive power injections:

$$\frac{\partial P_i}{\partial \theta_i} = \sum_{j=1}^n V_i V_j (-G_{ij} \sin(\theta_i - \theta_j) + B_{ij} \cos(\theta_i - \theta_j)) - V_i^2 B_{ii}, \quad (7.32)$$

$$\frac{\partial P_i}{\partial \theta_j} = V_i V_j (G_{ij} \sin(\theta_i - \theta_j) - B_{ij} \cos(\theta_i - \theta_j)), \quad i \neq j, \quad (7.33)$$

$$\frac{\partial P_i}{\partial V_i} = \sum_{j=1}^n V_j (G_{ij} \cos(\theta_i - \theta_j) + B_{ij} \sin(\theta_i - \theta_j)) + V_i G_{ii}, \quad (7.34)$$

$$\frac{\partial P_i}{\partial V_j} = V_i (G_{ij} \cos(\theta_i - \theta_j) + B_{ij} \sin(\theta_i - \theta_j)), \quad i \neq j, \quad (7.35)$$

$$\frac{\partial Q_i}{\partial \theta_i} = \sum_{j=1}^n V_i V_j (G_{ij} \cos(\theta_i - \theta_j) + B_{ij} \sin(\theta_i - \theta_j)) - V_i^2 G_{ii}, \quad (7.36)$$

$$\frac{\partial Q_i}{\partial \theta_j} = V_i V_j (-G_{ij} \cos(\theta_i - \theta_j) - B_{ij} \sin(\theta_i - \theta_j)), \quad i \neq j. \quad (7.37)$$

$$\frac{\partial Q_i}{\partial V_i} = \sum_{j=1}^N V_j (G_{ij} \sin(\theta_i - \theta_j) - B_{ij} \cos(\theta_i - \theta_j)) - V_i B_{ii}, \quad (7.38)$$

$$\frac{\partial Q_i}{\partial V_j} = V_i (G_{ij} \sin(\theta_i - \theta_j) - B_{ij} \cos(\theta_i - \theta_j)), \quad i \neq j. \quad (7.39)$$

b) active and reactive power branch flows:

$$\frac{\partial P_{ij}}{\partial \theta_j} = V_i V_j (g_{ij} \sin(\theta_i - \theta_j) - b_{ij} \cos(\theta_i - \theta_j)), \quad (7.40)$$

$$\frac{\partial P_{ij}}{\partial \theta_i} = -V_i V_j (g_{ij} \sin(\theta_i - \theta_j) - b_{ij} \cos(\theta_i - \theta_j)), \quad (7.41)$$

$$\frac{\partial P_{ij}}{\partial V_i} = -V_j (g_{ij} \cos(\theta_i - \theta_j) + b_{ij} \sin(\theta_i - \theta_j)) + 2(g_{ij} + g'_{ij}) V_i, \quad (7.42)$$

$$\frac{\partial P_{ij}}{\partial V_j} = -V_i (g_{ij} \cos(\theta_i - \theta_j) + b_{ij} \sin(\theta_i - \theta_j)), \quad (7.43)$$

$$\frac{\partial Q_{ij}}{\partial \theta_i} = -V_i V_j (g_{ij} \cos(\theta_i - \theta_j) + b_{ij} \sin(\theta_i - \theta_j)), \quad (7.44)$$

$$\frac{\partial Q_{ij}}{\partial \theta_j} = V_i V_j (g_{ij} \cos(\theta_i - \theta_j) + b_{ij} \sin(\theta_i - \theta_j)), \quad (7.45)$$

$$\frac{\partial Q_{ij}}{\partial V_i} = -V_j (g_{ij} \sin(\theta_i - \theta_j) - b_{ij} \cos(\theta_i - \theta_j)) - 2V_i (b_{ij} + b'_{ij}), \quad (7.46)$$

$$\frac{\partial Q_{ij}}{\partial V_j} = -V_i (g_{ij} \sin(\theta_i - \theta_j) - b_{ij} \cos(\theta_i - \theta_j)). \quad (7.47)$$

c) branch current magnitudes:

$$\frac{\partial I_{ij}}{\partial \theta_i} = \frac{g_{ij}^2 + b_{ij}^2}{I_{ij}} V_i V_j \sin(\theta_i - \theta_j), \quad (7.48)$$

$$\frac{\partial I_{ij}}{\partial \theta_j} = -\frac{g_{ij}^2 + b_{ij}^2}{I_{ij}} V_i V_j \sin(\theta_i - \theta_j), \quad (7.49)$$

$$\frac{\partial I_{ij}}{\partial V_i} = \frac{g_{ij}^2 + b_{ij}^2}{I_{ij}} (V_i - V_j \cos(\theta_i - \theta_j)), \quad (7.50)$$

$$\frac{\partial I_{ij}}{\partial V_j} = \frac{g_{ij}^2 + b_{ij}^2}{I_{ij}} (V_j - V_i \cos(\theta_i - \theta_j)), \quad (7.51)$$

d) nodal voltages

$$\frac{\partial V_i}{\partial V_i} = 1, \quad \frac{\partial V_i}{\partial V_j} = 0, \quad \frac{\partial V_i}{\partial \theta_i} = 0, \quad \frac{\partial V_i}{\partial \theta_j} = 0. \quad (7.52)$$

Example 7.4

Consider example 3-bus power system as shown in Fig. 7.5. For the given network model, measurement system, volt- and wattmeter readings find the estimates of state variables with use of WLS estimation. Parameter and measurement data:

Branch reactances: $\underline{X}_{12} = j0.15$ p.u., $\underline{X}_{13} = j0.10$ p.u., $\underline{X}_{23} = j0.09$ p.u..

Voltmeters: $V_1 = 1.020$ p.u., $V_2 = 1.015$ p.u., $V_3 = 1.012$ p.u..

Active power flows: $P_1 = 0.60$ p.u., $P_2 = 0.20$ p.u., $P_{13} = 0.47$ p.u., $P_{23} = 0.32$ p.u..

Measurement variances: $\sigma_{v_1}^2 = \sigma_{v_2}^2 = \sigma_{v_3}^2 = 0.001$, $\sigma_{p_1}^2 = \sigma_{p_2}^2 = \sigma_{p_{13}}^2 = \sigma_{p_{23}}^2 = 0.005$

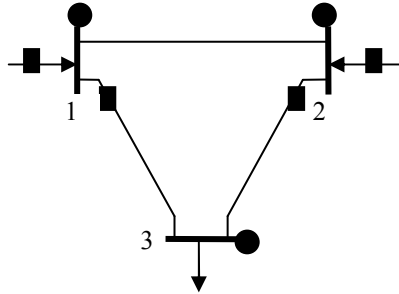


Fig. 7.5. Three-bus power system to illustrate state estimation.

■ - active power flow measurement ● - voltage measurement.

State variable and measurement vectors defined for example system:

$$\mathbf{x} = [x_1 \quad x_2 \quad x_3 \quad x_4 \quad x_5]^T = [\theta_2 \quad \theta_3 \quad V_1 \quad V_2 \quad V_3]^T$$

$$\mathbf{z} = [z_1 \quad z_2 \quad z_3 \quad z_4 \quad z_5 \quad z_6 \quad z_7]^T = [P_1 \quad P_2 \quad P_{13} \quad P_{23} \quad V_1 \quad V_2 \quad V_3]^T$$

Because branch resistances are assumed to be zero, the admittance matrix:

$$\underline{\mathbf{Y}} = \begin{bmatrix} jB_{11} & jB_{12} & jB_{13} \\ jB_{21} & jB_{22} & jB_{23} \\ jB_{31} & jB_{32} & jB_{33} \end{bmatrix} = \begin{bmatrix} -j\left(\frac{1}{0.15} + \frac{1}{0.1}\right) & j\frac{1}{0.15} & j\frac{1}{0.10} \\ j\frac{1}{0.15} & -j\left(\frac{1}{0.15} + \frac{1}{0.09}\right) & j\frac{1}{0.09} \\ j\frac{1}{0.10} & j\frac{1}{0.09} & -j\left(\frac{1}{0.1} + \frac{1}{0.09}\right) \end{bmatrix}.$$

Covariance matrix for measurements:

$$\mathbf{R} = \text{diag}\{\sigma_{P_1}^2 \sigma_{P_2}^2 \sigma_{P_{13}}^2 \sigma_{P_{23}}^2 \sigma_{V_1}^2 \sigma_{V_2}^2 \sigma_{V_3}^2\} =$$

$$= \begin{bmatrix} 0.005 & & & & & & \\ & 0.005 & & & & & \\ & & 0.005 & & & & \\ & & & 0.005 & & & \\ & 0 & & & 0.001 & & \\ & & & & & 0.001 & \\ & & & & & & 0.001 \end{bmatrix}.$$

Functions for the measurements are defined as follows:

a) measurement for power injection P_1 :

$$h_1(\mathbf{x}) = V_1 V_2 B_{12} \sin(\theta_1 - \theta_2) + V_1 V_3 B_{13} \sin(\theta_1 - \theta_3) = x_3 x_4 \frac{1}{0.15} \sin(-x_1) + x_3 x_5 \frac{1}{0.1} \sin(-x_2)$$

b) measurement for power injection P_2 :

$$h_2(\mathbf{x}) = V_1 V_2 B_{12} \sin(\theta_2 - \theta_1) + V_2 V_3 B_{23} \sin(\theta_2 - \theta_3) = x_3 x_4 \frac{1}{0.15} \sin(x_1) + x_4 x_5 \frac{1}{0.09} \sin(x_1 - x_2)$$

c) measurement for branch power flow P_{13} :

$$h_3(\mathbf{x}) = -V_1 V_3 b_{13} \sin(\theta_1 - \theta_3) = -x_3 x_5 \left(-\frac{1}{0.1}\right) \sin(-x_2) = x_3 x_5 \frac{1}{0.1} \sin(-x_2),$$

d) measurement for the branch power flow P_{23} :

$$h_4(\mathbf{x}) = -V_2 V_3 b_{23} \sin(\theta_2 - \theta_3) = -x_4 x_5 \left(-\frac{1}{0.09}\right) \sin(x_1 - x_2) = x_4 x_5 \frac{1}{0.09} \sin(x_1 - x_2),$$

e) measurement for the voltage magnitudes V_1, V_2, V_3 :

$$h_5(\mathbf{x}) = V_1 = x_3,$$

$$h_6(\mathbf{x}) = V_2 = x_4,$$

$$h_7(\mathbf{x}) = V_3 = x_5.$$

The measurement Jacobi matrix has the following structure:

$$\mathbf{H} = \begin{bmatrix} \frac{\partial P_1}{\partial \theta_2} & \frac{\partial P_1}{\partial \theta_3} & \frac{\partial P_1}{\partial V_1} & \frac{\partial P_1}{\partial V_2} & \frac{\partial P_1}{\partial V_3} \\ \frac{\partial P_2}{\partial \theta_2} & \frac{\partial P_2}{\partial \theta_3} & \frac{\partial P_2}{\partial V_1} & \frac{\partial P_2}{\partial V_2} & \frac{\partial P_2}{\partial V_3} \\ \frac{\partial P_{13}}{\partial \theta_2} & \frac{\partial P_{13}}{\partial \theta_3} & \frac{\partial P_{13}}{\partial V_1} & \frac{\partial P_{13}}{\partial V_2} & \frac{\partial P_{13}}{\partial V_3} \\ \frac{\partial P_{23}}{\partial \theta_2} & \frac{\partial P_{23}}{\partial \theta_3} & \frac{\partial P_{23}}{\partial V_1} & \frac{\partial P_{23}}{\partial V_2} & \frac{\partial P_{23}}{\partial V_3} \\ \frac{\partial \theta_2}{\partial V_1} & \frac{\partial \theta_3}{\partial V_1} & \frac{\partial V_1}{\partial V_1} & \frac{\partial V_2}{\partial V_1} & \frac{\partial V_3}{\partial V_1} \\ \frac{\partial \theta_2}{\partial V_2} & \frac{\partial \theta_3}{\partial V_2} & \frac{\partial V_1}{\partial V_2} & \frac{\partial V_2}{\partial V_2} & \frac{\partial V_3}{\partial V_2} \\ \frac{\partial \theta_2}{\partial V_3} & \frac{\partial \theta_3}{\partial V_3} & \frac{\partial V_1}{\partial V_3} & \frac{\partial V_2}{\partial V_3} & \frac{\partial V_3}{\partial V_3} \\ \frac{\partial \theta_2}{\partial \theta_2} & \frac{\partial \theta_3}{\partial \theta_2} & \frac{\partial V_1}{\partial \theta_2} & \frac{\partial V_2}{\partial \theta_2} & \frac{\partial V_3}{\partial \theta_2} \\ \frac{\partial \theta_3}{\partial \theta_2} & \frac{\partial \theta_3}{\partial \theta_3} & \frac{\partial V_1}{\partial \theta_3} & \frac{\partial V_2}{\partial \theta_3} & \frac{\partial V_3}{\partial \theta_3} \end{bmatrix} = \begin{bmatrix} \frac{\partial h_1(\mathbf{x})}{\partial x_1} & \frac{\partial h_1(\mathbf{x})}{\partial x_2} & \frac{\partial h_1(\mathbf{x})}{\partial x_3} & \frac{\partial h_1(\mathbf{x})}{\partial x_4} & \frac{\partial h_1(\mathbf{x})}{\partial x_5} \\ \frac{\partial h_2(\mathbf{x})}{\partial x_1} & \frac{\partial h_2(\mathbf{x})}{\partial x_2} & \frac{\partial h_2(\mathbf{x})}{\partial x_3} & \frac{\partial h_2(\mathbf{x})}{\partial x_4} & \frac{\partial h_2(\mathbf{x})}{\partial x_5} \\ \frac{\partial h_3(\mathbf{x})}{\partial x_1} & \frac{\partial h_3(\mathbf{x})}{\partial x_2} & \frac{\partial h_3(\mathbf{x})}{\partial x_3} & \frac{\partial h_3(\mathbf{x})}{\partial x_4} & \frac{\partial h_3(\mathbf{x})}{\partial x_5} \\ \frac{\partial h_4(\mathbf{x})}{\partial x_1} & \frac{\partial h_4(\mathbf{x})}{\partial x_2} & \frac{\partial h_4(\mathbf{x})}{\partial x_3} & \frac{\partial h_4(\mathbf{x})}{\partial x_4} & \frac{\partial h_4(\mathbf{x})}{\partial x_5} \\ \frac{\partial h_5(\mathbf{x})}{\partial x_1} & \frac{\partial h_5(\mathbf{x})}{\partial x_2} & \frac{\partial h_5(\mathbf{x})}{\partial x_3} & \frac{\partial h_5(\mathbf{x})}{\partial x_4} & \frac{\partial h_5(\mathbf{x})}{\partial x_5} \\ \frac{\partial h_6(\mathbf{x})}{\partial x_1} & \frac{\partial h_6(\mathbf{x})}{\partial x_2} & \frac{\partial h_6(\mathbf{x})}{\partial x_3} & \frac{\partial h_6(\mathbf{x})}{\partial x_4} & \frac{\partial h_6(\mathbf{x})}{\partial x_5} \\ \frac{\partial h_7(\mathbf{x})}{\partial x_1} & \frac{\partial h_7(\mathbf{x})}{\partial x_2} & \frac{\partial h_7(\mathbf{x})}{\partial x_3} & \frac{\partial h_7(\mathbf{x})}{\partial x_4} & \frac{\partial h_7(\mathbf{x})}{\partial x_5} \end{bmatrix},$$

Calculation of corresponding partial derivatives yields:

$$\mathbf{H} = \begin{bmatrix} -x_3 x_4 \frac{1}{0.15} \cos(-x_1) & -x_3 x_5 \frac{1}{0.1} \cos(-x_2) & x_4 \frac{1}{0.15} \sin(-x_1) + x_5 \frac{1}{0.1} \sin(-x_2) & x_3 \frac{1}{0.15} \sin(-x_1) & x_3 \frac{1}{0.1} \sin(-x_2) \\ x_3 x_4 \frac{1}{0.15} \cos(x_1) + x_4 x_5 \frac{1}{0.1} \cos(x_1 - x_2) & -x_4 x_5 \frac{1}{0.09} \cos(x_1 - x_2) & x_4 \frac{1}{0.15} \sin(x_1) & x_3 \frac{1}{0.15} \sin(x_1) + x_5 \frac{1}{0.09} \sin(x_1 - x_2) & x_4 \frac{1}{0.09} \sin(x_1 - x_2) \\ 0 & -x_3 x_5 \frac{1}{0.1} \cos(-x_2) & x_5 \frac{1}{0.1} \sin(-x_2) & 0 & x_3 \frac{1}{0.1} \sin(-x_2) \\ x_4 x_5 \frac{1}{0.09} \cos(x_1 - x_2) & -x_4 x_5 \frac{1}{0.09} \cos(x_1 - x_2) & 0 & x_4 \frac{1}{0.09} \sin(x_1 - x_2) & x_3 \frac{1}{0.9} \sin(x_1 - x_2) \\ 0 & 0 & 1 & 0 & 0 \\ 0 & 0 & 0 & 1 & 0 \\ 0 & 0 & 0 & 0 & 1 \end{bmatrix}$$

Assuming flat starting point for iterations:

$$\hat{\mathbf{x}}^{(0)} = [0.0 \quad 0.0 \quad 1.0 \quad 1.0 \quad 1.0]^T,$$

$$\mathbf{H}^{(0)} = \begin{bmatrix} -6.6667 & -10.0000 & 0.0000 & 0.0000 & 0.0000 \\ 16.6667 & -11.1111 & 0.0000 & 0.0000 & 0.0000 \\ 0.0000 & -10.0000 & 0.0000 & 0.0000 & 0.0000 \\ 11.1111 & -11.1111 & 0.0000 & 0.0000 & 0.0000 \\ 0.0000 & 0.0000 & 1.0000 & 0.0000 & 0.0000 \\ 0.0000 & 0.0000 & 0.0000 & 1.0000 & 0.0000 \\ 0.0000 & 0.0000 & 0.0000 & 0.0000 & 1.0000 \end{bmatrix},$$

$$\mathbf{z} - h(\hat{\mathbf{x}}^{(0)}) = [0.6000 \quad 0.2000 \quad 0.4700 \quad 0.3200 \quad 0.0200 \quad 0.0150 \quad 0.0120]^T.$$

The increment of state vector is found from:

$$\begin{aligned} \Delta \hat{\mathbf{x}}^{(0)} &= (\mathbf{H}^{(0)T} \mathbf{R}^{-1} \mathbf{H}^{(0)})^{-1} \mathbf{H}^{(0)T} \mathbf{R}^{-1} (\mathbf{z} - h(\hat{\mathbf{x}}^{(0)})) = \\ &= [-0.0192 \quad -0.0473 \quad 0.0200 \quad 0.0150 \quad 0.0120]^T. \end{aligned}$$

Updating the vector of state estimates according to:

$$\hat{\mathbf{x}}^{(1)} = \hat{\mathbf{x}}^{(0)} + \Delta \hat{\mathbf{x}}^{(0)} = [-0.0192 \quad -0.0473 \quad 1.0200 \quad 1.0150 \quad 1.0120]^T.$$

Repeating calculations until tolerance level $\max(|\Delta \hat{\mathbf{x}}|) < 10^{-4}$ is reached after 3 iterations gives the final solution (angles are given in rad and voltages in p.u.):

$$\hat{\mathbf{x}} = [-0.0178 \quad -0.0459 \quad 1.0199 \quad 1.0151 \quad 1.0120]^T.$$

Performance index for state estimation:

$$J(\hat{\mathbf{x}}) = [\mathbf{z} - h(\hat{\mathbf{x}})]^T \mathbf{R}^{-1} [\mathbf{z} - h(\hat{\mathbf{x}})] = 0.0060.$$

State vector estimates and measurement functions can be used for calculation of estimates of other quantities: power branch flows and node injections, currents, power losses etc.

PROBLEMS

- 7.1. In the DC circuit shown in Fig. P.7.1, the loop currents I_1 and I_2 are considered as state variables. Find WLS estimates of state variables. Using the estimates determine branch currents, source voltages and voltage drops at resistances.

Resistances: $R_1 = 1\Omega$, $R_2 = 2\Omega$, $R_3 = 3\Omega$.

Meter readings: $z_1 = V_1 = 7.98\text{V}$, $z_2 = V_2 = 9.03\text{V}$, $z_3 = I_1 = 1.96\text{A}$.
 Measurement weights are set to 10.0 for voltmeters and 1.0 for ammeter.

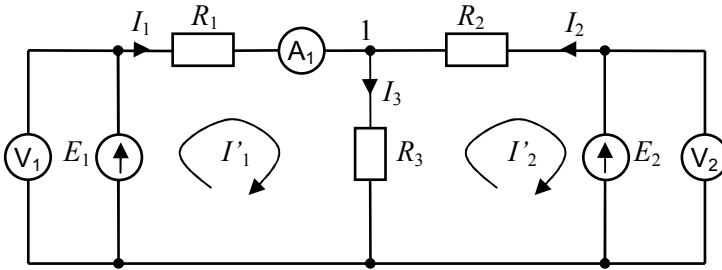


Fig. P.7.1. DC circuit for the state estimation.

7.2. In the simple power system shown in Fig. P.7.2 the meter readings are as follows:

$$\begin{aligned} z_1 = P_{12} = 2.50 \text{ p.u.}, & \quad \sigma^2_{P_{12}} = 0.05, \\ z_2 = P_{21} = -2.48 \text{ p.u.}, & \quad \sigma^2_{P_{21}} = 0.05, \\ z_3 = Q_{12} = 0.50 \text{ p.u.}, & \quad \sigma^2_{Q_{12}} = 0.05, \\ z_4 = V_1 = 1.00 \text{ p.u.}, & \quad \sigma^2_{V_1} = 0.01, \\ z_5 = V_2 = 0.99 \text{ p.u.}, & \quad \sigma^2_{V_2} = 0.01, \end{aligned}$$

Line reactance: $X_{12} = j0.10 \text{ p.u.}$

1. Determine WLS estimates of node voltages assuming stop criteria $|\Delta \mathbf{x}| < 10^{-3}$ and calculate performance index $J(\mathbf{x})$.
2. Change measurement deviations to: $\sigma^2_{V_1} = \sigma^2_{V_2} = 0.1$, $\sigma^2_{P_{12}} = \sigma^2_{P_{21}} = 0.5$, $\sigma^2_{Q_{12}} = 0.5$. Re-calculate WLS state estimation and performance index $J(\mathbf{x})$. Compare the results with values obtained in point 1.

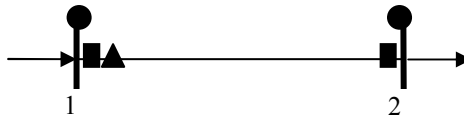


Fig. P.7.2. Two-bus system for the problem 1.

Measurements: • - voltage ■ - active power ▲ - reactive power

7.3. In the simple power system shown in Fig. P.7.3, the meter readings are as follows:

$$\begin{aligned} z_1 = P_1 = 1.3 \text{ p.u.}, & \quad \sigma^2_{P_1} = 0.01, \\ z_2 = P_2 = 0.5 \text{ p.u.}, & \quad \sigma^2_{P_2} = 0.01, \\ z_3 = P_3 = 0.8 \text{ p.u.}, & \quad \sigma^2_{P_3} = 0.01, \\ z_4 = Q_2 = 0.05 \text{ p.u.}, & \quad \sigma^2_{Q_2} = 0.01, \end{aligned}$$

$$z_5 = Q_3 = 0.10 \text{ p.u.}, \quad \sigma_{Q_3}^2 = 0.01,$$

$$z_4 = P_{13} = 0.70 \text{ p.u.}, \quad \sigma_{P_{13}}^2 = 0.01,$$

$$z_5 = P_{23} = 0.10 \text{ p.u.}, \quad \sigma_{P_{23}}^2 = 0.01,$$

$$z_6 = Q_{13} = 0.15 \text{ p.u.}, \quad \sigma_{Q_{13}}^2 = 0.01,$$

$$z_7 = Q_{23} = 0.02 \text{ p.u.}, \quad \sigma_{Q_{23}}^2 = 0.01,$$

$$z_8 = V_1 = 1.00 \text{ p.u.}, \quad \sigma_{V_1}^2 = 0.005,$$

branch reactances: $X_{12} = X_{13} = X_{23} = j0.10 \text{ p.u.}$

1. Determine WLS estimates of node voltages assuming stop criteria $|\Delta x| < 10^{-3}$ and calculate performance index $J(x)$.
2. Remove z_2, z_4, z_5, z_7 from measurement set. Re-calculate WLS state estimation, performance index and compare with results obtained in point 1.

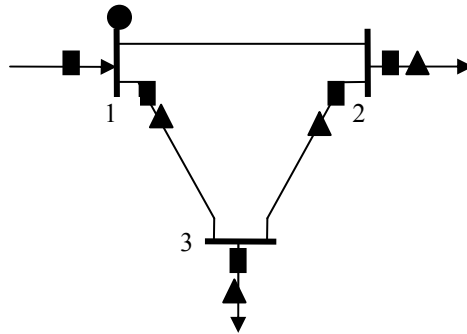


Fig. P.7.3. Three-bus system for the problem 2.
Measurements: ● - voltage ■ - active power ▲ - reactive power

REFERENCES

- [7.1] A. Abur, A. G. Exposito, *Power system state estimation. Theory and implementation*, Marcel Dekker, New York-Basel, 2004.
- [7.2] A. Monticelli, *State estimation in electric power systems - a generalized approach*, Kluwer Academic Publishers, Boston, 1999.
- [7.3] F. C. Schweppe, P. Wilders, *Power system static state estimation, part I: Exact model*, *IEEE Trans. on Power Apparatus and Systems*, Vol. 89, No. 2, Jan. 1970, pp. 120–125.
- [7.4] F. C. Schweppe, D. B. Rom, *Power system static state estimation, part II: Approximate model*, *IEEE Trans. on Power Apparatus and Systems*, Vol. 89, No. 2, Jan. 1970, pp. 125–130.

- [7.5] F. C. Schweppe, ***Power system static state estimation, part III: Implementation***, *IEEE Trans. on Power Apparatus and Systems*, Vol. 89, No. 2, Jan. 1970, pp. 130–135.
- [7.6] T. Okoń, K. Wilkosz, ***Weighted-least-squares power system state estimation in different coordinate systems***. *Przegląd Elektrotechniczny*, nr 11a, R. 86, 2010, s. 54-58.
- [7.7] R. Łukomski, K. Wilkosz, ***Methods of Measurement Placement Design for Power System State Estimation***, *AT&P Journal PLUS2*, No. 2, 2008, s. 75-79.

8. ALTERNATIVE FORMULATION OF THE POWER SYSTEM STATE ESTIMATION

8.1. INTRODUCTION

In this chapter, some alternative formulation of the power system state estimation are presented. Wide review of power system state estimation can be found in [8.5]. This chapter focuses on the decoupled formulation, the orthogonal factorisation, the hybrid method, and the Peters and Wilkinson method, the equality constrained normal equation formulation, and the augment matrix approach with the Hachtel matrix.

8.2. DECOUPLED FORMULATION OF WLS STATE ESTIMATION

It was observed that sensitivity of real power equations to changes in the magnitude of bus voltages and active power equations to changes in the phase angle of bus voltages are very low, especially for high voltage system which has large margin of stability [8.9], [8.10]. These observations allow to partition measurement equations into two parts:

- real power measurements,
- reactive power measurements, and voltage magnitude.

Basing on above observations, the vector of measurements can be partitioned in the following way:

$$\mathbf{z}^T = [\mathbf{z}_P^T \quad \mathbf{z}_{Q,V}^T], \quad (8.1)$$

and

$$\mathbf{H}(\mathbf{x}^{(k)}) = \begin{bmatrix} \mathbf{H}_{P/\delta}(\mathbf{x}^{(k)}) & \mathbf{H}_{P/V}(\mathbf{x}^{(k)}) \\ \mathbf{H}_{Q,V/\delta}(\mathbf{x}^{(k)}) & \mathbf{H}_{Q,V/V}(\mathbf{x}^{(k)}) \end{bmatrix}, \quad (8.2)$$

$$\mathbf{R} = \begin{bmatrix} \mathbf{R}_P & \mathbf{0} \\ \mathbf{0} & \mathbf{R}_{Q,V} \end{bmatrix}. \quad (8.3)$$

Ignoring off diagonal blocks $\mathbf{H}_{P/V}$ and $\mathbf{H}_{Q,V/\delta}$ in the Jacobi matrix \mathbf{H} , the gain matrix can be written in the following way:

$$\mathbf{G}(\mathbf{x}^{(k)}) = \begin{bmatrix} \mathbf{H}_{P/\delta}^T(\mathbf{x}^{(k)}) \cdot \mathbf{R}_P^{-1} \cdot \mathbf{H}_{P/\delta}(\mathbf{x}^{(k)}) & \mathbf{0} \\ \mathbf{0} & \mathbf{H}_{Q,V/V}^T(\mathbf{x}^{(k)}) \cdot \mathbf{R}_V^{-1} \cdot \mathbf{H}_{Q,V/V}(\mathbf{x}^{(k)}) \end{bmatrix} = \begin{bmatrix} \mathbf{G}_{P/\delta}(\mathbf{x}^{(k)}) & \mathbf{0} \\ \mathbf{0} & \mathbf{G}_{Q,V/V}(\mathbf{x}^{(k)}) \end{bmatrix}, \quad (8.4)$$

$$\mathbf{g}(\mathbf{x}^{(k)}) = \begin{bmatrix} -\mathbf{H}_{P/\delta}^T(\mathbf{x}^{(k)}) \mathbf{R}_P^{-1} [\mathbf{z}_P - \mathbf{h}_P(\mathbf{x}^{(k)})] \\ -\mathbf{H}_{Q,V/V}^T(\mathbf{x}^{(k)}) \mathbf{R}_V^{-1} [\mathbf{z}_{Q,V} - \mathbf{h}_{Q,V}(\mathbf{x}^{(k)})] \end{bmatrix} = \begin{bmatrix} \mathbf{g}_P(\mathbf{x}^{(k)}) \\ \mathbf{g}_{Q,V}(\mathbf{x}^{(k)}) \end{bmatrix}, \quad (8.5)$$

which leads to decoupled formulation where phase angle and magnitude of voltages are calculated alternately. The steps of two algorithms are given below:

Algorithm 1

1. Set the iteration index $k = 1$ and all bus voltages at the flat start, i.e. $V_i = 1$ pu $\delta_i = 0$ for all $i = 1, 2, \dots, N$.
2. Build $\mathbf{H}_{P/\delta}(\mathbf{x}^{(k)})$ and $\mathbf{H}_{Q,V/V}(\mathbf{x}^{(k)})$.
3. Calculate gain matrixes $\mathbf{G}_{P/\delta}(\mathbf{x}^{(k)})$ and $\mathbf{G}_{Q,V/V}(\mathbf{x}^{(k)})$.
4. Calculate $\mathbf{g}_P(\mathbf{x}^{(k)})$ and $\mathbf{g}_{Q,V}(\mathbf{x}^{(k)})$.
5. Solve $\mathbf{G}_{P/\delta}(\mathbf{x}^{(k)}) \cdot (\boldsymbol{\delta}^{(k+1)} - \boldsymbol{\delta}^{(k)}) = -\mathbf{g}_P(\mathbf{x}^{(k)})$.
6. Solve $\mathbf{G}_{Q,V/V}(\mathbf{x}^{(k)}) \cdot (\mathbf{V}^{(k+1)} - \mathbf{V}^{(k)}) = -\mathbf{g}_{Q,V}(\mathbf{x}^{(k)})$.
7. Check if $\|\boldsymbol{\delta}^{(k+1)} - \boldsymbol{\delta}^{(k)}\| < \varepsilon$ and $\|\mathbf{V}^{(k+1)} - \mathbf{V}^{(k)}\| < \varepsilon$. If yes, stop. Else, continue.
8. Go to step 2.

Algorithm 2

1. Set the iteration index $k = 1$ and all bus voltages at the flat start, i.e. $V_i = 1$ pu $\delta_i = 0$ for all $i = 1, 2, \dots, N$.
2. Build $\mathbf{H}_{P/\delta}(\boldsymbol{\delta}^{(k)}, \mathbf{V}^{(k)})$.
3. Calculate gain matrix $\mathbf{G}_{P/\delta}(\boldsymbol{\delta}^{(k)}, \mathbf{V}^{(k)})$.
4. Calculate $\mathbf{g}_P(\boldsymbol{\delta}^{(k)}, \mathbf{V}^{(k)})$.
5. Solve $\mathbf{G}_{P/\delta}(\boldsymbol{\delta}^{(k)}, \mathbf{V}^{(k)}) \cdot (\boldsymbol{\delta}^{(k+1)} - \boldsymbol{\delta}^{(k)}) = -\mathbf{g}_P(\boldsymbol{\delta}^{(k)}, \mathbf{V}^{(k)})$.
6. Build $\mathbf{H}_{Q,V/V}(\boldsymbol{\delta}^{(k+1)}, \mathbf{V}^{(k)})$.
7. Calculate gain matrix $\mathbf{G}_{Q,V/V}(\boldsymbol{\delta}^{(k+1)}, \mathbf{V}^{(k)})$.

8. Calculate $\mathbf{g}_{Q,V}(\boldsymbol{\delta}^{(k+1)}, \mathbf{V}^{(k)})$.
9. Solve $\mathbf{G}_{Q,V/V}(\boldsymbol{\delta}^{(k+1)}, \mathbf{V}^{(k)}) \cdot (\mathbf{V}^{(k+1)} - \mathbf{V}^{(k)}) = -\mathbf{g}_{Q,V}(\boldsymbol{\delta}^{(k+1)}, \mathbf{V}^{(k)})$.
10. Check if $(\boldsymbol{\delta}^{(k+1)} - \boldsymbol{\delta}^{(k)}) < \varepsilon$ and $(\mathbf{V}^{(k+1)} - \mathbf{V}^{(k)}) < \varepsilon$. If yes, stop. Else, continue.
11. Go to step 2.

8.3. DISADVANTAGES OF NORMAL EQUATION WLS ESTIMATION

It has been observed that under certain circumstances Normal Equation (NE) is prone to numerical instabilities. Numerical instabilities can appear when the calculation problem is ill-conditioned [8.3].

If the estimation process is ill-conditioned then measurement errors have significant influence on computational process. The measure of the ill-conditioning is a condition number. If the condition number is large, even small errors in measurement data may cause large errors in a state vector. The ill-conditioning of the estimation process often leads to a worse convergence of the process, convergence to wrong solution or even to lack of the convergence of this process. The reasons of ill-conditioning can be large differences in values of the elements of the matrix \mathbf{R} , existence long and short lines connected with the same bus, large proportion of injection measurements or existence of virtual measurements. The condition number is defined as:

$$\text{cond}(\mathbf{A}) = \frac{|\lambda_{GM}|}{|\lambda_{Gm}|}, \quad (8.6)$$

where: λ_{Gm} , λ_{GM} – a minimal eigenvalue and a maximal one (by moduli) of the matrix \mathbf{A} , $\mathbf{A} \in \{\mathbf{G}, \mathbf{U}, \mathbf{L}, \mathbf{F}\}$ respectively.

Example 8.1

If we recall normal equation formulation:

$$\mathbf{G}(\mathbf{x}^{(k)}) \cdot (\mathbf{x}^{(k+1)} - \mathbf{x}^{(k)}) = \mathbf{H}^T(\mathbf{x}^{(k)}) \mathbf{R}^{-1} [\mathbf{z} - \mathbf{h}(\mathbf{x}^{(k)})], \quad (8.7)$$

where

$$\mathbf{G}(\mathbf{x}^{(k)}) = \mathbf{H}^T(\mathbf{x}^{(k)}) \cdot \mathbf{R}^{-1} \cdot \mathbf{H}(\mathbf{x}^{(k)}). \quad (8.8)$$

It can be seen that for the matrix \mathbf{H} :

$$\mathbf{H} = \begin{bmatrix} 1 & 1 & 1 \\ \varepsilon & 0 & 0 \\ 0 & \varepsilon & 0 \\ 0 & 0 & \varepsilon \end{bmatrix}.$$

However $\text{rank}(\mathbf{H})=3$, if floating is $1\text{e-}10$ for $\varepsilon=0.5\text{e-}5$, the $\varepsilon^2=0$ and $\text{rank}(\mathbf{H}^T \cdot \mathbf{H})=1$

$$\mathbf{H}^T \mathbf{H} = \begin{bmatrix} 1+\varepsilon^2 & 1 & 1 \\ 1 & 1+\varepsilon^2 & 1 \\ 1 & 1 & 1+\varepsilon^2 \end{bmatrix} \approx \begin{bmatrix} 1 & 1 & 1 \\ 1 & 1 & 1 \\ 1 & 1 & 1 \end{bmatrix}.$$

Although such extreme situation never happens in practice, this example illustrates weakness of normal equations formulation [8.3].

In this chapter, several, numerically more robust methods will be presented.

8.3.1. ORTHOGONAL FACTORIZATION

For $\tilde{\mathbf{H}} = \mathbf{W}^{1/2} \mathbf{H}$ and $\Delta \tilde{\mathbf{z}} = \mathbf{W}^{1/2} [\mathbf{z} - \mathbf{h}(\mathbf{x})]$, where $\mathbf{W} = \text{diag}^{-1}(\sigma_k^2)$ is the weighting matrix, the normal equation of WLS can be written in the following way:

$$\underbrace{\tilde{\mathbf{H}}^T \cdot \tilde{\mathbf{H}}}_{\mathbf{G}} \Delta \mathbf{x} = \tilde{\mathbf{H}}^T \cdot \Delta \tilde{\mathbf{z}}. \quad (8.9)$$

In this method matrix $\tilde{\mathbf{H}}$ is decomposed in the following way:

$$\tilde{\mathbf{H}} = \mathbf{Q} \mathbf{R}, \quad (8.10)$$

where \mathbf{Q} - an $m \times m$ orthogonal matrix which $\mathbf{Q}^{-1} = \mathbf{Q}^T$,

\mathbf{R} - a $m \times n$ upper trapezoidal matrix (first n rows are upper triangular while remaining rows are null).

Further partitioning \mathbf{Q} and \mathbf{R} leads to the reduced form:

$$\tilde{\mathbf{H}} = [\mathbf{Q}_n \quad \mathbf{Q}_0] \cdot \begin{bmatrix} \mathbf{U} \\ \mathbf{0} \end{bmatrix} = \mathbf{Q}_n \mathbf{U}. \quad (8.11)$$

Using the property $\mathbf{Q} \cdot \mathbf{Q}^T = \mathbf{I}$. Equation (8.9) can be written as:

$$\tilde{\mathbf{H}}^T \cdot \mathbf{Q} \cdot \mathbf{Q}^T \cdot \tilde{\mathbf{H}} \Delta \mathbf{x} = \tilde{\mathbf{H}}^T \cdot \Delta \tilde{\mathbf{z}}, \quad (8.12)$$

$$\mathbf{R}^T \cdot \mathbf{R} \cdot \Delta \mathbf{x} = \mathbf{R}^T \cdot \mathbf{Q}^T \cdot \Delta \tilde{\mathbf{z}}, \quad (8.13)$$

$$\mathbf{U}^T \cdot \mathbf{U} \cdot \Delta \mathbf{x} = \mathbf{U}^T \cdot \mathbf{Q}_n^T \cdot \Delta \tilde{\mathbf{z}}. \quad (8.14)$$

Finally, last expression leads to:

$$\mathbf{U} \cdot \Delta \mathbf{x} = \mathbf{Q}_n^T \cdot \Delta \tilde{\mathbf{z}}. \quad (8.15)$$

Orthogonal factorization is more robust than Normal Equation. The drawback of this approach is the need to obtain and store matrix \mathbf{Q} which is much denser than the gain matrix \mathbf{G} [3, 5].

8.3.2. HYBRID METHOD

Using properties (8.11) that:

$$\tilde{\mathbf{H}} = \mathbf{Q}_n \mathbf{U} \Rightarrow \tilde{\mathbf{H}}^T = \mathbf{U}^T \cdot \mathbf{Q}_n^T. \quad (8.16)$$

And substituting for $\mathbf{U}^T \cdot \mathbf{Q}_n^T$ in equation (8.12) the hybrid method can be written in the following way:

$$\mathbf{U}^T \cdot \mathbf{U} \cdot \Delta \mathbf{x} = \tilde{\mathbf{H}}^T \cdot \Delta \tilde{\mathbf{z}}. \quad (8.17)$$

Hence, in the hybrid method, there is no need to store the matrix \mathbf{Q} .

In the hybrid method, the orthogonal transformation is made on the matrix $\tilde{\mathbf{H}}$ instead of the Cholesky decomposition of the gain matrix \mathbf{G} [8.3], [8.5], [8.6]. This fact allows avoiding situation mentioned in the example 8.1.

8.3.3. PETERS AND WILKINSON METHOD

In this method decomposition LU of $\tilde{\mathbf{H}}$ is performed [8.3], [8.5], [8.7].

$$\tilde{\mathbf{H}} = \mathbf{L} \cdot \mathbf{U}, \quad (8.18)$$

where \mathbf{L} – the $m \times n$ lower trapezoidal matrix (mark that it is not the same matrix as the matrix \mathbf{L} in the Cholesky decomposition),

\mathbf{U} – the $n \times n$ upper triangular matrix (note that this matrix is different from the \mathbf{U} matrix in the orthogonal or hybrid method).

Normal equation can be written in the following way:

$$\underbrace{\tilde{\mathbf{H}}^T \cdot \tilde{\mathbf{H}}}_{\mathbf{G}} \Delta \mathbf{x} = \tilde{\mathbf{H}}^T \cdot \Delta \tilde{\mathbf{z}} \quad (8.19)$$

which can be transformed as follows:

$$\mathbf{U}^T \cdot \mathbf{L}^T \cdot \mathbf{L} \cdot \mathbf{U} \cdot \Delta \mathbf{x} = \mathbf{U}^T \cdot \mathbf{L}^T \cdot \Delta \tilde{\mathbf{z}}, \quad (8.20)$$

$$\mathbf{L}^T \cdot \mathbf{L} \cdot \mathbf{U} \cdot \Delta \mathbf{x} = \mathbf{L}^T \cdot \Delta \tilde{\mathbf{z}}, \quad (8.21)$$

$$\mathbf{L}^T \cdot \mathbf{L} \cdot \Delta \mathbf{y} = \mathbf{L}^T \cdot \Delta \tilde{\mathbf{z}}, \quad (8.22)$$

where:

$$\Delta \mathbf{y} = \mathbf{U} \cdot \Delta \mathbf{x} \quad (8.23)$$

Algorithm of method

1. Perform the LU decomposition of $\tilde{\mathbf{H}}$
2. Using the Cholesky factorization of $\mathbf{L}^T \cdot \mathbf{L}$, followed by the forward/backward substitution, compute $\Delta \mathbf{y}$ (8.22)
3. Compute $\Delta \mathbf{x}$ by backward substitution using (8.23)

8.3.4. EQUALITY-CONSTRAINED WLS STATE ESTIMATION

Using of very high weights for virtual measurements, such zero-injections, cause ill-conditioning of the matrix \mathbf{G} [8.3], [8.5]. One way to solve this problem is considering equations related to zero-injection measurements as equality constrains. This problem of state estimation can be considered as minimization of the objective function $J(\mathbf{x})$ under the constraints $\mathbf{c}(\mathbf{x}) = \mathbf{0}$:

$$\text{Minimize } J(\mathbf{x}) = \frac{1}{2} [\mathbf{z} - \mathbf{h}(\mathbf{x})]^T \mathbf{R}^{-1} [\mathbf{z} - \mathbf{h}(\mathbf{x})], \quad (8.24)$$

$$\text{subjected to } \mathbf{c}(\mathbf{x}) = \mathbf{0}, \quad (8.25)$$

where $\mathbf{c}(\mathbf{x}) = \mathbf{0}$ - an equation set related to zero-injection measurements,

$\mathbf{R} = \text{diag}(\sigma_k^2) = \mathbf{W}^{-1}$ - a diagonal matrix of measurement covariances.

The formulated problem can be solved with the use of the method of Lagrange multipliers, using the function:

$$L(\mathbf{x}) = J(\mathbf{x}) - \boldsymbol{\lambda}^T \mathbf{c}(\mathbf{x}) \quad (8.26)$$

where $\boldsymbol{\lambda}$ - a vector of multipliers.

The solution of the state estimation is obtained in a certain iteration manner from the following equation set:

$$\mathbf{F} \cdot \begin{bmatrix} \mathbf{x}^{(k+1)} - \mathbf{x}^{(k)} \\ -\boldsymbol{\lambda} \end{bmatrix} = \begin{bmatrix} \mathbf{H}^T \mathbf{R}^{-1} [\mathbf{z} - \mathbf{h}(\mathbf{x}^{(k)})] \\ -\mathbf{c}(\mathbf{x}^{(k)}) \end{bmatrix} \quad (8.27)$$

\mathbf{F} is a coefficient matrix.

$$\mathbf{F} = \begin{bmatrix} \mathbf{H}^T \mathbf{R}^{-1} \mathbf{H} & \mathbf{C}^T \\ \mathbf{C} & \mathbf{0} \end{bmatrix} \quad (8.28)$$

Excluding zero-injections measurements in the NE/C method causes that matrix \mathbf{R}^{-1} has no longer so differentiated values and one of the main sources of ill-conditioning of the estimation calculation process has been eliminated. Consequently, the NE/C method should be more numerically stable than the NE method. However, the coefficient matrix \mathbf{F} from (8.28) is indefinite. This fact causes that row-pivoting must be combined with sparsity-oriented techniques during the LU factorization to preserve numerical stability. However, we can expect that additional computation should not be too extensive [8.3], [8.5].

It is noteworthy that the condition number of the coefficient matrix can be improved by scaling the term of the Lagrange function corresponding to the objective function. After the scaling, the Lagrange function can be written as [8.3]:

$$\mathbf{L}(\mathbf{x}) = \alpha \mathbf{J}(\mathbf{x}) - \lambda_s^T \mathbf{c}(\mathbf{x}) \quad (8.29)$$

where $\lambda_s = \alpha \lambda$.

Now, the following nonlinear-equation set is solved in following way:

$$\begin{bmatrix} \alpha \mathbf{H}^T \mathbf{R}^{-1} \mathbf{H} & \mathbf{C}^T \\ \mathbf{C} & \mathbf{0} \end{bmatrix} \cdot \begin{bmatrix} \mathbf{x}^{(k+1)} - \mathbf{x}^{(k)} \\ -\lambda_s \end{bmatrix} = \begin{bmatrix} \alpha \mathbf{H}^T \mathbf{R}^{-1} [\mathbf{z} - \mathbf{h}(\mathbf{x}^{(k)})] \\ -\mathbf{c}(\mathbf{x}^{(k)}) \end{bmatrix} \quad (8.30)$$

It is noteworthy that $\alpha = 1$ may lead to conditioning even worse than for the NE method. The factor α should be chosen as:

$$\alpha = \min_i R_{ii} \quad (8.31)$$

8.3.5. AUGMENT MATRIX APPROACH

The need to perform calculation of $\mathbf{H}^T \mathbf{R}^{-1} \mathbf{H}$ is a disadvantage of the equality constrained WLS method [8.3], [8.5]. Augmented matrix approach may overcome this drawback. The problem of state estimation can be considered as minimization of the objective function $J(\mathbf{x})$ under the constraints $\mathbf{c}(\mathbf{x}) = \mathbf{0}$ and $\mathbf{r} - \mathbf{z} + \mathbf{h}(\mathbf{x}) = \mathbf{0}$, i.e.:

$$\text{Minimize } J(\mathbf{x}) = \frac{1}{2} \mathbf{r}^T \cdot \mathbf{R}^{-1} \cdot \mathbf{r} \quad (8.32)$$

$$\text{subjected to } \mathbf{c}(\mathbf{x}) = \mathbf{0}$$

$$\mathbf{r} - \mathbf{z} + \mathbf{h}(\mathbf{x}) = \mathbf{0} \quad (8.33)$$

The formulated problem can be solved with the use of the method of Lagrange multipliers, using the function:

$$L(\mathbf{x}) = J(\mathbf{x}) - \lambda^T \mathbf{c}(\mathbf{x}) - \boldsymbol{\mu}^T (\mathbf{r} - \mathbf{z} + \mathbf{h}(\mathbf{x})) \quad (8.34)$$

The solution of the state estimation is obtained in a certain iteration manner from the following equation set

$$\begin{bmatrix} \mathbf{R} & \mathbf{H} & \mathbf{0} \\ \mathbf{H}^T & \mathbf{0} & \mathbf{C}^T \\ \mathbf{0} & \mathbf{C} & \mathbf{0} \end{bmatrix} \cdot \begin{bmatrix} \boldsymbol{\mu} \\ \mathbf{x}^{(k+1)} - \mathbf{x}^{(k)} \\ \lambda \end{bmatrix} = \begin{bmatrix} [\mathbf{z} - \mathbf{h}(\mathbf{x}^{(k)})] \\ \mathbf{0} \\ -\mathbf{c}(\mathbf{x}^{(k)}) \end{bmatrix} \quad (8.35)$$

The coefficient matrix in this method is called the Hachtel's matrix. As in the previous method proper scaling of weight matrix improves conditioning:

$$\begin{bmatrix} \alpha^{-1} \mathbf{R} & \mathbf{H} & \mathbf{0} \\ \mathbf{H}^T & \mathbf{0} & \mathbf{C}^T \\ \mathbf{0} & \mathbf{C} & \mathbf{0} \end{bmatrix} \cdot \begin{bmatrix} \boldsymbol{\mu} \\ \mathbf{x}^{(k+1)} - \mathbf{x}^{(k)} \\ \lambda \end{bmatrix} = \begin{bmatrix} [\mathbf{z} - \mathbf{h}(\mathbf{x}^{(k)})] \\ \mathbf{0} \\ -\mathbf{c}(\mathbf{x}^{(k)}) \end{bmatrix}. \quad (8.36)$$

8.4. GUIDELINES FOR PROGRAMMING IN MATLAB®

As it can be seen one of the major problem is solving linear equation $\mathbf{Ax} = \mathbf{b}$ where A is square $n \times n$ matrix, b, x are n rows vectors. It is not recommended to solve this problem in the following way [8.1]:

$$\mathbf{x} = \text{inv}(\mathbf{A}) * \mathbf{b}$$

It is recommended to use backslash divide “\”:

$$\mathbf{x} = \mathbf{A} \backslash \mathbf{b}$$

In this way the specific algorithm is used. Depends on A the appropriate method is used for solving this problem. Bellow there are information for sparse matrices. Checking which algorithm is used, during solving the mentioned equation, can be done in the following way

```
spparms('spumoni',1)
x=A\b
spparms('spumoni',0)
```

Example for normal equations:

```
Gx=H'*W*H      %H-Jacobi matrix, W-weighted matrix
gx=H'*W*dz     %dz=z-h(x) -residue of measurements
```

Theoretically the gain matrix should be symmetric, but because of some round off error during calculation of $\mathbf{H}' * \mathbf{W} * \mathbf{H}$, can be asymmetric. Therefore solving in this way:

```
del tax=Gx\gx
```

the LU decomposition instead Cholesky decomposition may be employed. If we want to use Cholesky decomposition it can be done in the following ways:

```
L=chol(Gx, 'lower');
del tax= L'(L\gx);
```

or we can made the gain matrix real symmetrical using $0.5*(Gx+Gx')$ instead of Gx ;

```
del tax=(0.5*(Gx+Gx'))\gx;
```

In this way Matlab® automatically uses Cholesky decomposition if the gain matrix is real sparse (band density is lower than 0.5).

Example for orthogonal factorization:

```
H_t=W.^0.5*H;
dz_t=W.^0.5*dz;
[Q,R]=qr(H_t);
[m,n]=size(H_t);
Qn=Q(:,1:n);
U=(R(1:n,:));
del tax=U\ (Qn'*dz_t);
```

Example for hybrid method:

```
del tax=U\ (U'\ (H_t'*dz_t));
```

Example for Peters Wilkinson Method:

$$[L,U]=lu(H_t);$$

$$Lt_L=L'*L;$$

In this method we need to use similar operation as in NE if we want to employ Cholesky factorization:

$$L_chol=chol(Lt_L,'lower');$$

$$\delta t_{ay}=L_chol \setminus (L_chol \setminus (L'*dz_t));$$

or:

$$\delta t_{ay}=(0.5*(Lt_L + Lt_L')) \setminus (L'*dz_t);$$

The delta_t is computed in the following way

$$\delta t_{ax}=U \setminus \delta t_{ay};$$

8.5. EXAMPLES OF MATRICES

Example 8.2

Considering the power system presented in the example 2.1 with measurements given in Tab. P.8.1.

Tab. P.8.1. Measurements of 4-bus power system

Measurement	Type	Value p.u.	$\sqrt{R_{kk}}$ p.u.
1	V ₁	1.0011	0.004
2	V ₂	0.9895	0.004
3	P ₂	0.0000	0.001
4	Q ₂	0.0000	0.001
5	P ₁₂	-0.5123	0.008
6	P ₁₃	-0.9731	0.008
7	Q ₁₂	0.0281	0.008
8	Q ₁₃	-0.1098	0.008

8.5.1. MATRICES FOR NORMAL EQUATION FORMULATION

$$\mathbf{H}(\mathbf{x}^{(0)}) = \begin{matrix} & \partial\delta_2 & \partial\delta_3 & \partial\delta_4 & \partial V_1 & \partial V_2 & \partial V_3 & \partial V_4 \\ \begin{matrix} \partial P_{12} \\ \partial P_{13} \\ \partial P_2 \\ \partial Q_{12} \\ \partial Q_{13} \\ \partial Q_2 \\ \partial V_1 \\ \partial V_2 \end{matrix} & \begin{bmatrix} 15.00 & 0 & 0 & -5.00 & 5.00 & 0 & 0 \\ 0 & 15.00 & 0 & -5.00 & 0 & 5.00 & 0 \\ 35.76 & -8.00 & -12.76 & -5.00 & 9.00 & -4.00 & 0 \\ -5.00 & 0 & 0 & -14.80 & 15.00 & 0 & 0 \\ 0 & -5.00 & 0 & -14.75 & 0 & 15.00 & 0 \\ -9.00 & 4.00 & 0 & -15.00 & 36.08 & -8.00 & -12.76 \\ 0 & 0 & 0 & 1.00 & 0 & 0 & 0 \\ 0 & 0 & 0 & 0 & 1.00 & 0 & 0 \end{bmatrix} \end{matrix}$$

$$\mathbf{G}(\mathbf{x}^{(0)}) = 10^9 \begin{bmatrix} 1.3633 & -0.3220 & -0.4561 & -0.0438 & -0.0029 & -0.0710 & 0.1148 \\ -0.3220 & 0.0839 & 0.1020 & -0.0200 & 0.0723 & 0 & -0.0510 \\ -0.4561 & 0.1020 & 0.1627 & 0.0638 & -0.1148 & 0.0510 & 0 \\ -0.0438 & -0.0200 & 0.0638 & 0.2577 & -0.5900 & 0.1362 & 0.1913 \\ -0.0029 & 0.0723 & -0.1148 & -0.5900 & 1.3840 & -0.3246 & -0.4601 \\ -0.0710 & 0 & 0.0510 & 0.1362 & -0.3246 & 0.0836 & 0.1020 \\ 0.1148 & -0.0510 & 0 & 0.1913 & -0.4601 & 0.1020 & 0.1627 \end{bmatrix}$$

Cholesky decomposition of \mathbf{G}

$$\mathbf{L}(\mathbf{x}^{(0)}) = 10^4 \cdot \begin{bmatrix} 3.6923 & 0 & 0 & 0 & 0 & 0 & 0 \\ -0.8722 & 0.2799 & 0 & 0 & 0 & 0 & 0 \\ -1.2352 & -0.2032 & 0.2450 & 0 & 0 & 0 & 0 \\ -0.1186 & -1.0848 & 1.1054 & 0.4049 & 0 & 0 & 0 \\ -0.0078 & 2.5587 & -2.6026 & -0.6132 & 0.4092 & 0 & 0 \\ -0.1923 & -0.5993 & 0.6157 & 0.0198 & -0.2433 & 0.0651 & 0 \\ 0.3109 & -0.8540 & 0.8591 & 0.1831 & -0.1609 & -0.0503 & 0.0321 \end{bmatrix}$$

8.5.2. MATRICES FOR ALTERNATIVE FORMULATION
OF WLS ESTIMATION METHOD

$$\mathbf{H}(\mathbf{x}^{(0)}) = 10^4 \cdot \begin{bmatrix} 0.1875 & 0 & 0 & -0.0625 & 0.0625 & 0 & 0 \\ 0 & 0.1875 & 0 & -0.0625 & 0 & 0.0625 & 0 \\ 3.5755 & -0.8000 & -1.2755 & -0.5000 & 0.9000 & -0.4000 & 0 \\ -0.0625 & 0 & 0 & -0.1850 & 0.1875 & 0 & 0 \\ 0 & -0.0625 & 0 & -0.1844 & 0 & 0.1875 & 0 \\ -0.9000 & 0.4000 & 0 & -1.5000 & 3.6076 & -0.8000 & -1.2755 \\ 0 & 0 & 0 & 0.0250 & 0 & 0 & 0 \\ 0 & 0 & 0 & 0 & 0.0250 & 0 & 0 \end{bmatrix}$$

$$\Delta \mathbf{z}(\mathbf{x}^{(0)}) = \begin{bmatrix} -64.0375 \\ -121.6375 \\ 0 \\ -8.9875 \\ -29.3500 \\ -160.3082 \\ 0.2750 \\ -2.6250 \end{bmatrix}$$

Orthogonal and hybrid method

$$\mathbf{R}(\mathbf{x}^{(0)}) = 10^4 \cdot \left. \begin{bmatrix} 3.6923 & -0.8722 & -1.2352 & -0.1186 & -0.0078 & -0.1923 & 0.3109 \\ 0 & 0.2799 & -0.2032 & -1.0848 & 2.5587 & -0.5993 & -0.8540 \\ 0 & 0 & -0.2455 & -1.1054 & 2.6026 & -0.6157 & -0.8591 \\ 0 & 0 & 0 & -0.4049 & 0.6132 & -0.0198 & -0.1831 \\ 0 & 0 & 0 & 0 & -0.4092 & 0.2433 & 0.1609 \\ 0 & 0 & 0 & 0 & 0 & 0.0651 & -0.0503 \\ 0 & 0 & 0 & 0 & 0 & 0 & 0.0321 \\ 0 & 0 & 0 & 0 & 0 & 0 & 0 \end{bmatrix} \right\} \mathbf{U}$$

$$\mathbf{Q}(\mathbf{x}^{(0)}) = \underbrace{\begin{bmatrix} 0.0508 & 0.1582 & -0.3872 & 0.7727 & -0.4691 & -0.0664 & 0.0099 & -0.0283 \\ 0 & 0.6699 & -0.5555 & -0.1236 & 0.4700 & 0.0789 & 0.0161 & 0.0000 \\ 0.9684 & 0.1593 & 0.1921 & 0.0000 & -0.0000 & 0.0000 & -0.0000 & 0.0000 \\ -0.0169 & -0.0527 & 0.1291 & 0.2508 & 0.4091 & -0.7676 & 0.3918 & -0.0850 \\ 0 & -0.2233 & 0.1852 & 0.5480 & 0.6029 & 0.4893 & -0.1126 & 0.0000 \\ -0.2437 & 0.6695 & 0.6735 & 0.1436 & -0.1261 & 0.0395 & -0.0251 & 0.0000 \\ 0 & 0 & 0 & -0.0617 & -0.0925 & 0.3271 & 0.6250 & -0.7000 \\ 0 & 0 & 0 & 0 & -0.0611 & 0.2284 & 0.6649 & 0.7085 \end{bmatrix}}_{\mathbf{Q}_n}$$

Peters and Wilkinson method

$$\mathbf{L}(\mathbf{x}^{(0)}) = \begin{bmatrix} 0.0524 & 0.2112 & 0.4444 & 1.0000 & 0 & 0 & 0 \\ 0 & 0.9440 & 1.0000 & 0 & 0 & 0 & 0 \\ 1.0000 & 0 & 0 & 0 & 0 & 0 & 0 \\ -0.0175 & -0.0704 & -0.1481 & 0.2595 & 0.5700 & 1.0000 & 0 \\ 0 & -0.3147 & -0.3333 & 0.5910 & 1.0000 & 0 & 0 \\ -0.2517 & 1.0000 & 0 & 0 & 0 & 0 & 0 \\ 0 & 0 & 0 & -0.0720 & -0.1218 & -0.3679 & 1.0000 \\ 0 & 0 & 0 & 0 & -0.0520 & -0.2434 & 0.9880 \end{bmatrix}$$

$$\mathbf{U}(\mathbf{x}^{(0)}) = 10^4 \cdot \begin{bmatrix} 3.5755 & -0.8000 & -1.2755 & -0.5000 & 0.9000 & -0.4000 & 0 \\ 0 & 0.1986 & -0.3211 & -1.6259 & 3.8341 & -0.9007 & -1.2755 \\ 0 & 0 & 0.3031 & 1.4723 & -3.6193 & 0.9127 & 1.2040 \\ 0 & 0 & 0 & -0.3472 & 0.8141 & -0.1944 & -0.2657 \\ 0 & 0 & 0 & 0 & -0.4811 & 0.3232 & 0.1570 \\ 0 & 0 & 0 & 0 & 0 & -0.0690 & 0.0680 \\ 0 & 0 & 0 & 0 & 0 & 0 & 0.0250 \end{bmatrix}$$

PROBLEMS

- 8.1. Consider power system from example 8.2. P_2 and Q_2 are zero-injection measurement. Obtain condition number of:
- the gain matrix from NE method,
 - U matrix from orthogonal method,

- coefficient matrix from NE with equally constrained,
 - Hachtel matrix.
- 8.2. The same as problem 1, investigate influence of weigh matrix on condition number.
- 8.3. Investigate influence of scaling parameters α on condition number of Hachtel matrix.

REFERENCES

- [8.1] MATLAB. The MathWorks, Inc., Natick, MA, USA.
<http://www.mathworks.com>.
- [8.2] J. A. Momoh, *Electric Power System Application of Optimization*. Second Edition. CRC Press, 2008.
- [8.3] A. Abur, A. G. Exposito, *Power System State Estimation: Theory and Implementation*. Marcel Dekker, Inc, New York – Basel, 2004.
- [8.4] A. Monticelly, *State Estimation in Electric Power Systems: A Generalized Approach*, Massachusetts, Kluwer Academic Publisher, 1999.
- [8.5] L. Holten, A. Gjelsvik, S. Aam., F. F. Wu, W. E. Liu, *Comparison of different methods for state estimation*. *IEEE Trans. on Power Systems*, Vol. 3, No. 4. 1988, pp. 1798-1806.
- [8.6] A. Monticelly, C.A.F. Murari, F.F. Wu, *A Hybrid State Estimator: Solving Normal Equations By Orthogonal Transformations*. *IEEE Trans. on Power Apparatus and Systems*, Vol. 104, No. 12. Dec 1985, pp. 3460-3468.
- [8.7] J. W. Gu, K. A. Clements, G. R. Krumpholz, P. W. Davis, *The solution of ill-conditioned power system state estimation problems via the method of Peters and Wilkinson*. *IEEE Trans. on Power Apparatus and Systems*, Vol. 102, No. 10, Oct. 1983, pp. 3473 – 3480.
- [8.8] A. Simoes-Costa, V.H. Quintana, *A Robust Numerical Technique for Power System State Estimation*. *IEEE Trans. on Power Apparatus and Systems*, Vol. 100, No. 2, Feb. 1981, pp. 691 – 698.
- [8.9] A. Garcia, A. Monticelli, P. Abreu, *Fast Decoupled State Estimation and Bad Data Processing*. *IEEE Trans. on Power Apparatus and Systems*, Vol. 98, No. 5, Sept./Oct. 1979, pp. 1645 – 1652.
- [8.10] B. Stott, O. Alsac, *Fast Decoupled Load Flow*. *IEEE Trans. on Power Apparatus and Systems*, Vol. 93, No. 3, May/June 1974, pp. 859 – 867.

9. NETWORK OBSERVABILITY ANALYSIS

9.1. INTRODUCTION

The set of available measurements in power system are used by power system state estimator in order to estimate the system state. Before installation of power system state estimator network, observability analysis should be carried out in order to check adequacy of existing measurements configuration. If system appears unobservable it is necessary to add additional meters in particular locations. During exploitation some measurements may fail, topology may change. Therefore it is necessary to perform observability analysis on-line. During this analysis there is no possibility to add any additional measurements if system appears unobservable, but it is possible to distinguish a observable islands. In this situation each island will have its own phase angle phase reference. Network observability analysis has to detect such cases and identify all existing observable islands before execution of power system state estimation [9.2].

Observability analysis can be carried out using fully coupled or decoupled measurement equations. Both approaches have some drawbacks. Using fully coupled model may lead to non-uniqueness of the solution. This can be illustrated by considering the following case of two bus system [9.2].

Example 9.1.

Consider the power line presented in Fig. 9.1, where: $V_1 = 1.00$ p.u., $V_2 = 0.99$ p.u., $Q_{12} = 0.80$ p.u., $X_{12} = 0.20$ p.u.

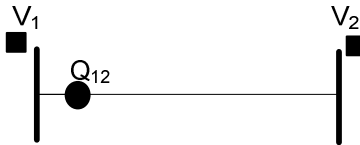


Fig. 9.1. 7-bus test system and its measurements

If we set $\theta_1 = 0$ as reference, the θ_2 can be calculated by solving the following equation:

$$Q_{12} = -\frac{V_1 \cdot V_2}{X_{12}} \cos \theta_2 + \frac{V_1^2}{X_{12}},$$

$$\theta_2 = \arccos\left(\frac{-Q_{12} \cdot X_{12} + V_1^2}{V_1 \cdot V_2}\right) = \arccos\left(\frac{-0.8 \cdot 0.2 + 1}{1 \cdot 0.99}\right) = \pm 31.95 \text{ degrees.}$$

Both solutions are equally likely. The decoupled approach does not have such disadvantage. At the beginning, analysis based on $P-\theta$ model and then on $Q-V$ model should be performed. Observability of power system consists of intersection of results from these two models. However, active and reactive power measurements usually occur in pairs and second step can be avoided.

The theory of observability has evolved into two classes of algorithms: numerically and topologically. In literature numerous algorithms of these approaches can be found. In [9.1], review of most of them is presented.

Topological approaches use the decoupled measurement model and graph theory. They are free of round-off errors because floating point operations are not employed. The topological methods can be several times faster than numerical ones [9.4]. However decoupled measurement model excludes using them when current magnitude measurements are present.

Numerical approaches may use fully coupled or decoupled models. They are based on the numerical factorization of the measurement Jacobi or gain matrix. Advantage of numerical methods is that they allow the use of existing routines for sparse triangular decomposition and sparse vector methods. However they require floating point operations so they are prone to round-off errors [9.1], [9.2], [9.4]. This chapter focuses on numerical method based on the nodal model and topological method.

9.2. THE METHOD BASED ON THE NODAL MODEL

For observability analysis a linearized measurement error free model can be employed:

$$\Delta \mathbf{z} = \mathbf{H} \cdot \Delta \mathbf{x}, \quad (9.1)$$

where: $\Delta \mathbf{z} = \mathbf{z} - \mathbf{h}(\mathbf{x}^{(0)})$, $\Delta \mathbf{x} = \mathbf{x} - \mathbf{x}^{(0)}$, $\mathbf{H} = \frac{\partial \mathbf{h}(\mathbf{x})}{\partial \mathbf{x}}$,

$\Delta \mathbf{z}$ - the mismatch between the measurement vector and its calculated value at an estimate $\mathbf{x}^{(0)}$.

Ignoring the weak coupling $P-V$ and $Q-\theta$, the decoupled formulation can be written as:

$$\Delta \mathbf{z}_p = \mathbf{H}_{p/\delta} \cdot \Delta \delta, \quad (9.2)$$

$$\Delta \mathbf{z}_{Q,V} = \mathbf{H}_{Q,V/V} \cdot \Delta \mathbf{V}. \quad (9.3)$$

As it was mentioned before, power and reactive power measurements usually occur in pairs only $P-\theta$ test can be performed. Further, it should be checked if at least one voltage measurements exists per observable island.

For observability analysis, all system branches can be assumed to have impedance of $j1.0$ p.u., shunt parameters are neglected and all bus voltages can be set equal 1.0 p.u. Therefore, power flows in all power system branches can be written as:

$$\mathbf{P}_b = \mathbf{A}\boldsymbol{\delta}, \quad (9.4)$$

where $\boldsymbol{\delta} = (\mathbf{H}_{p/\delta}^T \cdot \mathbf{H}_{p/\delta})^{-1} \mathbf{H}_{p/\delta}^T \mathbf{z}_p = (\mathbf{G}_{p/\delta})^{-1} \cdot \mathbf{t}_p,$ (9.5)

\mathbf{P}_b - a vector of branch flows,

\mathbf{A} - a branch-bus incidence matrix,

$\boldsymbol{\delta}$ - a vector of bus voltage phase angles,

Branches which have nonzero flows, i.e. $\mathbf{P}_b \neq 0$ are unobservable.

9.2.1. DETERMINING THE UNOBSERVABLE BRANCHES

For observability analysis, matrix $\mathbf{H}_{p/\delta}$ contains all columns unlikely in state estimation when reference bus (column) is removed. In practice, the equation (9.5) is solved using the Cholesky decomposition. Since $\mathbf{H}_{p/\delta}$ contains all columns it is not full-rank, therefore during Cholesky decomposition of the gain matrix $\mathbf{G}_{p/\delta} = \mathbf{L} \cdot \mathbf{L}^T$ at least one pivot point is zero. When zero pivot is encountered, it is replaced by 1.0 and the corresponding element of vector \mathbf{t}_p is assigned an arbitrary value. This values should be various, this can achieved by assigning integer numbers in increasing order, for example: 0,1,2, etc.[9.2]

Example 9.2.

Consider the system and measurement configuration shown in Fig. 9.2.

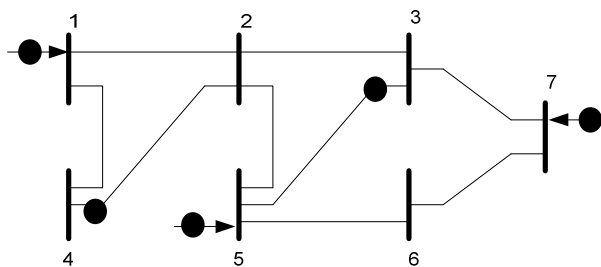


Fig. 9.2. 7-bus test system and its measurements

Incidence matrix \mathbf{A} is created in the following way:

$$\mathbf{A}(i, j) = \begin{cases} 1 & \text{if bus } j \text{ is the sending terminal of branch } i \\ -1 & \text{if bus } j \text{ is the receiving terminal of branch } i \\ 0 & \text{otherwise} \end{cases} \quad (9.6)$$

For considered system, the matrix \mathbf{A} can be written in the following way

$$\mathbf{A} = \begin{bmatrix} 1 & -1 & 0 & 0 & 0 & 0 & 0 \\ 1 & 0 & 0 & -1 & 0 & 0 & 0 \\ 0 & 1 & -1 & 0 & 0 & 0 & 0 \\ 0 & 1 & 0 & -1 & 0 & 0 & 0 \\ 0 & 1 & 0 & 0 & -1 & 0 & 0 \\ 0 & 0 & 1 & 0 & -1 & 0 & 0 \\ 0 & 0 & 1 & 0 & 0 & 0 & -1 \\ 0 & 0 & 0 & 0 & 1 & -1 & 0 \\ 0 & 0 & 0 & 0 & 0 & 1 & -1 \end{bmatrix}.$$

For observability analysis, as it was mentioned before, all system branches can be assumed to have impedance of $j1.0$ p.u., shunt parameters are neglected and all bus voltages can be set equal 1.0 p.u. Using this assumption The Jacobi matrix can be written in the following way:

- for power injection measurement

$$H(i, j) = \begin{cases} \sum & \text{for injection bus of } i^{\text{th}} \text{ measurement} \\ -1 & \text{for other ends of connected branches of } i^{\text{th}} \text{ measurement} \\ 0 & \text{otherwise} \end{cases} \quad (9.7)$$

where: \sum – a number of connected branches to the j -th bus,

- for power flow measurement

$$H(i, j) = \begin{cases} 1 & \text{for end of branch where } i^{\text{th}} \text{ measurement is placed} \\ -1 & \text{for other end of branch} \\ 0 & \text{otherwise} \end{cases} \quad (9.8)$$

For the considered power system the gain matrix can be written in the following way:

$$\mathbf{G}_{P/\delta} = \mathbf{H}_{P/\delta}^T \cdot \mathbf{H}_{P/\delta} = \begin{bmatrix} 4 & -2 & 0 & -2 & 0 & 0 & 0 \\ -2 & 3 & 1 & 0 & -3 & 1 & 0 \\ 0 & 1 & 3 & 0 & -4 & 2 & -2 \\ -2 & 0 & 0 & 2 & 0 & 0 & 0 \\ 0 & -3 & -4 & 0 & 10 & -3 & 0 \\ 0 & 1 & 2 & 0 & -3 & 2 & -2 \\ 0 & 0 & -2 & 0 & 0 & -2 & 4 \end{bmatrix},$$

where

$$\mathbf{H}_{P/\delta} = \begin{bmatrix} 2 & -1 & -1 & 0 & 0 & 0 & 0 \\ 0 & -1 & -1 & 0 & 3 & -1 & 0 \\ 0 & 0 & -1 & 0 & 0 & -1 & 2 \\ 0 & 0 & 1 & 0 & -1 & 0 & 0 \\ 0 & -1 & 0 & 1 & 0 & 0 & 0 \end{bmatrix}.$$

During Cholesky decomposition one zero pivot point is encountered and replaced by 1.0

$$\mathbf{L} = \begin{bmatrix} 2.0000 & 0 & 0 & 0 & 0 & 0 & 0 \\ -1.0000 & 1.4142 & 0 & 0 & 0 & 0 & 0 \\ 0 & 0.7071 & 1.5811 & 0 & 0 & 0 & 0 \\ -1.0000 & -0.7071 & 0.3162 & 0.6325 & 0 & 0 & 0 \\ 0 & -2.1213 & -1.5811 & -1.5811 & 0.7071 & 0 & 0 \\ 0 & 0.7071 & 0.9487 & 0.3162 & 0.7071 & \boxed{1.0000} & 0 \\ 0 & 0 & -1.2649 & 0.6325 & -1.4142 & 0 & \boxed{1.0000} \end{bmatrix}$$

and right hand side vector is equal to:

$$\mathbf{t}_p^T = [0 \ 0 \ 0 \ 0 \ 0 \ \boxed{0} \ \boxed{1}].$$

The estimated state is obtained by:

$$\delta = (\mathbf{L} \cdot \mathbf{L}^T)^{-1} \cdot \mathbf{t}_p = [4 \ 4 \ 2 \ 4 \ 2 \ 0 \ 1]^T,$$

and branch power flows are equal to:

$$\mathbf{P}_b = \mathbf{A}\delta = [0 \ 0 \ 2 \ 0 \ 2 \ 0 \ 1 \ 2 \ -1]^T.$$

Non-zero flow indicates that the corresponding branch is not observable.

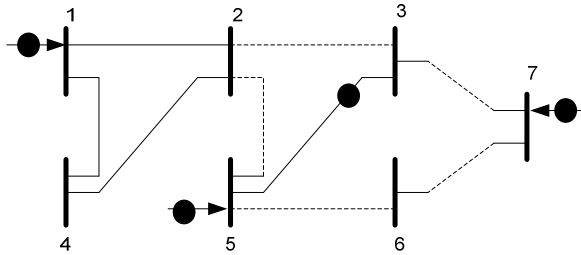


Fig. 9.3. 7-bus test system and its measurements and unobservable branches

9.2.2. DETERMINING THE OBSERVABLE ISLAND

The procedure of identifying unobservable branches can be also used in determination of the observable islands in the system. Procedure needs to be performed in the following way:

1. Perform procedure of determination unobservable branches.
2. Identify and remove all unobservable branches and all injections that are incident to these unobservable branches.
3. If unobservable branches are found go to step 1. Else determine observable branches.

It must be mentioned that sometimes the determination of observable islands is done in the first iteration as in the example 9.2.

Example 9.3.

For the system presented in Fig. 9.4, matrix A can be built in the following way:

$$\mathbf{A} = \begin{bmatrix} 1 & -1 & 0 & 0 & 0 & 0 & 0 \\ 1 & 0 & -1 & 0 & 0 & 0 & 0 \\ 0 & 1 & -1 & 0 & 0 & 0 & 0 \\ 0 & 1 & 0 & -1 & 0 & 0 & 0 \\ 0 & 0 & 1 & 0 & -1 & 0 & 0 \\ 0 & 0 & 0 & 1 & 0 & -1 & 0 \\ 0 & 0 & 0 & 0 & 1 & -1 & 0 \\ 0 & 0 & 0 & 0 & 1 & 0 & -1 \\ 0 & 0 & 0 & 0 & 0 & 1 & -1 \end{bmatrix}$$

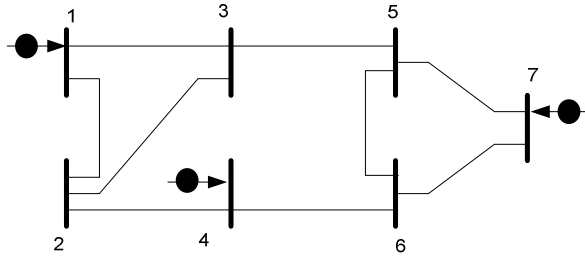


Fig. 9.4. 7-bus test system and its measurements

the Jacobi and gain matrices can be built as below:

$$\mathbf{H}_{P/\delta} = \begin{bmatrix} 2 & -1 & -1 & 0 & 0 & 0 & 0 \\ 0 & -1 & 0 & 2 & 0 & -1 & 0 \\ 0 & 0 & 0 & 0 & -1 & -1 & 2 \end{bmatrix},$$

$$\mathbf{G}_{P/\delta} = \begin{bmatrix} 4 & -2 & -2 & 0 & 0 & 0 & 0 \\ -2 & 2 & 1 & -2 & 0 & 1 & 0 \\ -2 & 1 & 1 & 0 & 0 & 0 & 0 \\ 0 & -2 & 0 & 4 & 0 & -2 & 0 \\ 0 & 0 & 0 & 0 & 1 & 1 & -2 \\ 0 & 1 & 0 & -2 & 1 & 2 & -2 \\ 0 & 0 & 0 & 0 & -2 & -2 & 4 \end{bmatrix}.$$

During Cholesky decomposition four zero pivot points are encountered and replaced by 1.0:

$$\mathbf{L} = \begin{bmatrix} 2 & 0 & 0 & 0 & 0 & 0 & 0 \\ -1 & 1 & 0 & 0 & 0 & 0 & 0 \\ -1 & 0 & \boxed{1} & 0 & 0 & 0 & 0 \\ 0 & -2 & 0 & \boxed{1} & 0 & 0 & 0 \\ 0 & 0 & 0 & 0 & 1 & 0 & 0 \\ 0 & 1 & 0 & 0 & 1 & \boxed{1} & 0 \\ 0 & 0 & 0 & 0 & -2 & 0 & \boxed{1} \end{bmatrix}$$

and right hand side vector is equal:

$$\mathbf{t}_P^T = [0 \ 0 \ \boxed{0} \ \boxed{1} \ 0 \ \boxed{2} \ \boxed{3}]$$

the estimate state is obtained by:

$$\delta = (\mathbf{L} \cdot \mathbf{L}^T)^{-1} \cdot \mathbf{t}_p = [0 \ 0 \ 0 \ 1 \ 4 \ 2 \ 3]^T$$

and branch flows are equal:

$$\mathbf{P}_b = \mathbf{A}\delta = [0 \ 0 \ 0 \ -1 \ -4 \ -1 \ 2 \ 1 \ -1]^T.$$

Non-zero flow indicates that the branch is not observable.

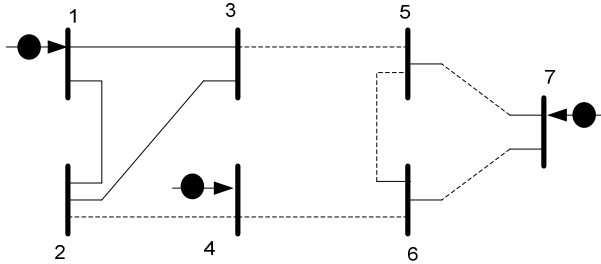


Fig. 9.5. 7-bus test system and its measurements and unobservable branches

It can be seen that after first procedure of determining the unobservable branches, branches: 2-4, 3-5, 4-6, 5-6, 5-7, 6-7 can be removed from further consideration. Measurements: P_4 , P_7 as injections incident to unobservable branches have to be removed.

Now matrix \mathbf{A} and can be written as follows:

$$\mathbf{A} = \begin{bmatrix} 1 & -1 & 0 & 0 & 0 & 0 & 0 \\ 1 & 0 & -1 & 0 & 0 & 0 & 0 \\ 0 & 1 & -1 & 0 & 0 & 0 & 0 \end{bmatrix}.$$

The Jacobi and gain matrices without P_4 and P_7 measurements can be written as:

$$\mathbf{H}_{P/\delta} = \begin{bmatrix} 2 & -1 & -1 & 0 & 0 & 0 & 0 \end{bmatrix}$$

$$\mathbf{G}_{P/\delta} = \begin{bmatrix} 4 & -2 & -2 & 0 & 0 & 0 & 0 \\ -2 & 1 & 1 & 0 & 0 & 0 & 0 \\ -2 & 1 & 1 & 0 & 0 & 0 & 0 \\ 0 & 0 & 0 & 0 & 0 & 0 & 0 \\ 0 & 0 & 0 & 0 & 0 & 0 & 0 \\ 0 & 0 & 0 & 0 & 0 & 0 & 0 \\ 0 & 0 & 0 & 0 & 0 & 0 & 0 \end{bmatrix}.$$

During Cholesky decomposition six zero pivot points are encountered and replaced by 1.0:

$$\mathbf{L} = \begin{bmatrix} 2 & 0 & 0 & 0 & 0 & 0 & 0 \\ -1 & \boxed{1} & 0 & 0 & 0 & 0 & 0 \\ -1 & 0 & \boxed{1} & 0 & 0 & 0 & 0 \\ 0 & 0 & 0 & \boxed{1} & 0 & 0 & 0 \\ 0 & 0 & 0 & 0 & \boxed{1} & 0 & 0 \\ 0 & 0 & 0 & 0 & 0 & \boxed{1} & 0 \\ 0 & 0 & 0 & 0 & 0 & 0 & \boxed{1} \end{bmatrix}$$

and right hand side vector is equal:

$$\mathbf{t}_p^T = [0 \quad \boxed{0} \quad \boxed{1} \quad \boxed{2} \quad \boxed{3} \quad \boxed{4} \quad \boxed{5}]$$

and branch flows are equal:

$$\mathbf{P}_b = \mathbf{A}\boldsymbol{\delta} = [0.5 \quad -0.5 \quad -1.0]^T.$$

Finally, all branches in considered system are declared unobservable.

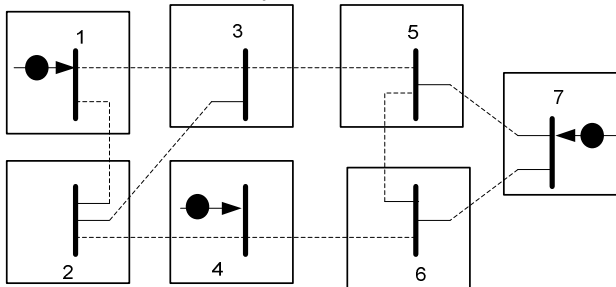


Fig. 9.6. 7-Final results of identified observable islands

9.3. TOPOLOGICAL OBSERVABILITY ANALYSIS METHOD

As it aforementioned, topological observability concept employs graph theory and decoupled measurement model. As it was defined in [9.8] that, given power network is solvable, if and only if, it is possible to find a tree which contains all buses. This leads to the concept of maximal forest of full rank (or simply maximal forest).

The tree is built according to the following rules:

- flow measurements, if assigned, must be assigned to the corresponding measured branch,

- injection measurements, if assigned, are assigned exactly to one of its incident branches.

Example 9.4.

For the power system from example 9.2., the following graph of possibilities of each measurement can be formed:

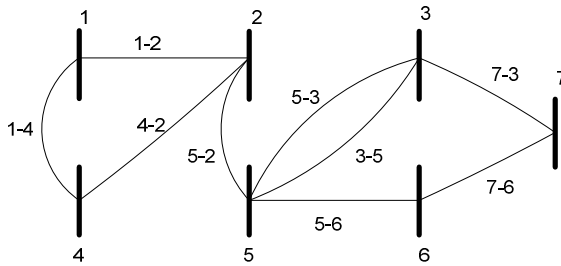


Fig. 9.7. The component graph for the 7-bus network from example 9.2.

At the beginning we have to construct the tree of flow measurements:

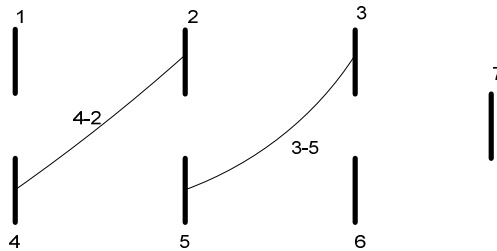


Fig. 9.8. Tree containing flow measurements

Injection measurements: at bus 1 we can assign to branches 1-2 or to 1-4, at bus 5 to branches 5-2, 5-3 or 5-6 and at bus 7 to branches 7-3 or 7-6. It must be mentioned that there is no way to predict the correct sequence for processing injections. Implementation of method requires proper back-up and re-assignment if injections if it is necessary. Fig. 9.9 presents tree containing flow measurements and proposition of injection measurements assigned to single branches.

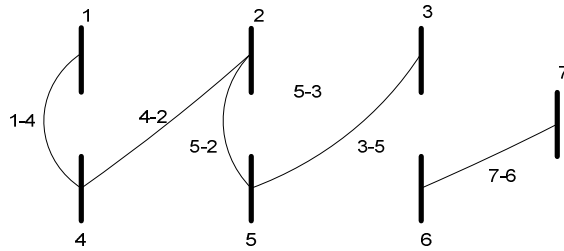


Fig. 9.9. Tree containing flow and injection measurements

It can be seen that it is impossible to build a single tree which will contain all busses. Therefore it is necessary to identify the observable islands. This can be done by removing the injections which have at least one incident branch and does not form a loop with the branches defined as a forest. Accordingly we have to discard injections at buses 5 and 7. According to Fig. 9.10 obtained results are the same as in numerical method.

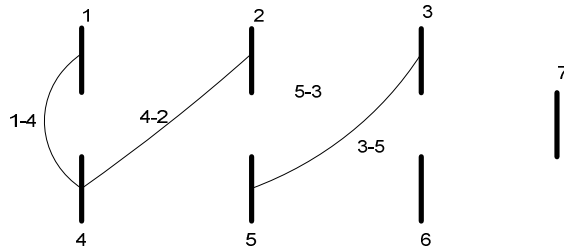


Fig. 9.10. Final tree containing flow and injection measurements

PROBLEMS

- 9.1. Consider system shown in Fig. P.9.1. Use the topological and numerical observability method to determine:
 - all irrelevant branches,
 - all irrelevant injection,
 - all observable islands,
 - all unobservable branches.
- 9.2. Suggest the location and type of a set minimum number of measurements to be added to the measurement list in order to make the system observable.

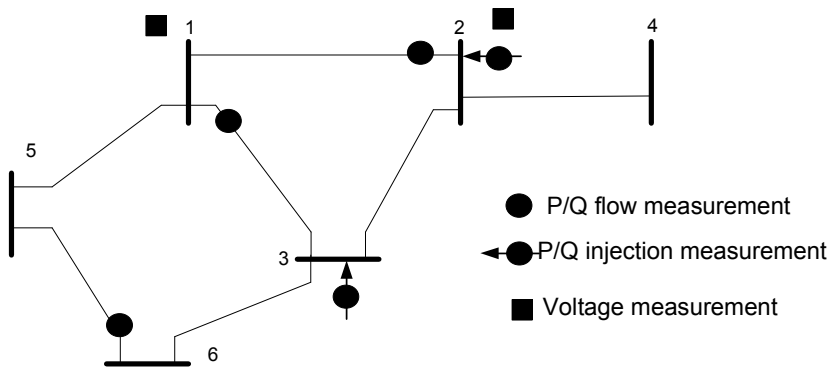


Fig. P.9.1. The 6-bus power system.

REFERENCES

- [9.1] R. Lukomski, K. Wilkosz, ***Power Network Observability for State Estimation Review of the Method***. *The 9th Inter. Scientific Conf. on Electric Power Engineering (EPE)*, Brno, Czech Republic, May 13-15, 2008, pp. 183-190.
- [9.2] A. Abur, A. G. Exposito, ***Power System State Estimation: Theory and Implementation***. Marcel Dekker, Inc, New York – Basel, 2004
- [9.3] A.G. Exposito, A. Abur, ***Generalized Observability Analysis and Measurement Classification***. *IEEE Trans. on Power Apparatus and Systems*, Vol. 13, No.3, Aug. 1998, pp.1090-1096.
- [9.4] Roberto R. Nucera, Michel L. Gilles, ***Observability Analysis: A New Topological Algorithm***. *IEEE Trans. on Power Systems*, Vol. 6, 1991, pp.466-473.
- [9.5] F.F. Wu, A. Monticelli, ***Network Observability: Identification of Observable Islands and Measurement Placement***. *IEEE Trans. on Power Apparatus and Systems*, Vol. 104, No.5, May 1985, pp.1035-1041.
- [9.6] F.F. Wu, A. Monticelli, ***Network Observability: Theory***. *IEEE Trans. on Power Apparatus and Systems*, Vol. 104, No.5, May 1985, pp. 1042-1048.
- [9.7] K. A. Clements, G. R. Krumpholz, P. W. Davis, ***Power System Estimation with Measurement Deficiency: An Algorithm that Determines The Maximal Observable Subnetwork***. *IEEE Trans. on Power Apparatus and Systems*, Vol. 101, No. 9, Sept. 1982, pp.3044-3052.
- [9.8] G. R. Krumpholz, K. A. Clements, P. W. Davis, ***Power System Observability: A Practical Algorithm Using Network Topology***. *IEEE Trans. on Power Apparatus and Systems*, Vol. 99, No.4, July/Aug. 1980, pp.1534-1542.

10. BAD DATA DETECTION AND IDENTIFICATION

10.1. INTRODUCTION

Power system state estimation is mainly aimed at providing a reliable information about power system ie.: power flows, bus powers, and voltages. In order to this, it should detect measurement errors, identify and eliminate them. We can distinguish the following errors:

- Small measurements errors may appear because of various reasons. They are related with uncertainty of metering systems and communications errors. Small measurements errors are filtered during standard state estimation procedure.
- Large measurement errors appear when the meters have large biases which can be caused by: wrong connections, damage. Unexpected interferences in telecommunication system may also lead to large errors. Large measurements errors should be: detected, identified and eliminate.
- Incorrect topology information may mislead state estimator and provide to wrong identification of large measurement errors. This situation is far more complicated.

Some bad data such: negative voltage magnitudes, measurements several orders of magnitude larger or smaller than expected values are easy to detect apriori state estimation. However, sometimes it is not possible to detect bad data in this way and it is necessary to equip state estimator with more advanced tool for bad data detection.

In this chapter we will focus on the bad data detection and identification techniques which related with WLS method. For this method bad data detection and identification is performed only after the estimation process by analyzing measurements residuals [10.1].

10.2. FEATURES OF MEASUREMENT ERRORS

The non-linear equation relating the measurements and the state vector are:

$$\mathbf{z} = \mathbf{h} \cdot (\mathbf{x}) + \mathbf{e}, \quad (10.1)$$

where: \mathbf{x} – a vector $n \times 1$ of true states (unknown),
 \mathbf{z} – a vector $m \times 1$ of measurement (known),
 $\mathbf{h}(\mathbf{x})$ – the nonlinear measurement function,
 \mathbf{e} – a vector $m \times 1$ of random errors.

Bad data detection and identification are performed by analyzing the measurement residual vector,

$$\mathbf{r} = \mathbf{z} - \mathbf{h}(\hat{\mathbf{x}}), \quad (10.2)$$

where: $\hat{\mathbf{x}}$ – the estimated value of \mathbf{x} .

It must be noted that however measurement errors are not correlated, independent measurement residuals may be correlated, which can be approximated as follows [10.1]:

$$\mathbf{r} = \mathbf{S} \cdot \mathbf{e}, \quad (10.3)$$

where residual sensitivity matrix \mathbf{S} is given by:

$$\mathbf{S} = \mathbf{I} - \mathbf{H} \cdot (\mathbf{H}^T \cdot \mathbf{R}^{-1} \cdot \mathbf{H})^{-1} \cdot \mathbf{H}^T \cdot \mathbf{R}^{-1}, \quad (10.4)$$

where $\mathbf{R} = \text{cov}(\mathbf{e}) = \text{diag}(\sigma_k^2)$.

Using above properties and fact that $E(\mathbf{e})=0$, the residual covariance matrix $\mathbf{\Omega}$ can be obtained as follows:

$$E(\mathbf{r}) = E(\mathbf{S} \cdot \mathbf{e}) = \mathbf{S} \cdot E(\mathbf{e}) = 0, \quad (10.5)$$

$$\text{Cov}(\mathbf{r}) = \mathbf{\Omega} = E[\mathbf{r} \cdot \mathbf{r}^T] = \mathbf{S} \cdot E[\mathbf{e} \cdot \mathbf{e}^T] \cdot \mathbf{S}^T = \mathbf{S} \cdot \mathbf{R} \cdot \mathbf{S}^T = \mathbf{S} \cdot \mathbf{R}. \quad (10.6)$$

10.3. TYPES OF MEASUREMENTS, BAD DATA DETECTABILITY AND IDENTIFIABILITY

Measurements may have various properties and influence on state estimation, according to their values and location. The following types of measurement can be distinguished [10.1]:

1. Critical measurements: Elimination of this measurement leads to unobservability of power system. Measurement residual of a critical measurement is always zero.
2. Redundant measurement: Non-critical measurements. Only redundant measurements may have nonzero measurement residuals
3. Critical pair: Two redundant measurements which simultaneous removal from set of measurements leads to unobservability of power system.

Detection belongs on determination if given set of measurements contains any bad data. Identification it is a finding out of specific “wrong” measurement. Only redundant measurement containing bad data can be identified. In other words critical measurements and critical pair may contain bad data and one never find out about it.

10.4. METHODS FOR BAD DATA DETECTION AND IDENTIFICATION

Problem of bad data processing has been presented in many papers. In this chapter, three methods are described: the χ^2 -test, normalized residuals and hypothesis testing identification (HTI).

10.4.1. USE OF χ^2 DISTRIBUTION FOR BAD DATA DETECTION IN WLS STATE ESTIMATION.

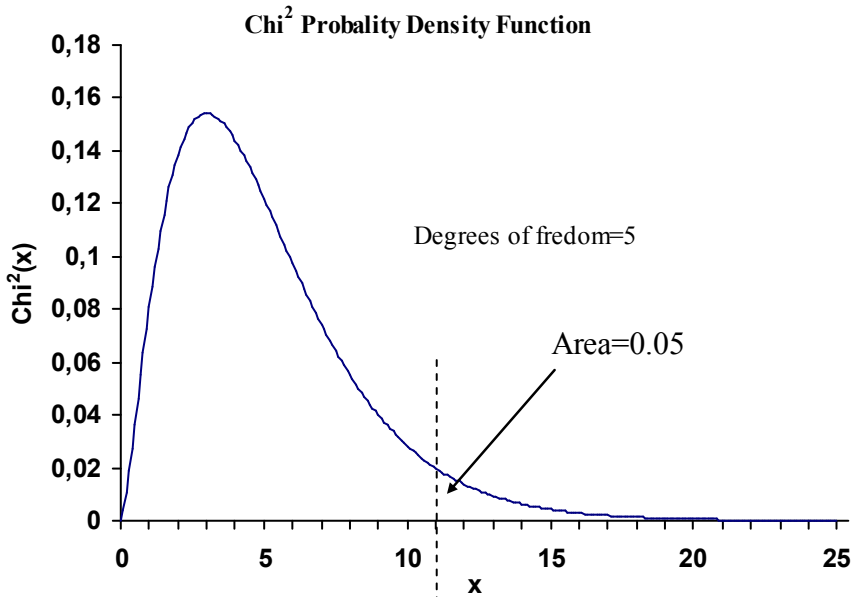


Fig.10.1. χ^2 Probability Density Function

Fig.10.1 presents the χ^2 probability density function (p.d.f). The area under curve represents the probability of finding x in a corresponding region, for example [10.1]:

$$\Pr\{x \geq x_t\} = \int_{x_t}^{\infty} \chi^2(u) du . \quad (10.7)$$

It represents the probability of x being larger than a certain threshold x_t . For error probability equal 0.05 and degrees of freedom equal 5, the threshold x_t is equal 11.071 which can be found in statistical tables or calculated in such software as Matlab®.

In WLS estimation when there is no bad data the index $J(x)$ follows Chi-square distribution. The computed value of $J(x)$ is compared as follows [10.5]:

$$J(x) > \chi^2_{m-n, \alpha} \quad (10.8)$$

where: $J(\mathbf{x}) = [\mathbf{z} - \mathbf{h}(\mathbf{x})]^T \mathbf{R}^{-1} [\mathbf{z} - \mathbf{h}(\mathbf{x})]$,
 m – a number of measurements,
 n – a number of state variables,
 α – the probability of false alarm.

If relation is true, then data is suspected to be biased by large error. The detection is calculated assuming a certain probability for false alarms.

Example 10.1.

Considering the following 4-bus system and its measurement configuration shown in Fig. 10.2

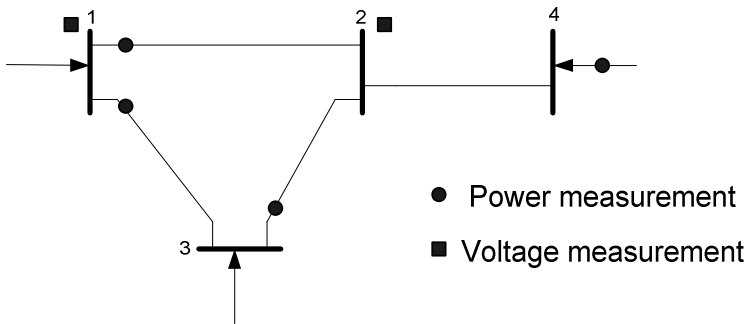


Fig.10.2. 4-bus system and its measurement

The corresponding network data are given below:

Tab. 10.1. Data of 4-bus power system

Bus k	Bus m	R p.u.	X p.u.	B p.u.	Tap
1	2	0.02	0.06	0.20	-
1	3	0.02	0.06	0.25	-
2	3	0.05	0.10	0.00	-
2	4	0.00	0.08	0.00	0.98

The number of state variables, n for considered system is 7 (four voltages magnitude and three voltage phase angles). There are altogether $m=12$ measurements, i.e. two voltage magnitude measurements 3 pairs of real/reactive flows and two pairs

of real/reactive injections, where bus 2 is a zeroinjection bus with attributed higher weights for measurements. Therefore, the degree of freedom is equal 5.

The base case of power flow is used to generation of measurements by adding Gaussian distributed errors. In first case no bad data is introduced, where in second one measurement P_{12} is changed intentionally in order to simulation bad data. Tables below present results for load flow and both cases of estimation.

Tab. 10.2. State Variables

Bus no:	Load Flow Results		Estimated State			
			No Bad Data		On Bad Data	
	V	δ	V	δ	V	δ
1	1.000	0.0000	1.0024	0.0000	1.0038	0.0000
2	0.9858	-1.7171	0.9881	-1.7162	0.9874	-2.0901
3	0.9682	-3.1426	0.9706	-3.1404	0.9707	-3.3505
4	0.9977	-2.8589	0.9999	-2.8629	1.0000	-3.8327

Tab. 10.3. Measurements

Meas. no:	Meas. Type	Real Value	No Bad Data		One Bad Data	
			Measured Value	Estimated Value	Measured Value	Estimated Value
1	V_1	1.0000	1.0011	1.0024	1.0011	1.0038
2	V_2	0.9858	0.9895	0.9881	0.9895	0.9874
3	P_2	0.0000	0.0000	0.0000	0.0000	0.0001
4	P_4	-0.2500	-2.2486	0.2503	-2.2486	-0.0882
5	Q_2	0.0000	0.0000	0.0000	0.0000	-0.0014
6	Q_4	-0.1000	-0.1010	-0.1019	-0.1010	-0.3830
7	P_{12}	-0.5162	-0.5123	-0.5178	-0.7684	-0.6279
8	P_{13}	-0.9625	-0.9731	-0.9666	-0.9731	-1.0287
9	P_{32}	0.2571	0.2452	0.2584	0.2452	0.2326
10	Q_{12}	0.0285	0.0281	0.0279	0.0281	0.0247
11	Q_{13}	-0.1087	-0.1098	-0.1089	-0.1098	-0.1125
12	Q_{32}	0.0393	0.0386	0.0389	0.0386	0.0434
J(x)			2.58		18.98	

The test threshold at 95% confidence level can be obtained using Matlab® function CHI2INV as [10.1]:

$$\text{CHI2INV}(0.95, 5) = 11.0705$$

As it can be seen $J(x)$ is lower than 11.0705 only in first case so no data is suspected, in the second $J(x)$ is higher, therefore the bad data is detected.

10.4.2. UTILIZATION OF NORMALIZED RESIDUALS FOR BAD DATA DETECTION AND IDENTIFICATION IN WLS STATE ESTIMATION

The main drawback of the χ^2 -test described above is indirect approach. Therefore normalized residuals should be more accurate for the bad data detection than the χ^2 -test. Normalized value of residuals can be obtained in the following way [10.1]:

$$r_i^N = \frac{|r_i|}{\sqrt{\Omega_{ii}}} \quad (10.9)$$

where: $\mathbf{r} = \mathbf{z} - \mathbf{h}(\mathbf{x})$, $\mathbf{\Omega} = \mathbf{R} - \mathbf{H} \cdot (\mathbf{H}^T \cdot \mathbf{R} \cdot \mathbf{H})^{-1} \cdot \mathbf{H}^T$,

- \mathbf{r} - a vector of measurement residues,
- \mathbf{R} - a variance matrix,
- \mathbf{H} - a Jacobi matrix.

The measurement with the largest normalized residual and larger than detection threshold is identified as bad data. The algorithm of identifying bad data is presented below [10.1]:

1. Determine estimate of x using WLS procedure.
2. Calculate normalized residuals as in (10.9)
3. Find measurement i which has the largest normalized residual (absolute value)
4. If $r_i > c$ then largest i -th measurement is suspected as bad data. Here, c is a chosen identification threshold and usually set on 3.0
5. Eliminate or correct the i -th measurement from measurement set and go to step 1.

Correction of measurement with bad data can be done in following way:

$$z_i \approx z_i^{bad} - \frac{R_{ii}}{\Omega_{ii}} r_i^{bad} \quad (10.10)$$

State estimation can be repeated after correcting the bad measurement. Sometimes iterative correction is required.

Example 10.2

The table below presents presented residuals for cases considered in example 10.1

Tab. 10.4. Measurement residuals

Measurement	Measurement	No bad data	One bad data
-------------	-------------	-------------	--------------

no:	type	r_i	r_i^N	r_i	r_i^N
1	V ₁	-0.0013	0.4452	-0.0027	0.9473
2	V ₂	0.0014	0.4849	0.0021	0.7451
3	P ₂	-0.0000	0.0380	0.0013	19.6213
4	P ₄	0.0017	0.2460	0.1345	19.8488
5	Q ₂	0.0000	0.2696	-0.0001	1.6377
6	Q ₄	0.0009	0.1360	-0.0128	1.8979
7	P ₁₂	0.0055	0.9028	-0.1406	23.2698
8	P ₁₃	-0.0065	1.8285	0.0556	15.6872
9	P ₃₂	-0.0132	1.8771	0.0126	1.7946
10	Q ₁₂	0.0002	0.0385	0.0034	0.5693
11	Q ₁₃	-0.0009	0.2623	0.0027	0.7620
12	Q ₃₂	-0.0003	0.0412	-0.0048	0.6839

It can be seen that the largest value for normalized residuals is related with P_{12} and simultaneously this value is greater than threshold equal 3. That means that measurement has been identified as a bad data. This measurement must be removed from measurement set or corrected according to (10.10).

10.4.3. HYPOTHESIS TESTING IDENTIFICATION

Identification of bad data by Hypothesis Testing Identification (HTI) method is based on computed estimates of measurement errors instead of measurement residuals as in normalized residuals. This approach may overcome problem when good and bad data have comparable residuals when multiple bad data appears [10.1], [10.2], [10.4].

Partitioning sensitivity matrix S and error covariance matrix R on suspected and true measurements we obtain:

$$S = \begin{bmatrix} S_{ss} & S_{st} \\ S_{ts} & S_{tt} \end{bmatrix}, \quad (10.11)$$

$$r_s = S_{ss}e_s + S_{st}e_t, \quad (10.12)$$

$$r_t = S_{ts}e_s + S_{tt}e_t, \quad (10.13)$$

$$R = \begin{bmatrix} R_s & \mathbf{0} \\ \mathbf{0} & R_t \end{bmatrix}, \quad (10.14)$$

where: r_s, r_t - the residual vectors of suspect and true measurement,
 e_s, e_t - the error vectors of suspect and true measurement.

Assuming that true measurements are free of errors ($E[\mathbf{e}_t] = \mathbf{0}$) the following equations can be derived:

$$\hat{\mathbf{e}}_s = \mathbf{S}_{ss}^{-1} \cdot \mathbf{r}_s, \quad (10.15)$$

$$\hat{\mathbf{e}}_s = \mathbf{e}_s + \mathbf{S}_{ss}^{-1} \cdot \mathbf{S}_{st} \cdot \mathbf{e}_t. \quad (10.16)$$

The $\hat{\mathbf{e}}_s$ has following properties:

Mean:

If $E[\mathbf{e}_t] = \mathbf{0}$, then $E[\hat{\mathbf{e}}_s] = \hat{\mathbf{e}}_s$

else $E[\hat{\mathbf{e}}_s] \neq \hat{\mathbf{e}}_s$

Covariance:

If $E[\mathbf{e}_t] = \mathbf{0}$, then

$$Cov(\hat{\mathbf{e}}_s) = Cov(\mathbf{e}_s) + \mathbf{S}_{ss}^{-1} \mathbf{S}_{st} Cov(\mathbf{e}_t) (\mathbf{S}_{ss}^{-1} \mathbf{S}_{st})^T, \quad (10.17)$$

$$Cov(\hat{\mathbf{e}}_s) = Cov(\mathbf{e}_s) + \mathbf{S}_{ss}^{-1} \mathbf{S}_{st} \mathbf{R}_t \mathbf{S}_{st}^T \mathbf{S}_{ss}^{-T}. \quad (10.18)$$

Using a following property:

$$\mathbf{S} \cdot \mathbf{R} \cdot \mathbf{S}^T = \mathbf{S} \cdot \mathbf{R}, \quad (10.19)$$

the following relation can be derived:

$$\mathbf{S}_{ss} \cdot \mathbf{R}_s \cdot \mathbf{S}_{ss}^T + \mathbf{S}_{st} \cdot \mathbf{R}_t \cdot \mathbf{S}_{st}^T = \mathbf{S}_{ss} \cdot \mathbf{R}_s, \quad (10.20)$$

and substituting equation (10.18)

$$\begin{aligned} Cov(\hat{\mathbf{e}}_s) &= Cov(\mathbf{e}_s) + \mathbf{S}_{ss}^{-1} (\mathbf{S}_{ss} \mathbf{R}_s - \mathbf{S}_{ss} \mathbf{R}_s \mathbf{S}_{ss}^T) \mathbf{S}_{ss}^{-T} \\ &= Cov(\mathbf{e}_s) + \mathbf{S}_{ss}^{-1} (\mathbf{R}_s \mathbf{S}_{ss}^T - \mathbf{S}_{ss} \mathbf{R}_s \mathbf{S}_{ss}^T) \mathbf{S}_{ss}^{-T} \\ &= Cov(\mathbf{e}_s) + (\mathbf{S}_{ss}^{-1} - \mathbf{I}_{ss}) \mathbf{R}_s \end{aligned} \quad (10.21)$$

Decision rules

Two alternative strategies can be distinguished:

Fixed probability of false alarm, α

$$\alpha = \Pr(\text{reject } H_0 \mid H_0 \text{ is true})$$

If H_0 is true $\Rightarrow \hat{\mathbf{e}}_s(i) \sim \mathbf{N}(\mathbf{0}, \mathbf{T}_{ii} \sigma_i^2)$ then:

$$\alpha = \Pr \cdot (|\hat{e}_{si}| > \lambda_i)$$

Substituting a \hat{e}_{si} by normalized absolute value of the estimated terror:

$$|\hat{e}_{si}^N| = \frac{|\hat{e}_{si}|}{\sigma_i \sqrt{T_{ii}}}$$

we obtain:

$$\alpha = \Pr \cdot \left(\frac{|\hat{e}_{si}|}{\sigma_i \sqrt{T_{ii}}} > N_{\left(1-\frac{\alpha}{2}\right)} \right)$$

and threshold is:

$$\lambda_i = \sigma_i \sqrt{T_{ii}} N_{\left(1-\frac{\alpha}{2}\right)}$$

Fixed probability of bad data identification, (1-β)

$$\beta = \Pr(\text{reject } H_1 \mid H_1 \text{ is true})$$

$$1 - \beta = \Pr(\text{accept } H_1 \mid H_1 \text{ is true})$$

If H_1 is true $\Rightarrow \hat{e}_s(i) \sim \mathbf{N} \cdot (e_{si}, (T_{ii} - 1)\sigma_i^2)$. Then

$$\beta = \Pr(\hat{e}_{si} \leq \lambda_i) - \Pr(\hat{e}_{si} \leq -\lambda_i)$$

$$\beta \approx \Pr(\hat{e}_{si} \leq \lambda_i)$$

The algorithm of bad data identification under fixed β [10.1]

Steps of the algorithm

1. Select set s_1 based on r^N and calculate

$$\mathbf{T}_{s_1} = \mathbf{S}_{s_1, s_1}^{-1} \text{ and } \hat{\mathbf{e}}_{s_1} = \mathbf{T}_{s_1} \mathbf{r}_{s_1}$$

2. Calculate $N_{\left(1-\frac{\alpha}{2}\right)_i}$:

$$N_{\left(1-\frac{\alpha}{2}\right)_i} = \frac{|e_{s_i}| + \sigma_i N_{\beta} \sqrt{T_{ii}} - 1}{\sigma_i \sqrt{T_{ii}}}$$

with $0 \leq N_{\left(1-\frac{\alpha}{2}\right)_i} \leq N_{\left(1-\frac{\alpha}{2}\right)_{\max}}$

3. Calculate the threshold for each s_{1i}

$$\lambda_i = \sigma_i \sqrt{T_{ii}} N_{\left(1-\frac{\alpha}{2}\right)_i}, i = 1, \dots, s_{1i}$$

4. Select measurement s_{1i} $|\hat{e}_{s_i}| > \lambda_i$

Form short list of suspect measurements selected at step 4. Repeat steps 1-4 until all measurements in the previous iteration are all selected again at step 4

PROBLEMS

- 10.1. Consider the following linear model:

$$y = a + b \cdot x + e$$

where, $E[e]=0$ and $\text{cov}[e]=\mathbf{I}$. The measurements are given as:

i	1	2	3	4	5	6	7	8	9
x_i	-4.000	-3.000	-2.000	-1.000	0.000	1.000	2.000	3.000	4.000
y_i	-4.002	-2.008	0.031	2.055	4.056	5.96	8.004	9.939	11.944

Find the WLS estimate for a and b . Use Chi2 test to detect any bad data. Use the largest normalised residue to identify bad data.

- 10.1. Consider example 10.2 if measurements: P_{32} and Q_{32} are removed. Find critical measurements.

REFERENCES

- [10.1] A. Abur, A. G. Exposito, ***Power System State Estimation: Theory and Implementation***. Marcel Dekker, Inc, New York – Basel, 2004
- [10.2] L.Mili, T. Van Cutsem, ***Implementation of the hypothesis testing identification in power system state estimation***. *IEEE Trans. on Power Systems*, Vol. 3, No.3, Aug 1988, pp. 887-893.
- [10.3] K. A. Clements, P. W. Davis, ***Multiple Bad Data Detectability and Identifiability: A Geometric Approach***. *IEEE Trans. on Power Delivery*, Vol. 1, No. 3, Nov. 1986, pp. 355 – 360.
- [10.4] Th. Van Cutsem, M. Ribbens-Pavella, L. Mili, ***Hypothesis Testing Identification: A New Method for Bad Data Analysis in Power System State***. *IEEE Trans. on Power Apparatus and Systems*, Vol. 103, No. 11, Nov. 1984, pp. 3239 – 3252.
- [10.5] A. Monticelli, A. Garcia, ***Reliable Bad Data Processing for Real-Time State Estimation***. *IEEE Trans. on Power Apparatus and Systems*, Vol. 102, No.5, May 1983, pp. 1126-1139.
- [10.6] Nian-de Xiang, Shi-ying Wang, Er-keng Yu, ***A New Approach for Detection and Identification of Multiple Bad Data in Power System State Estimation***. *IEEE Trans. on Power Apparatus and Systems*, Vol. 101, No.2, Feb 1982, pp.454-462.
- [10.7] A. Garcia, A. Monticelli, P. Abreu, ***Fast Decoupled State Estimation and Bad Data Processing***. *IEEE Trans. on Power Apparatus and Systems*, Vol. 98, No. 5, Sept 1979, pp.1645-1652.
- [10.8] E. Handschin, F.C. Schweppe, J. Kohlas, A. Fiechter, ***Bad data analysis for power system state estimation***. *IEEE Trans. on Power Apparatus and Systems*, Vol. 94, No. 2, 1975, pp.329-337.
- [10.9] H.M. Merrill, F.C. Schweppe, ***Bad Data Suppression in Power System Static State Estimation***. *IEEE Trans. on Power Apparatus and Systems*, Vol. 90, Nov./Dec. 1971, pp.2718-2725.

11. NETWORK PARAMETER ESTIMATION. TOPOLOGY ERROR IDENTIFICATION

11.1. NETWORK PARAMETER ESTIMATION

11.1.1. INTRODUCTION

The key element for power system security monitoring and analysis is a complete and correct network model. In the model two parts can be distinguished:

- the part including reported switching device statuses, branch power flows, the power supplied by generation and by used by loads,
- the part storing parameters of network components, e.g. series admittance and shunt susceptance of branches modeled as two port π equivalent, transformer tap changer positions. These values are stored in dispatching center database. The database is modified if new network component is added or existing element is upgraded.

The errors in network component parameters appear relatively rare. However, they can potentially degrade the results supplied by the state estimator. In addition these types of errors are much more difficult to detect than bad measurements and topology errors. The main reasons of network parameter errors are as follows:

- using non-adequate models describing network components, e.g. using π equivalents for very long transmission line modeling,
- inaccurate data supplied by the component manufacturers,
- network connectivity changes and component upgrading without updating relevant information stored in dispatching control center database,
- parameter changes resulting from environmental conditions (temperature, humidity etc.),
- erroneous information on transformer tap changes.

The most common parameter errors usually reveal as erroneous values of branch impedances/admittances and bad transformer tap changer positions. In the presence of branch parameter errors the power balance equations redistribute power flows in the adjacent branches and measurements with acceptable errors level can be recognized as bad data.

Significant degradation of state estimation results is observed in presence of parameter errors despite of the availability of highly redundant and accurate measurements.

Example 11.1

Parameter error in the considered 3-bus system (Fig. 11.1) relies on incorrect value of branch reactance in network model $X_{12} = j0.2$ p.u. instead the correct value $X_{12} = j0.15$ p.u.. The measurements are assumed to be correct.

Perform the estimation and compare the results in case of parameter error presence and without error. Measurement results are shown in Tab. 11.1

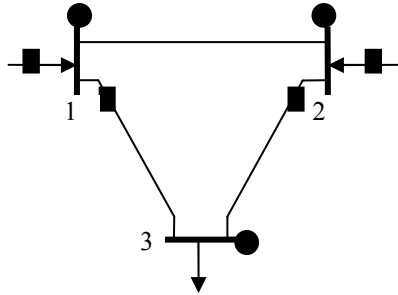


Fig. 11.1. Three-bus power system to illustrate state estimation.

■ - voltage ● active power flow measurement.

Tab. 11.1. Measurement data for example power system.

Measurement	Value, p.u.	Variance
P_1	0.60	0.005
P_2	0.20	0.005
P_{13}	0.47	0.005
P_{23}	0.32	0.005
V_1	1.020	0.001
V_2	1.015	0.001
V_3	1.012	0.001

The estimation results and measurement residuals are presented in Tab. 11.2 and 11.3.

Tab. 11.2. State estimation results for correct case and in case of network parameter error.

i	Correct case		Parameter error	
	\hat{V}_i , p.u.	$\hat{\theta}$, rad	\hat{V}_i , p.u.	$\hat{\theta}$, rad
1	1.0199	0.0000	1.0196	0.0000
2	1.0151	-0.0178	1.0157	-0.0201
3	1.0120	-0.0459	1.0117	-0.0472
$J(\mathbf{x})$	0.0060		0.1016	

Tab. 11.3. State estimation residuals for a correct case and in the case of a network-parameter error.

Measurement	Correct case	Parameter error
	r	r
P_1	0.0030	0.0096
P_2	0.0019	-0.0049
P_{13}	-0.0040	-0.0164
P_{23}	-0.0010	0.0110
V_1	0.0001	0.0004
V_2	-0.0001	-0.0007
V_3	0.0000	0.0003

One can observe that the performance index $J(\mathbf{x})$ residual absolute values are significantly larger in case of parameter error presence. Parameter errors can degrade the estimation quality and produce the effect similar to bad data occurrence.

Fig. 11.2 shows the influence of the error of the branch reactance X_{12} on the state-estimation performance index $J(\mathbf{x})$. It can be seen that branch parameter errors can seriously deteriorate the state estimation quality.

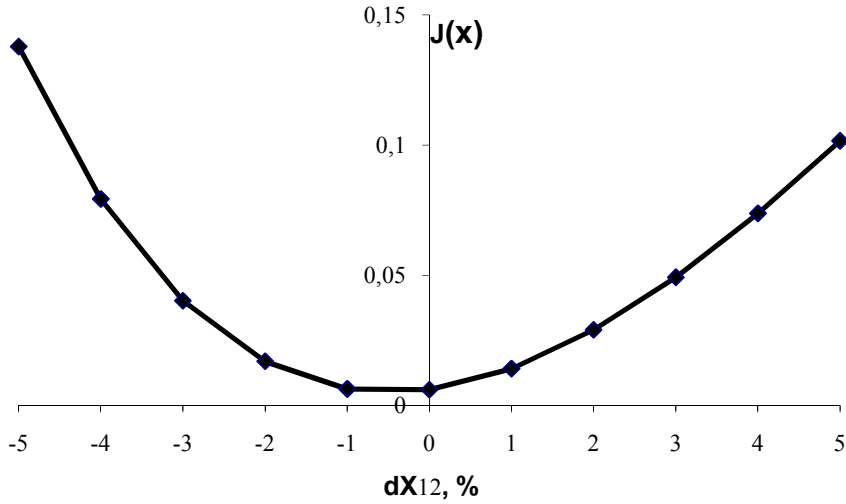


Fig. 11.2. Influence of branch reactance parameter error on state estimation performance.

11.1.2. DETECTION AND IDENTIFICATION OF PARAMETER ERRORS

Parameter error in the considered branch reflects in set of correlated errors burdening measurements incident with this branch: power flow at the ends of the branch and power injection located at the branch terminal nodes. Denoting by s the set of measurements related to the “suspicious” branch, the measurement vector can be formulated as [11.1]:

$$\mathbf{z}_s = h_s(\mathbf{x}, \mathbf{p}) + \mathbf{e}_s = h_s(\mathbf{x}, \mathbf{p}_0) + [h_s(\mathbf{x}, \mathbf{p}) - h_s(\mathbf{x}, \mathbf{p}_0)] + \mathbf{e}_s, \quad (11.1)$$

where: \mathbf{z}_s – a measurement vector,

\mathbf{x} – a state vector,

$h_s(\cdot)$ – a non-linear measurement function,

\mathbf{p} – a vector of real values of the network parameters,

\mathbf{p}_0 – a vector of bad values of the network parameters,

\mathbf{e}_s – a measurement-error vector,

s – a set of incident measurements.

One can be stated that if the parameter error is of significant value then the incident measurements will be probably observed by those having largest residuals. Using Taylor expansion the measurement error can be approximated as:

$$h_s(\mathbf{x}, \mathbf{p}) \approx h_s(\mathbf{x}, \mathbf{p}_0) + \frac{\partial h_s}{\partial \mathbf{p}} (\mathbf{p} - \mathbf{p}_0) = h_s(\mathbf{x}, \mathbf{p}_0) + \frac{\partial h_s}{\partial \mathbf{p}} \mathbf{e}_p, \quad (11.2)$$

where $\mathbf{e}_p = \mathbf{p} - \mathbf{p}_0$.

Detection of parameter error is based on the analysis of large normalized residuals of measurement related to the erroneously modeled branches.

Some of the methods of parameter error detection use the fact of presence of large residuals remain despite bad data rejection. Other methods consider analysis of state estimation performance index and statistical testing.

11.1.3. ESTIMATION OF NETWORK PARAMETER

Methods aimed at estimation of power network parameters basically use:

- residual sensitivity analysis,
- augmenting the state vector.

The main difference is that the first group of method use the classical state vector including voltage magnitudes and angles whereas new variables related to the network parameters are added to the state vector in the second group of methods.

More detailed explanation of the mentioned group of methods is given further.

Parameter estimation with the use of residual sensitivity analysis

This approach use state estimation results to asses network parameters. After successful execution of estimator the measurement residuals are calculated. The relationship between residuals and measurement errors is given by:

$$\mathbf{r} = (\mathbf{I} - \mathbf{H}\mathbf{G}^{-1}\mathbf{H}^T\mathbf{R}^{-1})\mathbf{e} = \mathbf{S} \cdot \mathbf{e} \quad (11.3)$$

where: \mathbf{r} – a measurement residual vector;

\mathbf{e} – a measurement error vector;

$\mathbf{S} = \mathbf{I} - \mathbf{H}\mathbf{G}^{-1}\mathbf{H}^T\mathbf{R}^{-1}$ – a sensitivity matrix;

\mathbf{I} – the identity matrix;

\mathbf{H} – a Jacobi matrix,

\mathbf{R} – a covariance matrix;

$\mathbf{G} = \mathbf{H}^T\mathbf{R}^{-1}\mathbf{H}$ – a gain matrix.

Note, that the set s of incident measurements comprise: erroneous branch, terminal buses, branches connected to the terminal buses, and the terminal buses of connected branches. The linearized relationship among residuals belonging to the set of incident measurement and parameter errors:

$$\mathbf{r}_s = \bar{\mathbf{r}}_s + \left(\mathbf{S}_s \frac{\partial h_s}{\partial \mathbf{p}} \right) (\mathbf{p} - \mathbf{p}_0) = \bar{\mathbf{r}}_s + \left(\mathbf{S}_s \frac{\partial h_s}{\partial \mathbf{p}} \right) \mathbf{e}_p, \quad (11.4)$$

where: \mathbf{S}_s – submatrix of sensitivity matrix corresponding to the adjacent measurements belonging to the set s ;

$\bar{\mathbf{r}}_s$ – a residual vector which can be obtained in case of correct network parameters.

Equation (11.4) determines the linear relationship between residuals \mathbf{r}_s and parameter errors \mathbf{e}_p to be found. In such case determination of parameter error estimates can be considered as local weighed least square estimation task. Assuming that \mathbf{e}_p are normally distributed with zero mean and diagonal covariance matrix $\mathbf{\Sigma}_s$, the optimal WLS estimates are given by:

$$\mathbf{e}_p = \left[\left(\mathbf{S}_s \frac{\partial h_s}{\partial \mathbf{p}} \right)^T \mathbf{\Sigma}_s^{-1} \mathbf{S}_s \frac{\partial h_s}{\partial \mathbf{p}} \right]^{-1} \left(\mathbf{S}_s \frac{\partial h_s}{\partial \mathbf{p}} \right)^T \mathbf{\Sigma}_s^{-1} \mathbf{r}_s, \quad (11.5)$$

where: $\hat{\mathbf{e}}_p$ - a vector of parameter error estimates.

The updated parameter vector can be obtained by:

$$\hat{\mathbf{p}} = \mathbf{p}_0 + \hat{\mathbf{e}}_p, \quad (11.6)$$

After modification of the network parameters, state estimation is re-calculated and checked for result improvement. In some cases, the parameter upgrading can be performed iteratively until no further state estimation improvement is reached.

Parameter estimation with use augmented state vector

The conventional way to solve weighted least squared estimation is to solve the normal equation:

$$\mathbf{G}\Delta\mathbf{x} = \mathbf{H}^T \mathbf{W}^{-1} \Delta\mathbf{z}, \quad (11.7)$$

Estimation of network parameters can be made by augmenting the state variable vector by parameters. The parameters of suspected branches are included in the state vector and the modified weighted least square objective function is given by:

$$\mathbf{J}(\mathbf{x}, \mathbf{p}) = \sum_{i=1}^m w_i^{-1} [z_i - h_i(\mathbf{x}, \mathbf{p})]^2, \quad (11.8)$$

where: z_i – the i -th element of a measurement vector,
 $h_i(\mathbf{x}, \mathbf{p})$ – a non-linear measurement function,
 \mathbf{p} – a vector of suspected parameters,
 w_i – weight of the i -th measurement or pseudomeasurement,
 m – a number of measurements.

Usually the approximate values of the parameters \mathbf{p}_0 can be obtained from the data base storing network model and can be incorporated as pseudomeasurements. The modified objective function is:

$$\mathbf{J}(\mathbf{x}, \mathbf{p}) = \sum_{i=1}^m w_i^{-1} [z_i - h_i(\mathbf{x}, \mathbf{p})]^2 + \sum_{j=1}^k w_{pj}^{-1} (p_j - p_{0j})^2, \quad (11.9)$$

where: w_{pj} – a weight assigned to the pseudomeasurement,

k – a number of pseudomeasurements related to the considered erroneous parameters.

To ensure the system observability, the number of additional state variables should be as low as possible. From that point of view the second formulation of objective function is preferred. The great impact on accuracy of the parameter estimation have the weighting coefficients w_{pj} .

Reduction of extra state variable number is possible for branches representing transmission lines. Usually the line impedance parameters per length unit are known with good accuracy and the single variable, normalized line length can describe the parameters. The parameter of the line connecting nodes i and j one can obtain:

$$\underline{y}_{ij}(l) = \frac{g_{ij} + jb_{ij}}{l}, \quad \underline{y}_{ijsh}(l) = jb_{ijsh}l \quad (11.10)$$

where: l – a normalized line length.

Parameter estimation with use of augmented state vector can be performed by solving classical normal equations. The modified, extended Jacobi matrix has the following structure:

$$\mathbf{H}_{ext} = \left[\begin{array}{c|c} \mathbf{H} & \mathbf{H}_p \\ \hline \mathbf{0} & \mathbf{I} \end{array} \right] \quad (11.11)$$

where: \mathbf{H} – the old Jacobi matrix with size $m \times n$,

n – a number of state variables;

\mathbf{H}_p – the Jacobi matrix including partial derivatives of the measurements with respect to the additional state variables.

Jacobi matrix elements corresponding to the power flow measurements:

$$\frac{\partial P_{ij}}{\partial l} = -\frac{P_{ij}}{l^2}, \quad \frac{\partial P_i}{\partial l} = -\frac{P_{ij}}{l^2}, \quad (11.12)$$

$$\frac{\partial Q_{ij}}{\partial l} = -\frac{Q_{ij} + V_i^2 b_{sij}(1+l^2)}{l^2}, \quad \frac{\partial Q_i}{\partial l} = -\frac{Q_{ij} + V_i^2 b_{sij}(1+l^2)}{l^2} \quad (11.13)$$

Example 11.2

For the three bus system from Example 11.1 find the estimate of relative length l_{12} of branch connecting nodes 1-2 by state vector augmentation. It is assumed that the branch reactance per length unit is $x_{12} = j0.1$.

State vector augmented by additional variable has a form:

$$\mathbf{x} = [\theta_2 \quad \theta_3 \quad V_1 \quad V_2 \quad V_3 \quad l_{12}]^T.$$

Hence, the addition of an extra column in the Jacobi matrix for WLS estimation is needed. The extra column terms are as follows:

$$\frac{\partial P_1}{\partial l_{12}} = -\frac{1}{l_{12}^2} V_1 V_2 \frac{1}{x_{12}} \sin(\theta_1 - \theta_2), \quad \frac{\partial P_2}{\partial l_{12}} = -\frac{1}{l_{12}^2} V_1 V_2 \frac{1}{x_{12}} \sin(\theta_2 - \theta_1),$$

$$\frac{\partial P_{13}}{\partial l_{12}} = \frac{\partial P_{23}}{\partial l_{12}} = \frac{\partial V_1}{\partial l_{12}} = \frac{\partial V_2}{\partial l_{12}} = \frac{\partial V_3}{\partial l_{12}} = 0.$$

Starting from flat point and assuming that the initial relative length $l_{12}^{(0)}=1.0$ one can obtain:

$$\mathbf{x}^{(0)} = [\theta_2 \quad \theta_3 \quad V_1 \quad V_2 \quad V_3 \quad l_{12}]^T = [0.0 \quad 0.0 \quad 1.0 \quad 1.0 \quad 1.0 \quad 1.0]^T.$$

It is easy to observe that the initial point results in zero column term in the Jacobi matrix and estimated variables cannot be calculated from normal equation for WLS. To overcome that the results of first iteration of estimation without an extra variable l_{12} are applied as starting point for second iteration:

$$\mathbf{x}^{(1)} = [\theta_2 \quad \theta_3 \quad V_1 \quad V_2 \quad V_3 \quad l_{12}]^T = [-0.019 \quad -0.047 \quad 1.020 \quad 1.015 \quad 1.012 \quad 1.0]^T.$$

Continuing the calculations the state estimates are as shown in Tab. 11.4. Relative length of branch 1-2 is $l_{12} = 1.459$. Hence, the estimated reactance of branch 1-2 is: $\underline{X}_{12} = l_{12} \underline{x}_{12} = 1.459 j0.1 = j0.146$ (the correct value is $\underline{X}_{12} = j0.150$). One can observe improvement of estimation by small reduction $J(\mathbf{x})$ value (see Example 11.1). Adding an extra variable the convergence was reached after 5 iterations (one extra iteration).

Tab. 11.4. State estimation residuals for the correct case and in the case of a network-parameter error.

i	\hat{V}_i , p.u.	$\hat{\theta}_i$, rad
1	1.0199	0.0000
2	1.0151	-0.018
3	1.0120	-0.046
l_{12}	1.459	
$J(\mathbf{x})$	0.0050	

Parameter estimation using series of past data

Network parameters are assumed to be constant and it enables to estimate them off-line with the use of great amount of measurements recorded in a data base. State vectors and measurement vectors are as follows:

$$\mathbf{x} = [\mathbf{x}_1 \quad \mathbf{x}_2 \quad \dots \quad \mathbf{x}_q \mid \mathbf{p}]^T, \quad (11.14)$$

$$\mathbf{z} = [\mathbf{z}_1 \quad \mathbf{z}_2 \quad \dots \quad \mathbf{z}_q]^T. \quad (11.15)$$

where: q – a number of used measurement sets,

\mathbf{x}_i – the i -th state vector,

\mathbf{z}_i – the i -th measurement vector,

\mathbf{p} – a vector of parameters.

The Jacobi matrix related to the extended model is as follows:

$$\mathbf{H} = \begin{bmatrix} \mathbf{H}_1 & & & \mathbf{h}_{1p} \\ & \mathbf{H}_2 & & \mathbf{h}_{2p} \\ & & \ddots & \vdots \\ & & & \mathbf{H}_q & \mathbf{h}_{qp} \end{bmatrix}. \quad (11.16)$$

Using the normal equations for finding the parameter estimates:

$$\mathbf{G}\Delta\mathbf{x} = \mathbf{H}^T \mathbf{W}^{-1} \Delta\mathbf{z}, \quad (11.17)$$

leads to the gain matrix with the following structure:

$$\mathbf{G} = \mathbf{H}^T \mathbf{W}^{-1} \mathbf{H} = \begin{bmatrix} \mathbf{G}_{11} & & & \mathbf{g}_{1p} \\ & \mathbf{G}_{22} & & \mathbf{g}_{2p} \\ & & \ddots & \vdots \\ & & & \mathbf{G}_{qq} & \mathbf{g}_{qp} \\ \mathbf{g}_{1p}^T & \mathbf{g}_{2p}^T & \dots & \mathbf{g}_{qp}^T & \mathbf{G}_{pp} \end{bmatrix}, \quad (11.18)$$

where:

$$\mathbf{G}_{ii} = \mathbf{H}_i^T \mathbf{W}_i^{-1} \mathbf{H}_i \quad i = 1, 2, \dots, q,$$

$$\mathbf{g}_{ip} = \mathbf{H}_i^T \mathbf{W}_i^{-1} \mathbf{h}_{ip} \quad i = 1, 2, \dots, q,$$

$$\mathbf{G}_{pp} = \sum_{i=1}^q \mathbf{h}_{ip}^T \mathbf{W}_i^{-1} \mathbf{h}_{ip}.$$

The right hand side of the normal equation:

$$\mathbf{H}^T \mathbf{W}^{-1} \Delta \mathbf{z} = [\mathbf{b}_1 \quad \mathbf{b}_2 \quad \dots \quad \mathbf{b}_q \mid \mathbf{b}_p]^T, \quad (11.19)$$

where:

$$\mathbf{b}_i = \mathbf{H}_i^T \mathbf{W}_i^{-1} \Delta \mathbf{z}_i \quad i = 1, 2, \dots, q,$$

$$\mathbf{b}_p = \sum_{i=1}^q \mathbf{h}_{ip}^T \mathbf{W}_i^{-1} \Delta \mathbf{z}_i .$$

The task leads to the processing the matrices with large size and special factorization techniques should be applied to perform the computations.

11.2. TOPOLOGY ERROR PROCESSING

11.2.1. INTRODUCTION

Elements of power systems (transmission lines, transformers, generators, loads etc.) are connected to the network buses. The buses are divided into the sections which can be connected or split by switching of circuit breakers. During the power system operation statuses of circuit breakers may change and network topology is then modified. The credible information on power network connectivity is very important from viewpoint of real-time modeling purposes. Conventional state estimation performs only bad data detection and it is based on the assumption that the network topology is correct. Current power network topology model is supplied by topology processor with use of telemetered statuses of switching devices. Unreported or falsely reported changes in switch statuses may result in wrong connectivity definition and topology errors. Topological errors can negatively affect the credibility of results obtained from state estimator. Incorrect connectivity model may cause:

- obtaining erroneous state variable values,
- detection of false, multiple bad data,
- determining of improper network model for security assessment,
- reporting of non existing violations of acceptable limits.

Topology errors are not so common as analog bad data. However, they are potentially more dangerous. Hence, checking the correctness of network connectivity model becomes very important task.

The further part of the chapter is aimed at the giving some consideration on the topological errors and the characteristic of method for connectivity error detection.

11.2.2. CHARACTERISTICS OF TOPOLOGY ERRORS

All the power network elements are connected to the bus sections through circuit breakers. Bus-sections at the same voltage level in certain substation can be linked together. Hence, substations are capable of operating with different configurations. Topology errors resulted from falsely reported statuses of switching equipment can be generally classified into the following groups:

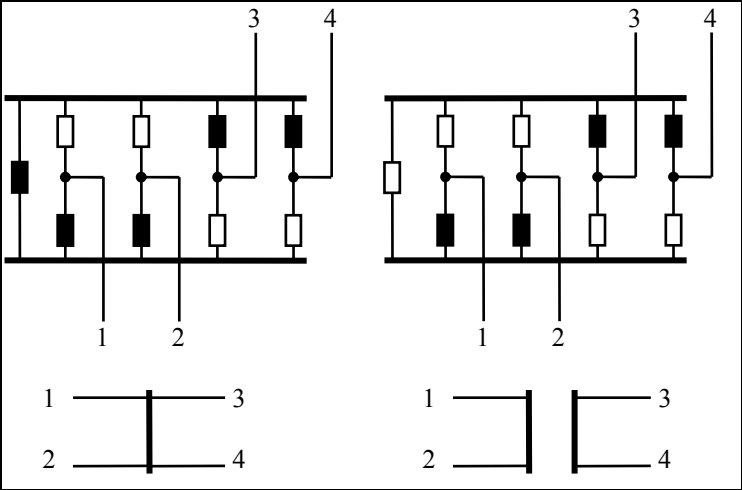
- substation configuration errors,
- shunt element status errors,
- branch status errors.

The brief description of the errors with some examples is shown in Tab. 11.5a – 11.5d. Considering the number of topology errors being at the same time, one can distinguish single and multiple errors.

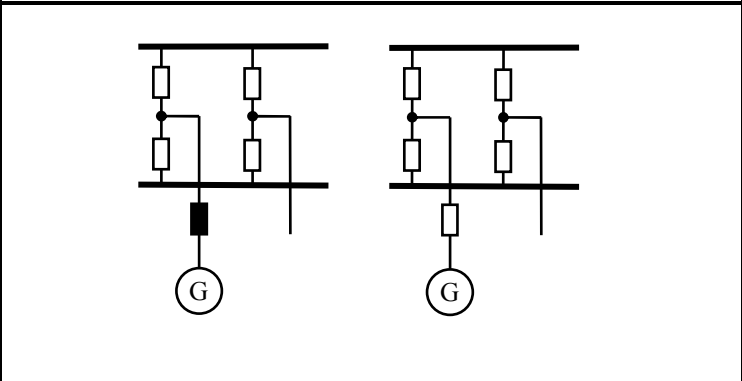
Tab. 11.5a. Substation topology errors. □ - open circuit breaker, ■ - closed circuit breaker.

Description	Example
<p><i>Substation reconfiguration – network element (branch, load, generator) modeled as connected to improper bus.</i></p>	

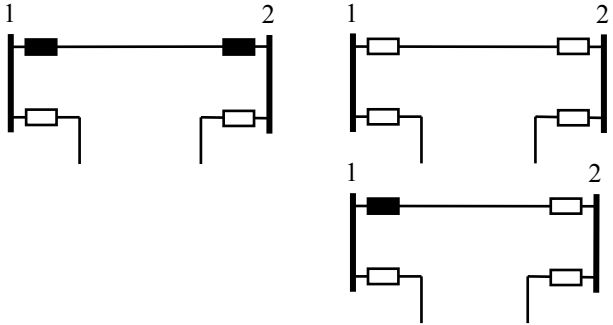
Tab. 11.5b. Bus topology errors. □ - open circuit breaker, ■ - closed circuit breaker.

Description	Example
<p><i>Bus split</i> – single bus is modeled as two or more buses.</p> <p><i>Bus merge</i> – two or more buses are modeled as single bus.</p> <p>Actual and modeled number of nodes are different</p>	 <p>1 ——— 3 2 ——— 4</p> <p>1 ——— 3 2 ——— 4</p>

Tab. 11.5c. Shunt element topology errors. □ - open circuit breaker, ■ - closed circuit breaker.

Description	Example
<p><i>Shunt element inclusion</i> – shunt element (generator, load, reactive shunt) out of operation included in the model.</p> <p><i>Shunt element exclusion</i> – shunt element (generator, load, reactive shunt) in operation excluded from the model.</p>	

Tab. 11.5d. Branch topology errors. □ - open circuit breaker, ■ - closed circuit breaker.

Description	Example
<p><i>Branch exclusion</i> – operating branch excluded from the model</p> <p><i>Branch inclusion</i> – branch out of operation included to the model</p>	

11.2.4. INFLUENCE OF TOPOLOGY ERROR ON STATE ESTIMATION

As mentioned earlier topology errors can be considered in some cases as parameter error with 100% error of branch admittance value. The topology error influence on state estimation is illustrated by the example 11.3.

Example 11.3

For the 5-bus system the active power measurements are available as shown in Fig. 11.2 and DC formulation of state estimation is considered. Variance of all measurements is assumed $\sigma=10^{-3}$ and susceptances of all the lines are equal to $b = 100$.

Tab. 11.6 shows the measurement values and corresponding estimation results with normalized measurements. It can be stated that estimation process was performed with good accuracy: all the residuals have relatively small absolute values.

In the next estimation run topology processor reported wrong topology: the branch linking nodes 2 and 5 being actually in operation was removed from the model. As a result measurement residuals grown significantly. The injection measurements P_2 and P_5 at the line terminal nodes having the largest residual absolute values were flagged as bad (Tab. 11.7). State estimator removed these measurements (the system remained observable). All the residuals have small values what can be observed in Tab. 11.8. Topology error remains to be undetected and two correct measurements were neglected in estimation.

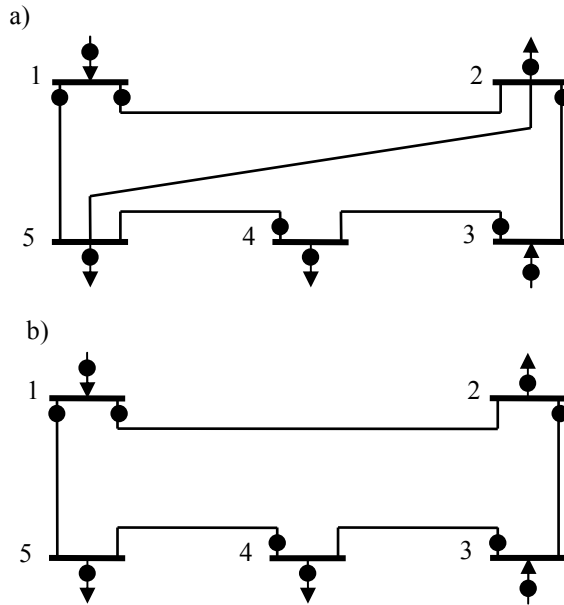


Fig. 11.3. Example power system: correct topology (a), erroneous topology (b).

Tab. 11.6. State estimation results for correct measurements and topology.

Type and location of measurement									
P_1	P_2	P_3	P_4	P_5	P_{12}	P_{15}	P_{23}	P_{34}	P_{45}
Measurement results, p.u.									
0.650	-0.500	0.650	-0.350	-0.450	0.286	0.363	-0.291	0.359	0.091
Power flow estimates, p.u.									
0.650	-0.500	0.650	-0.350	-0.450	0.286	0.364	-0.291	0.359	0.009
Normalized residuals									
0.013	-0.002	-0.002	-0.004	-0.007	-0.008	-0.017	-0.0009	-0.002	-0.002

Tab. 11.7. State estimation results for correct measurements and wrong topology:
branch 2-5 not included in the model.

Type and location of measurement									
P_1	P_2	P_3	P_4	P_5	P_{12}	P_{15}	P_{23}	P_{34}	P_{45}
Measurement results, p.u.									
0.650	-0.500	0.650	-0.350	-0.450	0.286	0.363	-0.291	0.359	0.091
Power flow estimates, p.u.									
0.6497	-0.528	0.643	-0.343	-0.422	0.258	0.392	-0.270	0.373	0.030
Normalized residuals									
0.013	1.318	0.328	-0.334	-1.325	1.019	-1.046	-0.772	-0.516	-0.773

Tab. 11.8. State estimation results for correct measurements and wrong topology:
branch 2-5 not included in the model, rejection of P_2 and P_5 .

Type and location of measurement									
P_1	P_2	P_3	P_4	P_5	P_{12}	P_{15}	P_{23}	P_{34}	P_{45}
Measurement results, p.u.									
0.650	-	0.650	-0.350	-	0.286	0.363	-0.291	0.359	0.091
Power flow estimates, p.u.									
0.650	-	0.650	-0.350	-	0.286	0.363	-0.291	0.359	0.009
Normalized residuals									
0.018	-	-0.0006	-0.0019	-	-0.014	-0.015	0.0003	-0.0002	0.0024

11.2.5. METHODS FOR TOPOLOGY ERROR DETECTION AND IDENTIFICATION

Detection of topology errors is not trivial problem and researchers have proposed great variety of topology error detection methods. The general classification of these methods is presented in Tab. 11.9.

The real-size transmission power network contains thousands of circuit breakers and the detailed modeling of individual circuit breakers is practically impossible. In such case methods using detailed representation apply the two-step procedure:

- “suspicious” network parts are detected by using the residual analysis,
- performing of detailed modeling of areas selected in the first step.

This procedure is more complicated and time-consuming than bus-branch representation based methods. However, the measurements neglected by bus-branch model can be taken into consideration.

Methods based on pre-estimation approach exploit the relationships among measured quantities and network topology. Using artificial intelligence techniques

(neural networks and expert systems) is also widely proposed. Validation of topology model before state estimation has many advantages in comparison to post-estimation approach: it usually much less sophisticated and time consuming. In addition in the presence of topology error state estimator may fail in convergence and detection of these errors may be impossible.

In the further part some more detailed considerations on the outstanding methods are presented.

11.2.6. PRE-ESTIMATION TOPOLOGY ERROR DETECTION AND IDENTIFICATION

This approach take advantage of checking raw measurement data before state estimation is running. Network topology validation is performed with use of data plausibility checking. For this purpose testing of fulfillment of relationships describing power network resulting from Kirchhoff and Ohms laws is applied, e.g.:

- sum of active and reactive power at node should be equal to zero or small value resulting from measurement noise,
- active power flows at terminals of branch should match if losses are also considered,
- active power flows in open ended branch should be near to zero and reactive power flows results from distributed shunt branch reactance. Large active power flows in such case may result from topology errors.

Tab. 11.9. Classification of topology error detection and identification methods.

Group	Approach	Description
Used network topology model representation	Bus-branch representation	Using conventional bus-branch model (breaker statuses are neglected)
	Detailed substation representation	“Suspicious” part of network modeled with individual breaker statuses
Source of data for topology error detection	Pre-estimation	Topology model validated with use of raw analog measurements and ON/OFF statuses of circuit breakers
	Post-estimation	Topology errors detected by state estimation residual analysis or by considering of circuit breakers statuses as state variables

Measurement checking is possible if high local measurement redundancy is available (e.g. all branch power flow and injections adjacent with certain node).

Except for simple measurement consistency testing some other pre-estimation topology verification methods have been proposed:

- graph search technique [11.2]: current and voltage consistency is checked by graph search: if voltage drops in loops or sum of powers in node exceeds tolerance level, then bad marks are assigned to the quantities which failed the test. Hence, the errors in topology can be detected. Additional measurements that are not used originally in calculation can be used for validation.
- application of artificial intelligence technique such as knowledge based systems, artificial neural networks, hybrid systems combining various techniques [11.5], [11.7], [11.8].

11.2.7. POST-ESTIMATION TOPOLOGY ERROR DETECTION AND IDENTIFICATION

This approach use the weighted least square method and detection of topology errors is based on the residual vector analysis 0, 0. However, the observed effect of wrong topology is reported in a false detection of bad data burdening node injections and branch flows.

The topology errors lead to the incorrect measurement function $h(\mathbf{x})$ and it reflects in the Jacobi matrix. This can be described by the following equation [11.3]:

$$\mathbf{H} = \mathbf{H}_e + \mathbf{E}, \quad (11.20)$$

where: \mathbf{H} – an actual Jacobi matrix,
 \mathbf{H}_e – an incorrect Jacobi matrix due to a topology error;
 \mathbf{E} – a Jacobi matrix error.

The true linearized equation for state estimation is:

$$\mathbf{z} = \mathbf{H}\mathbf{x} + \mathbf{e}, \quad (11.21)$$

and inserting (11.20) into (11.21) gives:

$$\mathbf{z} = \mathbf{H}_e\mathbf{x} + \mathbf{E}\mathbf{x} + \mathbf{e}, \quad (11.22)$$

Due to topology error measurement residual will have the following properties:

$$\mathbf{r} = \mathbf{z} - \mathbf{H}_e\hat{\mathbf{x}} = (\mathbf{I} - \mathbf{K}_e)(\mathbf{E}\mathbf{x} + \mathbf{e}), \quad (11.23)$$

$$E(\mathbf{r}) = (\mathbf{I} - \mathbf{K}_e)\mathbf{E}\mathbf{x}, \quad (11.24)$$

$$\text{cov}(\mathbf{r}) = (\mathbf{I} - \mathbf{K}_e)\mathbf{R}, \quad (11.25)$$

where: $\mathbf{K}_e = \mathbf{H}_e(\mathbf{H}_e^T\mathbf{R}^{-1}\mathbf{H}_e)^{-1}\mathbf{H}_e^T\mathbf{R}^{-1}$.

The measurement bias can be described as follows:

$$\mathbf{E}\mathbf{x} = \mathbf{M}\mathbf{f}, \quad (11.26)$$

where: \mathbf{M} – a measurement to branch incidence matrix,
 \mathbf{f} – a vector of branch flow errors.

The measurement residual are given by:

$$\mathbf{r} = (\mathbf{I} - \mathbf{K}_e)\mathbf{M}\mathbf{f}, \quad (11.27)$$

Now, it is possible to express the expected value of the normalized residuals in terms of branch flow error:

$$\mathbf{E}(\mathbf{r}^N) = \mathbf{\Omega}^{-\frac{1}{2}}(\mathbf{I} - \mathbf{K}_e)\mathbf{M}\mathbf{f} = \mathbf{S}\mathbf{f}, \quad (11.28)$$

where: $\mathbf{\Omega} = \text{diag}\{\text{cov}(\mathbf{r})\}$,

$\mathbf{S} = \mathbf{\Omega}^{-\frac{1}{2}}(\mathbf{I} - \mathbf{K}_e)\mathbf{M}$ - sensitivity matrix.

Assuming that bad measurement data are eliminated, normalized residual test can be then applied for detection of topology errors.

Let consider the linear relationship between the measurement residuals and branch error flows:

$$\mathbf{r} = (\mathbf{I} - \mathbf{K}_e)\mathbf{M}\mathbf{f} = \mathbf{T}\mathbf{f}, \quad (11.29)$$

If the single topology error exist in the j -th branch, there will be a change in the corresponding branch flow $f_j = \alpha$ and $f_k = 0$ for $k \neq j$, where α is the scalar corresponding to the topology error. Hence, the measurement residual vector \mathbf{r} will be collinear with the vector \mathbf{T}_j , being the j -th column of matrix \mathbf{T} .

The geometric interpretation of the measurement residual can be used for detection of single branch topological error. Geometrically based method contains the following steps [11.3]:

- solving weighted least squares estimation and calculation of residuals ,
- calculation of sensitivity matrix \mathbf{T} for measurement residuals with respect to branch flow errors \mathbf{f} ,
- testing the co-linearity between the measurement residual vector and the columns of the sensitivity matrix \mathbf{T} using the dot product:

$$\cos \theta_j = \frac{\mathbf{T}_j^T \mathbf{r}}{\|\mathbf{T}_j\| \|\mathbf{r}\|}, j = 1, 2, \dots, b, \quad (11.30)$$

where: b – number of branches in the power network,

- if $\cos \theta_j \approx 1$ and for other branches $\cos \theta_k < 1$ for $k \neq j$, a single topology error may occur in the j -th branch.

It should be noted that detection and identification of topology errors based on the measurement residuals analysis will require high enough measurement redundancy. In

some cases of errors, the capability of detection and identification can be significantly limited by the network configuration.

Example 11.4

For 5-bus system shown in Fig. 11.4 DC state estimation is performed. However, the branch *d* connecting the nodes 2 and 5 is assumed to be open but actually it is in operation.

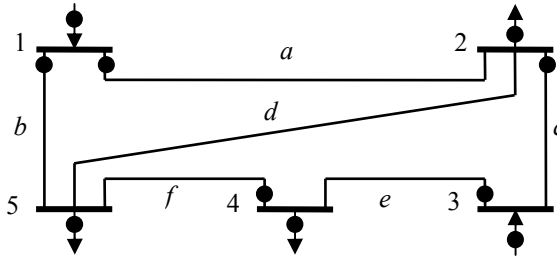


Fig. 11.4. Example power network and its measurement system.

For simplicity all measurement weights are assumed to be 1, and branch reactances are 0.01 p.u.. Measurement data are gathered in Tab. 11.10.

Tab. 11.10. Measurement data for the exemplary power system.

P_1	P_2	P_3	P_4	P_5	P_{12}	P_{15}	P_{23}	P_{34}	P_{45}
0.65	-0.50	0.65	-0.35	-0.45	0.28	0.36	-0.29	0.36	0.01

The Jacobi matrix with correct topology:

$$\mathbf{H} = \begin{bmatrix} -100 & 0 & 0 & -100 \\ 300 & -100 & 0 & -100 \\ -100 & 200 & -100 & 0 \\ 0 & -100 & 200 & -100 \\ -100 & 0 & -100 & 300 \\ -100 & 0 & 0 & 0 \\ 0 & 0 & 0 & -100 \\ 100 & -100 & 0 & 0 \\ 0 & 100 & -100 & 0 \\ 0 & 0 & 100 & -100 \end{bmatrix} . \tag{11.31}$$

Due to exclusion error (actually closed branch *d* is modeled as open) the Jacobi matrix is modified:

$$\mathbf{H}_e = \begin{bmatrix} -100 & 0 & 0 & -100 \\ 200 & -100 & 0 & 0 \\ -100 & 200 & -100 & 0 \\ 0 & -100 & 200 & -100 \\ 0 & 0 & -100 & 200 \\ -100 & 0 & 0 & 0 \\ 0 & 0 & 0 & -100 \\ 100 & -100 & 0 & 0 \\ 0 & 100 & -100 & 0 \\ 0 & 0 & 100 & -100 \end{bmatrix} \quad (11.32)$$

The measurement to branch incidence matrix is defined as follows:

$$\mathbf{M} = \begin{matrix} P_1 \\ P_2 \\ P_3 \\ P_4 \\ P_5 \\ P_{12} \\ P_{15} \\ P_{23} \\ P_{34} \\ P_{45} \end{matrix} \begin{bmatrix} a & b & c & d & e & f \\ 1 & 1 & 0 & 0 & 0 & 0 \\ -1 & 0 & -1 & 1 & 0 & 0 \\ 0 & 0 & 1 & 0 & 1 & 0 \\ 0 & 0 & 0 & 0 & -1 & 1 \\ 0 & -1 & 0 & -1 & 0 & -1 \\ 1 & 0 & 0 & 0 & 0 & 0 \\ 0 & 1 & 0 & 0 & 0 & 0 \\ 0 & 0 & -1 & 0 & 0 & 0 \\ 0 & 0 & 0 & 0 & 1 & 0 \\ 0 & 0 & 0 & 0 & 0 & 1 \end{bmatrix} \quad (11.33)$$

Using equations. (11.27) - (11.30) the geometric test is performed and the results are shown in Tab. 11.11

Tab. 11.11. Measurement data for example power system.

Branch j	$\cos \theta_j$
a	0.0007
b	0.0007
c	0.0007
d	1.0000
e	0.0007

If $\cos \theta_d = 1.0000$ and other values significantly smaller than 1.0, single topology error affecting branch d is detected with use the test.

11.2.8. SUBSTATION CONFIGURATION ERRORS

Power system substations can operate in many different configurations. The most common used circuit breaker schemes are: single bus, double bus-double breaker, main and transfer bus, breaker and a half, ring bus. The number of electrical nodes depends on the substation connectivity scheme and circuit breaker statuses.

Many methods of topology error detection concern on modeling of individual circuit breakers statuses in substations. After validation procedure substation connectivity scheme is converted into bus-branch model. If the status of every breaker in certain substation needs to be checked, a sufficient measurement redundancy within substation is needed. Otherwise the statuses cannot be correctly estimate because different configurations can correspond to the available measurement set.

The closed circuit breakers is represented by zero-impedance, and open by zero admittance. Inserting very small impedance or admittance values of breakers into estimation equations usually leads to the ill-conditioning of estimation computations and may cause convergence difficulties. The more suitable representation concerns on power flow through breaker.

Considering the state estimation equation with augmented measurement set:

$$\mathbf{z}_a = h(\mathbf{x}) + \mathbf{M}\mathbf{f} + \mathbf{e}, \quad (11.34)$$

where: \mathbf{z}_a – an augmented measurement vector,

$h()$ – a nonlinear function relating measurements to the states assuming all breakers are open,

\mathbf{x} – a state vector containing bus voltage magnitudes and angles,

\mathbf{M} – a measurement to circuit breaker incidence matrix,

\mathbf{f} – a vector of power flows through the circuit breakers,

\mathbf{e} – a vector of measurement errors.

State variables and breaker flows form the augmented state vector:

$$\mathbf{x}_a = \begin{bmatrix} \mathbf{x} \\ \mathbf{f} \end{bmatrix}, \quad (11.35)$$

and new nonlinear measurement function h_a is formulated. The state estimation equation:

$$\mathbf{z}_a = h_a(\mathbf{x}_a) + \mathbf{e}, \quad (11.36)$$

Measurements and constraints including in (11.36) comprise the following types:

- “regular” analog measurements:

$$\mathbf{z} = h(\mathbf{x}_a) + \mathbf{e}, \quad (11.37)$$

- operational constraints imposed by status of the circuit breaker as presented in Fig. 11.5,

These constraints can be expressed in matrix form as :

$$\mathbf{A}_0 \mathbf{x}_a + \mathbf{e}_0 = 0. \quad (11.38)$$

- structural constraints imposed by network connectivity structure, e.g. zero injection constraints at some nodes:

$$c(\mathbf{x}_a) = 0. \quad (11.39)$$

The estimation objective function and constraints are as follows:

$$\begin{aligned} & \min J(\mathbf{r}, \mathbf{r}_0) \\ & \text{s.t. } h(\hat{\mathbf{x}}) + \mathbf{r} = \mathbf{z} \\ & \quad \mathbf{A}_0 \hat{\mathbf{x}} + \mathbf{r}_0 = 0 \\ & \quad c(\hat{\mathbf{x}}) = 0 \end{aligned}, \quad (11.40)$$

where: J – an objective function;

\mathbf{r}, \mathbf{r}_0 – residuals for conventional measurements and operational constraints,

$\hat{\mathbf{x}}$ - an augmented vector of state estimates containing voltage angles, magnitudes and power flows through circuit breakers.



Fig. 11.5. Operational constraints for circuit breakers in the generalized state estimation:
 (a) closed circuit breaker, (b) open circuit breaker.

Example 11.5

For the substation presented in Fig. 11.6 create detailed substation model of DC state estimation for augmented state variable vector.

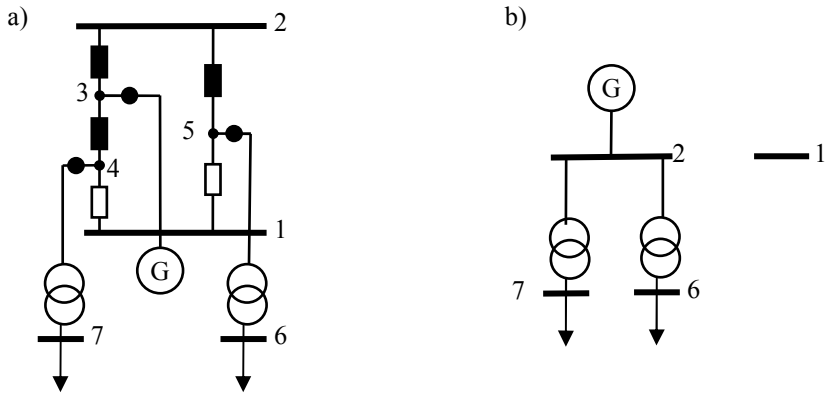


Fig. 11.6. Detailed substation representation (a) and its bus-branch model (b).

As the state variables the substation internal node angles and two external node angles (θ_6, θ_7) are considered. In addition power flows through switching branches are also included into the state vector.

$$x = [\theta_2 \quad \theta_3 \quad \theta_4 \quad \theta_5 \quad P_{14} \quad P_{15} \quad P_{23} \quad P_{25} \quad P_{34}]^T$$

Measurements in terms of state variables are as follows:

$$P_3 = -P_{23} + P_{34} + e,$$

$$P_5 = -P_{15} - P_{25} + e.$$

The constraints related to the circuit breaker statuses:

$$\theta_3 - \theta_4 = 0,$$

$$\theta_2 - \theta_3 = 0,$$

$$\theta_2 - \theta_5 = 0,$$

$$P_{14} = 0,$$

$$P_{15} = 0.$$

The constraints related to the zero-injection pseudo-measurements:

$$P_1 = 0: \quad P_{14} + P_{15} = 0,$$

$$P_2 = 0: \quad P_{23} + P_{25} = 0,$$

$$P_4 = 0: \quad -P_{14} - P_{34} - X_{T1}^{-1}(\theta_6 - \theta_4) = 0,$$

One can observe that variable θ_1 does not appear in state vector because it is considered as reference.

Running local weighted least square calculations for detailed bus section level for substation with suspicious measurement or switching device statuses is possible. It enables detection of bad data and doubt statuses of switching branches if the local observability is ensured.

Example 11.6

In the substation presented in Fig. 11.6 the state of switching branch connecting nodes 3 and 4 is assumed to be unknown. Measurement values: $P_3= 2.50$ p.u., $P_{64}= -1.10$ p.u., $P_5= -1.45$ p.u. Measurement variances are set to 0.01. Transformer T_1 reactance is 0.1 p.u..

Three separated areas can be distinguished in substation: node 1, nodes 2, 3, 5 and nodes 4, 6. The measurement, topological and operational constraints can be written in matrix form as:

$$\begin{bmatrix}
 0 & 0 & 0 & 0 & 0 & -1 & 0 & 1 \\
 0 & 0 & 10 & 0 & 0 & 0 & 0 & 0 \\
 0 & 0 & 0 & 0 & -1 & 0 & -1 & 0 \\
 0 & -1 & 0 & 0 & 0 & 0 & 0 & 0 \\
 1 & 0 & 0 & 0 & 0 & 0 & 0 & 0 \\
 0 & 0 & 0 & 1 & 0 & 0 & 0 & 0 \\
 0 & 0 & 0 & 0 & 1 & 0 & 0 & 0 \\
 0 & 0 & 0 & 1 & 1 & 0 & 0 & 0 \\
 0 & 0 & 0 & 0 & 0 & 1 & 1 & 0 \\
 0 & 0 & -10 & -1 & 0 & 0 & 0 & -1
 \end{bmatrix}
 \begin{bmatrix}
 \hat{\theta}_3 \\
 \hat{\theta}_5 \\
 \hat{\theta}_6 \\
 \hat{P}_{14} \\
 \hat{P}_{15} \\
 \hat{P}_{23} \\
 \hat{P}_{25} \\
 \hat{P}_{34}
 \end{bmatrix}
 =
 \begin{bmatrix}
 \hat{P}_3 \\
 \hat{P}_{64} \\
 \hat{P}_5 \\
 \hat{\theta}_{25} \\
 \hat{\theta}_{34} \\
 \hat{P}_{14} \\
 \hat{P}_{15} \\
 \hat{P}_1 \\
 \hat{P}_2 \\
 \hat{P}_4
 \end{bmatrix}$$

The results of weighted least squares estimation are:

$$\begin{bmatrix}
 \hat{\theta}_3 \\
 \hat{\theta}_5 \\
 \hat{\theta}_6 \\
 \hat{P}_{14} \\
 \hat{P}_{15} \\
 \hat{P}_{23} \\
 \hat{P}_{25} \\
 \hat{P}_{34}
 \end{bmatrix}
 =
 \begin{bmatrix}
 0.0000 \\
 0.0000 \\
 -0.1091 \\
 0.0029 \\
 0.0029 \\
 -1.4294 \\
 1.4382 \\
 1.0794
 \end{bmatrix}$$

It can be observed that power flow P_{34} differs considerably from zero and doubt circuit breaker status is assumed to be closed.

PROBLEMS

- 11.1. For three-bus power system from Problem 7.2 (chapter 7) find the relative length estimation of branch 2-3 by state vector augmentation (see Example 7.2). Assume that reactance per unit length is $\underline{x} = j0.15$. Compare the obtained estimated branch reactance with actual value and assess the estimation performance index.
- 11.2. Five-bus system as presented in Fig. 11.7 the branch e shown as dotted line is modeled as closed but in fact it is open. All measurement shown in Tab. 11.12 have weights assumed to be 1, and branch reactances are 0.01 p.u.. Perform the DC state estimation and make colinearity test with (11.30) for detecting the topology errors. Is topology error in branch e detectable? Why?

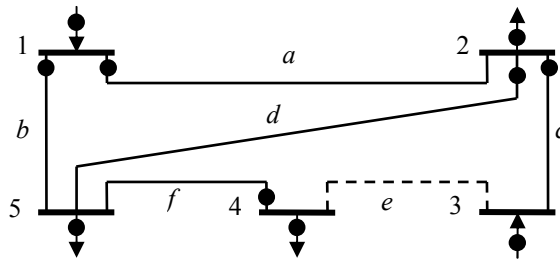


Fig. 11.7. Power system for Problem 2.

Tab. 11.12. Measurement data for example power system.

P_1	P_2	P_3	P_4	P_5	P_{12}	P_{15}	P_{23}	P_{25}	P_{45}
0.65	-0.50	0.65	-0.35	-0.45	0.16	0.48	-0.65	0.31	-0.35

REFERENCES

- [11.1] A. Abur, A. G. Exposito, *Power system state estimation. Theory and implementation*, Marcel Dekker, New York-Basel, 2004.
- [11.2] P. Bonanomi, G. Gramberg, *Power system data validation and state calculation by network search technique*, *IEEE Trans. on Power Apparatus and Systems*, Vol. 102, No. 1, Jan. 1983, pp. 238-249.

- [11.3] K. A. Clements, P. W. Davis, ***Detection and identification of topology errors in electric power system***, *IEEE Trans. on Power Systems* Vol. 3, No. 4, Nov. 1988, pp. 1748-1753.
- [11.4] A. Monticelli, ***State estimation in electric power systems - a generalized approach***, Kluwer Academic Publishers, Boston, 1999.
- [11.5] D. M. V. Kumar, S. C. Srivastava, S. Shah, S. Mathur, ***Topology processing and static state estimation using artificial neural networks***, *IEE Proc. Generation, Transmission and Distribution*, Vol. 143, No. 1, Jan. 1996, pp. 99-105.
- [11.6] N. Logic, G. T. Heydt, ***An approach to network parameter estimation in power system state estimation***, *Electric Power Components and Systems*, Vol. 33, No. 11, pp. 1191 – 1201.
- [11.7] R. Łukomski, K. Wilkosz, ***Power system topology verification method: utilization of different types of artificial neural networks***. *The 16th Inter. Conf. on Systems Science*, Vol. 3, Wrocław, Sept. 2007, pp. 149-157.
- [11.8] R. Lukomski, K. Wilkosz, ***Method for power system topology verification with use of radial basis function networks***, *Lecture Notes in Computer Science*, Vol. 4507, 2007, pp. 862-869.
- [11.9] K. Wilkosz, ***A Multi-Agent System Approach to Power System Topology Verification***. *Lecture Notes in Computer Science*, Vol. 4881, 2007, pp. 970 - 979.
- [11.10] N. Singh, H. Glavitsch, ***Detection and identification of topological errors in online power system analysis***, *IEEE Trans. on Power Systems*, Vol. 6, No. 1, Feb. 1991, pp. 324-331.
- [11.11] F. F. Wu, W.-H. E. Liu, ***Detection of topology errors by state estimation***, *IEEE Trans. on Power Systems*, Vol. 4, No. 1, Feb. 1989, pp. 176-183.

12. STATE ESTIMATION USING AMPERE MEASUREMENTS

12.1. INTRODUCTION

Nowadays, state estimation is also applied to lower voltage networks where measurement set usually consist of a large proportion of voltage magnitude and ampere measurements. Power measurements usually are used for power transformers. In this situation there is need to incorporate of ampere measurements into the state estimation. Using ampere measurements instead of pair of power measurements causes several problems, such as possibility of non-unique solution and lack a possibility of decoupling [12.1].

12.2. MODELING OF AMPERE MEASUREMENTS

For a branch connecting nodes k and m (Fig. 12.1), the following current equation can be derived:

$$I_{km} = \text{abs} \left(\begin{bmatrix} -\left(\frac{y_{sh}}{2} + y_{km}\right) & y_{km} \end{bmatrix} \cdot [V_k \quad V_m]^T \right). \quad (12.1)$$

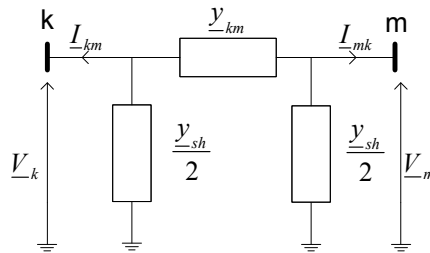


Fig. 12.1. Two port Π -model of transmission line.

Current can be calculated also from the following equations:

$$I_{km} = \frac{\sqrt{P_{km}^2 + Q_{km}^2}}{V_k}. \quad (12.2)$$

However for distribution network shunt elements of branch are negligible and for polar coordinate system the following equation can be derived [12.1]:

$$I_{km} = \sqrt{(g_{km}^2 + b_{km}^2)(V_k^2 + V_m^2 - 2V_k V_m \cos \delta_{km})}. \quad (12.3)$$

From (12.3) it is easy to obtain the Jacobi-matrix elements for state variables of the bus k :

$$\frac{\partial I_{km}}{\partial \delta_k} = \frac{g_{km}^2 + b_{km}^2}{I_{km}} V_k V_m \sin \delta_{km}, \quad (12.4)$$

$$\frac{\partial I_{km}}{\partial \delta_m} = -\frac{g_{km}^2 + b_{km}^2}{I_{km}} V_k V_m \sin \delta_{km}, \quad (12.5)$$

$$\frac{\partial I_{km}}{\partial V_k} = \frac{g_{km}^2 + b_{km}^2}{I_{km}} (V_k - V_m \cos \delta_{km}), \quad (12.6)$$

$$\frac{\partial I_{km}}{\partial V_m} = \frac{g_{km}^2 + b_{km}^2}{I_{km}} (V_m - V_k \cos \delta_{km}). \quad (12.7)$$

Figures below present I_{km} and its derivatives as a function of V_k and δ_k for $\delta_m = 0$, $V_m = 1$, $R_{km} = 0.02$, $X_{km} = 0.06$ and shunt admittance equal 0.

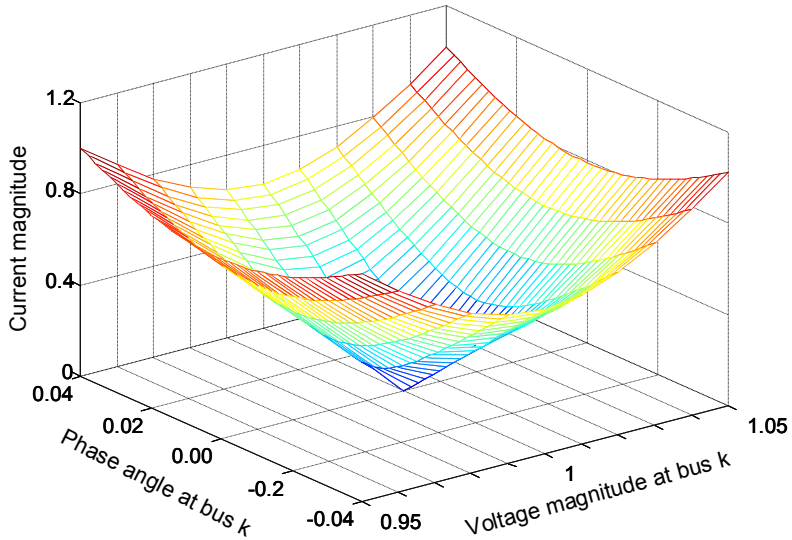


Fig. 12.2. Current magnitude.

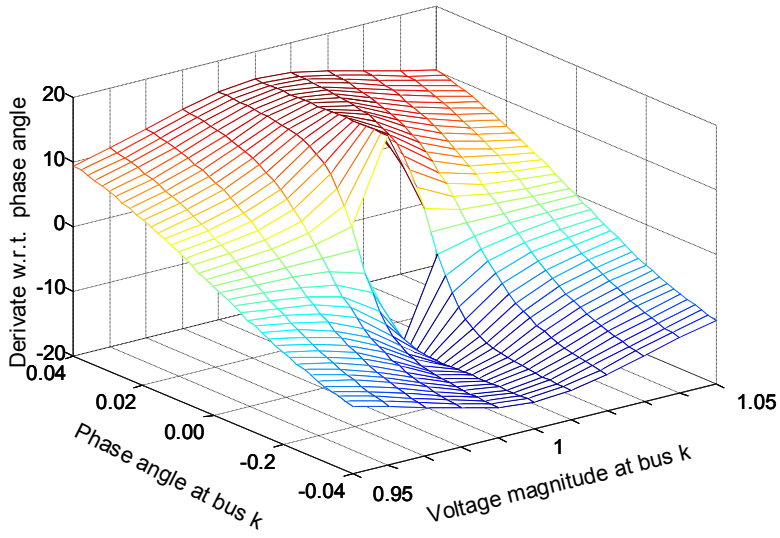


Fig. 12.3. Derivate of current magnitude with respect to phase angle.

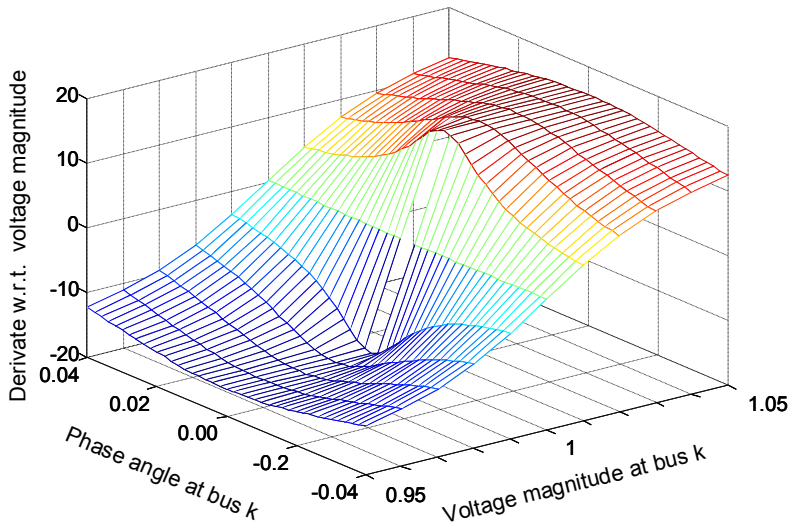


Fig. 12.4. Derivate of current magnitude with respect to voltage magnitude.

It can be seen that for strong non-linearity at $V_k = 1$ and $\delta_k = 0$ derivatives abruptly change which is shown in Fig. 12.3 and Fig. 12.4. That means that derivatives of I_{km} are undefined at this point. The solution of this problem is using I_{km}^2 instead of I_{km} . Then derivatives can be written as:

$$\frac{\partial I_{km}^2}{\partial \delta_k} = 2(g_{km}^2 + b_{km}^2) V_k V_m \sin \delta_{km}, \quad (12.8)$$

$$\frac{\partial I_{km}^2}{\partial \delta_m} = -2(g_{km}^2 + b_{km}^2) V_k V_m \sin \delta_{km}, \quad (12.9)$$

$$\frac{\partial I_{km}^2}{\partial V_k} = 2(g_{km}^2 + b_{km}^2) (V_k - V_m \cos \delta_{km}), \quad (12.10)$$

$$\frac{\partial I_{km}^2}{\partial V_m} = 2(g_{km}^2 + b_{km}^2) (V_m - V_k \cos \delta_{km}). \quad (12.11)$$

Figures below present plot of I_{km}^2 and its derivatives as a function of V_k and δ_k .

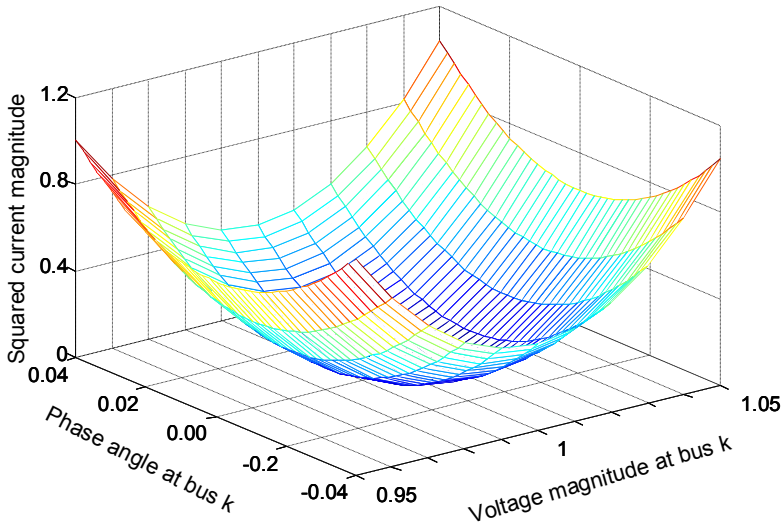


Fig. 12.5. Square current magnitude.

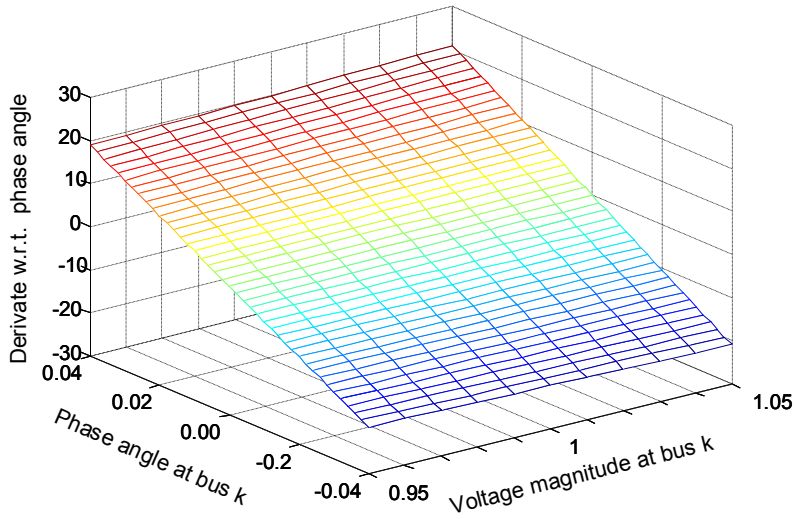


Fig. 12.6. Derivate of square current magnitude with respect to phase angle.

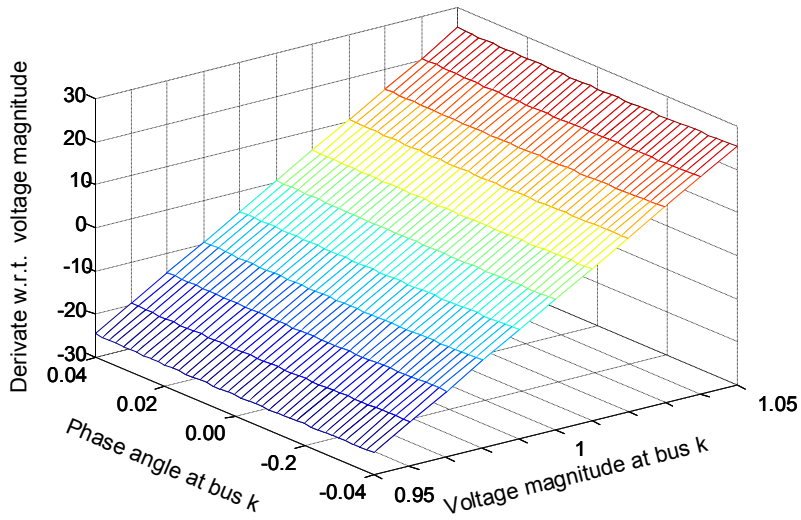


Fig. 12.7. Derivate of square current magnitude with respect to voltage magnitude.

It can be seen that derivatives for the flat start are null which can cause ill-conditioning of the gain matrix. Therefore, the following solutions to overcome this problem can be suggested [12.1]:

- initiate state variables with a random small perturbation,
- add artificial shunt elements which are removed after first iteration.

If b_{sh} is considered, the I_{km} has following derivatives:

$$\frac{\partial I_{km}}{\partial \delta_k} = \frac{V_k V_m \left[\left(g_{km}^2 + b_{km} \left(\frac{b_{sh}}{2} + b_{km} \right) \right) \sin \delta_{km} + g_{km} \frac{b_{sh}}{2} \cos \delta_{km} \right]}{I_{km}}, \quad (12.12)$$

$$\frac{\partial I_{km}}{\partial \delta_m} = - \frac{V_k V_m \left[\left(g_{km}^2 + b_{km} \left(\frac{b_{sh}}{2} + b_{km} \right) \right) \sin \delta_{km} + g_{km} \frac{b_{sh}}{2} \cos \delta_{km} \right]}{I_{km}}, \quad (12.13)$$

$$\frac{\partial I_{km}}{\partial V_k} = \frac{\left(g_{km}^2 + \left(\frac{b_{sh}}{2} + b_{km} \right)^2 \right) V_k}{I_{km}}, \quad (12.14)$$

$$- \frac{V_m \left[\left(g_{km}^2 + b_{km} \left(\frac{b_{sh}}{2} + b_{km} \right) \right) \cos \delta_{km} - g_{km} b_{km} \frac{b_{sh}}{2} \sin \delta_{km} \right]}{I_{km}}$$

$$\frac{\partial I_{km}}{\partial V_m} = \frac{(g_{km}^2 + b_{km}^2) V_m}{I_{km}} - \frac{V_k \left[\left(g_{km}^2 + b_{km} \left(\frac{b_{sh}}{2} + b_{km} \right) \right) \cos \delta_{km} - g_{km} \frac{b_{sh}}{2} \sin \delta_{km} \right]}{I_{km}}, \quad (12.15)$$

where I_{km} is calculated from (12.1) or (12.2).

Derivates of I_{km}^2 can be written in the following way:

$$\frac{\partial I_{km}^2}{\partial \delta_k} = 2V_k V_m \left[\left(g_{km}^2 + b_{km} \left(\frac{b_{sh}}{2} + b_{km} \right) \right) \sin \delta_{km} + g_{km} \frac{b_{sh}}{2} \cos \delta_{km} \right], \quad (12.16)$$

$$\frac{\partial I_{km}^2}{\partial \delta_m} = -2V_k V_m \left[\left(g_{km}^2 + b_{km} \left(\frac{b_{sh}}{2} + b_{km} \right) \right) \sin \delta_{km} + g_{km} \frac{b_{sh}}{2} \cos \delta_{km} \right], \quad (12.17)$$

$$\frac{\partial I_{km}^2}{\partial V_k} = 2 \left(g_{km}^2 + \left(\frac{b_{sh}}{2} + b_{km} \right)^2 \right) V_k - 2V_m \left[\left(g_{km}^2 + b_{km} \left(\frac{b_{sh}}{2} + b_{km} \right) \right) \cos \delta_{km} - g_{km} \frac{b_{sh}}{2} \sin \delta_{km} \right], \quad (12.18)$$

$$\frac{\partial I_{km}^2}{\partial V_m} = 2 \left(g_{km}^2 + b_{km}^2 \right) V_m - 2V_k \left[\left(g_{km}^2 + b_{km} \left(\frac{b_{sh}}{2} + b_{km} \right) \right) \cos \delta_{km} - g_{km} \frac{b_{sh}}{2} \sin \delta_{km} \right]. \quad (12.19)$$

12.3. OBSERVABILITY ANALYSIS FOR POWER SYSTEM WITH AMPERE MEASUREMENTS

Observability is defined as the ability to uniquely estimate the state of system using given measurements. In classical state estimation where measurements come in real and reactive pairs observability analysis can be performed using decoupled models. But, when ampere measurements are considered, the decoupled model of power system cannot be employed and for observability analysis fully coupled model must be used. However, as it was written chapter 9. observability analysis for fully coupled model doesn't guarantee uniqueness of solution. This can be illustrated by considering the following case of two bus system:

Example 12.1.



Fig. 12.8. One-line diagram of a 2-bus power system

$$\cos \delta_{km} = \frac{V_k^2 + V_m^2 - I_{km}^2 z_{km}^2}{2 \cdot V_k \cdot V_m}. \quad (12.20)$$

It can be seen that two opposite values of δ_{km} fulfill equation above ($\arccos\delta_{km} = \pm\delta_{km}$). Therefore according to equations below one can notice that two solutions for active and reactive power are possible:

$$P_{km} = b_{km}V_kV_m \sin \delta_{km} + \frac{1}{2} [g_{km}(V_m^2 - V_k^2) - I_{km}^2 r_{km}], \quad (12.21)$$

$$Q_{km} = \frac{1}{2} [b_{km}(V_k^2 - V_m^2) - I_{km}^2 x_{km}] + g_{km}V_kV_m \sin \delta_{km}. \quad (12.22)$$

Problem does not exist if power system is observable without ampere measurements or if they are added in order to improve accuracy of state estimation instead of extending the observable network. Extending observability by adding ampere measurement is possible if power flow direction is known a priori which usually is true for radial networks.

12.3.1. PROCEDURE BASED ON THE RESIDUAL COVARIANCE MATRIX

The covariance matrix Ω can be obtained from [12.3]:

$$\Omega = \mathbf{S} \cdot \mathbf{R} = \mathbf{R} - \mathbf{H} \cdot \mathbf{G}^{-1} \cdot \mathbf{H}^T. \quad (12.23)$$

where: Ω – a residual covariance matrix,

\mathbf{S} – a residual sensitive matrix,

\mathbf{R} – a covariance matrix of measurement error vector.

If column of Ω is equal null then corresponding measurement is critical. If a measurement belongs to a residual spread component then, k^{th} column is null except entries corresponding to the same residual spread component. Therefore, only for the current magnitude measurements residual spread component need to be determined.

Ω_k can be calculated as follows:

1. Solve $\mathbf{G} \cdot \mathbf{y}_k = \mathbf{h}_k^T$,
where \mathbf{h}_k : k^{th} row of \mathbf{H} .
2. Compute Ω_k as: $\Omega_k = \mathbf{R}_k - \mathbf{H} \cdot \mathbf{y}_k$,
where \mathbf{R}_k is the k^{th} column of \mathbf{R} .

The algorithm of the method [12.3]

1. Compute the columns of Ω corresponding to the current magnitude measurements.
2. If column k of Ω contains a nonzero entry corresponding to a power flow or an injection measurements, skip that column.

3. If column k of Ω contains a zero entry corresponding to a power flow or an injection measurements, flag the current measurements together with all the other measurements with nonzero entries in that column, as a v-i residual spread component that has potential to yield multiple solutions.
4. If the column is completely zero, flag the current magnitude measurements as critical

If no measurement is flagged then the system is uniquely observable. During steps 2-4 it is necessary to decide if a given entry is zero. This decision must be made based on numerical threshold which can be different for different system. Therefore Ω should be normalized in order to make threshold independent of the system. Decision of zero can be made as follows:

$$|\Omega_{jk}| / \Omega_{\max} \leq \varepsilon$$

where: e.g. $\varepsilon = 1.0e-4$

Example 12.2.

Consider following 4-bus power system

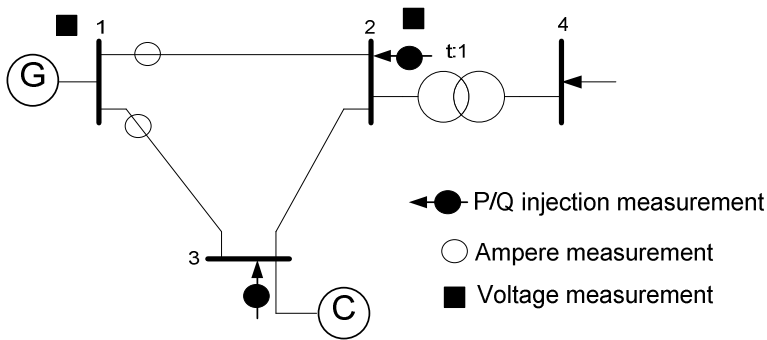


Fig. 12.9. One-line diagram of a 4-bus power system

Assuming unity reactances and null resistances and non-flat start:

Tab. 12.1. Initial values for state vector

Bus	V	$\delta(^{\circ})$
1	0.95	0
2	1	-1
3	1.05	-2
4	1.1	-3

The following Jacobi matrix is obtained:

$$\mathbf{H} = \begin{matrix} & \partial\delta_2 & \partial\delta_3 & \partial\delta_4 & \partial V_1 & \partial V_2 & \partial V_3 & \partial V_4 \\ \begin{matrix} \partial P_2 \\ \partial P_3 \\ \partial Q_2 \\ \partial Q_3 \\ \partial V_1 \\ \partial V_2 \\ \partial I_{12}^2 \\ \partial I_{13}^2 \end{matrix} & \begin{bmatrix} 36.66 & -8.47 & -14.02 & -5.26 & 9.44 & -3.86 & 0.44 \\ -8.32 & 23.10 & 0 & -5.80 & -4.35 & 9.52 & 0 \\ -8.56 & 4.05 & -0.49 & -14.91 & 35.17 & -8.07 & -12.75 \\ 4.35 & -9.85 & 0 & -15.56 & -8.32 & 24.98 & 0 \\ 0 & 0 & 0 & 1 & 0 & 0 & 0 \\ 0 & 0 & 0 & 0 & 1 & 0 & 0 \\ -8.29 & 0 & 0 & -24.92 & 25.07 & 0 & 0 \\ 0 & -17.41 & 0 & -49.68 & 0 & 50.29 & 0 \end{bmatrix} \end{matrix}$$

If R is assumed to be the identity matrix then:

$$\mathbf{\Omega} = \begin{matrix} & \partial P_2 & \partial P_3 & \partial Q_2 & \partial Q_3 & \partial V_1 & \partial V_2 & \partial I_{12}^2 & \partial I_{13}^2 \\ \begin{matrix} \partial P_2 \\ \partial P_3 \\ \partial Q_2 \\ \partial Q_3 \\ \partial V_1 \\ \partial V_2 \\ \partial I_{12}^2 \\ \partial I_{13}^2 \end{matrix} & \begin{bmatrix} -0.000 & 0.000 & 0.000 & -0.000 & -0.000 & 0.000 & 0.000 & 0.000 \\ -0.000 & 0.000 & 0.000 & 0.002 & 0.006 & -0.008 & 0.001 & -0.001 \\ -0.000 & 0.000 & 0.000 & -0.000 & 0 & 0 & -0.000 & -0.000 \\ 0.000 & 0.002 & -0.000 & 0.049 & 0.129 & -0.170 & 0.023 & -0.025 \\ 0.000 & 0.006 & -0.000 & 0.129 & 0.339 & -0.447 & 0.062 & -0.065 \\ -0.000 & -0.008 & 0.000 & -0.170 & -0.447 & 0.588 & -0.081 & 0.086 \\ -0.000 & 0.001 & -0.000 & 0.023 & 0.062 & -0.081 & 0.011 & -0.012 \\ 0.000 & -0.001 & -0.000 & -0.025 & -0.065 & 0.086 & -0.012 & 0.012 \end{bmatrix} \end{matrix}$$

It can be seen that measurements: $P_3, Q_3, V_1, V_2, I_{12}, I_{13}$, forms a v-i residual spread component, while P_2 and Q_2 are critical. That means that system is not uniquely observable and more than one solution are possible. Solution depends on initiate point.

12.3.2. PROCEDURE BASED ON THE JACOBI MATRIX

Observability analyses are also possible without computing residual covariance matrix. Presence of v-i residual spread components can be obtained from the Jacobi matrix [12.2].

Partitioning a linearized error-free measurement equation leads to:

$$\begin{bmatrix} \mathbf{H}_1 \\ \mathbf{H}_2 \end{bmatrix} \mathbf{x} = \begin{bmatrix} \mathbf{z}_1 \\ \mathbf{z}_2 \end{bmatrix}, \quad (12.24)$$

$$\mathbf{z}_2 = \mathbf{H}_2 \cdot \mathbf{H}_1^{-1} \cdot \mathbf{z}_1 = \mathbf{S}_z \cdot \mathbf{z}_1, \quad (12.25)$$

$$\mathbf{S}_z = \mathbf{H}_2 \cdot \mathbf{H}_1^{-1} \quad (12.26)$$

or using Peters-Wilkinson decomposition

$$\mathbf{H} = \begin{bmatrix} \mathbf{H}_1 \\ \dots \\ \mathbf{H}_2 \end{bmatrix} = \begin{bmatrix} \mathbf{L} \\ \dots \\ \mathbf{M} \end{bmatrix} [\mathbf{U}] \quad (12.27)$$

$$\mathbf{L} \cdot \mathbf{S}_z = \mathbf{M}, \quad (12.28)$$

where: $\mathbf{H}_1 = \mathbf{L} \cdot \mathbf{U}$ – $n \times n$ square matrix,
 \mathbf{H}_2, \mathbf{M} – $(m-n) \times n$ rectangular matrices,
 \mathbf{L} – $n \times n$ lower triangular matrix,
 \mathbf{U} – $n \times n$ upper triangular matrix.

Matrix \mathbf{S}_z is called the measurement sensitivity matrix where each row correspond to redundant measurement. Null column indicates that corresponding measurement is a critical and nonzero element in each row indicates that those measurements belong to the same residual spread as the redundant measurement.

Example 12.3.

$$\begin{bmatrix} \mathbf{H}_1 \\ \dots \\ \mathbf{H}_2 \end{bmatrix} = \begin{array}{c} \partial P_2 \\ \partial P_3 \\ \partial Q_2 \\ \partial Q_3 \\ \partial V_1 \\ \partial V_2 \\ \partial I_{12}^2 \\ \partial I_{13}^2 \end{array} \begin{array}{cccccccc} \partial \delta_2 & \partial \delta_3 & \partial \delta_4 & \partial V_1 & \partial V_2 & \partial V_3 & \partial V_4 & \\ \begin{bmatrix} 36.66 & -8.47 & -14.02 & -5.26 & 9.44 & -3.86 & 0.44 \\ -8.32 & 23.10 & 0 & -5.80 & -4.35 & 9.52 & 0 \\ -8.56 & 4.05 & -0.49 & -14.91 & 35.17 & -8.07 & -12.75 \\ 4.35 & -9.85 & 0 & -15.56 & -8.32 & 24.98 & 0 \\ 0 & 0 & 0 & 1 & 0 & 0 & 0 \\ 0 & 0 & 0 & 0 & 1 & 0 & 0 \\ -8.29 & 0 & 0 & -24.92 & 25.07 & 0 & 0 \\ \dots & \dots & \dots & \dots & \dots & \dots & \dots & \dots \\ 0 & -17.41 & 0 & -49.68 & 0 & 50.29 & 0 \end{bmatrix} \end{array}$$

$$\mathbf{S}_z = \mathbf{H}_2 \mathbf{H}_1^{-1} = \begin{bmatrix} \partial P_2 & \partial P_3 & \partial Q_2 & \partial Q_3 & \partial V_1 & \partial V_2 & \partial I_{12}^2 \\ 0.000 & 0.090 & -0.000 & 1.978 & 5.214 & -6.866 & 0.946 \end{bmatrix}$$

P_2 and Q_2 are critical measurements where remaining ones belong to v-i redundant set.

12.3.3. PROBLEM OF BAD DATA

As it was explained in chapter 10, measurements may have various properties and influence on state estimation, according to their values and location. When ampere measurements are considered the following types of measurement can be distinguished [12.1], [12.4]:

- Noncritical: when deleted, the system remains uniquely observable.
- Critical: when removed, the system becomes unobservable.
- Uniqueness-Critical: when eliminated, the system becomes not uniquely observable, i.e., several solutions are possible.

Bad data detection and identification are carried out according to the procedure presented in chapter 10. They include:

- Standard bad data detection and identification.
- Checking whether or not the identified bad data correspond to noncritical measurements.

It must be noted that when only conventional measurements are used there is no risk of eliminating critical measurement. However if ampere measurements are used there is need to check if identified bad data correspond to noncritical measurements. Procedure of checking of noncriticality is presented below:

- If the measurement belongs to residual spread component containing only power and voltage measurements, then declare it as noncritical. Else, continue.
- If the measurement refers to power flow or injection and the residual spread component does not contain any other power measurement then declare it as uniqueness-critical. Else, continue,
- Check if any of the remaining ampere measurements in the same residual spread component will become critical when this measurement is eliminated. If, yes, then declare the measurement as uniqueness-critical, else declare it as noncritical.

PROBLEMS

- 12.1. Consider if adding measurement Q_{km} in the example 12.1. will make a Power system observable.
- 12.2. Consider example 12.2. Suggest the location and type of a set minimum number of measurements to be added to the measurement list in order to make the power system observable.

12.3. Perform observability analysis of the power system shown in Fig. P.12.1.

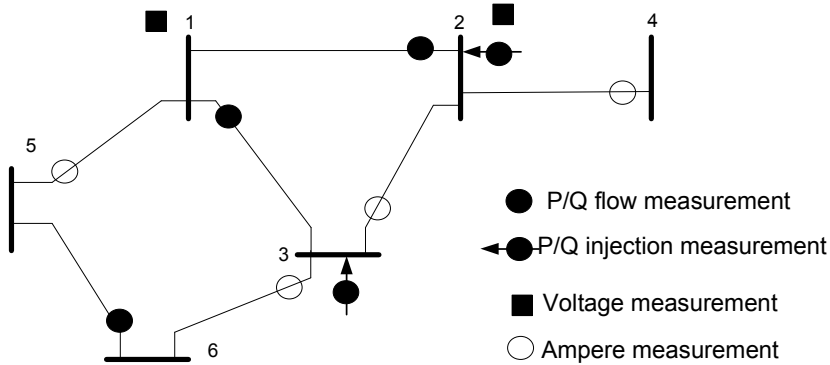


Fig. P.12.1. The 6 bus power system

REFERENCES

- [12.1] A. Abur, A. G. Exposito, *Power System State Estimation: Theory and Implementation*. Marcel Dekker, Inc, New York – Basel, 2004.
- [12.2] A. G. Exposito, A. Abur, *Generalized Observability Analysis and Measurement Classification*. *IEEE Trans. on Power Systems*, Vol. 13, No. 3, Aug. 1998, pp. 1090-1095.
- [12.3] A. Abur, A. G. Exposito, *Detecting Multiple Solutions in State Estimation in the Presence of Current Magnitude Measurements*. *IEEE Trans. on Power Systems*, Vol. 12, No. 1, Feb. 1997, pp. 370-375.
- [12.4] A. Abur, A. G. Exposito, *Observability and Bad Data Identification When Using Ampere Measurements in State Estimation*. *IEEE Inter. Conf. on Circuits and Systems*, paper No. 958, May 3-6, 1993, Chicago.
- [12.5] J. M. Ruiz Munoz, A. G. Exposito, *A Line Current Measurement Based State Estimator*. *IEEE Trans. on Power Systems*, Vol. 7, No.2, May 1992, pp. 513-519
- [12.6] K. Geisler, *Ampere Magnitude Line Measurements for Power System*. *IEEE Trans. on Power Apparatus and Systems*, Vol. 103, No. 8, Aug. 1984, pp.1962-1969.

13. DISTRIBUTION POWER SYSTEM STATE ESTIMATION – SPECIFIC PROBLEMS

13.1. INTRODUCTION

In the past, load flow was used for planning and operation. Recently, with installing in distribution system SCADA systems real-time control becomes possible. New methods are proposed for obtaining the consistent and accurate real-time data needed for monitoring and operation of distribution systems.

Distribution automation is the real-time monitoring and control of distribution circuits to facilitate feeder analysis function such as: voltage and reactive power control, network reconfiguration, demand side management etc. To perform these tasks distribution system state estimation is recognized as efficient tool which enables providing the real-time state estimates.

Using the results of state estimation for distribution systems can contribute to:

- improve reliability by faster failure detection and supply restoration, detection of overloads,
- improve network operation efficiency,
- develop energy customer response.

State estimation of distribution power network differs considerably from state estimation routines applied to transmission network and should be re-defined. This chapter is aimed at presenting some special problem regarded to this subject.

13.2. DISTRIBUTION POWER NETWORK CHARACTERISTIC

The methods of conventional state estimation originally developed for transmission systems cannot be simply adopted for distribution networks. The essential differences between both types of power systems result in fact that transmission system state estimation assumptions are not longer valid. Tab. 13.1 provides comparison between transmission and distribution networks. Essential differences among these systems result in developing some special methods for distribution system state estimation.

Tab.13.1. Transmission and distribution system comparison.

Characteristic	Transmission systems	Distribution systems
Symmetry	The degree of phase unbalance is small and only positive sequence network can be analyzed Single phase representation possible	The degree of phase unbalance is usually significant and three phase representation is required
Network topology	Meshed	Radial or weakly meshed; substation supply independent radial feeders
Line parameters	Long lines with low R/X ratio	Short or medium long lines with relatively high and varying R/X ratio
Measurement and redundancy	Very good, much of the network has measurement redundancy and network is observable as a whole	Poor, there is much more loads than available measurements Network highly unobservable, Loads usually need to be estimated
Network size	From several hundred up to several thousand nodes	From several thousand to several dozen thousand nodes

13.3. MODELS OF DISTRIBUTION POWER SYSTEM COMPONENTS

13.3.1. DISTRIBUTION SYSTEM STRUCTURE

General structure of distribution system is shown in Fig. 13.1. It has usually radial structure with possible lateral connections. The loads are connected to the nodes by transformers and are supplied from main feeder via overhead or cable lines. Some of the branches are equipped with switching sections. To improve power factor capabilities capacitor banks can be inserted into power network. Distributed generation can be also embedded in network.

Recently distribution system have been equipped with Distribution Automation Systems (DAS) enabling monitoring and control of network elements installed in substation and feeders: switching equipment, capacitor banks, transformer tap position etc. Modern DAS are capable of providing real-time measurements of voltages, currents, active and reactive power flows. Theses data can be processed in order to

support operator decisions. In such environment state estimation for distribution system can be implemented.

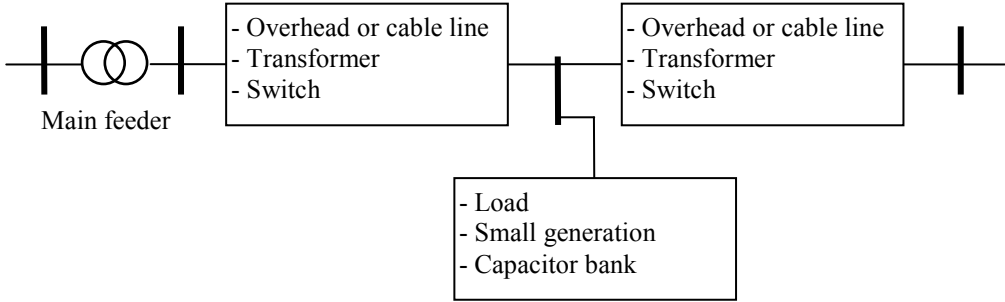


Fig. 13.1. Power distribution system structure.

13.3.2. DISTRIBUTION LINE MODELS

Fig. 13.2 presents a three-phase line section m connected between nodes i and j . The relations between node voltages and branch currents is as follows:

$$\begin{bmatrix} \underline{V}_{a,i} \\ \underline{V}_{b,i} \\ \underline{V}_{c,i} \end{bmatrix} = \begin{bmatrix} \underline{V}_{a,j} \\ \underline{V}_{b,j} \\ \underline{V}_{c,j} \end{bmatrix} + \begin{bmatrix} \underline{Z}_{aa,ij} & \underline{Z}_{ab,ij} & \underline{Z}_{ac,ij} \\ \underline{Z}_{ba,ij} & \underline{Z}_{bb,ij} & \underline{Z}_{bc,ij} \\ \underline{Z}_{ca,ij} & \underline{Z}_{cb,ij} & \underline{Z}_{cc,ij} \end{bmatrix} \begin{bmatrix} \underline{I}_{a,ij} \\ \underline{I}_{b,ij} \\ \underline{I}_{c,ij} \end{bmatrix}, \quad (13.1)$$

or in concise matrix form:

$$\underline{\mathbf{V}}_{abc,i} = \underline{\mathbf{V}}_{abc,j} + \underline{\mathbf{Z}}_{abc,ij} \underline{\mathbf{I}}_{abc,ij}. \quad (13.2)$$

where: $\underline{\mathbf{Z}}_{abc}$ – an impedance matrix of line section,

$\underline{\mathbf{V}}_{abc,i} = [\underline{V}_{a,i} \ \underline{V}_{b,i} \ \underline{V}_{c,i}]^T$ – a vector of phase voltages at the node i ,

$\underline{\mathbf{I}}_{abc,ij} = [\underline{I}_{a,ij} \ \underline{I}_{b,ij} \ \underline{I}_{c,ij}]^T$ – a vector of phase currents in the branch m connecting the nodes i and j .

The impedance matrix comprising self- and mutual terms is given by:

$$\underline{\mathbf{Z}}_{abc,ij} = \begin{bmatrix} \underline{Z}_{aa,ij} & \underline{Z}_{ab,ij} & \underline{Z}_{ac,ij} \\ \underline{Z}_{ba,ij} & \underline{Z}_{bb,ij} & \underline{Z}_{bc,ij} \\ \underline{Z}_{ca,ij} & \underline{Z}_{cb,ij} & \underline{Z}_{cc,ij} \end{bmatrix}. \quad (13.3)$$

The elements of matrix can be derived from Carson's equations, by assumption that well grounded distribution system is well grounded and ground voltages are zero. Then Kron reduction matrix method can be applied to obtain 3×3 impedance matrix of line section. Rearranging equation (13.1) the phase currents are given as:

$$\begin{bmatrix} \underline{I}_{a,ij} \\ \underline{I}_{b,ij} \\ \underline{I}_{c,ij} \end{bmatrix} = \begin{bmatrix} \underline{Y}_{aa,ij} & \underline{Y}_{ab,ij} & \underline{Y}_{ac,ij} \\ \underline{Y}_{ba,ij} & \underline{Y}_{bb,ij} & \underline{Y}_{bc,ij} \\ \underline{Y}_{ca,ij} & \underline{Y}_{cb,ij} & \underline{Y}_{cc,ij} \end{bmatrix} \begin{bmatrix} \underline{V}_{a,i} - \underline{V}_{a,j} \\ \underline{V}_{b,i} - \underline{V}_{b,j} \\ \underline{V}_{c,i} - \underline{V}_{c,j} \end{bmatrix}, \quad (13.4)$$

or in matrix form:

$$\underline{I}_{abc,ij} = \underline{V}_{abc,j} + \underline{Y}_{abc,ij} (\underline{V}_{abc,i} - \underline{V}_{abc,j}),$$

where: $\underline{Y}_{abc,ij} = \underline{Z}_{abc,ij}^{-1}$ – a line section admittance matrix.

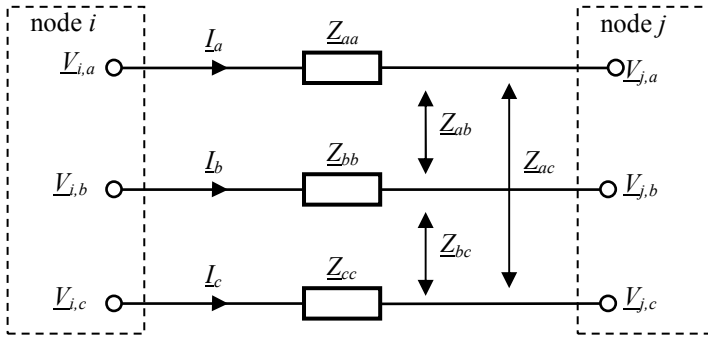


Fig. 13.2. Three phase line section.

13.3.3. STATIC LOAD MODELS

Loads can be represented in the following connections:

- four wire wye system: phase to phase or phase to neutral connection,
- three wire delta system: phase to phase connection.

The loads can operate as symmetric or asymmetric in single-phase, two-phase and three-phase mode and can be modeled as:

- constant apparent power (constant PQ),
- constant current,
- constant impedance,
- combination of the above mentioned models.

Fig. 13.3a presents the wye connected load.

1. Load model with constant apparent power:

$$\underline{I}_a = \left(\frac{\underline{S}_a}{\underline{V}_{an}} \right)^*, \quad \underline{I}_b = \left(\frac{\underline{S}_b}{\underline{V}_{bn}} \right)^*, \quad \underline{I}_c = \left(\frac{\underline{S}_c}{\underline{V}_{cn}} \right)^*. \quad (13.5)$$

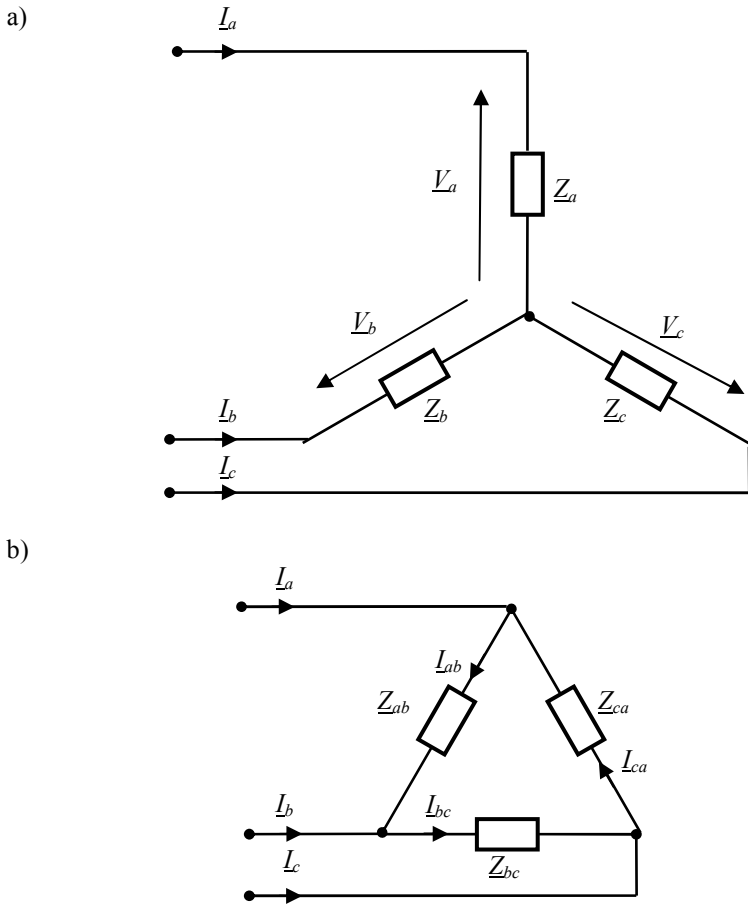


Fig. 13.3. Three phase load configurations: wye (a), delta (b).

2. Load model with constant impedance.

The impedance is first obtain:

$$\underline{Z}_a = \frac{V_{an}^2}{\underline{S}_a^*}, \quad \underline{Z}_b = \frac{V_{bn}^2}{\underline{S}_b^*}, \quad \underline{Z}_c = \frac{V_{cn}^2}{\underline{S}_c^*}, \quad (13.6)$$

and then the currents as a function of constant impedance are derived:

$$\underline{I}_a = \frac{V_{an}}{\underline{Z}_a}, \quad \underline{I}_b = \frac{V_{bn}}{\underline{Z}_b}, \quad \underline{I}_c = \frac{V_{cn}}{\underline{Z}_c}. \quad (13.7)$$

3. Load model with constant current.

The current magnitudes are obtained from equation (13.5).

Fig. 13.3b shows the delta connected load model.

1. Load model with constant apparent power.

$$\underline{I}_{ab} = \left(\frac{\underline{S}_{ab}}{\underline{V}_{ab}} \right)^*, \quad \underline{I}_{bc} = \left(\frac{\underline{S}_{bc}}{\underline{V}_{bc}} \right)^*, \quad \underline{I}_{ca} = \left(\frac{\underline{S}_{ca}}{\underline{V}_{ca}} \right)^*. \quad (13.8)$$

In this model the line to line voltages are adjusted to maintain constant power.

2. Load model with constant impedance.

The impedance is first obtain:

$$\underline{Z}_{ab} = \frac{V_{ab}^2}{\underline{S}_{ab}^*}, \quad \underline{Z}_{bc} = \frac{V_{bc}^2}{\underline{S}_{bc}^*}, \quad \underline{Z}_{ca} = \frac{V_{ca}^2}{\underline{S}_{ca}^*}. \quad (13.9)$$

and then the currents as a function of constant impedance are derived:

$$\underline{I}_{ab} = \frac{V_{ab}}{\underline{Z}_{ab}}, \quad \underline{I}_{bc} = \frac{V_{bc}}{\underline{Z}_{bc}}, \quad \underline{I}_{ca} = \frac{V_{ca}}{\underline{Z}_{ca}}. \quad (13.10)$$

3. Load model with constant current.

The current magnitudes are obtained from equation (13.8).

Calculation of load parameters for different load models is shown in Tab. 13.2.

Tab. 13.2. Load model parameter calculations. $k \in \{a, b, c\}$ for wye, $k \in \{ab, bc, ca\}$ for delta connection.

Load model	Impedance \underline{Z}_k	Current \underline{I}_k	Power \underline{S}_k
Constant impedance	\underline{Z}_k	$\frac{V_k}{\underline{Z}_k}$	$\frac{V_k^2}{\underline{Z}_k^*}$
Constant current	$\frac{V_k}{\underline{I}_k}$	\underline{I}_k	$\underline{V}_k \underline{I}_k^*$
Constant power	$\frac{V_k^2}{\underline{S}_k^*}$	$\frac{\underline{S}_k^*}{\underline{V}_k}$	\underline{S}_k

The methods for state estimation of distribution networks usually use the grounded wye load model irrespective of number of phases. In such case the load power:

$$\underline{S}_k = \underline{V}_k \underline{I}_k^*, k \in \{a, b, c\} \quad (13.11)$$

13.3.4. LOAD PSEUDOMEASUREMENT ESTIMATION

As mentioned, network observability analysis determines whether the given numbers and location of measurement are adequate to estimate the state vector.

The number and localization of these measurement is insufficient to obtain network observability. The way of increase of measurement number is estimation of loads. Obtaining of credible estimates of loads is not simple task. The information on loads concerns on basic customer information: group of customer, its location in power network, and historical data regarding to energy consumption, weather conditions. Customers are usually classified into groups with common demand profile. Usually the residential, commercial, industrial classes are distinguished.

Load demand depends on great variety of factors and estimates based on load curves have very limited forecasting capabilities. For customer classes with similar load profiles, standard load curves illustrating power demand as a function of time (Fig. 13.4) . These standard curves are based on historical data obtained by monitoring of customers within the considered time period. For state estimation purposes it is necessary do develop algorithms estimating loads with respect to statistical data analyses of customer loads.

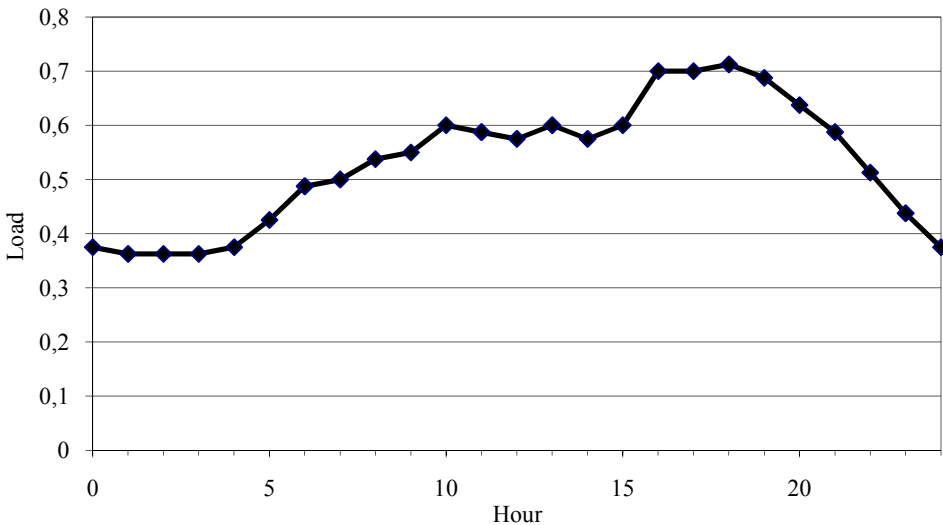


Fig. 13.4. Example averaged daily load curve for residential customers.

Great number of methods for load estimation have been presented in technical literature. Brief characteristics of load estimation methods are given in Section 14.

13.4. DISTRIBUTION POWER SYSTEM STATE ESTIMATION METHODS

Initially, distribution power system state estimation methods originated from weighted least square estimation formulated for transmission systems. Recently, the great variety of state estimation methods have been developed and they can be categorized into the following groups:

- weighted least squares based methods:
 - three phase node voltages as state variables: [13.1], [13.6], [13.8], [13.9],
 - branch currents flowing in each phase as state variable: [13.2], [13.3], [13.7], [13.11],
- load flow calculation based methods – using the backward-forward sweep load flow method for radial distribution networks. Measurement data are used in calculations as possible [13.10].

Some more detailed information on will be given in the further part.

13.4.1. NODE VOLTAGES-BASED STATE ESTIMATION

The weighted least square estimation described in Chapter 7 is adapted for three phase distribution network representation. Objective function formulation and solution scheme of state variable estimates given by equations (7.36), (7.37) is still valid in three phase case.

State variable vector

Node voltage angles and magnitudes are selected as state variables:

$$\mathbf{x} = [\boldsymbol{\theta}_2 \quad \boldsymbol{\theta}_3 \quad \dots \quad \boldsymbol{\theta}_n \quad \mathbf{V}_1 \quad \mathbf{V}_2 \quad \dots \quad \mathbf{V}_n]^T, \quad (13.12)$$

where: $\boldsymbol{\theta}_i = [\theta_{a,i} \quad \theta_{b,i} \quad \theta_{c,i}]$ – a vector of angles of voltages at the node i for the phases a , b and c respectively;

$\mathbf{V}_i = [V_{a,i} \quad V_{b,i} \quad V_{c,i}]$ – a vector of magnitudes of voltages at the node i for the phases a , b and c respectively,

n – a number of nodes.

Note that $\boldsymbol{\theta}_1 = [0 \quad \exp(j2\pi/3) \quad \exp(-j2\pi/3)]$ is assumed to be reference angles and this term is neglected in state vector.

Derivation of measurement functions

The measurement functions $h(\mathbf{x})$ are considered for branch current magnitudes, branch power flows and power injections and node voltage magnitudes.

Assuming the line section model as shown in Fig. 13.2 the branch current in phase k is given by:

$$\underline{I}_{k,ij} = I_{k,ij}^r + jI_{k,ij}^x = \sum_{m \in \{a,b,c\}} \underline{Y}_{km,ij} (\underline{V}_{m,i} - \underline{V}_{m,j}), \quad (13.13)$$

where: $\underline{Y}_{km,ij}$ – an element of the line section admittance matrix $\underline{Y}_{abc,ij}$;

$I_{k,ij}^r, I_{k,ij}^x$ – a real and an imaginary part of the complex branch current $\underline{I}_{k,ij}$,

$k \in \{a, b, c\}$.

The measurement function related to the branch current magnitude:

$$h_c(\mathbf{x}) = I_{k,ij} = \sqrt{(I_{k,ij}^r)^2 + (I_{k,ij}^x)^2}, \quad (13.14)$$

Branch power flow measurement at node i , $\underline{S}_{k,ij}^* = P_{k,ij} - jQ_{k,ij}$, is expressed as:

$$h_{Pij}(\mathbf{x}) - jh_{Qij}(\mathbf{x}) = \underline{S}_{k,ij}^* = \underline{V}_{k,i}^* \sum_{m \in \{a,b,c\}} \underline{Y}_{km,ij} (\underline{V}_{m,i} - \underline{V}_{m,j}), \quad (13.15)$$

where: $k \in \{a, b, c\}$.

Power injection measurement at node j , $\underline{S}_{k,j}^* = P_{k,j} - jQ_{k,j}$, is given by:

$$h_{Pi}(\mathbf{x}) - jh_{Qi}(\mathbf{x}) = \underline{S}_{k,i}^* = \underline{V}_{k,i}^* \sum_{j \in N_i} \sum_{m \in \{a,b,c\}} \underline{Y}_{km,ij} (\underline{V}_{m,i} - \underline{V}_{m,j}), \quad (13.16)$$

where: N_i – a set of nodes connected with the node i ; $k \in \{a, b, c\}$.

Measurement function for voltage magnitude at node i for phase k is given by:

$$h_v(\mathbf{x}) = V_{k,i}. \quad (13.17)$$

where: $k \in \{a, b, c\}$.

One can observe that measurement functions, except the functions for voltage magnitudes, are non-linear functions of state variables. Three phase representation results in more complicated form of these function in comparison to single phase representation described in chapter 7. The number of state estimates and the Jacobi and gain matrix sizes are much larger. However, due to radial network configuration they are sparse and some modifications concerned on maintaining the Jacobi matrix with constant terms are possible.

Derivation of Jacobi-measurement-matrix terms

Measurement functions are derived for hybrid network equations: voltages are represented in polar form and admittances in rectangular form.

Expanding the measurement function for power flows one can obtain:

$$h_P(\mathbf{x}) = P_{k,ij} = V_{k,i} \sum_{m \in \{a,b,c\}} [G_{km,ij} (V_{m,i} \cos(\theta_{k,i} - \theta_{m,i}) - V_{m,j} \cos(\theta_{k,i} - \theta_{m,j})) + B_{km,ij} (V_{m,i} \sin(\theta_{k,i} - \theta_{m,i}) - V_{m,j} \sin(\theta_{k,i} - \theta_{m,j}))] \quad (13.18)$$

$$h_Q(\mathbf{x}) = Q_{k,ij} = V_{k,i} \sum_{m \in \{a,b,c\}} [G_{km,ij} (V_{m,i} \sin(\theta_{k,i} - \theta_{m,i}) - V_{m,j} \sin(\theta_{k,i} - \theta_{m,j})) + B_{km,ij} (V_{m,i} \cos(\theta_{k,i} - \theta_{m,i}) - V_{m,j} \cos(\theta_{k,i} - \theta_{m,j}))] \quad (13.19)$$

where: $Y_{km,ij} = G_{km,ij} + jB_{km,ij}$ - an element of line section admittance matrix,
 $k, m \in \{a, b, c\}$.

Significant simplification of Jacobi matrix terms is possible if the approximations concerned on constant voltage magnitude and small angle differences are used and it can be expressed as:

$$V_{k,i} \approx 1.0, \quad \cos(\theta_{k,i} - \theta_{m,j}) \approx 1.0, \quad \sin(\theta_{k,i} - \theta_{m,j}) \approx 0.0, \quad (13.20)$$

The non-zero terms of the approximated Jacobi matrix are:

- branch power flows:

$$\frac{\partial P_{k,ij}}{\partial \theta_{m,l}} \approx \frac{\partial Q_{k,ij}}{\partial V_{m,l}} \approx -B_{km,ij}, \quad i = l, k \in \{a, b, c\}, m \in \{a, b, c\}. \quad (13.21)$$

$$\frac{\partial P_{k,ij}}{\partial \theta_{m,l}} \approx \frac{\partial Q_{k,ij}}{\partial V_{m,l}} \approx B_{km,ij}, \quad j = l, k \in \{a, b, c\}, m \in \{a, b, c\}. \quad (13.22)$$

$$\frac{\partial P_{k,ij}}{\partial V_{m,l}} \approx \frac{\partial Q_{k,ij}}{\partial \theta_{m,l}} \approx G_{km,ij}, \quad i = l, k \in \{a, b, c\}, m \in \{a, b, c\}. \quad (13.23)$$

$$\frac{\partial P_{k,ij}}{\partial V_{m,l}} \approx \frac{\partial Q_{k,ij}}{\partial \theta_{m,l}} \approx -G_{km,ij}, \quad j = l, k \in \{a, b, c\}, m \in \{a, b, c\}. \quad (13.24)$$

- power node injections:

$$\frac{\partial P_{k,i}}{\partial \theta_{m,l}} \approx \frac{\partial Q_{k,i}}{\partial V_{m,l}} \approx -\sum_{l \in N_i} B_{km,il}, \quad i = l, k \in \{a, b, c\}, m \in \{a, b, c\}. \quad (13.25)$$

$$\frac{\partial P_{k,i}}{\partial \theta_{m,l}} \approx \frac{\partial Q_{k,i}}{\partial V_{m,l}} \approx B_{km,ij}, \quad l \in N_i, k \in \{a, b, c\}, m \in \{a, b, c\}. \quad (13.26)$$

$$\frac{\partial P_{k,i}}{\partial V_{m,l}} \approx \frac{\partial Q_{k,i}}{\partial \theta_{m,l}} \approx \sum_{l \in N_i} G_{km,il}, \quad i = l, k \in \{a, b, c\}, m \in \{a, b, c\}. \quad (13.27)$$

$$\frac{\partial P_{k,i}}{\partial V_{m,l}} \approx \frac{\partial Q_{k,i}}{\partial \theta_{m,l}} \approx -G_{km,ij}, \quad l \in N_i, k \in \{a, b, c\}, m \in \{a, b, c\}. \quad (13.28)$$

– branch current magnitudes:

$$\frac{\partial I_{k,ij}^r}{\partial \theta_{m,l}} \approx -\frac{\partial I_{k,ij}^x}{\partial V_{m,l}} \approx -B_{km,ij}, \quad i=l, k \in \{a, b, c\}, m \in \{a, b, c\}. \quad (13.29)$$

$$\frac{\partial I_{k,ij}^r}{\partial \theta_{m,l}} \approx -\frac{\partial I_{k,ij}^x}{\partial V_{m,l}} \approx B_{km,ij}, \quad j=l, k \in \{a, b, c\}, m \in \{a, b, c\}. \quad (13.30)$$

$$\frac{\partial I_{k,ij}^r}{\partial V_{m,l}} \approx \frac{\partial I_{k,ij}^x}{\partial \theta_{m,l}} \approx G_{km,ij}, \quad i=l, k \in \{a, b, c\}, m \in \{a, b, c\}. \quad (13.31)$$

$$\frac{\partial I_{k,ij}^r}{\partial V_{m,l}} \approx \frac{\partial I_{k,ij}^x}{\partial \theta_{m,l}} \approx -G_{km,ij}, \quad j=l, k \in \{a, b, c\}, m \in \{a, b, c\}. \quad (13.32)$$

State estimation algorithm

Computational algorithm is very similar to the weighted least squares estimation for transmission system presented in Chapter 7:

1. Initialization of the iteration counter $k=0$.
2. Initialization of the state vector with use of the flat start or with use measured values if available.
3. Forming the Jacobi and gain matrices.
4. Calculation of $\mathbf{H}^T \mathbf{R}^{-1}(\mathbf{z}-h(\mathbf{x}))$ and decomposition of the gain matrix for finding $\Delta \mathbf{x}$.
5. Check for convergence, $\max(|\Delta \mathbf{x}|) < \varepsilon$ or $k > k_{max}$?
6. If yes stop, otherwise updating the solution $\mathbf{x}^{(k+1)} = \mathbf{x}^{(k)} + \Delta \mathbf{x}$ and the iteration counter $k=k+1$. Go to step 3.

When the Jacobi and gain matrices are formed some problem occurs with current measurement. The phase of measured current is required to determine real and imaginary part of complex branch current (see equation (13.14)). However, only magnitude is available. It is proposed to eliminate current measurements (without losing the observability) and perform first few iterations. Then the estimated current phase values, current measured magnitude are included onto the Jacobi matrix, and state estimation is re-calculated.

Example 13.1

For radial distribution system shown in Fig. 13.6 find the estimates of 3 phase node voltages.

Line section impedance and admittance matrices in p.u:

$$\underline{Z}_{abc,12} = \underline{Z}_{abc,23} = 10^{-3} \begin{bmatrix} 2.4388 + j6.1727 & 0.4132 + j3.2579 & 0.4132 + j3.2579 \\ 0.4132 + j3.2579 & 2.4388 + j6.1727 & 0.4132 + j3.2579 \\ 0.4132 + j3.2579 & 0.4132 + j3.2579 & 2.4388 + j6.1727 \end{bmatrix},$$

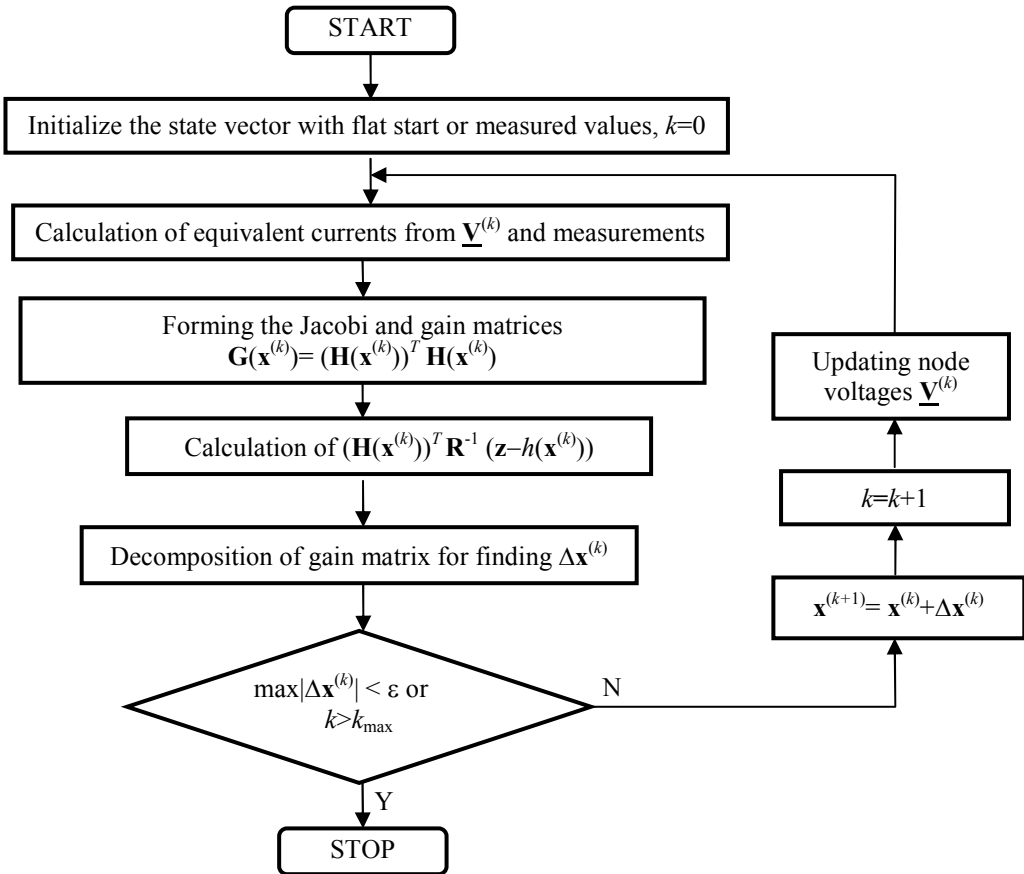


Fig. 13.5. Flowchart for state estimation calculations .

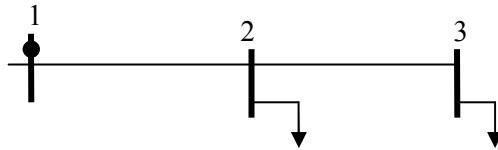


Fig. 13.6. Example simple radial distribution system. • voltage measurement.

$$\underline{Y}_{abc,12} = \underline{Y}_{abc,23} = 10^2 \begin{bmatrix} 1.1352 - j1.7887 & -0.4725 + j0.5248 & -0.4725 + j0.5248 \\ -0.4725 + j0.5248 & 1.1352 - j1.7887 & -0.4725 + j0.5248 \\ -0.4725 + j0.5248 & -0.4725 + j0.5248 & 1.1352 - j1.7887 \end{bmatrix}$$

Load pseudomeasurements obtained from load estimation step are in Tab. 13.3.

Tab. 13.3. Load pseudomeasurements.

i	$P_{a,i}$	$Q_{a,i}$	$P_{b,i}$	$Q_{b,i}$	$P_{c,i}$	$Q_{c,i}$
1	0.0000	0.0000	0.0000	0.0000	0.0000	0.0000
2	0.0640	0.0128	0.0040	0.0018	0.0010	0.0028
3	0.0180	0.0048	0.0180	0.0048	0.0180	0.0048

Voltage at main feeder as reference: $V_1 = 1.0 [1 \quad \exp(j2\pi/3) \quad \exp(-j2\pi/3)]^T$

Power flow in branch 1-2: $P_{a,12} = P_{b,12} = P_{c,12} = 0.080$ $Q_{a,12} = Q_{b,12} = Q_{c,12} = 0.017$

Measurements weights (elements of \mathbf{R} matrix) are set to 1.

Convergence criterion is assumed as $\max(|\Delta \mathbf{x}|) < 10^{-3}$.

The structure of the simplified Jacobi matrix built with use equations (13.21) - (13.28) is presented in Fig. 13.7.

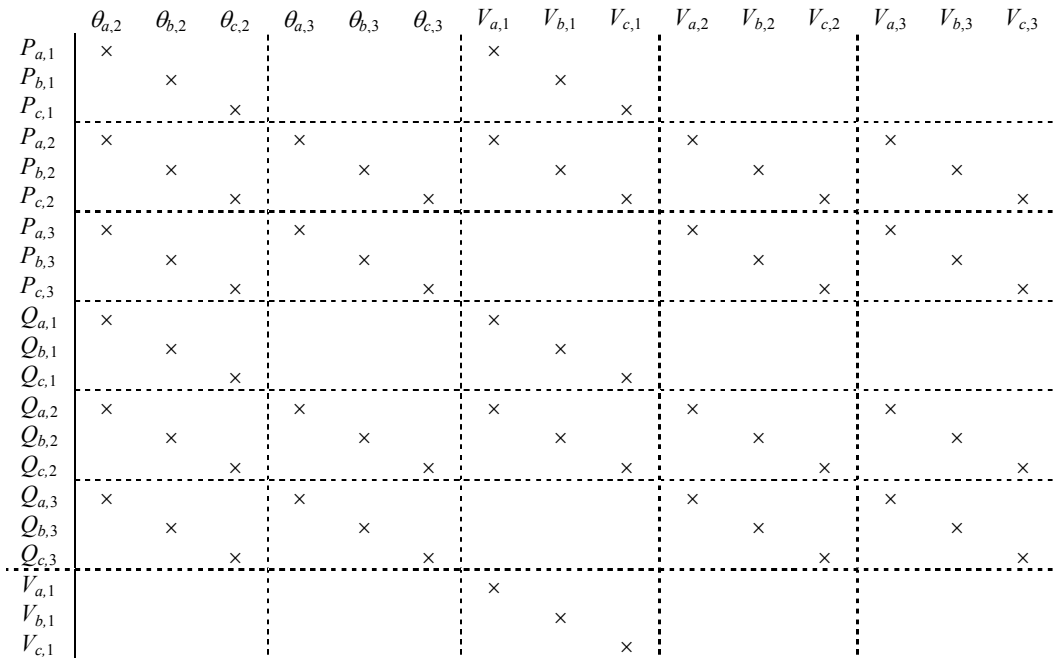


Fig. 13.7. Structure of the simplified Jacobi matrix \mathbf{H} . \times - non-zero term.

The values of measurement functions in vector of measurement mismatches $[\mathbf{z}-h(\mathbf{x})]$ are calculated with use of equation (7.37) for flat initial point.

After calculation the state variable vector the following results are obtained.

Tab. 13.4. State vector estimates.

Node i	$\hat{V}_{a,i}$, p.u.	$\hat{\theta}_{a,i}$, deg	$\hat{V}_{b,i}$, p.u.	$\hat{\theta}_{b,i}$, deg	$\hat{V}_{c,i}$, p.u.	$\hat{\theta}_{c,i}$, deg
1	1.0000	0.000	1.0000	120.000	1.0000	-120.000
2	0.9999	0.027	1.0001	119.998	0.9998	-119.998
3	0.9999	0.030	1.0001	120.001	0.9998	-119.995

Tab. 13.5. Branch current estimates.

Branch, ij	$\hat{I}_{a,ij}$, p.u.	$\hat{\phi}_{a,ij}$, deg	$\hat{I}_{b,ij}$, p.u.	$\hat{\phi}_{b,ij}$, deg	$\hat{I}_{c,ij}$, p.u.	$\hat{\phi}_{c,ij}$, deg
1-2	0.0839	-12.0865	0.0230	103.3013	0.0290	-135.1820
2-3	0.0186	-14.9013	0.0186	105.0698	0.0186	-134.9263

The convergence were achieved after 3 iterations.

13.4.2. BRANCH CURRENTS-BASED STATE ESTIMATION

Alternative formulation of state estimation problem for three phase distribution network is using branch current as state variables. Knowing these currents other quantities as complex node voltages, power branch flow and power injections can be calculated. The node voltages can be found by forward sweep procedure. Starting from substation voltage and moving toward leaf nodes of the radial network using equation (13.1). Current and power injection can be found with use of Kirchhoff Current Law.

The state variable vector is former as:

$$\mathbf{x} = [\mathbf{I}_1^r \quad \mathbf{I}_2^r \quad \dots \quad \mathbf{I}_n^r \quad \mathbf{I}_1^x \quad \mathbf{I}_2^x \quad \dots \quad \mathbf{I}_n^x]^T, \quad (13.33)$$

where: $\mathbf{I}_i^r = [I_{a,i}^r \ I_{b,i}^r \ I_{c,i}^r]$ – real parts of the branch current flowing into the bus i for the phases a , b and c respectively,
 $\mathbf{I}_i^x = [I_{a,i}^x \ I_{b,i}^x \ I_{c,i}^x]$ – imaginary parts of the branch current flowing into the bus i for the phases a , b and c respectively,
 n – a number of branches.

Measurement function

Regarding to the power measurements it is assumed that the actual power flows measurement and load pseudo-measurements are available. These measurements are converted into currents with use of the following relationship:

$$\underline{I}_{k,ij} = I_{k,ij}^r + jI_{k,ij}^x = \left(\frac{P_{k,ij} + jQ_{k,ij}}{\underline{V}_{k,i}^{(t)}} \right)^*, \quad (13.34)$$

where: $P_{k,ij}$, $Q_{k,ij}$ – an active and a reactive branch power flow measurements at the node i for the phase k ,

$\underline{V}_{k,i}^{(t)}$ – a voltage at the node i and the phase k in t -th iteration of solution process, $k \in \{a, b, c\}$.

The load pseudo-measurements can be obtained from:

$$\underline{I}_{k,i} = I_{k,i}^r + jI_{k,i}^x = \left(\frac{P_{k,i} + jQ_{k,i}}{\underline{V}_{k,i}^{(t)}} \right)^*, \quad (13.35)$$

where: $P_{k,i}$, $Q_{k,i}$ – active and reactive load pseudo-measurements at the node i for the phase k ,

$\underline{V}_{k,i}^{(t)}$ – a voltage at the node i and the phase k in the t -th iteration of solution process,

$$k \in \{a, b, c\},$$

Note that the actual node voltages are not available and they are obtained from calculations.

Measurement functions for equivalent currents are linear:

$$h_r(\mathbf{x}) + j h_x(\mathbf{x}) = I_{k,ij}^r + j I_{k,ij}^x. \quad (13.36)$$

where: $k \in \{a, b, c\}$.

Node (load) currents are linear function of state variables and they can be calculated from Kirchhoff Current Law. The concise form for describing that uses the node-branch incidence matrix \mathbf{A} defined as:

$$a_{ij} = \begin{cases} 1, & \text{if branch } j \text{ is directed away from node } i \\ -1, & \text{if branch } j \text{ is directed towards from node } i \\ 0, & \text{if branch } j \text{ is not incident to node } i \end{cases}$$

The relation between node currents and branch currents (state variables) is:

$$h_{ri}(\mathbf{x}) = \mathbf{A}' \mathbf{I}^r, \quad h_{xi}(\mathbf{x}) = \mathbf{A}' \mathbf{I}^x, \quad (13.37)$$

where: $\mathbf{I}^r = [\mathbf{I}_1^r \quad \mathbf{I}_2^r \quad \dots \quad \mathbf{I}_n^r]^T$ – a vector of real part of branch currents,

$\mathbf{I}^x = [\mathbf{I}_1^x \quad \mathbf{I}_2^x \quad \dots \quad \mathbf{I}_n^x]^T$ – a vector of imagine part of branch currents,

\mathbf{A}' – the three phase incidence matrix with the following terms:

$$\mathbf{a}'_{ij} = \begin{cases} \mathbf{I}_{3 \times 3}, & \text{if branch } j \text{ is directed away from node } i \\ -\mathbf{I}_{3 \times 3}, & \text{if branch } j \text{ is directed towards from node } i \\ \mathbf{0}_{3 \times 3}, & \text{if branch } j \text{ is not incident to node } i \end{cases}$$

Current magnitude measurements are directly incorporated into the state estimation. However, it is non-linear function of state variables:

$$h_c(\mathbf{x}) = I_{k,ij} = \sqrt{(I_{k,ij}^r)^2 + (I_{k,ij}^x)^2}, \quad (13.38)$$

Voltage measurements are neglected in measurement vector, except the main feeder voltage to be the reference, because they do not have significant influence on state estimation results quality.

where: $\phi_{k,ij} = \arctan\left(\frac{I_{k,ij}^x}{I_{k,ij}^r}\right)$.

Objective function

The objective function for state estimation can be decomposed into three terms as it can be seen in the following fomula:

$$J(\mathbf{x}) = [\mathbf{z}^r - h_r(\mathbf{I}^r)]^T (\mathbf{R}^r)^{-1} [\mathbf{z}^r - h_r(\mathbf{I}^r)] + [\mathbf{z}^x - h_x(\mathbf{I}^x)]^T (\mathbf{R}^x)^{-1} [\mathbf{z}^x - h_x(\mathbf{I}^x)] + [\mathbf{z}^m - h_C(\mathbf{I}^m)]^T (\mathbf{R}^m)^{-1} [\mathbf{z}^m - h_C(\mathbf{I}^m)] \quad (13.42)$$

where: $\mathbf{z}^r, \mathbf{z}^x$ – measurement vectors related to the real and imaginary parts of equivalent current phasors obtained from actual power flow measurements and load pseudo- measurements,

\mathbf{z}^m – a vector of current magnitude measurements,

$h(\mathbf{I}^r), h(\mathbf{I}^x), h(\mathbf{I}^m)$ – measurement functions involving real, imaginary parts and magnitudes of current phasors,

$\mathbf{R}^r, \mathbf{R}^x, \mathbf{R}^m$ – measurement error covariance matrices.

First term of objective function relates to the power flow measurements and the second to measured current magnitude. The notation for phases is neglected for better clarity.

State estimation algorithm

Computation of branch current estimates is performed in the following steps:

1. Initialization of the iteration counter $k=0$.
2. Initialization of the voltages with use of the flat start or with use measured values if available.
3. Calculation of equivalent currents with use of the voltages $\underline{\mathbf{V}}^{(k)}$, power flows measurements and load pseudomeasurements.
4. Forming the Jacobi and gain matrix.
5. Calculation of $\mathbf{H}^T \mathbf{R}^{-1}(\mathbf{z}-h(\mathbf{x}))$ and decomposition of the gain matrix for finding $\Delta \mathbf{x}$.
6. Check for convergence, $\max(|\Delta \mathbf{x}|) < \varepsilon$ or $k > k_{max}$?
7. If yes stop, otherwise updating the solution $\mathbf{x}^{(k+1)} = \mathbf{x}^{(k)} + \Delta \mathbf{x}$ and the iteration counter $k=k+1$. For given branch currents update the voltages by the forward sweep procedure. Go to step 3.

Note, that when the Jacobi and gain matrices are formed some problem with current measurement occurs, because its phase is not available. It is proposed to eliminate current measurements (without losing the observability) and perform first few iterations. Then the estimated current phase and measured magnitude are included into the Jacobi matrix and the state estimation is re-calculated.

Modifications of the described method are concerned on maintaining the Jacobi and gain matrix with constant terms and phase decoupling.

Example 13.2

For the distribution network shown in Fig. 13.6 in Example 13.1 find the state estimate with use of branch current based state estimation formulation.

Active power flow measurements: $P_{a,12} = 0.082$ $P_{b,12} = 0.022$ $P_{c,12} = 0.028$

Reactive power flow measurements: $Q_{a,12} = 0.017$ $Q_{b,12} = 0.006$ $Q_{c,12} = 0.007$

The Jacobi matrix has the following structure:

	$I'_{a,12}$	$I'_{b,12}$	$I'_{c,12}$	$I'_{a,23}$	$I'_{b,23}$	$I'_{c,23}$	$I^x_{a,12}$	$I^x_{b,12}$	$I^x_{c,12}$	$I^x_{a,23}$	$I^x_{b,23}$	$I^x_{c,23}$
$P_{a,12}$	1											
$P_{a,12}$		1										
$P_{b,12}$			1									
$P_{a,1}$	-1											
$P_{b,1}$		-1										
$P_{c,1}$			-1									
$P_{a,2}$	1			-1								
$P_{b,2}$		1			-1							
$P_{c,2}$			1			-1						
$P_{a,3}$				1								
$P_{b,3}$					1							
$P_{c,3}$						1						
$Q_{a,12}$							1					
$Q_{b,12}$								1				
$Q_{c,12}$									1			
$Q_{a,1}$							-1					
$Q_{b,1}$								-1				
$Q_{c,1}$									-1			
$Q_{a,2}$							1			-1		
$Q_{b,2}$								1			-1	
$Q_{c,2}$									1			-1
$Q_{a,3}$										1		
$Q_{b,3}$											1	
$Q_{c,3}$												1

Note that the Jacobi matrix contains only constant term and its recalculation during iterations is not needed.

During each iteration, once the voltages are updated the load pseudomeasurements and power flow are also modified to obtain new equivalent current values (equation (13.5)).

Final branch current estimates converted into polar form are shown in Tab. 13.6.

Tab. 13.6. State estimation results.

Branch, ij	$\hat{I}_{a,ij}$, p.u.	$\hat{\Phi}_{a,ij}$, deg	$\hat{I}_{b,ij}$, p.u.	$\hat{\Phi}_{b,ij}$, deg	$\hat{I}_{c,ij}$, p.u.	$\hat{\Phi}_{c,ij}$, deg
1-2	0.0839	-12.0865	0.0230	103.3013	0.0290	-135.1820
2-3	0.0186	-14.9013	0.0186	105.0698	0.0186	-134.9263

13.4.3. ESTIMATION

BY BACKWARD-FORWARD SWEEP LOAD FLOW CALCULATIONS

Load flow based state estimation methods use backward-forward sweep in three-phase networks with radial configuration. Conventional weighted least squares methods suffer from ill-conditioning of the gain and Jacobi matrices. The backward-forward scheme is usually much more robust to low R/X values and fast in convergence.

Scheme of simple radial distribution network is shown in Fig. 13.9. For better legibility single phase representation is used.

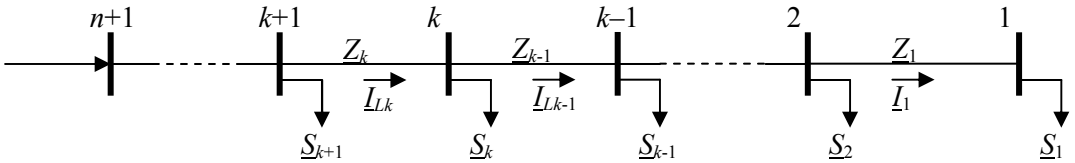


Fig. 13.9. Radial distribution network scheme.

Initially the node voltage magnitudes are set to the measured values if available, otherwise the flat starting point is applied.

To calculate node voltages and branch current the following equation based on Kirchhoff laws can be written:

$$\mathbf{I}_{abc,Lk} = \mathbf{I}_{abc,k} + \mathbf{I}_{abc,Lk-1}, \quad (13.43)$$

$$\mathbf{V}_{abc,k+1} = \mathbf{V}_{abc,k} + \mathbf{Z}_{abc,k} \mathbf{I}_{abc,Lk}, \quad (13.44)$$

where: $\mathbf{I}_{abc,m}$ – a vector of phase currents at the node m ,

$$\mathbf{I}_{abc,Lk} = \sum_{m=1}^k \mathbf{I}_{abc,m} \text{ – a vector of phase currents in the branch } k,$$

$\mathbf{Z}_{abc,k}$ – an impedance matrix for the section corresponding to the branch k ,

$k \in \{1, 2, \dots, n\}$.

The node current is calculated from:

$$\underline{\mathbf{I}}_{abc,k} = \begin{bmatrix} \underline{I}_{a,k} \\ \underline{I}_{b,k} \\ \underline{I}_{c,k} \end{bmatrix} = \begin{bmatrix} (\underline{S}_{a,k} / \underline{V}_{a,k})^* \\ (\underline{S}_{b,k} / \underline{V}_{b,k})^* \\ (\underline{S}_{c,k} / \underline{V}_{c,k})^* \end{bmatrix} = \begin{bmatrix} (P_{a,k} - jQ_{a,k}) / (\underline{V}_{a,k})^* \\ (P_{b,k} - jQ_{b,k}) / (\underline{V}_{b,k})^* \\ (P_{c,k} - jQ_{c,k}) / (\underline{V}_{c,k})^* \end{bmatrix}. \quad (13.45)$$

where: $k = 1, 2, \dots, n$.

Hence, the nodal voltages can be obtained:

$$\begin{bmatrix} \underline{V}_{a,k+1} \\ \underline{V}_{b,k+1} \\ \underline{V}_{c,k+1} \end{bmatrix} = \begin{bmatrix} \underline{V}_{a,k} \\ \underline{V}_{b,k} \\ \underline{V}_{c,k} \end{bmatrix} + \begin{bmatrix} \underline{Z}_{aa,k} & \underline{Z}_{ab,k} & \underline{Z}_{ac,k} \\ \underline{Z}_{ba,k} & \underline{Z}_{bb,k} & \underline{Z}_{bc,k} \\ \underline{Z}_{ca,k} & \underline{Z}_{cb,k} & \underline{Z}_{cc,k} \end{bmatrix} \begin{bmatrix} (P_{a,k} - jQ_{a,k}) / (\underline{V}_{a,k})^* \\ (P_{b,k} - jQ_{b,k}) / (\underline{V}_{b,k})^* \\ (P_{c,k} - jQ_{c,k}) / (\underline{V}_{c,k})^* \end{bmatrix} \quad (13.46)$$

Analytical solution of the equation (13.46) is difficult and the iterative method are applied to solve it. To maintain observability it is assumed that load pseudomeasurements for all nodes are available.

Backward sweep

First, the initial voltage at node 1 is set and node current is calculated. Current in branch connecting nodes 1 and 2 is equal to the node current. Next, voltage node 2 is calculated with equation (13.46). Current in branch connecting nodes 2 and 3 is calculated with equation (13.43) as sum of node current in node 2 and branch current of former branch. Once the branch current is calculated, the voltage at node 3 can be found. The propagation moves towards the main feeder until node n is reached. Then all branch currents are calculated.

Forward sweep

Having branch current calculated during forward sweep voltages at each node starting from main feeder can be calculated. The voltage magnitude of main source is set to measured value. Phase angles are assumed as the reference:

$$\theta_{abc,n+1} = [0 \quad 2\pi/3 \quad -2\pi/3]^T. \quad (13.47)$$

The node voltages are calculated starting from feeder with use of:

$$\underline{\mathbf{V}}_{abc,k} = \underline{\mathbf{V}}_{abc,k+1} - \underline{\mathbf{Z}}_{abc,k} \underline{\mathbf{I}}_{abc,Lk}, \quad (13.48)$$

Once the node 1 is reached all the node voltages are available.

Convergence condition

The steps in backward and forward sweep are performed during each iteration. The convergence condition is that, the voltage magnitudes are compared with previous iteration:

$$\max(|V_{abc,k}^{(i)} - V_{abc,k}^{(i-1)}|) < \varepsilon, k=1, 2, \dots, n + 1, \tag{13.49}$$

where: $V_{abc,k}^{(i)}$ - a voltage magnitude vector at the node k for i -th iteration.

If the voltage mismatches exceeds the assumed threshold the computation are continued, otherwise stop. Having node voltages calculated all branch currents, real and reactive power flows, losses can be calculated.

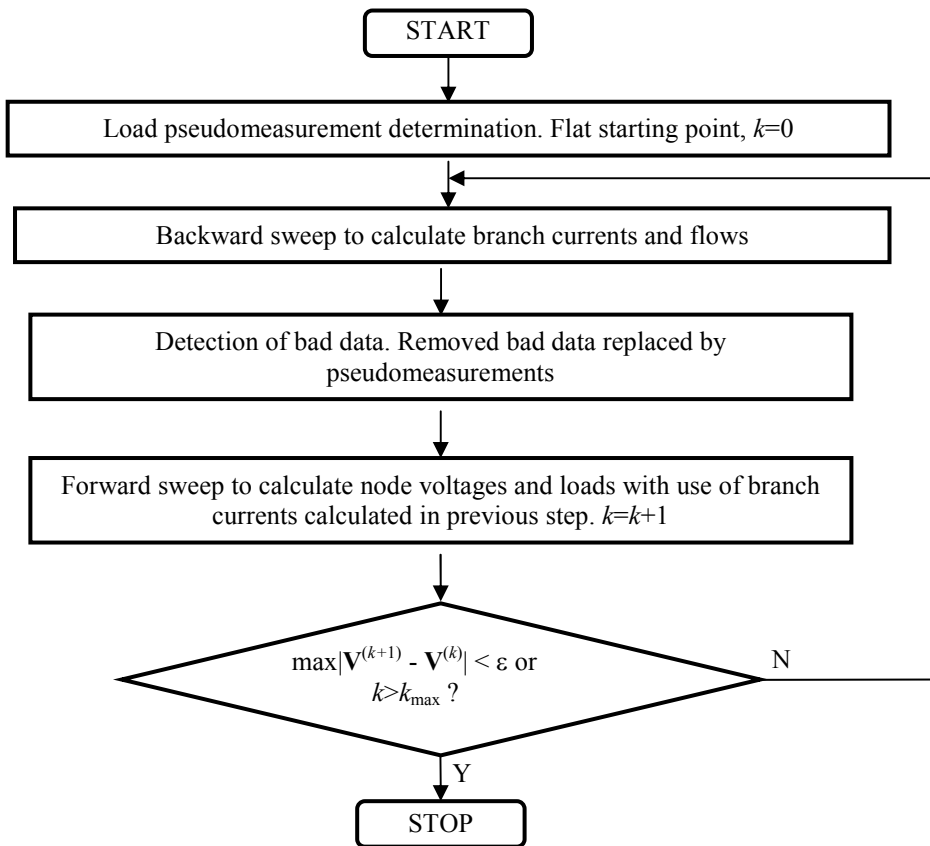


Fig. 13.10. Flowchart of backward-forward distribution state estimation.

Measurement handling and bad data detection

The calculated values are compared with measurements: voltages, branch currents and power flows. If the difference exceeds the assumed threshold the measurement is suspected as bad data and replaced by calculated value.

Example 13.3

For the radial system shown in Fig. 13.6 find the node voltages and branch currents estimates with use of the backward-forward sweep methods.

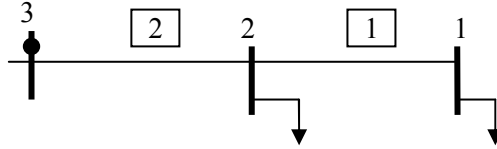


Fig. 13.11. Example simple radial distribution system. • voltage measurement.

Branch impedance/admittance parameters:

$$\underline{Z}_{abc,12} = \underline{Z}_{abc,23} = 10^{-3} \begin{bmatrix} 2.4388 + j6.1727 & 0.4132 + j3.2579 & 0.4132 + j3.2579 \\ 0.4132 + j3.2579 & 2.4388 + j6.1727 & 0.4132 + j3.2579 \\ 0.4132 + j3.2579 & 0.4132 + j3.2579 & 2.4388 + j6.1727 \end{bmatrix},$$

$$\underline{Y}_{abc,12} = \underline{Y}_{abc,23} = 10^2 \begin{bmatrix} 1.1352 - j1.7887 & -0.4725 + j0.5248 & -0.4725 + j0.5248 \\ -0.4725 + j0.5248 & 1.1352 - j1.7887 & -0.4725 + j0.5248 \\ -0.4725 + j0.5248 & -0.4725 + j0.5248 & 1.1352 - j1.7887 \end{bmatrix}.$$

Load pseudomeasurements obtained from load estimation step are in Tab. 13.3.

Tab. 13.7. Load pseudomeasurements for network in Fig. 13.6.

i	P_{a1i} p.u.	Q_{a1i} p.u.	P_{b1i} p.u.	Q_{b1i} p.u.	P_{c1i} p.u.	Q_{c1i} p.u.
3	0.0000	0.0000	0.0000	0.0000	0.0000	0.0000
2	0.0640	0.0128	0.0040	0.0018	0.0010	0.0028
1	0.0180	0.0048	0.0180	0.0048	0.0180	0.0048

Voltage at main feeder as reference: $\underline{V}_3 = 1.0 [1 \quad \exp(j2\pi/3) \quad \exp(-j2\pi/3)]^T$

Convergence criterion is assumed as $\max(|\Delta \mathbf{x}|) < 10^{-4}$.

1. Backward sweep

The voltage at node 1 is set to the flat start value:

$$\underline{\mathbf{V}}_{abc}^{(0)} = \begin{bmatrix} \underline{V}_{a,1}^{(0)} \\ \underline{V}_{b,1}^{(0)} \\ \underline{V}_{c,1}^{(0)} \end{bmatrix} = \begin{bmatrix} 1.0 \\ 1.0 \exp(j2\pi/3) \\ 1.0 \exp(-j2\pi/3) \end{bmatrix} = \begin{bmatrix} 1.0000 \\ -0.5000 + j0.8660 \\ -0.5000 - j0.8660 \end{bmatrix}$$

$$\underline{I}_{a,L1}^{(1)} = \underline{I}_{a,1}^{(1)} = \left(\frac{\underline{S}_{a,1}}{\underline{V}_{a,1}^{(0)}} \right)^* = \left(\frac{0.0180 + j0.0048}{1.0000} \right)^* = 0.0180 - j0.0048,$$

$$\underline{I}_{b,L1}^{(1)} = \underline{I}_{b,1}^{(1)} = \left(\frac{\underline{S}_{b,1}}{\underline{V}_{b,1}^{(0)}} \right)^* = \left(\frac{0.0180 + j0.0048}{-0.5000 + j0.8660} \right)^* = -0.0048 + j0.0180,$$

$$\underline{I}_{c,L1}^{(1)} = \underline{I}_{c,1}^{(1)} = \left(\frac{\underline{S}_{c,1}}{\underline{V}_{c,1}^{(0)}} \right)^* = \left(\frac{0.0180 + j0.0048}{-0.5000 - j0.8660} \right)^* = -0.0132 - j0.0132.$$

$$\underline{\mathbf{I}}_{abc,L1}^{(1)} = [0.0180 - j0.0048 \quad -0.0048 + j0.0180 \quad -0.0132 - j0.0132]^T$$

Voltage in node 2:

$$\begin{aligned} \underline{\mathbf{V}}_{abc,2}^{(0)} &= \underline{\mathbf{V}}_{abc,1}^{(0)} + \underline{\mathbf{Z}}_{abc,12} \underline{\mathbf{I}}_{abc,L1}^{(1)} = \begin{bmatrix} 1.0000 \\ -0.5000 + j0.8660 \\ -0.5000 - j0.8660 \end{bmatrix} + \\ &+ 10^{-3} \begin{bmatrix} 2.4388 + j6.1727 & 0.4132 + j3.2579 & 0.4132 + j3.2579 \\ 0.4132 + j3.2579 & 2.4388 + j6.1727 & 0.4132 + j3.2579 \\ 0.4132 + j3.2579 & 0.4132 + j3.2579 & 2.4388 + j6.1727 \end{bmatrix} \times \\ &\times \begin{bmatrix} 0.0180 - j0.0048 \\ -0.0048 + j0.0180 \\ -0.0132 - j0.0132 \end{bmatrix} = \begin{bmatrix} 1.0000 + j0.0001 \\ -0.5000 + j0.8661 \\ -0.5001 - j0.8660 \end{bmatrix} \end{aligned}$$

Load current in node 2

$$\underline{I}_{a,2}^{(1)} = \left(\frac{\underline{S}_{a,2}}{\underline{V}_{a,2}^{(0)}} \right)^* = \left(\frac{0.0640 + j0.0128}{1.0000 + j0.0001} \right)^* = 0.0640 - j0.0128,$$

$$\underline{I}_{b,1}^{(1)} = \left(\frac{\underline{S}_{b,2}}{\underline{V}_{b,1}^{(0)}} \right)^* = \left(\frac{0.0040 + j0.0018}{-0.5000 + j0.8661} \right)^* = -0.0004 + j0.0044,$$

$$\underline{I}_{c,1}^{(1)} = \left(\frac{\underline{S}_{c,2}}{\underline{V}_{c,1}^{(0)}} \right)^* = \left(\frac{0.0100 + j0.0028}{-0.5001 - j0.8660} \right)^* = -0.0074 - j0.0073.$$

$$\underline{\mathbf{I}}_{abc,2}^{(1)} = [0.0640 - j0.0128 \quad -0.0004 + j0.0044 \quad -0.0074 - j0.0073]^T$$

Branch current

$$\underline{\mathbf{I}}_{abc,L2}^{(1)} = \underline{\mathbf{I}}_{abc,L1}^{(1)} + \underline{\mathbf{I}}_{abc,2}^{(1)} = \begin{bmatrix} 0.0180 - j0.0048 \\ -0.0048 + j0.0180 \\ -0.0132 - j0.0132 \end{bmatrix} + \begin{bmatrix} 0.0640 - j0.0128 \\ -0.0004 + j0.0044 \\ -0.0074 - j0.0073 \end{bmatrix} = \begin{bmatrix} 0.0820 - j0.0176 \\ -0.0053 + j0.0224 \\ -0.0206 - j0.0204 \end{bmatrix}$$

Voltage in node 3:

$$\begin{aligned} \underline{\mathbf{V}}_{abc,3}^{(0)} &= \underline{\mathbf{V}}_{abc,2}^{(0)} + \underline{\mathbf{Z}}_{abc,23} \underline{\mathbf{I}}_{abc,L2}^{(1)} = \begin{bmatrix} 1.0000 + j0.0001 \\ -0.5000 + j0.8661 \\ -0.5001 - j0.8660 \end{bmatrix} + \\ &+ 10^{-3} \begin{bmatrix} 2.4388 + j6.1727 & 0.4132 + j3.2579 & 0.4132 + j3.2579 \\ 0.4132 + j3.2579 & 2.4388 + j6.1727 & 0.4132 + j3.2579 \\ 0.4132 + j3.2579 & 0.4132 + j3.2579 & 2.4388 + j6.1727 \end{bmatrix} \times \\ &\times \begin{bmatrix} 0.0820 - j0.0176 \\ -0.0053 + j0.0224 \\ -0.0206 - j0.0204 \end{bmatrix} = \begin{bmatrix} 1.0003 + j0.0004 \\ -0.5001 + j0.8663 \\ -0.4999 - j0.8660 \end{bmatrix} \end{aligned}$$

2. Forward sweep

Note, that the f in superscript denotes forward direction of sweep.

Node 3 is considered as reference and $\underline{\mathbf{V}}_{abc,3}^{(1)}$ and needs to be replaced by reference voltage. The remaining node voltages are updated with use of branch currents calculated in forward sweep:

$$\begin{aligned} \underline{\mathbf{V}}_{abc,2}^{(1)} &= \underline{\mathbf{V}}_{abc,3}^{(1)} - \underline{\mathbf{Z}}_{abc,23} \underline{\mathbf{I}}_{abc,L2}^{(1)} = \begin{bmatrix} 1.0000 + j0.0000 \\ -0.5000 + j0.8660 \\ -0.5000 - j0.8660 \end{bmatrix} + \\ &- 10^{-3} \begin{bmatrix} 2.4388 + j6.1727 & 0.4132 + j3.2579 & 0.4132 + j3.2579 \\ 0.4132 + j3.2579 & 2.4388 + j6.1727 & 0.4132 + j3.2579 \\ 0.4132 + j3.2579 & 0.4132 + j3.2579 & 2.4388 + j6.1727 \end{bmatrix} \times \\ &\times \begin{bmatrix} 0.0820 - j0.0176 \\ -0.0053 + j0.0224 \\ -0.0206 - j0.0204 \end{bmatrix} = \begin{bmatrix} 1.0002 + j0.0004 \\ -0.5001 + j0.8660 \\ -0.4999 - j0.8661 \end{bmatrix} \end{aligned}$$

$$\underline{\mathbf{V}}_{abc,1}^{(1)} = \underline{\mathbf{V}}_{abc,2}^{(1)} - \underline{\mathbf{Z}}_{abc,12} \underline{\mathbf{I}}_{abc,L1}^{(1)} = \begin{bmatrix} 1.0002 + j0.0004 \\ -0.5001 + j0.8660 \\ -0.4999 - j0.8661 \end{bmatrix} +$$

$$+ 10^{-3} \begin{bmatrix} 2.4388 + j6.1727 & 0.4132 + j3.2579 & 0.4132 + j3.2579 \\ 0.4132 + j3.2579 & 2.4388 + j6.1727 & 0.4132 + j3.2579 \\ 0.4132 + j3.2579 & 0.4132 + j3.2579 & 2.4388 + j6.1727 \end{bmatrix} \times$$

$$\times \begin{bmatrix} 0.0180 - j0.0048 \\ -0.0048 + j0.0180 \\ -0.0132 - j0.0132 \end{bmatrix} = \begin{bmatrix} 1.0000 + j0.0000 \\ -0.5000 + j0.8661 \\ -0.5001 - j0.8660 \end{bmatrix}$$

The convergence checking:

$$\max\left(\max\left(\left|\underline{\mathbf{V}}_{abc,1}^{(1)} - \underline{\mathbf{V}}_{abc,1}^{(0)}\right|\right), \max\left(\left|\underline{\mathbf{V}}_{abc,2}^{(1)} - \underline{\mathbf{V}}_{abc,2}^{(0)}\right|\right), \max\left(\left|\underline{\mathbf{V}}_{abc,3}^{(1)} - \underline{\mathbf{V}}_{abc,3}^{(0)}\right|\right)\right) = 0.543 \cdot 10^{-4} < 10^{-3}$$

The convergence is reached after one iteration. Otherwise the calculations need to be repeated for updated voltage values until meeting the performance.

Backward-forward sweep algorithm is very fast and efficient for state estimation and load flow calculations in radial feeders.

PROBLEMS

- 13.1. Calculate state estimation for radial distribution system with lateral link as shown in Fig. P.13.1 with the use of three phase WLS node voltage formulation.

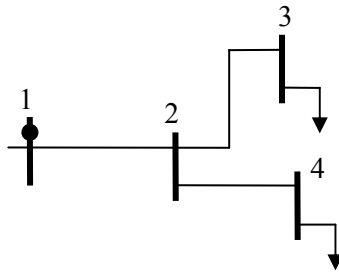


Fig. P.13.1. Radial distribution system with laterals. • - voltage magnitude measurement.

Branches are assumed to be three phase line sections with impedance/admittance parameters (in p.u.):

$$\begin{aligned} Z_{abc,12} &= Z_{abc,23} = Z_{abc,24} = \\ &= 10^{-3} \begin{bmatrix} 2.4388 + j6.1727 & 0.4132 + j3.2579 & 0.4132 + j3.2579 \\ 0.4132 + j3.2579 & 2.4388 + j6.1727 & 0.4132 + j3.2579 \\ 0.4132 + j3.2579 & 0.4132 + j3.2579 & 2.4388 + j6.1727 \end{bmatrix} \\ Y_{abc,12} &= Y_{abc,23} = Y_{abc,24} = \\ &= 10^2 \begin{bmatrix} 1.1352 - j1.7887 & -0.4725 + j0.5248 & -0.4725 + j0.5248 \\ -0.4725 + j0.5248 & 1.1352 - j1.7887 & -0.4725 + j0.5248 \\ -0.4725 + j0.5248 & -0.4725 + j0.5248 & 1.1352 - j1.7887 \end{bmatrix} \end{aligned}$$

Voltage measurement at main feeder (in p.u.):

$$\underline{V}_1 = 1.0 [1 \quad \exp(j2\pi/3) \quad \exp(-j2\pi/3)]^T$$

Measurements weights (elements of \mathbf{R} matrix) are set to 1.

Convergence criterion is assumed as $\max(|\Delta \mathbf{x}|) < 10^{-3}$.

Load pseudomeasurements are shown in Tab. P.13.1.

Tab. P.13.1. Load pseudomeasurements.

i	$P_{a, i}$ p.u.	$Q_{a, i}$ p.u.	$P_{b, i}$ p.u.	$Q_{b, i}$ p.u.	$P_{c, i}$ p.u.	$Q_{c, i}$ p.u.
1	0.000	0.000	0.000	0.000	0.000	0.000
2	0.000	0.000	0.000	0.000	0.000	0.000
3	0.060	0.015	0.004	0.002	0.001	0.002
4	0.020	0.004	0.020	0.004	0.020	0.004

- 13.2. Calculate state estimation for the distribution system described in problem 13.1, as shown in Fig. P.13.2 with WLS branch current as state variables.

Voltage at main feeder as reference (in p.u.):

$$\underline{V}_1 = 1.0 [1 \quad \exp(j2\pi/3) \quad \exp(-j2\pi/3)]^T$$

Power flow in branch 1-2: $P_{a,12} = P_{b,12} = P_{c,12} = 0.080$,

$$Q_{a,12} = Q_{b,12} = Q_{c,12} = 0.017$$

Measurements weights (elements of \mathbf{R} matrix) are set to 1.

Convergence criterion is assumed as $\max(|\Delta \mathbf{x}|) < 10^{-3}$.

Load pseudomeasurements are shown in Tab. P.13.2.

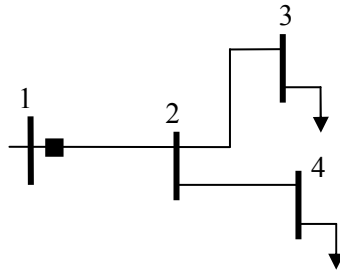


Fig. P.13.2. Radial distribution system with laterals. ■ - active/reactive power measurement.

Tab. P.13.2. Load pseudomeasurements (in p.u.).

i	$P_{as\,i}$ p.u	$Q_{as\,i}$ p.u	$P_{bs\,i}$ p.u	$Q_{bs\,i}$ p.u	$P_{cs\,i}$ p.u	$Q_{cs\,i}$ p.u
1	0.000	0.000	0.000	0.000	0.000	0.000
2	0.000	0.000	0.000	0.000	0.000	0.000
3	0.064	0.0128	0.004	0.0018	0.001	0.0028
4	0.018	0.0048	0.018	0.0048	0.018	0.0048

REFERENCES

- [13.1] M. E. Baran, A.W. Kelley, *State estimation for real-time monitoring of distribution systems*, *IEEE Trans. on Power Systems*, Vol. 9, No. 3, Aug. 1994, pp. 1601-1609.
- [13.2] M. E. Baran, A. W. Kelley, *A branch current based state estimation method for distribution systems*, *IEEE Trans. on Power Systems*, Vol. 10, No. 1, Feb. 1995, pp. 483-491.
- [13.3] Y. Deng, Y. He, B. Zhang , *A branch current estimation based state estimation method for radial distribution systems*, *IEEE Trans. on Power Delivery*, Vol. 17, No. 4, Oct. 2002, pp. 1057-1062.
- [13.4] A.K. Ghosh, D.L. Lubkeman, R.H. Jones, *Load modeling for distribution circuit state estimation*, *IEEE Trans. on Power Delivery*, April 1997, pp. 999-1005.
- [13.5] L. Grigsby, *Electric power generation, transmission and distribution*, CRC, 2007.
- [13.6] W.-M. Lin, J.-H. Teng, *Distribution fast decoupled state estimation by measurement pairing*, *IEE Proc. Generation, Transmission and Distribution*, Vol. 143, No. 1, Jan. 1996, pp. 43-48.

- [13.7] W.-M. Lin, J.-H. Teng, S.-J. Chen, ***A highly efficient algorithm in treating current measurements for the branch current based distribution state estimation***, *IEEE Trans. on Power Delivery*, Vol. 16, No. 3., July 2001, pp. 433-439.
- [13.8] C. N. Lu, J. H. Teng, W.-H., E. Liu, ***Distribution system state estimation***, *IEEE Trans. on Power Systems*, Vol. 10, No. 1, Feb. 1995, pp. 229-240.
- [13.9] I. Roytelman, S. M. Shahidepour, ***State estimation for electric power distribution system in quasi real-time conditions***, *IEEE Trans. on Power Delivery*, Vol. 8, No. 4, Oct. 1993, pp. 2009-2015.
- [13.10] D. Thukaram, J. Jerome, C. Surapong, ***A robust three-phase state estimation algorithm for distribution networks***, *Electric Power System Research*, Vol. 55, No. 3, Sept. 2000, pp. 191-200.
- [13.11] H. Wang, N. N. Schultz, ***A revised branch current based distribution state estimation algorithm and meter placement impact***, *IEEE Trans. on Power Delivery*, Vol. 19, No. 1, Jan. 2004, pp. 207-213.

14. ESTIMATION OF LOADS IN DISTRIBUTION SYSTEM

The procedure of load estimation in distribution power systems provides static real and reactive load estimates for each node in the system given synchronized measurements [14.1] – [14.10].

These procedures require possession of such data as:

- customer information (type, location, etc.),
- historical data (billing data, monthly power consumption in kWh, etc.),
- load forecasts (at the 5-minute, 15-minute and hourly basis),
- load profiles,
- real-time measurements:
 - load data,
 - bus voltages,
- switch status,
- control device status/settings.

In load estimation for power distribution systems the following issues are considered:

- the load-driven nature of power distribution system: there is no need to maintain system voltages if no loads are connected,
- the interdependence between system states and loads,
- three-phase modelling,
- operating and loading constraints,
- on-line measurements.

Methods for load estimation can be classified as follows:

- simple load estimation methods [14.4],
- Distribution State Estimation (DSE) based methods [14.3], [14.9], [14.10],
- statistical load modelling techniques [14.2], [14.6],
- fuzzy set based methods [14.1], [14.5], [14.7],
- a Bayesian linear model method [14.8].

14.1. SIMPLE LOAD ESTIMATION METHODS

Simple load estimation methods are based on historic data or operator's experience [14.4]. They allocate load to individual line sections, using:

- monthly peak load readings,
- transformer peak load analysis,

- existing diversified load curves.

Such methods are more suitable for peak load estimation. They give results which are affected by diversity of load groups and coincidence of peak loads.

14.2. DISTRIBUTION STATE ESTIMATION BASED METHODS

There are two approaches used in DSE based methods [14.3], [14.9], [14.10]:

- distribution load estimation is a by-product of DSE,
- distribution load estimation is a beginning step in a two-step method, which combines load allocation and DSE techniques.

The two-step method with use of distribution state estimation assumes that:

- the network is balanced, and single phase analysis is used,
- in the first step, loads are allocated according to billing data and typical load curves,
- in the second step, apart from on-line measurements, the rough load estimates from the first step are used as load pseudo-measurements,
- in the second step, WLS (Weighted Least Squares) state estimation is performed,
- real and reactive loads are computed based on state estimates.

14.2.1. EXAMPLE OF LOAD ESTIMATION WITH THE USE OF WLS ESTIMATION METHODS

Weighted least square is also used for load estimation [14.3], [14.9], [14.10]. State variable vector comprises conventional system states and parameters related to the loads. For the loads the following relationship is taken into account:

$$\tilde{\mathbf{S}}_L = \tilde{\mathbf{S}}_L^0 + \mathbf{\Lambda} \tilde{\mathbf{S}}_L^0, \quad (14.1)$$

where: $\tilde{\mathbf{S}}_L = [\tilde{P}_{L,1} \quad \tilde{P}_{L,2} \quad \dots \quad \tilde{P}_{L,n} \quad \tilde{Q}_{L,1} \quad \tilde{Q}_{L,2} \quad \dots \quad \tilde{Q}_{L,n}]^T$ - a vector of load estimates,
 $\tilde{\mathbf{S}}_L^0$ - an initial load vector,

- the network is balanced, single phase analysis is used, and no operating and loading constraints are considered,
- class-specific daily load curves that model the behaviour of loads as a function of season, day-of-week, hour, and temperature, are used.

The considered methods have performance characteristics, which significantly depend upon the time of the day, the size of the network, the number of the customer groups and the locations of each group of loads.

14.3.2. EXAMPLE OF STATISTICAL LOAD ESTIMATION

A simple method of the load estimation concerns on using substation power flows to different load points by using weighting coefficients resulting from transformer capacity [14.2]:

$$P_i = P_m \left(\frac{TC_i}{\sum_{i \in I_m} TC_i} \right), \quad (14.3)$$

where: $i \in I_m$ – a number of nodes,

I_m – a set of nodes served by power flowing through the node m ,

P_i – a real power demand at the node i ,

P_m – a real power flow measurement at the node m ,

TC_i – a transformer capacity at the node i .

However, transformer capacity is not recognized as adequate for estimation and an average daily customer is introduced:

$$P_i = P_m \left(\frac{ADC_i}{\sum_{i \in I_m} ADC_i} \right). \quad (14.4)$$

where: ADC_i – the average daily customer at the node i usually defined as monthly energy consumption divided by number of days in a billing period.

To take into consideration real-time load changes the load model factor LMF stated to group of customers is used:

$$P_{i,j,t} = P_{m,t} \left(\frac{E\{LMF_{j,t}\}ADC_{i,j}}{\sum_{i \in I_m} \sum_{j \in I_c} E\{LMF_{j,t}\}ADC_{i,j}} \right), \quad (14.5)$$

where: I_c – a set of load classes,

t – a time of analysis,

$ADC_{i,j}$ – a demand consumption at the node i for a load belonging to class j ,

$LMF_{j,t}$ – a load model factor for the group j at the time t .

The factor LMF is derived from normalized daily load curves obtained from historical-data statistical analysis made for all the distinguished customer classes. Accuracy of the statistical approach depends on time of the day, number of customers belonging to the certain class, availability of historical data etc. A reactive power of a load can be estimated by an approximate power factor.

14.4. FUZZY SET BASED METHODS

The characteristic feature of the methods is modelling system uncertainty and also inexactness and random nature of customer demands [14.1], [14.5], [14.7].

One can distinguish the following approaches:

- application of a fuzzy regression model,
- utilization of operator experience and expert knowledge,
- application of neural network and fuzzy set techniques.

14.4.1. APPLICATION OF A FUZZY REGRESSION MODEL

The following characteristic features of the approach based on application of a fuzzy regression model can be enumerated:

- the applied model expresses the correlation between a substation peak active load and supplied customer active loads in radial networks,
- single phase modelling is used in radial distribution systems,
- system voltages, operating and loading constraints are not considered.

14.4.2. UTILIZATION OF OPERATOR EXPERIENCE AND EXPERT KNOWLEDGE

The approach, which assumes utilization of operator experience and expert knowledge, can be characterized as follows:

1. Linguistic description for the size of loads is utilized.
2. The load current at a bus is estimated as a fuzzy variable described by the membership function.
3. Single phase modelling is used in radial distribution systems.
4. System voltages, operating and loading constraints are not considered.

14.4.3. APPLICATION OF NEURAL NETWORK AND FUZZY SET TECHNIQUES

The approach, based on application of neural network and fuzzy set techniques is proposed for active demand estimation in radial networks. Neural network and fuzzy set techniques are applied to generate standard load curves for classes of customers based on their monthly energy consumption and a large set of data of load curves obtained from measurement data. Loading constraints are incorporated in the method. As it is in the case of the previously-presented approaches also in the case of the considered approach, system voltages and operating constraints are not considered. Actual real power losses are neglected in the estimator.

14.5. OTHER METHODS FOR LOAD ESTIMATION

Other methods for load estimation are:

- Bayesian estimator used to estimate normalized load curves [14.8],
- a weighted least absolute value estimation method introduced to decrease the effect of gross errors in measurements [14.3].

14.6. REMARKS ON METHODS FOR LOAD ESTIMATION

Generally, the methods can be categorized into two groups by problem formulations:

- load estimation is formulated as a post-processing procedure of state estimation,
- power flows or customer demands are defined as the estimated variables of the load estimation problem.

In the second case, load estimation is a procedure which is independent from DSE.

Characterising the first group of the methods for load estimation, one can state:

1. The DSE based methods belong to this group.
2. Loads decide about system states, therefore methodology which treats load estimation as a by-product of DSE, may not provide satisfactory results.

Characteristics of the second group of the methods for load estimation are as follows:

- In this group, there are:
 - statistical load modelling methods,
 - the Bayesian linear model method,
 - fuzzy set based methods,
 - the WLAV estimation method.

- The loads (power flow/customer demand) are estimated directly.
- These methods separate loads from system states, which simplifies the interdependence between system states and loads.

General remarks on methods for load estimation

None of the methods formally considers operating and loading constraints, such as power flow equations and thermal limits of conductors/cables/switches.

1. Most of the methods are designed for radial networks or exploit the radial structure.
2. None of the methods rigorously studies the effects of the radial structure on the problem of load estimation and takes advantage of them.

PROBLEMS

- 14.1. What is a purpose of estimation of loads in distribution system?
- 14.2. What data are inputs for procedures of estimation of loads in distribution system?
- 14.3. What issues are considered in load estimation for power distribution systems?
- 14.4. How can we classify methods for load estimation for power distribution systems?
- 14.5. Characterize simple load estimation methods.
- 14.6. What are main features of distribution state estimation based methods?
- 14.7. Shortly describe statistical load modelling technique.
- 14.8. Give different solution of load estimation for power distribution systems with the use of the idea of fuzzy sets.

REFERENCES

- [14.1] M. Gavrilas, V.C. Sfintes and M.N. Filimon, ***Identifying Typical Load Profiles Using Neural-fuzzy Models***. *2001 IEEE/PES Transmission and Distribution Conf. and Exposition*, Vol. 1, 2001, pp. 421 -426.
- [14.2] K. Ghosh, D. L. Lubkeman and R. H. Jones, ***Load Modeling for Distribution Circuit State Estimation***. *IEEE Trans. on Power Delivery*, Vol. 12, No. 2, Apr. 1997, pp. 999-1005.
- [14.3] M.R. Irving and C. N. Macqueen, ***Robust Algorithm for Load Estimation in Distribution Networks***. *IEE Proc. Generation, Transmission and Distribution*, Vol. 145, No. 5, Sept. 1998, pp. 499-504.

- [14.4] J.A. Jardini, C.M.V. Tahan, M.R. Gouvea, S.U. Ahn and F. M. Figueiredo, ***Daily Load Profiles for Residential, Commercial and Industrial Low Voltage Consumers***. *IEEE Trans. on Power Delivery*, Vol. 15, No. 1, Jan. 2000, pp. 375 -380.
- [14.5] H. Kuo and Y. Hsu, ***Distribution System Load Estimation and Service Restoration Using a Fuzzy Set Approach***. *IEEE Trans. Power Delivery*, Vol. 8, No. 4, Oct. 1993, pp. 1950-1957.
- [14.6] H. Liao and D. Niebur, ***Load Profile Estimation in Electric Transmission Networks Using Independent Component Analysis***. *IEEE Trans. on Power Systems*, Vol. 18, No. 2, May 2003, pp. 707 -715.
- [14.7] J. Nazarko and W. Zalewski, ***The Fuzzy Regression Approach to Peak Load Estimation in Power Distribution Systems***. *IEEE Trans. on Power Systems*, Vol. 14, No. 3, Aug. 1999, pp. 809-814.
- [14.8] S. A. Villalba and C. A. Bel, ***Hybrid Demand Model for Load Estimation and Short Term Load Forecasting in Distribution Electric Systems***. *IEEE Trans. on Power Delivery*, Vol. 15, No. 2, Apr. 2000, pp. 764-769.
- [14.9] J. Wan and K. Miu, ***A Zonal Load Estimation Method for Unbalanced, Radial Distribution Networks***. *IEEE Trans. on Power Delivery*, Vol. 17, No. 4, Oct. 2002, pp. 1106-1112.
- [14.10] J. Wan and K. Miu, ***Weighted Least Squares Methods for Load Estimation in Distribution Networks***. *IEEE Trans. on Power Systems*, Vol. 18, No. 4, Nov. 2003, pp. 1338-1345.